Novel Coatings for Hard Tissue Implants

Submitted to the National University of Ireland, Cork,

in fulfilment of the requirements for the degree of

Doctor of Philosophy In Pharmacy-Pharmaceutics

By

Caroline O' Sullivan B.Sc., M.Sc.

School of Pharmacy, University College Cork, Ireland

Under the direction and supervision of

Abina Crean, B.Sc., Ph.D., M.P.S.I.

Katie Ryan, B.Sc., Ph.D., M.A.

Head of School: Professor Catriona O' Driscoll, B.Sc., Ph.D., M.A.

2013

Table of Contents

Declaration

This thesis has not been previously submitted, in part or in whole, to this or any other University for any degree and is, unless otherwise stated the original work of the author.

Signed: .....

Caroline O'Sullivan

The cell biology work was conducted by Dr. Peter O'Hare, Nanotechnology and Integrated BioEngineering Centre, NIBEC, University of Ulster, UK. The surgery in the *in vivo* trial and chemiluminescence test was executed by Prof. John Hunt. UKBioTEC, University of Liverpool.

A range of analysis was outsourced to various consultant laboratories: XPS was conducted by Dow Corning, Belgium; ICP-OES was perfomed by CERAM, UK; XRD analysis was executed by Greg Byrne, Surface Engineering Research Group, UCD and tensile bond strength analysis was carried out by APS, Waterford.

'Chance favors the prepared mind'

I would like to dedicate this thesis to my parents,

John and Mary O' Sullivan

and

to my husband, James McAuliffe.

Acknowledgements

I would like to sincerely thank my supervisors Dr. Abina Crean and Dr. Katie Ryan for their patience, encouragement and guidance throughout this Ph.D. programme. I have gained valuable knowledge on all levels from this experience with working with them. I can honestly say that this achievement would not have been possible without their limitless support, for which I am truely grateful.

I would also like to acknowledge the following for their assistance and contribution to the work involved:

- School of Pharmacy in UCC for the opportunity to complete this work.
- Technical officers Suzanne Crotty, Dr. Michael Cronin and Dr. Tom O' Mahony (UCC).
- EnBio for supplying the CoBlast samples and Dr. Liam O'Neill for his technical support.
- Dr. Peter O'Hare NIBEC for the cell biology work.
- Prof. Alan Dobson and Dr. Niall O'Leary for the use of the facilities in the Department of Microbiology in Environmental Research Institute (ERI), UCC, for supplying the *S. aureus* strain ATCC 1448 and training.
- Dr. Jim O'Gara for use of the facilities in the School of Biomolecular and Biomedical Science and for supplying the clinical isolate strains.
- Prof. John Hunt, UKBioTEC, University of Liverpool for his guidance in the *in vivo* trial.
- Kathleen O'Sullivan for her assistance in the statistical analysis, School of Mathemathical Sciences, UCC.

Publications and Presentations

Peer-reviewed Publications

O'Sullivan, C., O'Hare, P., Byrne, G., O'Neill, L., Ryan, K.B. and Crean, A.M., (2011) 'A modified surface on titanium deposited by a blasting process'. Coatings, 1(1): 53-71.

O'Sullivan, C., O'Hare, P., O'Leary, N.D., Crean, A.M., Ryan, K., Dobson, A.D. and O'Neill, L.D. (2010) 'Deposition of substituted apatites with anticolonising properties onto titanium surfaces using a novel blasting process.' Journal of Biomedical Materials Research B: Applied Biomaterials, 95(1): 141-149.

Submitted Publications

O'Sullivan, C., O'Hare, P., Byrne, G., O'Neill, L., Ryan, K.B. and Crean, A.M., (2012) 'A modified surface on titanium deposited by a blasting process'. Surface and Coatings Technology.

Publications in Preparation

O'Sullivan, C., Paramanathan, N., O'Hare, P., O'Leary, N.D., Dobson, A.D.,O'Gara, J., Crean, A.M. and Ryan, K. 'Evaluation of increased ion concentration on the antimicrobial and anticolonising properties of substituted apatite coatings'.

O'Sullivan, C., Paramanathan, N., Hunt, J.,Crean, A.M. and Ryan, K., '*In vivo* evaluation of silver substituted apatite coatings to combat infection on hard tissue implants'

Presentations

O'Sullivan, C. (2011) In at the Deep End: Learning to Teach in Higher Education- Lost in Translation. Postgraduate Symposium, University College Cork, Cork, February 16.

O'Sullivan, C., Crean ,A. and Ryan, K. (2010) Novel Coatings for Hard Tissue Implants. Joint Schools of Pharmacy Research Seminar. Queens University of Belfast, Belfast, March 29-30.

O'Sullivan, C., Crean, A. and Ryan, K. (2010) Novel Coatings for Hard Tissue Implants. School of Pharmacy Research Seminar. University College Cork, Cork, January 29.

Poster Presentations

O'Sullivan, C., Crean, A. and Ryan, K. (2011) The Use of Substituted Apatites to Combat Bacterial Infections on Hard Tissue Implants. Poster presentation at PhD Research Day, School of Pharmacy, UCC, September 15.

O'Sullivan, C., Crean, A. and Ryan, K. (2010) The Use of Substituted Apatites to Combat Bacterial Infections on Hard Tissue Implants. Poster presentation at Molecules to Medicine Research Conference, College of Medicine & Health, UCC, June 16.

Abbreviations

AaP:	Accumulation associated proteins
ATCC:	American Type Culture Collection
ACS:	American Chemical Society
ACP:	Amorphous calcium phosphate
Ag:	Silver
AgA:	Silver substituted apatite
AgSrA:	Silver strontium substituted apatite
Al:	Aluminium
ALP	Alkaline phosphatase
Al_2O_3:	Alumina
ALBC:	Antibiotics loaded bone cements
AmP:	Antimicrobial peptides
atm:	Atomis
BAI:	Biomaterial associated infections
ASTM:	American Society of Test Methods
BC:	Bone cement
BCP:	Biphasic calcium phosphate
BHI:	Brains heart infusion
BMP:	Bone morphogenic proteins
°C:	Degree celsius
Ca:	Calcium
CaO:	Calcium oxide
CaP:	Calcium phosphate
Ca/P:	Calcium to phosphate
CDHA:	Calcium deficient HA
CFU:	Colony forming unit
cm:	Centimetres
Co:	Cobalt
CoCr:	Cobalt-chromium alloy
Cr:	Chromium
Cu:	Copper
2D	Two dimensional
3D	Three dimensional
DCP:	Dicalcium phosphate
DNA:	Deoxyribonucleic acid
E.coli:	*Escherichia coli*
EDTA:	Ethylenediaminetetra acetic acid
EDX:	Energy dispersive X-ray analysis
FDA:	Food Drug Adminstration
fMLP:	N-formyl-methionyl-leucyl-phenylalanine
FTIR:	Fourier transform infrared spectroscopy

GPa:	Gigapascal
HA:	Hydroxyapatite
HCl:	Hydrochloric acid
HMDS:	Hexamethyldisilizane
HPLC:	High performance liquid chromatography
h:	Hour
ICP-OES:	Inductively coupled plasma optical emission spectroscopy
ISO:	International Standard Organisation
IPA:	Isopropanol
g:	Gram
KBr:	Potassium bromide
KCl:	Potassium chloride
keV:	Kiloelectron volt
Kg:	Kilogram
kV:	Kilovolt
K-wire:	Kirshner wire
l:	Litres
LAF:	Laminar air flow
LB:	Luria Bertoni
m:	Meter
M:	Molarity
mMol:	Millimole
µm:	Micrometer
MCD:	Apatitic abrasive
MEM:	Minimum Essential Medium
MIC:	Minimum inhibitory concentration
mins:	Minutes
ml:	Millilitres
Mpa:	Megapascals
mRNA:	Messenger ribonucleic acid
MSSA:	*Methicillin sensitive Staphylococcus aureus*
MRSA	*Methicillin resistant Staphylococcus aureus*
MTT:	3-(4,5-dimethylthiazol-2-yl)-2,5-diphenyltetrazolium bromide
N:	Newton
Ni:	Nickel
NiTi:	Nitinol
NY:	New York
nm:	Nanometre
O:	Oxygen
OA:	Oxyapatite
OD:	Optical density
mA:	Milliamp
mM:	Millimolar
M:	Molar

OCP:	Octacalcium phosphate
OHA:	Octa-hydroxyapatite
%:	Percentage
p:	Probability
P:	Phosphorous
P. aeruginosa:	*Pseudomonas aeruginosa*
PBS:	Phosphate buffer saline
PC:	Phosphorylcholine
PEG:	Poly(ethylene glycol)
PGA:	Poly(glycolic acid)
PHA:	Poly(hydroxyl alkanoates)
PIA:	Polysaccharide intercellular adhesin
PLA:	Poly(lactic acid)
PLD:	Pulsed laser deposition
PLGA:	Poly(lactic-co-glycolic acid)
PMA:	Phorbol-12-myristate-13-acetate
PMMA:	Poly(methyl methacrylate)
ppm:	Parts per million
PRG:	Poly(ethlene glycol)
psi	Pound per square inch
PXRD:	Powder X-ray diffraction
QAC:	Quaternary ammonium compounds
Ra:	Surface roughness- arithmetic mean value
RF:	Radio frequency
RGD:	Arginine-glycine-aspartic
rpm:	Revolutions per minute
s:	Second
SD:	Standard deviation
S.aureus:	*Staphylococcusaureus*
S.epidermis:	*Staphylococcus epidermis*
SBF:	Simulated body fluid
SEM:	Scanning electron microscopy
Sr:	Strontium
SrA:	Strontium substituted apatite
SS:	Stainless steel
TCP:	Tricalcium phosphate
Ti:	Titanium
TTCP:	Tetracalcium phosphate
THA:	Total hip arthroplasty
THR:	Total hip replacement
TSA:	Tryptone soya agar
TSB:	Tryptone soya broth
U/ml:	Units per millilitre
UK:	United Kingdom

µl:	Microlitres
USA:	United States of America
V:	Vanadium
wt:	Weight
XRD:	X-ray diffraction
XPS:	X- ray photo spectroscopy
Zn:	Zinc
ZnA:	Zinc substituted apatite
ZrO_2:	Zirconia

Summary of Thesis

Hydroxyapatite (HA) coating of hard tissue implants is widely employed for its biocompatible and osteoconductive properties as well as its improved mechanical properties (Borsari *et al*., 2005; Stoch *et al*., 2005; Lu *et al.,* 2004). The provision of this bioactive surface (modified surface) onto which the bone can strongly bond will in turn limit micromotions at the implant-host interface (Borsari *et al*., 2005; Stoch *et al*., 2005). Plasma technology is the principal deposition process for coating HA on bioactive metals for this application (Campbell *et al*., 2003). However, thermal decomposition of HA can occur during the plasma deposition process, resulting in coating variability in terms of purity, uniformity and crystallinity, which can lead to implant failure caused by aseptic loosening (Mohammadi *et al*., 2008; Gross *et al*., 2004; Chang and Khor., 1996; Søballe and Overgaard, 1996). An alternative coating technology, CoBlast^{TM}, based on grit blasting technology, has been used to deposit HA onto titanium (Ti) metal using a dopant/abrasive regime. This is an ambient temperature and low cost deposition process which retains the chemical composition of the starting materials thereby offering better control of the coating properties. However, one of the major drawbacks in the use of biomedical materials is the occurrence of biomaterials associated infections (BAI) (Schmidmaier *et al*., 2006). These infections are the result of colonisation of bacterial microbes leading to the inevitable biofilm formation on the surface of the implant. Biomaterial-associated infections pose great surgical problems, as revision surgery is not always easy and patients suffer severe discomfort (Van Howelingen, 2012; Schmidmaier *et al*., 2006). Traditional therapeutic approaches are complicated with a number of drawbacks including poor delivery and impact of antibiotics at the localised site or

development of antibiotic resistance microbes (Jiranek *et al*., 2006; Amyes and Gemmell, 1997; Gold and Moellering, 1996). Prophylactic treatment involving large doses of antibiotics administered before and after surgery increases the risks of systemic toxicity and organ failure (Ruszczak and Fress, 2003; Price *et al*., 1996). Recently, there has been an emergence of resistant bacterial strains, which are proven difficult to eradicate using conventional antibiotics (Parvizi *et al*., 2009). Therefore, there is a need for a bioceramic coating on hard tissue implants that not only promotes bone-implant integration but also inhibits bacterial colonisation.

The thesis is structured over a number of chapters as follows:

In **Chapter 1**, a literature review has been prepared which covers the main topics focused in this study. Typical biomaterials used for hard tissue implants are outlined. Moreover, HA and its importance as a bioceramic coating on hard tissue implants is discussed. The bone fixation process at the implantation site involving the biological and chemical interactions at the implant-bone interface is covered. In addition, the surface properties of the implant which influences cellular response of the osteoblasts (bone forming cells) are summarised. Problems associated with hard tissue implants and possible solutions that have been extensively studied are included. The process involved in biofilm formation is detailed. An overview of the deposition processes used to deposit HA as well as the CoBlast technology are presented.

Similar materials and methods were used to characterise the modified surfaces in the various studies **(Chapters 3-7)** as a result, a general overview of these materials and

methods are outlined in **Chapter 2.** The materials and modified surfaces were characterised where appropriate, using various analytical techniques to understand the elemental and chemical composition (EDX, XPS, XRD, FT-IR), physical properties (SEM, surface roughness, coating mass and thickness) and cell culture analysis (cell proliferation and cytotoxicity). Details of the microbiology assessments executed (antimicrobial and anticolonising studies) are outlined. The antimicrobial studies consisted of evaluating the impact of the leached ion released from the surface and the effect of the immobilised ion on the surface (permanent, non leaching surface effect) using *Staphylococcus aureus* (*S. aureus*) and clinical strains (methicillin resistant *Staphylococcus aureus (MRSA),* methicillin sensitive *Staphylococcus aureus (MSSA) and Staphylococcus epidermis (S. epidermis*). In addition, anticolonising assessments were performed to investigate the potential biofilm formation of bacterial microbes onto the surfaces. An *in vivo* study was also performed to assess the efficacy of the implants' surfaces against *S. aureus* in an infection model using nude mice. In **Chapter 7**, the methods used to characterise the implants surfaces for microbial attachment (% kill, SEM), and subsequent inflammatory and systemic responses are summarised.

In **Chapter 3**, CoBlast has been used to successfully modify a Ti substrate with a HA treatment. A series of apatitic abrasives under the trade name MCD, was investigated to determine the effect of abrasive particle size on the surface properties of both microblast (abrasive only) and CoBlast (HA/abrasive) treatments. The CoBlast HA substrates were compared to the microblast substrates and an untreated Ti. The various powders (HA powder, apatitic abrasives) and the treated substrates were characterised for chemical composition, coating coverage, crystallinity and

topography including surface roughness. The results revealed that the surface roughness of the HA blasted modification was affected by the particle size of the apatitic abrasives used. More importantly, the CoBlast process did not alter the chemistry of the crystalline HA during deposition. Enhanced viability of osteoblastic cells was observed on the CoBlast HA surfaces compared to the microblast and untreated Ti.

Chapter 4, compares in an *in vitro* study, the HA coating deposited using CoBlast and also using the standard plasma spraying process. Ion release from the HA surfaces over 3 days are assessed and the bioactivity of these surfaces in stimulating body fluid (SBF) were evaluated. The HA surface induced the formation of a carbonated apatite (CHA) on its surfaces following incubation in SBF. Possible mechanisms for this formation are outlined however further analysis is required for confirmation. Both surfaces are characterised before and after the bioactivity study for chemical and physical properties. The HA surfaces were analysed for osteoblast cell viability using MG-63 osteoblasts. The mechanical properties of the adhesion bond strength between the HA coating and the Ti substrate was assessed before and after the formation of the carbonated apatite. The data revealed that the deposition of the HA coating using plasma technology resulted in a rougher and thicker coating however, the quality of the coating was inferior to the CoBlast surface. The CoBlast HA coating was more crystalline, uniform, exhibited higher levels of osteoblast proliferation *in vitro* and produced higher levels of mechanical stability despite its lower rate of dissolution.

In **Chapter 5**, CoBlast technology was used to successfully deposit a series of substituted apatites onto Ti. The 5% wt substituted apatite powders (AgA, SrA and ZnA) were deposited due to their potential use as antimicrobial materials and coatings to combat BAI. The modified surfaces were assessed for their chemical and physical properties as well as cell viability of osteoblasts. Surfaces demonstrated good cell proliferation without any cytotoxicity observed. The antimicrobial and non-colonising behaviour of the surfaces were assessed using *S. aureus* as the bacterial challenge. Promising levels of initial microbial inhibition were observed from all of the substituted surfaces. The anticolonising behaviour was attributed to the surface impact of the immobilised ions in conjunction with the low levels of ions released from the surface. The Ag substituted apatite was observed to outperform both the SrA and ZnA in terms of biofilm inhibition. However, better surface impact was observed for the SrA with enhanced osteoblast proliferation compared to the ZnA surface. Promising results of the anticolonising and preliminary osteoconductive potential of 5% wt substituted apatites were revealed in **Chapter 5**.

Chapter 6 evaluates the use of substituted apatites with an increased loading of 12% wt (AgA, SrA) in a similar study to **Chapter 5**. In addition, a co-substituted silver-strontium (AgSr) apatite was evaluated due to the enhanced cell proliferation behaviour of SrA and anticolonising behaviour of AgA in the previous study. 12% AgA was seen to again outperform the other surfaces in terms of its anticolonising behaviour and as a result was subjected to further antimicrobial and anticolonising studies using clinical strains (*MRSA, MSSA and S. epidermis*). The results revealed that the AgA surface demonstrated good antibacterial activity (eluted and immobilised ion) against *MRSA* followed by *MSSA*. Good anticolonising activity

was only observed at day 1 against *MRSA*. Poor impact against *S. epidermis* was observed compared to the other clinical isolates assessed. AgA demonstrates promising potential as a coating to combat BAI.

AgA of two different loadings (5% wt and 12% wt) were deposited onto a Ti K-wire implants using CoBlast technology and the anticolonising behaviour of these implants were assessed in an *in vivo* model in **Chapter 7.** EDX and SEM were used to determine the chemical composition and morphology of the surfaces. The implants were subcutaneously implanted into nude mice and inoculated with *S. aureus* as the bacteria challenge, which delivered a localised infection. Following two days, the explanted 12% wt AgA coated K-wire was seen to outperform the 5% wt AgA. Lower inflammatory responses were activated with the insertion of the Ag loaded K-wires in an infection model. These results indicate that the AgA coating on the surface of orthopeadic implants inhibits adhesion preventing colonising behaviour with good biocompatibility potential.

Finally, in **Chapter 8** a general discussion on the findings of the studies performed in Chapters 3-7 is given. This discussion is divided into four sections, in order to address the main objectives of the thesis and the research questions probed:

(i) Ultimate aim: Added value and key benefits of CoBlast technology. CoBlast, a room temperature process, has the ability to deposit the 'as-received' powders and tailor the surface composition and properties. Surfaces with enhanced

osteoblast cell viability, osteoconductive potential and promising anticolonising activity can be deposited.

(ii) Objective 1: Evaluations of HA coatings deposited using CoBlast technology in *in vitro* studies. CoBlast HA coatings could positively influence the long-term success of hard tissue implants and offers an attractive alternative to the industry standard plasma process.

(iii) Objective 2: Evaluation of substituted apatites with antimicrobial metals as an infection preventing strategy in *in vitro* studies. Substituted apatite coatings were shown to inhibit bacterial colonisation without compromising osteoblast cell viability.

(iv) Objective 3: Evaluation of AgA as an infection preventing surface in an *in vivo* model. AgA at a silver loading of 12% wt was shown to be effective in inhibiting *S. aureus* colonisation compared to 5% wt AgA with a lower inflammatory response activated in a subcutaneous model in nude mice.

Conclusions, limitations of this work and future work are also included.

Chapter 1

1.0 Introduction and Literature Review

Hydroxyapatite (HA) and doped apatites were deposited onto titanium (Ti) (V) metal using a grit blasting CoBlast technology. The HA surface was deposited as a bioactive surface to induce chemical and biological responses whereas the substituted apatites, which comprised of antimicrobial metals, offer the dual purpose of being osteoconductive in addition to its anticolonising activity. The coatings are characterised to investigate the effectiveness of the CoBlast technology to deposit the bioceramics onto Ti metal and also to assess the quality of the coatings deposited, which will affect the stablity and degradation. The literature review focuses on these keys areas so as to understand the important factors which must be studied so as to critically evaluate CoBlast coatings. The keys areas comprises of understanding the following: properties of biomaterials; implant fixation process; problems that undermine long-term fixation focusing on biofilm formation as a main reason; biofilm formation process and preventative measures and competing technologies. A summary of the literature review is as follows:

Bioceramics and metals are commonly used biomaterials for hard tissue implants. (Dorozhkin, 2010). Hard tissue implants find applications in both the dental and orthopaedic areas where the implants must form a secure bond with the bone in order to promote stability to the load bearing implants (Borsari *et al*., 2005; Stoch *et al*., 2005; Lu *et al*., 2004). These biomaterials evoke specific biological responses which are responsible for successfully integrating and securing the implant to living tissue ensuring longevity of the implant in order to enhance everyday functionality

(Arinzeh *et al*., 2005; Xue *et al*., 2004; Overgaard, *et al*., 1999). HA is a bioceramic applied as a coating onto metallic implants to induce good quality bone formation at the implants surface and to minimise micromotions which could undermine the implants stability (Borsari *et al*., 2005; Lu *et al*., 2004). In this literature review, the different types of biomaterials used are discussed as well as the important properties they must posess to ensure successful integration with host tissue. Once the implant is inserted into the body, there is a casade of chemical and biological reactions which occur at the surface-bone interface responsible for fixating the implant to bone. Fixation is a complex process involving a variety of biological cells. This review describes this complex fixation process (chemical and biological interactions, bone formation, remodelling). The attachment and proliferation of osteoblasts, bone forming cells to the implants surface is considered an important step in this fixation process. Constructing surfaces with the surface properties that enhance these interactions will ensure successful implantation. In addition the surface properties that influence osteoblast adhesion is discussed.

The review outlines the two main problems which compromise the long-term success of hard tissue implants: aseptic loosening and biomaterial associated infections (BAI). Aseptic loosening may be caused by an unstable mechanical bond between the implant and bone due to poor initial fixation, incompatible mechanical properties or poor coating properties such as cracking or delamination (Abu-Amer *et al*., 2007; Huiskes *et al*., 1993). Other sources include corrosion or degradation of the biomaterial surface resulting in inflammation. On the other hand, BAI are predominatly caused by the introduction of bacteria during surgery (Schmidmaier *et*

al., 2006, Van de Belt *et al*., 2001). These microbes attach onto the implant surface and subsequently proliferate into a resiliant biofilm which can be difficult to eradicate. The steps involved in biofilm formation are outlined and the prevention strategies that are established to combat such infections are presented. These namely include biocide release, which involves the release of antibiotics or antimicrobial ions from the implants surface to kill bacterial microbes (Liu and Chang, 2009; Chai *et al*., 2007). Surfaces that have been designed to repell microbes from the surface through charge and surface chemistry interactions (Russell, 2009; Berry *et al*., 2000; Gottenbos *et al*., 2000). Finally, the utilisation of non-leaching surfaces capable of killing microbes on contact is discussed (Antoci *et al*., 2008; Hu *et al*., 2007; Gabriel *et al*., 2006). These surfaces include immobilising or tethering antimicrobial materials through covalently bonding onto the implants surface. Research performed in these areas is discussed.

Conventional methods used to deposit biocermics onto metals are discussed. There are advantages and disadvantages associated with these processes which are summarised. Problems include non-uniformity, reproducibility, delamination and degradation leading to aseptic loosening (Mohammadi *et al*., 2007; Gross *et al*., 2004; Chang and Khor., 1996; Søballe and Overgaard, 1996). Coating adhesion, chemical composition and purity are problematic and results in pre- and post-treatment steps so as to overcome these failings. CoBlast offers an attractive alternative to conventional methods as this low temperature deposition process deposits a higher quality coating compared to plasma.

1.1 Hard Tissue Implants

With an ageing human population who participate regularly in physical activites, there has been an increase in degenerative diseases such as osteoporosis (weaken of bones), osteoarthritis (inflammation in bone joints) and bone infections (osteomyelitis and peridontitis), also bone fractures (open and closed traumatic fractures) which result in pain or loss in function. It has been estimated that one out of two Americans will require medical care for a bone or joint issue in their lifetime and the cost of dealing with denegerative diseases is approximately $849 billion dollars a year in the USA (Gunnigle, 2011). It is also estimated that 15% of the world's population experiences pain and joint degeneration due to the presence of osteoarthritis (Vallejo *et al*., 2004). Bone-related disesases and bone fractures account for the need for hard tissue implants whose function is to provide and enhance a bodily function thus, improving the quality and longevity of human life (Dorozhkin, 2010).

Hard tissue implants are widely used in repair, replacement or augumetation of diseased or damaged parts of the body system such as bones, joints and teeth. Hard tissue implants are prostheses that will bond with bone and needs to be successfully integrated with the living tissue for long-term stability. These types of medical implants are predominantly composed of metals and are often coated with a bioactive coating, which are surgically implanted. Through the bone fixation process in the body, a structural and functional connection between the living bone and the implant is made. Hard tissue implants find application in two main areas; dental and orthopaedic settings.

A dental implant is an artificial tooth root replacement used in prosthetic dentistry and can have a number of manifestations including screws, cylinders or blades which are surgically placed into the jawbone and can hold one or more prosthetic teeth. There are many types of orthopaedic implants such as joint arthroplasties, spinal fixation devices, fracture plates, wires, pins, screws, artificial ligament attachment implants, craniofacial implants and maxillofacial implants (Ryan *et al*., 2006). Joint arthroplasties are used to relieve pain or restore range of motion by reconstructing lower limb joints such as the hip, knee and ankle. Total hip replacement (THR) involves using components such as acetabular cups and femoral heads. Whereas knee implants consist of two types 1) unilateral replacement, patella femoral joint replacement or 2) total knee replacement. Even though the focus of this research is based on orthopaedic implants, in particular those associated with THR, it may also be applied to dental implants. Hard tissue implants are engineered from a wide range of biomaterials and should posses fundamental properties such as good mechanical and biological compatibility, enhanced wear and corrosion resistance and superior bioactivity to improve the mechanical interlocking between the implants surface and living tissue.

1.1.1 Biomaterials for Hard Tissue Implants

A biomaterial is defined as ‘a substance that has been engineered to take a form which, alone or as part of a complex system, is used to direct, by control of interactions with components of living systems’ (Williams, 2009). They play a vital role in ‘ensuring the success of a medical device and are intended to interface with biological systems to evaluate, treat, augment or replace any tissue, organ or function of the body’ (Williams, 1999). Biomaterials can be described as being bioactive,

bioinert and biocompatible. A bioactive material is one that elicits a specific response at the interface of the material which results in the formation of a bond between tissues and the material (Williams, 1999) including bonding directly to bone (Ducheyne and Qiu, 1999). For the purposes of biomedical implants, the term bioinert can be defined as 'a minimal level of response from the host tissue in which the implant becomes covered in a thin fibrous layer which is non-adherent' (Best *et al*., 2008). Finally in the context of the development of novel biomaterials, biocompatibility is an important property and represents 'a material that does not elicit an unresolved inflammatory response or demonstrate immunogenicity or cytotoxicity' (Rezwan *et al*., 2006).

The evolution of biomaterials according to Hench and Polak, encompasses three generations: bioinert materials such as the use of biomedical metals (first generation); bioactive and biodegradable materials e.g. calcium phosphate coatings and drug delivery systems (second generation) and materials designed to stimulate specific cellular responses at the molecular level are classed as third generation biomaterials (third generation) (Hench and Polak, 2002). Most of the research to date on hard tissue implants has been specifically focused on first and second generation materials whereas approaches in tissue engineering has been related to the design and evolution of third generation biomaterials which are engineered to release growth factors and osteoprogenitor cell populations (Hench and Polak, 2002). Table 1.1 shows the types of materials that can be chosen for specific applications. Common biomaterials used in hard tissue implants include metals, ceramics, polymers or composites (e.g. mixtures of ceramics and polymers).

Table 1.1: Implant materials used in the body (Navarro *et al*., 2008; Park and Bronino, 2003).

Material Category	Material for Implant Use	Examples
Metals	Titamium and its alloys, cobalt-chromium alloys, stainless steels, gold, silver, plantium	Joint replacements, bone plate, screws
Ceramics	Aluminum oxide, calcium phosphates, bioactive glasses	Dental abutments, orthopaedic femoral heads, bone grafts, bone cements
Polymers	Nylon, silicon, rubber, polyester,polyethylene, poly(methacrylic acid)	Hip sockets, soft tissues, liner of acetabular cups, spacers

The design and selection of a biomaterial for hard tissue implant is an important consideration and Geetha *et al*., reported that these implants must possess the following properties (Geetha *et al*., 2009):

- *Biocompatibility*: The success of the implant is mainly dependent on the reaction of the human body to the implant. The two main factors that affect the biocompatibility are the host's response which is induced by the material and the material's degradation within the host. The biomaterial itself and the degradation products must be highly non-toxic and should not cause any inflammatory response or allergic reaction.
- *Suitable mechanical properties*: Implants are used for high load bearing applications which are subjected to repeated cyclic loads and strains. It is important for the implant to have high mechanical strength (tensile strength) and low Young's modulus (stiffness) comparable to that of bone in order to prevent implant loosening and ensure lifetime functionality. Table 1.2 summarises the mechanical properties of typical biomaterials used for hard tissue implants.

- *High corrosion and wear resistance*: Low resistance to corrosion and wear results in the release of ions or wear debris into the body, which will elicit allergic or toxic reactions.
- *Osteointegration*: If the implant surface fails to integrate with the adjacent bone micromotions can result, which will subsequently lead to failure due to implant loosening (Geetha *et al*., 2009).

Table 1.2: Comparison of mechanical properties between implant material and bone (Bonfield, 1998; Thompson and Hench, 1998).

Material	Young's Modulus (GPa)	Tesile Strength (MPa)
Alumina	365	6-55
Sintered HA	70-90	50-110
HA coating	0.5-5.3[2]	>51 [1,3]
Stainless steel 316L	193	540
Cobalt-chromium alloys	230	900-1540
Titanium (Grade V)	106	900
Poly(methyl methacrylate) bone cement	3.5	70
High density polyethyene	1	30
Cortical bone	7-30	50-150

([1]ISO Standard, 2008; [2]Tsui *et al*, 1998; [3] FDA, 1992)

1.1.1.1 Metals

Bioinert metals are excellent biomaterials for load-bearing orthopaedic applications, some of which include 316L stainless steel (SS), cobalt-chromium alloy (CoCr), and titanium based alloys including shape memory nitinol (NiTi). A major problem with the use of alloys such as SS and CoCr is the release of elements such as nickel, chromium and cobalt due to the corrosion in the body's environment (Okazaki and Gotoh, 2005). Other drawbacks include the 'stress shielding effect' arising from the

mismatch of Young's modulus properties between metal and bone (higher stiffness than bone (>30 GPa)), which leads to insufficient stress transfer to bone and results in bone cell death around the implant (Sumner *et al*., 1998) or the formation of fibrous membrane. This 'stress shielding effect' will lead to implant failure due to implant loosening (Geetha *et al.*, 2009; Sun *et al.*, 2001; Sumner *et al*., 1998). NiTi is commonly used as the biomaterial in stents due to its unique property of 'shape memory', which is the ability of the material to recover its shape after applied stress is favoured (Navarro *et al*., 2008; Eggeler *et al*., 2004). This is attractive in the context of hard tissue metal implants which undergo excessive cyclic loading. However, its use for hard tissue implants of large surface area is still being investigated due to concerns relating to the release of toxic nickel, a potential carcinogen (Kapanen *et al*., 2001). Ti (V) is the most commonly used metal for implantation, due to its excellent mechanical properties (high strength and low modulus relative to bone), high corrosion resistance, biocompatibility, light weight and excellent osteointegration properties (Niinomi, 2002). A new generation of metals for orthopaedic implants include porous Ti metals, which are sintered metals with increased surface roughness as a result of their three dimensional (3D) structures. The attractiveness of these materials is due to their ability to reduce modulus mismatch at the bone-implant interface and enhance long-term fixation (Levine, 2008).

1.1.1.2 Ceramics

Ceramics are defined as 'non metallic, inorganic and which can be shaped and consolidated at high temperatures' (Ravaglioli and Krajewski, 1992). Hench and Wilson defined bioceramics as 'biomaterials designed and fabricated from ceramic

origins used for repair and reconstruction of diseased, damaged or worn-out' parts of the body (Hench and Wilson, 1993). Bioceramics are categorised as either 'bioinert' or 'bioactive', examples of the former include alumina (Al_2O_3) and zirconia (Zr_2O). Alumina is the most commonly used inert bioceramic due to its excellent mechanical properties. Due to their similarity in chemical composition to that of bone and teeth, calcium phosphates (CaP) have emerged as an important family of bioceramics. CaP coatings are bioactive as they can form interfacial bonding system with living tissue. Different types of CaP with varying degrees of calcium to phosphate (Ca/P) molar ratios are available including hydroxyapatite (HA), tricalcium phosphate (TCP), biphasic calcium phosphate (BCP), amorphous calcium phosphate (ACP), or calcium deficient HA (CDHA). BCP is a mixture of HA with either α-TCP or β-TCP (Dorozhkin, 2010). The chemical composition and the calcium to phosphate molar ratio of these CaP compounds and a number of other CaP compounds are outlined in Table 1.3.

CaP have been extensively used for clinical applications relating to bone cements, bone filling, bone substituting and bone tissue engineering materials, due mainly to their bioactivity, biocompatibility and osteoconductive properties (Tan *et al.*, 2011; Best *et al*. 2008; Saikia *et al*., 2008; Habraken *et al*., 2007; Jiranek *et al*., 2006; Knaack *et al*., 1998). Despite their poor mechanical properties in a bulk form (brittle and low tensile strength), these bioceramics are employed as coatings on metallic implants (Borsari *et al*., 2005; Oh *et al*., 2005; Stoch *et al*., 2005; Lu *et al*., 2004). Thus, CaP coatings on metallic implant devices offers the possibility of combining the strength of the metals and the bioactivity of the ceramics. The biodegradation properties of ceramics such as thermodynamic solubility, crystallinity feature

(crystalline/amorphous), presence of impurities and additives, and structural properties (dense/porous) are considered important parameters for their success in bone repair and regeneration.

Table 1.3: CaP compounds commonly used as biomaterials (Dorozhkin, 2010).

Abbreviation	Compound	Formula	Ca/P molar ratio
DCPD	Dicalcium phosphate dehydrate, mineral brushite	$CaHPO_4 \cdot 2H_2O$	1.0
DCP	Dicalcium phosphate anhydrous, mineral monetite	$CaHPO_4$	1.0
OCP	Octacalcium phosphate	$Ca_8(HPO_4)_2(PO_4)_4 \cdot 5H_2O$	1.33
α-TCP	α-Tricalcium phosphate	$\alpha\text{-}Ca_3(PO_4)_2$	1.5
β-TCP	β-Tricalcium phosphate	$\beta\text{-}Ca_3(PO_4)_2$	1.5
ACP	Amorphous calcium phosphate	$CaxHy(PO_4)_z \cdot nH_2O$, n = 3–4.5; 15–20% H_2O	1.0–2.2
CDHA	Calcium-deficient hydroxyapatite	$Ca_{10-x}(HPO_4)x(PO_4)_{6-x}(OH)_{2-x}$[f] $(0 < x < 1)$	1.5–1.67
HA	Hydroxyapatite	$Ca_{10}(PO_4)_6(OH)_2$	1.67
OA	Oxyapatite	$Ca_{10}(PO_4)_6O$	1.67
TTCP	Tetracalcium phosphate, mineral hilgenstockite	$Ca_4(PO_4)_2O$	2.0

Bioactive bioceramics maybe resorbable or non-resorbable. CaP, such as TCP are classed as resorbable ceramics as they degrade and are completely resorbed *in vivo* (Ginebra *et al*., 2006). Whereas other CaP compounds such as HA have low solubility, are more stable under physiological conditions and therefore are classed as non-resorbable although there is the potential for dissolution of the CaP system through slow ion release. HA are attractive as coatings as they have demonstrated enhanced bone apposition and maintain integration with the regenerated bone tissues after implantation compared to the resorbable TCP (Ginebra *et al*., 2006).

Bioglasses are also resorbable bioceramics and were first developed by Hench in the 1970's. Bioglasses have excellent biocompatibility as well as bone bonding ability. Typical bioglass formulations consist of the following: sodium oxide, calcium oxide, phosphorus pentoxide and silicon oxide and these formulation induce bone growth three times faster than HA (Cao and Hench, 1996). However, bioglasses have poor mechanical properties which limits their use to non-loading applications such as bone fillers in the orthopaedic and dental arenas (Jones *et al*., 2006; Rezwan *et al.*, 2006). Commerically available bioglasses include Perioglas® for the treatment of periodontitis and Novabone® used a bone filler. Release of silicon, calcium, oxygen and sodium ions contribute to intracellular and extracellular responses in addition to their chemical bonding to host bone (Xynos *et al*., 2001). Studies have shown that bioactive glasses enhance the wound healing of soft tissues due to its anti-inflammatory response (Verrier *et al*., 2004; Bendall *et al*., 1998). Bioglass performs at a higher level being osteostimulative (bone healing properties), due to its ability to stimulate growth factor production in addition to its osteoconductivity (enhanced recruitment, proliferation and differentiation properties) (Tan *et al.*, 2011; Hu and Zhong, 2009). Through chemical formulation, properties can be varied resulting in control of the resorption rate, however, increase in crystallinity reduces the level of bioactivity (Peitl Filho *et al*., 1996; Pereira *et al*., 1994).

Current investigations involve the use of composites, which are composed of biodegradable polymers reinforced with ceramic particles. The aim is to replicate the natural micro-environment and encourage the development of tissue with good mechanical properties. The composite matrix functions purely as a scaffold since the the composite degrades as regeneration proceeds (Navarro *et al*., 2005 and Navarro *et al*., 2004). Scaffolds can be either porous or dense composed of bioglasses, HA,

ACP and BCP as the ceramic component in a poly(lactic-co-glycolic acid) derived co-polymers (PLGA) or polycaprolactone matrix. Stem cells, growth factors and peptide sequences have been incorporated into the composites for tissue engineering purposes such as tissue repair and regeneration (Hardouin *et al*., 2000).

1.2 Hydroxyapatite

The bioceramic, hydroxyapatite (HA), $Ca_{10}(PO_4)_6(OH)_2$, constitutes 65% of the mineral fraction of human bone and stoichiometric HA has a Ca/P molar ratio of 1.67 (Kim *et al*., 1998). HA is crystalline and therefore, offers higher stability in aqueous media compared to other CaP compounds. However, biological apatites differ chemically to HA, in that carbonate is a major substitute in biological bone (5-8%) (Kumta *et al*., 2005) and they contain trace elements such as fluorine, chlorine, magnesium, sodium and potassium (Bertinetti *et al*., 2006). Consequently, biological bone is deficient in calcium ions (Ca^{+2}) with respect to HA and has an average Ca/P molar ratio of 1.5. The deviation from a Ca/P molar ratio of 1.67, lowers the crystallinity and increases the solubility of the CaP compound (Tampieri *et al*., 2005; Landi *et al*., 2003), whereas highly crystalline stoichiometric HA exhibits a lower solubility *in vitro* and *in vivo* (Mavropoulos *et al*., 2003).

The thermodynamic instability of HA results in the decomposition of this crystalline material into various CaP phases when processed at high temperatures (>1300 ºC) (Muralithran and Ramesh, 2000; Gross and Berndt, 1998; Gross *et al*., 1998; Zhou *et al*.,, 1993). This can lead to the formation of intermediates such as calcium oxide (CaO), octa-hydroxyapatite (OHA), α-TCP, β-TCP and tetra-calcium phosphate (TTCP) (Gross and Berndt, 1998; Gross *et al*., 1998). The presence of these

impurities in a HA material can decrease the crystallinity and subsequently, make it more prone to dissolution. Thermal degradation products including α-TCP, β-TCP, TTCP and OHA are resorbable and biodegrade more rapidly in an aqueous environment compared to pure HA (Ginebra *et al*., 2006; Ducheyne *et al*., 1990). The dissolution rate decreases in the following order: ACP>DCP>TTCP>α-TCP>β-TCP>>HA. It was demonstrated in an animal study that 99% of ACP was degraded in twenty-six weeks after implantation (Knaack *et al*., 1998). The accelerated resorption of TCP before bone ingrowth is a major problem as it undermines the stability of the implant leading to failure (Heimann and Wirth, 2006). Alternatively, it was determined that a more crystalline HA surface (75-95%) demonstrated higher stability *in vivo* with slower dissolution and better mechanical fixation after 12 weeks, suggesting a better choice for long-term mechanical and biological fixation of implants compared to a lower crystalline surface (50-55%) (Xue *et al*., 2004; Overgaard *et al*., 1999). Dekker *et al.*, (2005) reported better osteointegration as a result of a higher quality and quantity of lamellar bone formed on a crystalline CaP surface compared to an amorphous carbonated apatite surface *in vivo*. The authors hypothesised that osteoblasts were unable to maintain adhesion on the implant surface due to the resorbability of the lower crystalline surface (Dekker et al., 2005). Peraire *et al*., (2006) reported that following 6 months implantation, a thin crytalline HA coating had remained intact with no signs of dissolution or degradation. However, these studies were in agreement, that the highly crystalline HA coating is suitable for long-term implantation and the low crystalline coating has superiority in promoting faster initial bone fixation (Peraire *et al*., 2006, Xue *et al*, 2005; Overgaard *et al*, 1999).

One of the main reasons supporting the use of HA as a bone substitute material is its versatility. Along with the other documented bioactive characteristics, it can undergo thermal treatments in order to increase (or decrease) phase purity, cystallinity, HA particle size and change chemical composition (dehydration and functional group alteration) (LeGeros, 2001; LeGeros and Craig, 1993). This type of processing is usually required to varying degrees to confer HA material with desired chemical, structural and dissolution properties, to enhance its capability in an *in vivo* setting (Yang *et al*., 2007; Yang *et al*, 2005). There has been much interest in BCP for this reason. The biodegradation of the BCP can be tailored by altering the HA and TCP ratio to achieve rapid fixation and long-term stability of the implant (Steward *et al*., 2004; Overgaard *et al*., 1999).

For many years, HA has been used for the coating of orthopaedic implants due to its biocompatible properties. Commerically available orthopaedic hip protheses coated with HA includes: S-ROM® sleeve (Depuy, US); McMin® acetabular component (Corin Medical Ltd, UK); ABG® femoral stem (Howmedica, US); Omifit® acetabular shell (Osteonics, US) (Gross *et al*., 2004). To date, much investigation has been carried out regarding the use of hydroxyapatite as an osteoinductive material, with uses as both bone graft implants in the bulk form and also as a coating on metal implants. HA has shown ability to bind chemically to bone with enhanced bone apposition to implants without the formation of fibrous tissues. As a bone graft substitute, porous forms of bulk HA have been shown to induce bony apposition at the cell-biomaterial interface and to also encourage the mineralisation (Hile *et al*., 2005; Hing *et al*., 2004). There have been short- and long- term studies performed to evaluate HA as an implant material. In one study by Marcacci *et al.* they showed that

when HA was used as a bone defect filler, complete fusion between the implant and the host bone occurred five to seven months after surgery (Marcacci *et al*., 2007). In all patients, a good integration of the implant with the host tissue was maintained at the end of the investigation (six to seven years post surgery). No late fractures in the implant zone were observed. This study demonstrated the long-term durability of bone regeneration achieved by the use of HA. They concluded that the use of osteoprogenitor cells in conjunction with porous bioceramics such as HA were a viable alternative to the use of autologous bone for the repair of critical-sized long bone defects (Marcacci *et al*., 2007*)*. Extensive clinical research has demonstrated the continued fixation of HA coated orthopaedic implants over test periods (two-ten years), illustrating the beneficial properties of HA as a successful osteoconductive coating (D'Lima *et al*., 1999; Røkkum *et al*., 1999; Dorr *et al*., 1998; Donnelly *et al*., 1997). D'Lima *et al.*, (1999) followed up on Omifit-HA titanium stem in 56 patients for 2-5 years with excellent clinical and radiographic results. Subsidence was non-progressive after 1 year. Stable bone ingrowth fixation was evident at the hydroxyapatite coated part of the implant (D'Lima *et al*, 1999).

1.3 Implant Fixation

When an implant is inserted into the body, there are a number of key interactions both biological and chemical which govern events leading to the formation of bonds between the biomaterial and bone, and the ultimate integration of the implant with the host tissue. Integral to this area, a number of cellular components are involved in the formation and regulation of bone development. The interactions of osteoblasts, the bone forming cells, with the implant surface is of great importance and the

surface properties of the implant will influence this interaction process. Concurrently, there is also a series of chemical reactions that occur between the bioceramic and the physicological environment that involves dissolution and modification of the bioceramic. A number of terms commonly used to describe the fixation of the implant to bone, in addition to the different events that occur at the implant-bone interface, are summarised in the next section.

1.3.1 Fixation Terms

The process of osteoinduction refers to the recruitment and differentiation of specialised cells, osteoconduction is the bone forming process seen on the surface of hard tissue implants and finally osteointegration is the fixation or anchorage of the implant to the living tissues. The osteoconduction phase is dependent on osteoblasts formation during the osteoinduction stage and the osteointegration is dependent on the activity of these osteoblasts for the stability of the implant. Albrektsson and Johansson, offered a more comprehensive definition of these terms:

- *Osteoinduction:* Involves the recruitment of immature cells, osteoprogenitor cells and the stimulation (induction agents, hormones and inflammation response) of these cells to develop into pre-osteoblasts which then mature into osteoblasts (bone forming cells). In trauma events, such as fractures, induction agents are released to initiate the healing process (induction period) (Albrektsson and Johansson, 2001).
- *Osteoconduction:* Process by which bone grows on the surface with a provision of a scaffold, such as the case with an implant. Osteoblasts are the cells that are responsible for the synthesis, deposition and mineralisation of the extracellular matrix of the bone, described in the next section **(1.3.2).** Adhesion of

osteoblasts is considered an important step in osteoconduction (Albrektsson and Johansson, 2001).

- *Osteointegration*: Is the stable anchorage of an implant achieved by direct bone-to-implant contact. Successful integration involves the process where the implant is connected to the living tissues by the formation of bony tissue around the implant without the growth of fibrous tissue at the bone implant interface. Osteoblastic and osteoclastic activities are mainly responsible for the osteointegration of implants (Albrektsson and Johansson, 2001).

Histological sections reveal bone to implant contact of the order of 10-20 microns (μm) is only needed for osteointegration and also interfacial implant movement of more than 150 μm will inevitably lead to soft tissue formation instead of bone (Brunski, 1999).

1.3.2 Bone Formation and Remodelling

Bone is an extremely dense form of connective tissues (osseous tissues), which in its various shapes makes up the human skeleton frame. Bone has three main functions. The first is the mechanical role in the support of surrounding tissues and organs whilst providing sites for attachment for ligaments, tendons and muscles which are involved in the bodily movements. The second is its function in calcium homeostasis. Bone is a calcium reservoir which exchanges bone minerals with the fluids of the body. Finally, its role in haematopoiesis (blood cell renewal), where the bone marrow is the only source that supplies the body with the nutrient-carrying blood cells and infection fighting white blood cells (Martini, 2005). Osseous tissues contain specialised cells and a matrix consisting of 65% mineral (inorganic) and 35% organic materials. The mineral phase is largely made up of HA (crystalline calcium

phosphate). The HA provides rigidity to the organic matrix which is composed of 90% collagen and 10% non-collagenous proteins. The collagen fibers provide an organic framework on which HA is inserted. The non-collagenous proteins include osteocalcin, osteonectin and osteopontin (Martini, 2005). There are two types of bone a) the structural protective layer called compact or cortical bone and b) spongy cancelleous bone (Puckett *et al*., 2008).

The bone is regulated by four different types of specialised cells, these include osteoprogenitor, osteoblasts, osteocytes and osteoclasts. The activities of these cells are responsible for growth and development and remodelling of bone (Figure 1.1).

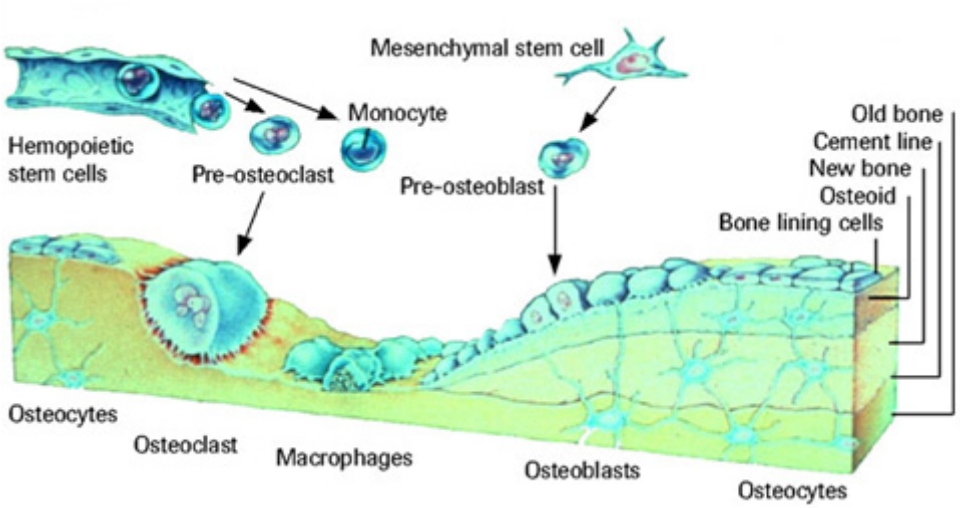

Figure 1.1: Bone remodelling process illustrating the resorption and formation of bone (Roche, 2012).

Osteoblasts are the main cells responsible for bone formation. Osteoprogenitor cells are derived from stem cells originating in the mesenchyme (tissue from which all the connective tissues are formed) (Albrektsson and Johansson, 2001). Osteoprogenitor cells lack many of the known osteoblast markers such as ALP or osteocalcin (Jäger *et al*., 2007; Boyan *et al*., 1996). External stimuli including induction agents (hormones

and growth factors) and also an inflammation response are responsible for the differentiation of the osteoprogenitor cells into pre-osteoblast and then to osteoblast cells (Jäger *et al*., 2007; Boyan *et al*., 1996). Bone morphogentic proteins (BMP) are responsible for the stimulation of stem cells into the active osteoblast.

Osteoblast cells play a vital role in the bone repair and also in success of implantation. They are responsible for synthesising bone through the production of new bone matrix in a process called osteogenesis. Osteoblasts synthesise and release organic bone matrix (osteoid), certain hormones (cytokines) and growth factors (Raggart and Partridge, 2010; Jäger *et al*., 2007*).* This is followed by mineralisation around the osteoid where the osteoblasts are responsible for elevating the local concentrations of CaP and promoting the deposition of the calcium salts in the organic matrix (Raggart and Partridge, 2010; Jäger *et al*., 2007; Martini, 2005). Alkaline phosphatase (ALP) is an important enzyme responsible for the crystallisation of the calcium salts (HA form) which leads to the subsequent hardening and calcification of the matrix (Jäger *et al*., 2007; Barrère *et al*., 2006; Martini, 2005). The osteoblasts themselves become embedded into the mineralised matrix and these mature osteoblasts are termed osteocytes. Osteocyctes are responsible for maintaining the protein and mineral content of the matrix and also participate in the repair process of damaged bone (Barrère *et al*., 2006; Martini, 2005).

Osteoclasts are cells produced by hematopoietic stem cells that remove and recycle bone matrix (Lu *et al.*, 2002). They do this by secreting acids and proteolyic enzymes that dissolve bone. This erosion process is important in the regulation of

calcium and phosphate concentrations in body fluid. In living bone, the osteoclasts are constantly removing matrix and the osteoblasts are constantly adding to it, a process called "remodelling" (Martini, 2005). This antagonistic behaviour is extremely important process in order to repair bone micro-damage that occurs during normal daily activity and also to replace bone during the growth process and following fracture injuries (Aubin, 2001). When the osteoclasts remove calcium salts faster than the osteoblasts deposit it, then the bone becomes weak leading to osteoporosis. However, dense and stronger bone results from muscular stress as a result of exercise due to enhanced osteoblast activity (Martini, 2005). Macrophages, also from the same lineage as osteoclasts, are crucial in early inflammatory phases of bone healing removing debris as a result of bone fracture and surgical implantations (McKee *et al*., 2011). Recently, specialised macrophages termed osteomacs, have been suggested to play important roles in bone remodelling such as regulating osteoblast mineralisation, stimulating osteoblast differentiation and regulating osteoclast recruitment, formation and function (Raggatt *et al*., 2008; Chang *et al*., 2008; Pettit *et al*., 2008).

1.3.3 Osteoblastic Adhesion to Implants

The success of the implantation is governed by how well the first phase of osteoblast attachment and adhesion occur. This will then lead to the subsequent osteoblast proliferation and differentiation on contact with the implant surface resulting in deposition of the bone matrix and ALP (osteogenesis process). When an implant comes in contact with a biological environment, the implant surface becomes conditioned with a layer of adsorbed protein. Osteoblasts attach themselves to the conditioned layer on the implant surface through electrostatic interactions and van der

Waals forces. Several extracellular matrix and plasma proteins, such as fibronectin and vibronectin, have been shown to mediate cell-substrate attachment (Garcia *et al*., 1999). Cell attachment to these proteins is the result of their chemotactic behaviour (adhesive properties) due to their Arg-Gly-Asp (RGD) sequence which is specific to the fixation of cell membrane receptors like integrin (Grzesik and Robey, 1994). Integrins plays an important role not only in cell-substrate adhesion but also in proliferation, cell migration and consequently cell growth and differentiation. Cell-implant adhesion activation is essential for signal transduction and regulation of gene expression for collagen and other bone proteins. The process of Ca ion influx is also activated by the cell adhesion (Anselme, 2000).

Attachment and adhesion will be indicated by morphology changes of the osteoblast cultured on the surface. Evidence of cytoskeleton organisation (lamellipodia and filopodia) will indicate the cell's ability to adhere to the surface. Extension of the plasma membrane combined with the larger surface area of a flattened cell on the surface will signify adhesion as cell spreading is an essential step in cell adhesion (Zhu *et al.*, 2004). This morphology of flattened shaped and filopodia and lamellipodia formation promotes cell migration.

1.3.4 Surface Properties that Alter Cell-Implant Interactions

The cell-substrate interaction is a critical factor in the success of the osteoblast adhesion and the subsequent osteoconduction process, and consequently the physicochemical and biological properties of the biomaterial play an important role. The specific properties of the implant's surface such as the chemistry, topography, wettability and biocompatibility can all be augmented to induce a desired cellular

response. As previously mentioned, cells do not interact directly with the naked implant's surface however, they do bind to a conditioned protein layer which is deposited after implantation. It is well established that the surface characteristics of the naked implant's surface will determine which biomolecules will be adsorbed. The composition, type, amount and conformation of this protein coated surface will consquently influence osteoblast attachment, proliferation and osteogenic differentiation (Baujard-Lamotte *et al*., 2008; Yang *et al*., 2003). Water molecules reach the implant surface first, hence, it has been hypothesised that increased wettabilty enhances interactions between the implant surface and the biological environment (Rupp *et al*., 2004). The surface chemistry of a material is influenced by the outer functional groups present and dictates which biological molecules adsorb on the surface (Keselowsky *et al*., 2004). In addition it affects the orientation and adhesion of the cells and how they form the first monolayer of tissue (Rouahi *et al*., 2006; Webb *et al*., 2000; Schwartz and Boyan, 1994). It is generally thought that hydrophilic surfaces will adsorb lower levels of a more active conformation of the bulky proteins in the conditioned layer (Baujard-Lamotte *et al*., 2008). However, it has been reported that fibronectin absorbs on both hydrophilic and hydrophobic surfaces but has a higher affinity for hydrophobic surfaces whereas albumin preferentially absorbs onto hydrophobic substrates (Roach *et al*., 2005). An increase in fibronectin was observed on Ti compared to the larger protein, albumin. The conformation of fibronectin governed the osteoblast attachment through the arginine-glycine-aspartic acid (RGD) receptor site sequence (Yang *et al*., 2003). In general, RGD-functionalised surfaces have been shown to significantly increase osteointegration (*in vivo*) compared to unmodified Ti substrates (Elmengarrd *et al*., 2005; Kroese-Deutman *et al*, 2005).

It is generally accepted that the three dimensional (3D) surface topography (shape, size and surface texture) of the implant is one of the most important parameters that influences cellular reactions (Puckett *et al*., 2008; Bigerelle and Anselme, 2005; Anselme *et al*., 2000). There is much research evaluating the osteoblast behaviour (attachment, proliferation and osteogenic differentiation) on the micro (1-10 μm) and nano (<1μm) structure of substrates (Puckett *et al*., 2008; Schuh *et al*., 2004; Cho and Park, 2003; Wennenberg *et al*., 1997). The micron range of roughness maximises the interlocking between the mineralised bone and the surface of the implant. Smoother implant surfaces induced fibrous tissue growth and implant loosening *in vivo* compared to significant osteoconductive properties of roughened implants (Schwartz *et al*., 2008; Grizon *et al*., 2002; Wennenberg *et al*., 1997). Different techniques are used to promote osteointegration such as chemical etching and sand-blasting as a means to alter the surface roughness (Schuh *et al*., 2004; Cho and Park, 2003; Wennenberg *et al*., 1997). Even though roughened surfaces were found to reduce osteoblast proliferation, increased roughness was found to promote osteogenic differentiation (expressed ALP and collagen) (Boyan, 2003; Martin, 1995). In recent studies, it has been demonstrated that cells use of the nano-topography of the surface for adhesion and that the osteoblasts aligned themselves along defined substrate morphology (Pukett *et al.*, 2008). Enhanced protein and cell binding interactions by larger surface areas/increased roughness was also confirmed using porous HA (Rouahi *et al*., 2006). Lin *et al.,* (2008) demonstrated that porous HA can interact with the stem cells and generate potent inductive substances other than BMPs, that are responsible for stimulating differentiation into osteoblasts, thereby, highlighting the osteoinductive properties of the HA material.

Cell adhesion is generally better on hydrophilic surfaces compared to hydrophobic surfaces (Zhao *et al*., 2005; Massaro *et al*., 2001; Redey *et al*., 2000). These studies suggested that a high surface energy surface (high polar content) was favorable for osteoblast adhesion as a result of better wetting characteristics (Maxian *et al*., 1993) As previsously mentioned, CaP and HA are known for their excellent osteoconductivity due to their bioactive properties. The release of calcium and phosphate ions has been linked to early bone formation *in vivo* (Arinzeh *et al*., 2005; Gosain *et al*., 2002) as well as the differentiation of osteoprogenitor cells determined by the expression of a number of different differentiation markers *in vitro* (Arinzeh *et al*., 2005 Siebers *et al*., 2004). However, it was reported that crystalline HA and a BCP mixture containing a 70/30 ratio of HA/TCP demonstrated significantly increased expression of messenger ribonucleic acid (mRNA) for ALP from osteoblasts at day six compared to the other surfaces containing BCP mixtures of lower HA content (Wang *et al*., 2004). It was suggested that the difference of mRNA expression for ALP maybe related to the differences in chemistry, surface energy and/or topography of CaP surfaces, however, no conclusive evidence was given (Wang *et al*., 2004).

1.3.5 Bone-Biomaterial Interface

When an implant is inserted into the body, a dynamic complex process between the implant and surrounding tissues is initiated. Interactions involving water, dissolved ions, biomolecules (proteins) and cells surround the implant following implantation. Bioactive materials such as HA and bioglasses can stimulate a direct bond to form between the implant and the surrounding bone, and thus enhance osteointegration. Gross and Berndt defined that bioactivity is determined by the ability of material to

invoke a crystallised carbonate apatite layer from physiological fluid (Gross and Brendt, 1998). Hench was the first to propose a bonding mechanism for bioglass and also introduced the concept that all bioactive ceramics form a 'bone like apatite layer on their surfaces in the living body and bond to bone through this apatite layer' (Hench, 1998; Cao and Hench, 1996). This is brought about through the partial dissolution of the HA coating which will increase the calcium and phosphate concentration at the local environment followed by precipitation of CaP crystals with the incorporation of the collagenous matrix and bone growth toward the implant (Sun *et al*., 2001). It has even been postulated that growth factors such as BMPs could be co-precipitated with the HA crystals onto the surface which in turn recruit cells and induce differentiation (Yuan *et al*., 1998). Later Ducheyne and Qui proposed a similar bonding mechanism for bioceramics, however they postulated the theory of ion exchange and structural rearrangement at the bioceramic-tissue interface, which leads to interdiffusion from the surface boundary layer into the bioceramic (Ducheyne and Qui, 1999). Xin *et al*., (2005) reported differences with respect to apatite formation on various porous bioceramic solids such that formation was less likely to occur on HA (low dissolution) and α-TCP (rapid dissolution) surfaces compared to other bioceramics (bioglass, glass-ceramics and β-TCP). Differences in precipitation between the *in vivo* and *in vitro* samples were also observed (Xin *et al*., 2005).

According to Dorozhkin, HA dissolution occurs through five steps which show that throughout the process of HA dissolution, the surface changes in composition forming $Ca_3(PO_4)_2$ (TCP) and $CaHPO_4$ (DCP) (Dorozhkin, 1999; Dorozhkin 1997). These two different chemical components of the surfaces take part in a dissolution

reaction (Eq 1.1-1.5). The dissolution of HA coatings increase as the porosity and surface area increase and the particle size and crystallinity decrease.

$$Ca_5(PO_4)_3OH_{(s)} + H^+_{(aq)} \leftrightarrow Ca_5(PO_4)_3(H_2O)^+_{(s)} \quad \text{(Eq 1.1)}$$

$$2Ca_5(PO_4)_3(H_2O)^+_{(s)} \leftrightarrow 3Ca_3(PO_4)_{2(s)} + Ca^{2+}_{(aq)} + 2H_2O_{(aq)} \quad \text{(Eq 1.2)}$$

$$Ca_3(PO_4)_{2(s)} + 2H^+_{(aq)} \leftrightarrow Ca^{2+}_{(aq)} + 2CaHPO_{4(s)} \quad \text{(Eq 1.3)}$$

$$CaHPO_{4(s)} + H^+ \leftrightarrow Ca^{2+}_{(aq)} + H_2PO_4^-{}_{(aq)} \quad \text{(Eq 1.4)}$$

$$CaHPO_{4(s)}{}^+ \leftrightarrow Ca^{2+}_{(aq)} + HPO_4^{2-}{}_{(aq)} \quad \text{(Eq 1.5)}$$

However, recently a mechanism to explain the bioactivity of HA was described by Bertazzo *et al*., (2005) and is based on a combination of those proposed by the Hench and Dulcheyne and Qui models. The steps involved in bone formation are presented in Figure 1.2. HA surface is solubilised (surface transformation Eq 1.1-1.5) when dissolution of the HA layer is initiated (Step 1); continuation of the solubilisation of the HA surface (Step 2) and finally equilibrium between physiological solutions and the modified surface of HA is achieved (Step 3). Step 4 involves adsorption of proteins and/or other biological moieties. Steps 5 and 6, cell adhesion and cell proliferation, followed by the osteogenic differentiation (Step 7), are the subsequent stages which lead to new bone formation (Step 8).

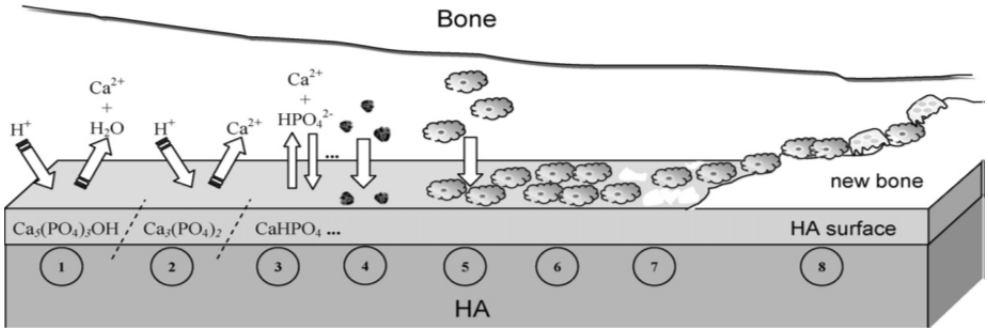

Figure 1.2: Diagram representing the phenomena that occur on the surface of HA after implantation (Bertazzo *et al.*, 2010).

The bone-implant surface is subjected to further bone ingrowth and remodelling and a biological fixation can be achieved as described earlier in **Section 1.3.2**. However, the stability associated with crysalline HA surfaces inhibits their transformation. The acid environment produced at the implantation site as result of cellular actitivity and enzymes produced can initiate the dissolution of the HA surface (Baron *et al*., 1985). LeGeros *et al.,* (2001). described the dissolution initiated by host enzymes leads to the release of calcium ions with supersaturation of ions at the interfacial region between surface and physiological solution. Subsequent precipitation of carbonated apatites can occur through seeded growth on the HA crystalline surface (LeGeros *et al*., 2001). On the otherhand, Cao and Hench postulated that a highly crystalline HA surface with low dissolution will not experience dramatic morphological change and that bone tissue will bond directly to the HA crystal through epitaxial growth (Cao and Hench, 1996).

The successful incorporation of an orthopaedic implant into the body relies heavily on the ability of the surface to conduct bone growth and bond to bone directly. This in turn allows mechanical stability of the implant and aids in its functioning by becoming an active part of the system.

1.4 Problems Associated with Hard Tissue Implants

Biomaterial selection for coating hard tissue implants poses a number of challenges, these include aseptic loosening and biofilm formation.

1.4.1 Aseptic Loosening

Aseptic loosening describes implant failure that is the direct result of loosening of the implant without the presence of infection. Aseptic loosening is a disabling condition that can affect patients 10 to 20 years following total hip arthroplasties (THA) and clinical symptoms of inflammation, impaired function and excessive pain are generally not apparent until late stages of failure (Abu-Amer *et al*., 2007; Huiskes, 1993). Revision surgergy is often neccessary to overcome this problem. According to Abu-Amer *et al*., aseptic loosening can be the result of poor initial fixation (bone-implant bonding), mechanical loss of fixation over time or biological loss of fixaton caused by particulate debris (metallic, polymeric and ceramic) inducing osteolysis around the implant (Abu-Amer *et al*., 2007). Huiskes proposed the following concept of failure scenarios for aseptic loosening of cemented and cementless implants (Huiskes *et al*., 1993):

- *Damage accumulation failure*: Is the gradual cracking of cement or coating over time as a consequence of load bearing activities and/or cyclic loading. This results in interfacial de-bonding called delamination. These will influence the long-term mechanical integrity of the implant resulting in implant failure.
- *Wear debris inflammation:* This describes particulates breaking off from the implant surface either from the coating/metal interface or metal/metal interface of the implant. The debris can migrate to the implant/bone interface and result in tissue inflammation causing bone cell death, a condition known as osteolysis.
- *Stress shielding failure:* As mentioned previously, for increased longevity of the implant the biomaterial must possess similar mechanical properties to that

of bone, if mismatches exist, alteration of the transfer of stress to the underlying tissue will result, leading to bone cell death.

- *Stress bypass failure:* Sometimes fixations in the body can be heterogeneous leading to stress transfer over the localised spots. Bone ingrowth can be patchy at the implant-bone interface and stability of the implant is weakened.
- *Growth failure:* A high frequency of micromotion of the implant relative to the bone can inhibit osseous growth giving rise to inadequate bonding as a result of gaps between the implant and bone (>3 mm). If bonding does not occur a fibrous membrane will form on the implant surface, the strength of the bonding between the implant-bone is compromised.
- *Destructive wear failure*: The dis-integration of the joint replacement prosthesis as a result of load bearing activities. The modular components of the implant gradually wear out and the mechanical integrity can no longer be maintained.

It has been reported that aseptic loosening which is a major complication and causes more that 52% of the revisions of hip arthroplasty continues to be major complication in the USA (Ulrich *et al*., 2008). The provision of a bioactive surface onto which the bone can strongly bond will successfully limit micromotions at the implant-host interface. Also the biological, chemical and mechanical attachment between an implant surface and osseous tissue has been reported to limit aseptic loosening (Dumbleton and Manley, 2004). Attachment can be achieved by positively enhancing the interactions that occur at the implant-bone interface through the deposition of bioactive coatings onto the implant surface.

1.4.2 Biomaterial Associated Infections

One of the main problems that occurs with hard tissue implant surgery is biomaterial associated infections (BAI). It has been reported that on average about 5% of initially inserted internal fixation devices become infected (Darouiche, 2004). The prevalence of infection two years after surgery was 1.63% for hips and 1.86% for knees (Huo *et al*., 2010). These infections are the result of bacterial adhesion and subsequent colonisation, leading to the biofilm formation at the implantation site (Van de Belt *et al*., 2001; Dougherty, 1998; Van Loosdrecht *et al*., 1990). The formation of the biofilm on the implant surface leads to reduced stability and ultimately its failure. The most common bacteria responsible for such infections are *Staphylococcus* species in particular *Staphylococcus aureus* (*S. aureus*) and *Staphylococcus epidermidis* (*S. epidermidis*). Common sources of BAI include contaminated implant/device surfaces, exogeneous pathogens from skin, surgical instrumentation, local environment, distant local infections in the patient (An and Friedman, 1996).

Irradicating such infections remains a challenge and BAI remains one of the most common reasons leading to revision surgery (Van Houwelingen *et al*., 2012; Huo *et al.*, 2010; Hendriks *et al*., 2004). Treatment of infections at the implant site can be complicated and the approaches routinely employed have major drawbacks. Systemic delivery of antibiotics can result in poor delivery of the therapeutic to the implantation site. The high doses required may result in systemic toxicity with associated renal and liver complications (Ruszczak and Friess, 2003; Price *et al*., 1996). Another approach is to use antibiotic-loaded biomaterials, however, this is not always the most effective treatment, as prolonged elution of low levels of the

therapeutic agents below the minimum inhibitory concentration (MIC) increases the risk of the development of antibiotic resistance (Jiranek *et al*., 2006; Amyes and Gemmell, 1997; Gold and Moellering, 1996). Resistant strains of bacteria have become more prevalent. Methicillin-resistant organisms, most prominently methicillin-resistant *S. aureus* (*MRSA*) infections were noted to increase from 16% in 1999 to 37% in 2006 and methicillin-resistant *S. epidermis* (*MRSE*) infections showed a similar increase from 11% to 15% in the same time period (Parvizi *et al*., 2009). Regarding these methicillin resistant infections as well as chronic BAI, two stage reconstruction surgery is the standard treatment consisting of the removal of the prosthesis, surgical debridement and insertion of an antibiotic loaded cement spacer (first stage). Following antibiotic therapy for a minimium of 6 weeks, the artifical prosthesis is implanted (second stage) (Van Houwelingen *et al*., 2012). Comparing single stage and two stage treatment of methicillin resistant staphlyococcus species, debridement and antibiotic therapy (single stage treatment) was successful in 37% whereas two stage procedure had success rate of 60% for total knee replacement and 75% for THR (Parvizi *et al*., 2009). While single-stage revision has had good results, two-stage re-implantation remains the gold standard for the treatment of chronically infected THA where non methicillin strains were identified as the cause (90% success rate). Inhibiting bacterial adhesion is often regarded as an alternative approach in preventing implant associated infections (Zibermann and Elsner, 2008). Therefore, there is a need for a bioceramic coating that will not only have osteointegrative properties but can also effectively resist bacterial colonisation.

1.4.2.1 Biofilm Formation

Bacterial adherence is a complex multi-step process that is influenced by the host, the device and the microbe. This complex phenomena has been simplified into the following phases: attachment, adhesion and aggregation (Gristina, 1987). However, prior to the attachment stage there is the formation of a 'conditioning film' (biomolecules) within seconds on exposure of the implant to the biological environment which suggests that the microbes adhere to the formed conditioning film and not to the bare implant surface. The initial adhesion (attachment stage) of the microbes depends on the physicochemical characteristics of the biomaterial surface, microbe cell surface and the biological fluid in the environment (Van Loosdrecth *et al*., 1990). Hetrick and Schoenfisch, summarised the process involved in biofilm formation (Hetrick and Schoenfisch, 2006). The attachment can be divided into two time dependent stages (Figure 1.3).

Phase I involves reversible cellular association with the biomaterial surface through long and short range chemical interactions, which occurs in the first 1-2 hours of implantation (Vacheethasanee and Marchant, 2000). Phase II (2-3 hours post implantation) involves a stronger adhesion mechanism through molecular bridges between the organism and the implant surface formed through specific cell surface chemical reactions (Vacheethasanee and Marchant, 2000). At this stage (24 hour post implantation), the attached microorganisms secrete an exopolysaccharide layer which anchors the biofilm and forms an outer lining of the biomaterial called 'glycocalyx' (Gristina and Costerton, 1985). The glycocalyx, in addition to anchoring the biofilm, also protects against environmental attacks and treatment with antibiotics (Isiklar *et al*., 1996; Gristina, 1987). The aggregation step involves the

colonisation of the bacteria subsequently leading to the formation of a thick film of 'slime'. Organisms on the outside of the slime may detach and give rise to septic infection (Van de Belt *et al*., 2001).

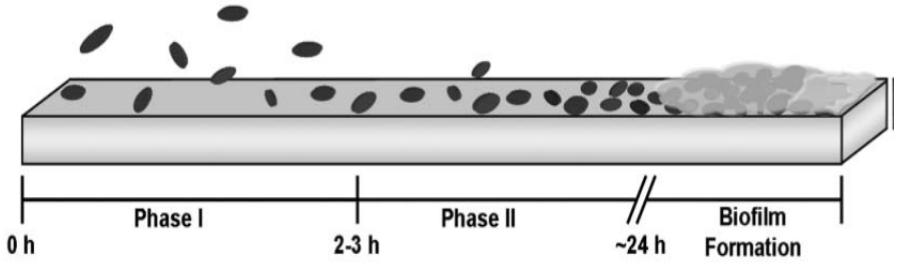

Figure. 1.3: Representation of bacterial adhesion to a biomaterial substrate (Hetrick and Schoenfisch, 2006).

1.5 Biofilm Preventative Strategies

Many different strategies have been developed to combat the incidence of BAI. Three main approaches have been developed to construct anticolonising coatings for biomedical applications: biocide releasing, microbe-repelling and contact-active anticolonising coatings. The former approach is well established and has received much research attention compared to the other strategies. However, microbe repelling and contact-active coatings are relatively new approaches and these novel methods offer potential in the treatment of infection in the orthopaedic setting.

1.5.1 Biocide Release

This involves the release of antimicrobial agents, namely antibiotics and antimicrobial metals from a matrix impregnated coating on hard tissue implants, which kills microbes at the localised site. Biocide release can be tailored to have burst and controlled release components in order to combat infection in the perioperative and post-surgical phase (Liu and Chang, 2009; Chai *et al*., 2007; Teller *et al*., 2007; Rossi *et al*., 2004; Lucke *et al*., 2003). Release proceeds through diffusion from the coating matrix or coincides with erosion of the coating matrix (Liu and Chang, 2009; Chai *et al*., 2007; Teller *et al*., 2007). Alternatively, bioglass was shown to posses antimicrobial properties as a result of the dissolution of the bioglass matrix elevating the pH at the localised site (Hu *et al*., 2009).

1.5.1.1 Antibiotic Loaded Bone Cements

The development of antibiotic loaded bone cements (ALBC) have been extensively studied since their discovery in the 1960's. These frontier materials consisting of drug loaded poly(methyl methacrylate) (PMMA) bone cements (BC) are commercially available today e.g. Simplex P (Stryker, United Kingdom (UK)) and Palacos G (Biomet, Warsaw). Alternatively, cements are also available which are vacuum-mixed with antibiotics such as ampicillin, erythromycin, colistin, cefazolin, gentamicin, vancomycin and tobramycin by surgeons and then moulded with the implant like a putty (Zilberman and Elsner, 2008). The antibiotic dosage in ALBC's for treatment of musculosketal infection can be as high as 6-8 g per 40 g BC (Springer *et al*., 2004). The release of antibiotics from BC follows a biphasic mechanism. Initial release, during the first hours after exposure of antibiotic loaded cement to a fluid, is mainly a surface phenomenon (first phase) while prolonged

release over several days is a bulk diffusion process (second phase) (Van de belt *et al*., 2000). The second phase relies on the availability of pores and connecting capillaries in the cements through which the fluids can penetrate and dissolve the antibiotics that slowly diffuse through the matrix. Factors that affect antibiotic release include antibiotic type, BC type and mixing conditions (Jiranek *et al*., 2006*).* The main advantage of BC usage is that it works in the treatment of deep infections with much clinical data to support its success (Jiranek *et al*., 2006). The disadvantages of using these materials includes (i) the presence of unreacted monomer which may cause cyctotoxic effects leading to chemical necrosis of the bone; (ii) some are non-degradable e.g. PMMA; (iii) 80% of the antibiotic has been reported to be effectively locked in the BC for many years resulting in sub-inhibitory exposure and induction of resistance in subjected strains and (iv) the mechanical strength of the BC can be compromised due to the addition of the drug and the subsequent drug release (Hendriks *et al*., 2004; Powles *et al*., 1998). Some of these problems can be overcome with resorbable bone cements such as those composed of CaP and brushite cements. The resorbable bone cement can lead to faster and more prolonged drug release, at higher concentration, with efficacy against militant bacteria strains without toxicity (Habraken *et al*., 2007; Jiranek *et al*., 2006).

1.5.1.2 Antibiotic Loaded Implant Coatings-Cementless Implants

The use of bioactive materials such as CaO, HA, TCP as drug eluting orthopaedic coatings pose a simple cementless solution for the treatment of BAI. Extensive research has been carried out to develop a simple means of impregnating the drug into the HA pores (Chai *et al*., 2007; Pham *et al*., 2002) or into the HA matrix (Teller *et al*., 2007; Stigter *et al*., 2002). *In vitro* release of antibiotics from these materials

has been reported for vancomycin, gentamicin and ciprofloxacin with no antibacterial impact beyond three days for materials loaded using a soakage method (Chai *et al*., 2007). The antibacterial assessments demonstrated inhibition of *S. auerus* after 24 hours with short loading times of 15 mins however, the authors hypothesised that efficiacy of only up to 2 days could be achieved (Brohede *et al*., 2009). The downfall associated with using these materials loaded with antibiotics through a soakage method is that a short elution profile results (1-3 days). Recent research has shown a simple 'fast-loading slow-release' mechanism of incorporating antibiotics through loading HA coated Ti surfaces in antibiotic solutions where the antibiotics (tobramycin, cephalothin, amoxicillin) chemically bind to the CaP (Brohede *et al*., 2009, Stigter *et al*., 2004).

In order to further extend the period of drug liberation, the addition of different biodegradable polymers has been employed. Biopolymers are also attractive alternatives to PMMA with the key benefit of being completely bioresorable, which eliminates the need for surgical removal. These drug delivery systems allow for increased antibiotic loading and more controllable release kinetics that can be modified by the polymer's degradation profile. Biodegradable, Food and Drug Administration (FDA) approved polyesters such as poly(lactic acid) (PLA), poly(glycolic acid) (PGA) and poly(ethlene glycol) (PEG), and their co-polymers have been manufactured into different forms (microspheres, films, beads) and are successfully used on orthopaedic devices (Habraken *et al*., 2007). These combination coatings demonstrate low burst release and a linear drug release up to 24 weeks (Zilberman *et al*., 2008), with clinical data reported in the prevention of infections on intra-medullary implants up to 6 weeks after implantation (Schmidmaier *et al*., 2006;

Lucke *et al*., 2003). Poly(hydroxy alkanoates) (PHA) have demonstrated excellent control over gentamicin release over a period of 6 weeks with bacterial eradication within 24-48 hours (Rossi *et al*., 2004). Other novel approaches use polymerisation techniques to produce drug loaded PLGA/HA microspheres (Shi *et al*., 2009) and novel polymer-drug microspheres developed with a HA shell (Xu and Czernuszka, 2008). Toxicological studies with PLGA devices suggest that local tissue reactions at the site of application may occur (Dailey *et al*., 2006; Sundback *et al*., 2005) with strong inflammatory responses after 24 months *in vivo* when composites of PLA and TCP were implanted. The degradation of the PLA was linked to the inflammatory response (Ignatius *et al*., 2001). Despite concerns that the acidic by-products of the biocompatable PLGA may denature proteins (Nair and Laurencin, 2007), it has been recently shown to release BMP-2 from PLGA based microspheres (Kirby *et al*., 2011).

1.5.1.3 Substituted Apatites

Alternatives to antibiotics have also been researched, and the use of substituted or doped apatites which can deliver the added functionality of antimicrobial surfaces to the HA bioactive surfaces. Substituted apatites are CaP materials where the Ca ion has been replaced by other cations. Investigations into the use of ions such as silver (Ag), zinc (Zn) and copper (Cu) which were incorporated into HA have shown to have a positive antimicrobial effect (Zhou *et al*., 2008; Ahmed 2006; Chen *et al*., 2006; Chung *et al*., 2006; Kim *et al*., 1998). Strontium ions, an element present in trace quantities in the mineral phase of bone has also been reported to have an antimicrobial effect *in vitro* (Lin *et al*., 2008; Guida *et al*., 2003). Of these antimicrobial ions investigated, Ag doped apatites have been the most extensively

studied. Silver has strong inhibitory and bactericidal effects aswell as a broad spectrum of activity against a wide range of pathogens (Feng *et al*., 2000b). Concerns relating to the toxicological issues surrounding systemic or local accumulation of metals have been raised (Campoccia *et al*., 2006). Several proposed mechanisms have been reported to explain the antimicrobial mode of action of the metal ions. These mechanisms include disruption of the electron transport chain, inhibition of deoxyribonucleic acid (DNA) replication, DNA cleavage, membranous disruptions, formation of reactive oxygen species and enzyme inhibition (Applerot *et al*., 2009; Zhou *et al*., 2008; Park *et al*., 2009; Feng *et al*., 2000b; Fagian *et al*., 1986; Richards, 1984; Yakabe *et al*., 1980; Bragg and Rainnie, 1975; Kasahara and Anraku, 1974).

Recently, it has been reported that Ag containing HA coatings demonstrated good antibacterial and osteogenic properties with low toxicity *in vitro* (Roy *et al*., 2012, Ruan *et al*., 2009). Good osteoblast adhesion and proliferation was observed on Ag loaded HA surfaces however it was noted that the Ag content should be limited to between 1-3% wt *in vitro* (Sandukas *et al*., 2011). The osteoconductivty of Ag containing HA coatings on Ti was evaluated in rat tibiae confirming that there was good bone formation for a 3% wt loading. However, inhibition of bone formation was observed at higher Ag loadings of 50% wt (Yonekura *et al*., 2011). Ag loaded CaP coatings have also demonstrated antibacterial activity against *MRSA in vitro* (Ando *et al*., 2010) and *in vivo* (Shimazaki *et al*., 2010) without cytotoxic effects.

1.5.2 Microbe Repelling Strategies

Microbe repelling coatings are still under development and find applications in many medical areas but to date are rarely found in the orthopaedic setting. These materials include tailoring coating properties such as surface charge and hydrophobicity by altering the surface chemistry in order to reduce bacterial attachment, thus preventing microbial colonisiation (Russell, 2009; Berry *et al*., 2000; Gottenbos *et al*., 2000).

The infection risk associated with each biomaterial varies according to the material and is determined by the interplay between adhesion and surface growth of the infecting organism. Hydrophobic polymers such as fluoroplastic coated implants for otolaryngology applications have proven to inhibit biofilm formation using *S. aureus* as the challenge organism (Berry *et al*., 2000). Research including clinical trials on a lipophilic coating, phosphorylcholine (PC), demonstrated that biofilm formation was reduced on PC coated materials compared to the uncoated material for biomedical applications (Russell, 2009; Shigeta *et al*., 2006). Other approaches used protein coatings of heparin and albumin to inhibit bacterial adhesion (Kinnari *et al*., 2005; Galliani *et al*., 1994; Nagaoka and Kawakami, 1995). Even though these biomaterials reduce the adhesion of the bacteria cells they do not exhibit bactericidal effects (Gottenbos *et al*., 2000).

Studies have concluded that the surface growth of initially adhering bacteria is influenced by the surface charge of the biomaterials (Gottenbos *et al*. 2000; Harkes

et al., 1992). A wide range of postive and negative charged polymeric surfaces were investigated (poly(dimethyl siloxane), teflon, polyethylene, polypropylene, polyurethane, poly(ethylene terephthalate) (PET) and PMMA as well as postively and negatively charged co-polymers of methacrylic acid) (Gottenbos *et al*. 2000; Harkes *et al*., 1992). The surface growth of *Escherichia coli (E. coli)* was slow or absent on positively charged surfaces due to the resultant tight binding between the bacteria and the charged surface as compared to negatively charged surfaces (Harkes *et al*., 1992). The growth of *P. aeruginosa* on biomaterial surfaces also decreased with an increasing binding strength to the surface (Gottenbos *et al*., 2000). It has been shown that when a biomaterial surface is more negatively charged, the chance of coagulase negative bacteria adhering is reduced thereby delaying the formation of the biofilm as a result of electostatic repulsion. Alternatively, positively charged surfaces are more adhesive but the strong electrostatic attraction of the organisms impedes surface growth of Gram negative bacteria (Gottenbos *et al*., 2000).

1.5.3 Contact Active Anticolonising Coatings

This novel and less established approach uses non leaching biocidal agents, which kill microbes on contact with the coating surface, without the need for release of the antimicrobial agent. 'Self sterilising' surfaces containing quaternary ammonium compounds (QAC) polycaionic materials, anchored to the implant surface through covalent bonds, exert their effects by damaging cell membranes (Murata *et al*., 2007; Milović *et al*., 2005). The permanent attachment of drugs to surfaces through the different functional groups of antibiotics (amine, carboxyl or aldehyde) which form covalent bonds or electrostatic interactions with the specific groups on the coating

has been investigated (Ginalska *et al*., 2005). In the study by Ginalska *et al*., gentamicin sulphate was covalently immobilised on a PET prosthesis and sealed with gelatin. Ninety-seven percent of the antibiotic remained bound on the biomaterial for at least 30 days. A bacteriostatic effect against *S. aureus*, *E. coli* and *P. aeruginosa* was exerted with no biofilm formation (Ginalska *et al*., 2005).

Functionality can also be introduced to the surface through the use of linkers which can then tether antibiotics to the surface through weak electrostatic or covalent interactions. Research has shown the effective use of silanes as linkers to bind drugs to Ti surfaces (Antoci *et al*., 2008; Jose *et al*., 2005). Vancomycin was coupled to a Ti surface using two linkers, 3-aminopropyltriethoxysilane and 8-amino-2,6-dioxoctanoic acid and demonstrated 88% reduction in *S. aureus* attachment compared to uncoated Ti over 2 hours (Jose *et al*, 2005). Colonisation of *S. epidermis* for 30 hours was also inhibited and the anticolonising activity was maintained following 7 repeated cycles of 24 hour incubation with the strain (Antoci *et al*., 2008). Other research has used glycol spacers in addition to silanes to link vancomycin to Ti (V) in order to functionalise the Ti surface. Anticolonising effects of up to 44 days against *S. aureus* were observed *in vitro* (Edupuganti *et al*., 2007*)*. Natural polycations such as chitosan have been immobilised onto Ti to confer antimicrobial activity on the surface through disruption of cell membrane of microbes. Coatings prepared through coupling chitosan to silanised Ti using a glutaraldehyde linker demonstrated enhanced osteoblast proliferation and antimicrobial effect against a wide range of strains for 55 hours compared to Ti (Carlson *et al*., 2008). The use of antimicrobial peptides (AmP) (Faber *et al.*, 2003) as a non-leaching material for medical devices has been developed (Ferreira *et al*.,

2008). The mode of action of AmP includes the formation of pores in the cell membrane leading to cell lysis (Tzoris *et al*., 2003) and demonstrated antibacterial, antiviral and antifungal activity (Zasloff *et al*., 2002). AmP, tethered using PEG spacer to a silanised Ti surface, was responsible for killing *E.coli* on contact (Gabriel *et al.*, 2006).

Another alternative includes immobilising antimicrobial metals in CaP coatings on implant substrates. Recent studies have shown that the catalytic action of metals in coatings has the capacity to produce reactive oxygen species which induce apoptosis (Hu *et al*., 2007). There has been some formulation development of doped apatites to reduce the elution of microbial ions (Ag^{+}) through the addition of other metals (Zn, Cu) to modify the TCP network thus reducing the rate of the material's breakdown (Matsumoto *et al*., 2009). Even though there is some elution of ions, a synergistic effect has been reported whereby the antimicrobial effect was attributed not only to the low concentrations of ions released but also to the free radical species formed by the immoblised antimicrobial metals (Matsumoto *et al*., 2009; Hu *et al*., 2007).

The advantage of using contact active anticolonising coatings includes the reduced toxicity as a result of the antimicrobial agent not being released. However, antibiotic coupled surfaces may give rise to the development of resistant pathogens (Ferreira and Zumbuehl, 2009). The synthetic preparation of polycations is cheap, they are not susceptible to degradation and do not give rise to bacterial resistance (Milović *et al*., 2005). Unfortunately, not much is known about their cytotoxicity and biocompatability *in vivo* (Milović *et al*., 2005). Synthetic polycationic compounds

with antimicrobial activity have not yet been approved by the FDA and European Medicines Agency for applications on medical device coatings whereas immobolisation of FDA approved antibiotics may have less regulatory hurdles to overcome (Ferreira and Zumbuehl., 2009). AmP are reported to be less likely to induce bacterial resistance than traditional antibiotics because they kill quickly and specificantly target the microbial membranes. However, it was also observed that the activity of the tethered AmP does not directly correspond to that of their analogs in free solution (Hilpert *et al*., 2009).

1.6 Deposition Techniques

A number of HA coating deposition techniques have been employed to confer a bioactive layer onto metallic substrates. Plasma spraying is a form of thermal spraying and is the most extensively used to generate HA coating of various thicknesses (Lombardi *et al*., 2006; Talib and Toff, 2004; Xue *et al*., 2004; Khor *et al*., 2003; Ong and Chan, 2000). It is the most common method utilised in the medical device industry, to apply HA surface coatings. These do not always lead to the ideal surface being engineered as the coating is deposited at temperatures ranging between 10,000-12,000 ^{o}C which subsequently leads to the formation of undesirable phases of CaP (Narayanan *et al*., 2008, Campbell *et al*., 2003). This results in problems with respect to coating uniformity, reproducibility and adhesion of the coating onto the substrate. (Heimann and Wirth, 2006; Gross and Berndt, 1998; Gross *et al*., 1998; Chen *et al*., 1994; LeGeros *et al*., 1991*).* As a result, research has been directed towards finding similar deposition processes that can achieve improved coating performance. These include pulsed laser deposition (PLD) (Koch

et al., 2007; Katto *et al*., 2005), radio frequency (RF) magnetron sputtering (Nelea *et al*., 2003; Long *et al*., 2002), sol-gel immersion techniques (Stoch *et al*., 2005; Weng *et al*., 2003) and electrophoretic deposition (Wang *et al*., 2002; Stoch *et al*., 2001; Ducheyne *et al*., 1990). Table 1.4 outlines the advantages and disadvantages of various techniques used to deposit a HA layer onto metals. Unfortunately, none of these techniques can provide the perfect coating due to the formation of cracks, residual stresses and secondary phases (impurities) as a result of the process conditions, which reduce the long-term coating durability leading to implant failure (Geesink *et al*., 2002).

The increased solubility associated with the formation of undesirable CaP phases produced during plasma spray processes can eventually lead to the poor direct apposition of bone and compromise the mechanical stability of the implant (Heimann and Wirth, 2006; LeGeros *et al*., 1991). Poor integration with the host tissue occurs when the coating itself delaminates over time due to the poor bonding strength of the HA onto the underlying surface or as the coating itself resorbs into the surrounding environment (Mohammadi *et al*., 2007), leading to implant failure and the requirement for revision surgery (Gross *et al*., 1998).

Table 1.4: Various techniques to deposit CaP on metal implants (Narayanan *et al*, 2008; Yang *et al*, 2005).

Category	Technique	Summary	Thick-ness	Advantages	Disadvantages
Thermal	Thermal Spraying including plasma spraying	High temperature process 10,000 -12,000ºC producing thick homogenous HA coatings.	30–200 µm	High deposition rates; low cost.	High temperatures induce decomposition; rapid cooling produces amorphous coatings.
	Sputter coating	Radio frequency (RF)-magnetron sputtering from CaP glass targets. Thin but dense HA coatings with strong adhesion and compact microstructure.	0.5–3 µm	Uniform coating thickness on flat substrates; dense coating.	Expensive; time consuming; produces amorphous coatings.
	Pulsed laser deposition	Inside a vacuum chamber, a pulsed laser beam is focused on a rotating HA target. Thin coatings with high fatigue resistance.	0.05–5 µm	Coating by crystalline and amorphous phases; dense and porous coating.	Expensive.
	Hot isostatic pressing	Hot pressing of HA granules onto titanium surface. Uniform coating.	0.2–2.0 nm	Produces dense coatings.	Cannot coat complex substrates; high temperature required; thermal expansion mismatch; elastic property differences; expensive; removal/interaction of encapsulation material.
Wet Methods	Sol-gel technique	Prepared by soaking in Ca and P gel following by a sintering process.	<1 µm	Can coat complex shapes; low processing temperatures; relatively cheap as coatings are thin.	Some processes require controlled atmosphere processing; expensive raw materials; time consuming process; post sintering process.
	Biomimetic coating	Immersion in simulating biological fluid (SBF).	<30 µm	Low processing temperatures; can form bonelike apatite; can coat complex shapes.	Time consuming; requires replenishment and a pH constancy of simulated body fluid.
Electo-chemical	Electro-phoresis	Cathodic deposition of CaP from electrolyte.	0.1–2.0 mm	Uniform coating thickness; rapid deposition rates.	Difficult to produce crack-free coatings; requires high sintering temperatures.

From a commercial standpoint, plasma spraying offers a rapid deposition approach with coatings produced at a sufficiently low cost (Ong and Chan, 2000). Controlling the deposition parameters of high temperature methods can be hard to achieve especially when considering that HA becomes unstable at temperatures above 1300 ºC (Muralithran and Ramesh, 2000). The production of reproducible coatings with uniform thickness is a common problem which in turn can lead to weakening of the HA layer. A thickness of 50-75 μm has been employed by most manufactures for commercially used orthopaedic implants (Sun *et al*., 2001). However, HA coating thickness affects both its resorption and mechanical properties. Thicker coatings usually exhibit poorer mechanical properties. Whilst the efficacy of thin coatings produced from ion beam or RF spluttered coatings is unknown (Sampathkumaran *et al*., 2001), a CaP coating thickness of 10 μm is required for good bond apposition (Narayanan *et al*., 2008).

Even in the commercial setting many of the coating methods listed would require a number of steps to be performed to prepare the implant surface before and after deposition. In many cases the surface needs to be roughened or acid etched for the HA coating to adhere to the surface of the implant (Schuh *et al*., 2004; Cho and Park, 2003; Wennenberg *et al*., 1997). Also, many techniques require a post sintering step to improve coating density, crystallinity and adhesion (bond strength). Post treatment conditions include thermal treatment for 2-5 hours at 1000-1250 °C with a heating program at 0.5-3 °C/min (Oktar *et al*., 2004). ACP crystallises generally at a temperature of 700 °C leading to a mixture of HA, TTCP and CaO (Feng *et al*., 2000a). As the process occurs at high temperature it also limits the co-deposition of

therapeutic drugs and biologics which would be destroyed or rendered irreversibly inactive (O'Hare *et al*., 2010).

There are also similar problems encountered with wet chemical methods for the application of bioactive coatings. Many steps are often required to prepare the surface for the deposition of the HA layer, which are very time consuming, expensive and complicated. In addition a post treatment step may be required (Stoch *et al*., 2005; Yang *et al*., 2005; Oktar *et al*., 2004; Weng *et al*., 2003; Wang *et al*., 2002). For this reason, very few have been commercialised.

In general, the crystallinity of HA coatings on hard tissue implants ranges from 65-75%. Crystalline HA coatings are required for long-term implantation however, lower crystallinity promotes faster initial bone fixation (Peraire *et al*., 2006; Xue *et al*., 2004; Overgaard *et al*., 1999). Irrespective of the short falls of wet chemical methods, they have great potential in producing HA materials with enhanced hydrophilicity, which will increase the osteoconductive properties of the coating. Massaro et al., (2001) reported that sol-gel coating (higher OH ion content) promoted high cell growth, greater ALP and greater osteocalcin production compared to the spluttered and plasma sprayed coating (lower OH ion concentration). Silver loaded apatites have been deposited using sol-gel, plasma, thermal spraying and ion beam techniques (Roy *et al.*, 2012; Sandukas, 2011; Yonekura *et al.*, 2011; Ruan *et al.*, 2009; Chen *et al.*, 2007b), however the same coating issues prevail.

1.6.1 CoBlast™ Process

In order to overcome the drawbacks noted for some of the methods discussed previously a novel approach using a grit blasting technique, CoBlast, has been developed. It is a novel process for the modification of active metal and active metal alloy surfaces (Ti, NiTi, CoCr, etc.) utilising existing conventional microblasting processes which are commonly used to provide a clean and roughened surface on orthopaedic implants. Derived from sandblasting, microblasting mixes fine abrasive powders with dry air, which is then propelled through a small nozzle onto the implant surface. This impact removes any unwanted debris and also provides a roughened surface. Micro-abrasive blasting is a straightforward, cost-efficient and environmentally friendly way to perform a variety of surface treatments (Schuh *et al*., 2004; Cho and Park, 2003; Wennenberg *et al*., 1994).

CoBlast uses two powders, an abrasive (e.g. alumina, apaptitic abrasive (MCD)) and a dopant (e.g. bioceramic). CoBlast is the controlled co-incidental blasting of abrasive and coating particles onto a reactive metal substrate. The process consists of either two separate flow systems or one combined flow of the abrasive and the dopant, Figure 1.5. The flow systems are microblasters which use dry compressed air to blast the abrasive and dopant powders through the respective nozzles or a single nozzle onto the surface. In the case of a dual nozzle system, both powder streams meet at the surface of the metal to be coated whereas there is a single stream of powders with a single nozzle regime.

The substrate can be stationary on a stage or fixed on a rotationary axis. The nozzles move over the substrate in the X, Y and Z directions using a computer numerical

control table. The CoBlast process is a single step process that can be conducted at ambient temperature. The abrasive disrupts the oxide layer on the metal, removes any unwanted debris and also provides a roughened surface. Concomitantly, the exposed underlying pure metal is forced to passivate, through the formation of chemical bonds with the dopant particles. The passivating substrate has a higher affinity to bond with the desired coating over the abrasive and therefore produces a unique conformal surface typically devoid of abrasive particles (O'Donoghue and O'Neill, 2009).

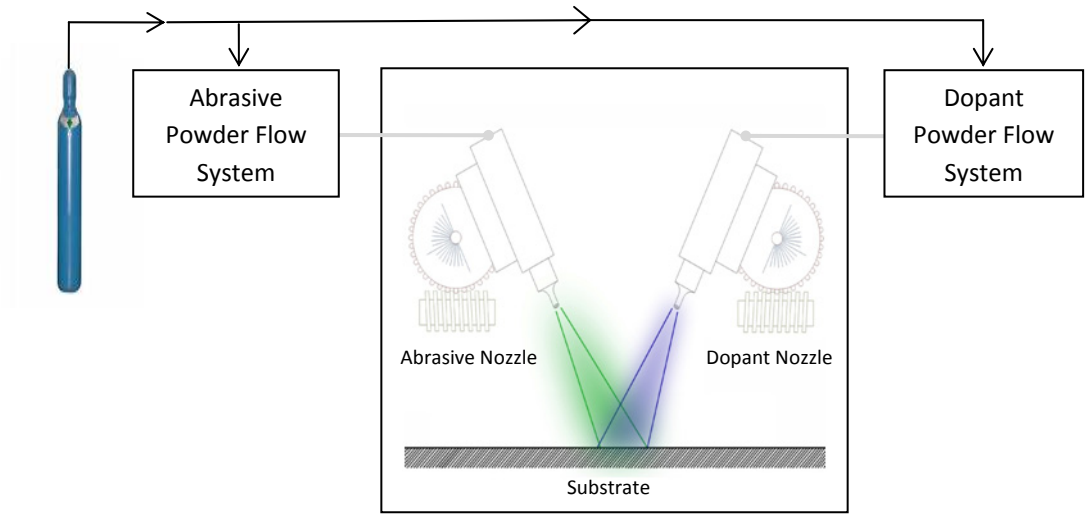

Figure 1.4: Schematic of the CoBlast process (O'Neill *et al*., 2009).

Roughening of the metal surface using the grit blasting approach, creates active sites through the removal of the metal oxide layer, which subsequently provides for impregnation, mechanical locking and chemical bonding of the dopant (O'Hare *et al*., 2010). Modifications of less than 10 μm were observed using this technology (O'Neill *et al*., 2009). Tribochemical bonding as observed by Gbureck *et al*, is believed to produce a well adhered and stable uniform coating of the dopant on the

metal using the CoBlast technology (Tan *et al*., 2012; O'Hare *et al*.,2010; Gbureck *et al*., 2003).

Research has shown the deposition of various substituted apatites (fluoro apatite and carbonate apatite) on Ti substrates (O'Neill *et al*., 2009). CoBlast HA surface demonstrated enhanced osteoblast attachment *in vitro* and early stage lamellar bone growth (O'Hare *et al*., 2010). CoBlast deposition has been seen to produce bioceramic coatings consisting of HA, bioglass and HA/Bioglass. Bioglass derived surfaces demonstrated superior osteoconductity to HA (cell attachment, proliferation and osteogenic differentiation) (Tan, *et al*., 2011). CoBlast HA surface has been compared to a plasma sprayed HA surface in *in vitro* and *in vivo* (Tan *et al*., 2012). CoBlast HA surface was less rough with slower cell proliferation but exhibited enhanced hydrophilicity, higher crystallinity, improved stem cell adhesion and attachment compared to plasma sprayed HA *in vitro*. In an *in vivo* setting, the two HA coatings demonstrated enhanced osteointegration compared to the uncoated Ti surface, however, no significant differences in the torque out force values were seen between the HA surfaces irrespective of the coating technique (Tan *et al.,* 2012).

CoBlast offers the following advantages compared to the conventional coating methods used in the orthopaedic arena, these include:

- It is a single step process carried out at room temperature and pressure. Therefore, the chemical composition of the dopant is preserved in the coating. This room temperature process also allows for the deposition of active pharmaceutical ingredients (Tan *et al*., 2012).

- It is a chemical free and therefore an environmentally friendly process (O'Donoghue and O'Neill, 2009).
- Two-dimenstional (2D) and 3D substrates can be used. The system can cater for large implants such as hip arthroplasties as well as smaller fixation implants e.g. dental screws (O'Donoghue and O'Neill, 2009).
- The deposited dopants are an integral part of the metal oxide layer and therefore no lamination of the surface modification occurs. As a result, it takes on the inherent strength of the bulk metal (O'Donoghue and O'Neill, 2009).
- Easy integration of the CoBlast system into a manufacturing environment. The single CoBlast processing step (using conventional equipment) plus cleaning replaces five steps required to obtain a HA coating using the industry standard plasma spray, the CoBlast process integrates roughening and the application of the HA in one step (O'Donoghue and O'Neill, 2009).
- Normal sterilisation such as chemical and irradation techniques can be used to sterilise CoBlast surfaces.

1.7 Objectives

The ultimate aim of this work was to develop and characterise novel coatings that will provide key benefits and added value to hard tissue implants. However, this work can be divided into three main objectives surrounding this central theme with specific research questions addressed:

1. Evaluate HA coatings deposited using CoBlast technology in *in vitro* studies.
   (i) Can the technology effectively deposit a HA layer onto Ti substrates?

(ii) How does CoBlast HA surface compare to uncoated surface in a preliminary biological study?

(iii) Can surface properties be altered or tailored into the modified surfaces?

(iv) How does the surface compare to the competing technology such as plasma spraying process?

2. Evaluate substituted apatites containing antimicrobial metals as an infection preventing strategy in *in vitro* studies.

(i) Can CoBlast effectively deposit substituted apatites?

(ii) Do CoBlast coatings of substituted apatites offer dual benefits of being anticolonising and osteoconductive?

3. Evaluation of AgA as an infection preventing surface in *in vivo* model.

(i) Do the *in vitro* and *in vivo* study results correlate?

(ii) Does the surface elicit an inflammatory and cytotoxic response?

(iii) Does the infection stay localised at the implantation site?

(iv) What improvements are seen to the anticolonising impact in an infection model using *S. aureus* as the bacterial challenge?

Chapter 2

2.0 General Materials and Methods

In this chapter, an overview of the materials and methods used are given. Figure 2.1 outlines the analysis performed on the CoBlast surfaces.

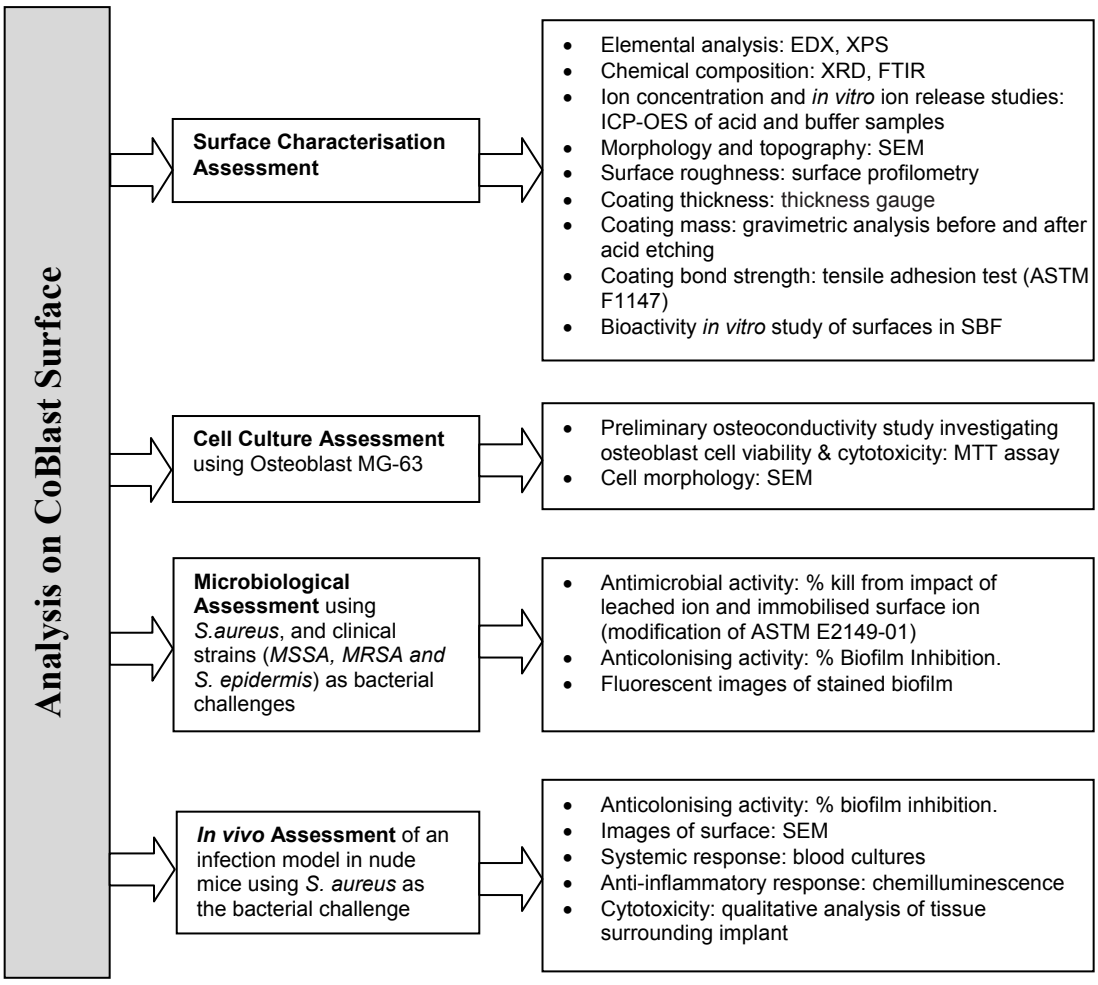

Figure 2.1: An outline of the analysis performed on the CoBlast samples (where EDX is energy dispersive X-ray; XPS is X-ray photoelectron spectroscopy; SEM is scanning electron microscopy; XRD is X-ray diffraction; ICP-OES is inductively coupled plasma optical emission spectroscopy; SBF is stimulating body fluid; MTT is 3-(4, 5-dimethylthiazol-2-yl)-2, 5-diphenyltetrazolium bromide).

Due to the different studies investigated in each chapter (**Chapters 3-7**), variations in the experimental methodology were undertaken which was consistent with the research focus of each chapter. Surface characterisation was performed to determine elemental analysis, chemical composition, surface morphology, topography, coating thickness, coating mass, the concentration of ions released from the surface, coating adhesion strength. A MTT (3-(4, 5-dimethylthiazol-2-yl)-2, 5-diphenyltetrazolium bromide) assay was performed to determine the osteoconductive potential of the surfaces in a preliminary study which investigated the osteoblast viability and cytotoxicity. Scanning electron microcopy (SEM) images of osteoblast cultured on the surfaces were taken to investigate the attachment and spreading of the cells on HA surfaces. Microbiological assessments were performed to determine the impact of the leached ion from the surface as well as the surface effect from the immobilised ion and were expressed as % kill. The % biofilm inhibition was also assessed (anticolonising study). Fluorescent images were taken to illustrate the presence of active microbial cells on sample surfaces. Finally, an infection *in vivo* model was performed to evaluate the potential of CoBlast coated implants as an infection preventing surface in nude mice**.**

Even though, this chapter outlines the materials used and methodology performed in the overall project, a brief summary of the analysis performed with details on sample numbers, time points and statistical analysis executed will be presented in the individual chapters.

2.1 Materials

Titanium (Grade 5, Ti-6Al-4V) coupons (15mm x 15mm x 1mm), were obtained from Lisnabrin Engineering Ireland. Titanium (Grade 5, Ti-6Al-4V) Kirskner wires (K-wire) 0.8 mm x 180 mm were obtained from Smantec.USA. Crystalline HA powder was sourced from Science Applications Industries, France. Silver substituted apatite (5% and 12% wt AgA), strontium substituted apatite (5% and 12% wt SrA), zinc substituted apatite (5% and 12% wt ZnA) and co-doped silver strontium substituted apatite (12% wt AgSrA) were sourced from Himed Inc. (NY, USA). The substituted apatites were described as being low crystallinity in the unsintered condition. The alumina abrasive was purchased from Comco (NY, USA). The MCD apatite abrasives (MCD-106, MCD-180 and MCD-425) were all purchased from Himed Inc. (NY, USA). The dopants (HA, AgA, SrA, ZnA, AgSrA) and the abrasives (alumina and MCD series) were all biomedical grade materials. HPLC grade 1M hydrochloric acid (HCl), de-ionised water, isopropanol (IPA), ethanol, phosphate buffer solution (PBS), potassium bromide (KBr) FTIR grade, tris (hydroxmethyl) aminomethane, sodium chloride (NaCl), sodium bicarbonate ($NaHCO_3$), potassium chloride (KCl), dipotassium hydrogen phosphate trihydrate ($K_2HPO_4.3H_2O$), magnesium chloride hexahydrate ($MgCl_2.6H_2O$), calcium chloride ($CaCl_2$), sodium sulphate (Na_2SO_4) and hydroxymethylaminomethane ($(CH_2OH)_3CNH_2$), trypsin, ethylenediaminetetraacetic acid (EDTA), MTT assay kit, ACS reagent grade dimethyl sulphoxide, paraformaldehyde, glutaraldehyde, osmium tetroxide and hexamethyldisilizane (HMDS), Luria Bertoni (LB) broth, LB agar, brains heart infusion (BHI) broth, BHI agar, acridine orange, dextrose, tryptone soya broth (TSB) and tryptone soya agar (TSA), Columbia blood agar plates and Columbia agar were all purchased from Sigma-Aldrich, UK. MG-63 osteoblast cells

were obtained from American Type Culture Collection (ATCC), (UK). Minimum Essential Medium (MEM), foetal calf serum, penicillin G sodium, streptomycin, amphotericin B were purchased from PAA Laboratories GmbH, Austria. *S. aureus* (ATCC 1448) was obtained from the laboratory of Prof. Alan Dobson at the Microbiology Department, University College Cork. The clinical isolates, *MRSA* (BH1CC), *MSSA* (BH48) and *S. epidermis* (BH1457) were sourced from Dr. James O'Gara (Microbiology Department, University College Dublin). Catheter needles (BD 16 G Pro Venflon) were sourced from Becton, Dickinson and Company, UK. Vetbond was sourced from 3M, UK. Commercially available Biorad Pastorex Staph-Plus latex (Biorad Laboratories, UK) was used as the agglutination test. Chemiluminescent kit was purchased from Knight Scientific, UK.

2.2 Sample Preparation

Prior to surface modification, the coupons were cleaned ultrasonically in 1M HCl and then in isopropanol to remove any contaminants. The HA and substituted apatites were deposited onto the titanium coupons using EnBIO's proprietary CoBlast technique according to the deposition conditions outlined in Table 2.1 for the various studies (**Chapters 3-7**). The working distance of the dopant and abrasive nozzles were approximately 20 mm and 8 mm from the surface, respectively with a speed of 13 mm/sec.

The microblast surfaces were prepared under the same corresponding conditions as above, however no HA was delivered through the dopant nozzle (**Chapters 3** and **4**). After the surface treatment step, all samples were air-cleaned for 30 seconds to

remove any loose powder from the surface. The CoBlast surfaces in **Chapters 3, 4** and **7** were ultrasonically washed in de-ionised water for 3-5 minutes. HA plasma coated Ti substrates were prepared by APS Materials, Ireland (**Chapter 4**). *The in vivo* implants in **Chapter 7** were sterilised by gamma radiation with a dose of 29.1-29.7 kGy according to EN552:1994 (British Standards Institution, 1994).

Table 2.1: CoBlast Deposition Process Conditions.

Chapter	Study	Abrasive	Dopant	Pressure (psi) Dopant/Abrasive
3	Physicochemical and biological characterisation of CoBlast HA surface	MCD-106, MCD-180, MCD-425	HA	90/75
4	A comparison of CoBlast and plasma sprayed HA coating stability following SBF immersion	Al_2O_3	HA	90/75 90/60
5	Deposition of substituted apatites with anticolonising properties onto titanium surfaces using CoBlast technology	Al_2O_3	HA, ZnA, SrA, AgA,	90/60
6	Evaluation of increased ion concentration on the antimicrobial and anticolonising properties of substituted apatite coatings	MCD-106	HA, ZnA, SrA, AgA, AgSrA	90/75
7	*In vivo* evaluation of silver substituted apatite coatings to combat infection on hard tissue implants	MCD-106	HA, AgA	90/75

2.3 Sample Characterisation

Surface characterisation can be divided into elemental and chemical analysis, *in vitro* ion release studies, physical analysis, mechanical analysis and bioactivity study in SBF. These were performed on a range of CoBlast surfaces.

2.3.1 Elemental and Chemical Composition

The elemental composition of the powders and the coatings was carried out using a Jeol JSM 5510 scanning electron microscope (SEM) in conjunction with an INCA

X-sight Energy Dispersive X-ray (EDX) spectroscopy detector (Oxford Instruments, UK). X-ray photoelectron spectroscopy (XPS) was performed using a Kratos Analytical Axis Ultra photoelectron spectrometer with a monochromated aluminium (Al Ka) X-ray source. X-ray diffraction (XRD) data was collected on a Siemens GAXRD diffractometer using CuKα1 radiation, with an anode current of 30 mA and an accelerating voltage of 40 keV. Data was collected in the range of 20 to 60 2θ degrees with a step size of 0.02 and a scan rate of 1 second per step. A Perkin Elmer Spectrum One Fourier Transform Infrared Spectrometer (FTIR) was used to determine the structural fingerprint of the powders and the coatings. The coating was scrapped off and pressed into a KBR disc (2% wt sample in KBR). The sample in KBR discs were analysed in transmittance mode with an average of 20 scans taken for each sample. A background scan of a blank KBR disc was automatically subtracted from the sample spectrum. The spectra gave approximately 70-90% transmittance however the results are presented in an overlay fashion. Powders (HA, MCD series, Al_2O_3) for FTIR analysis were prepared in a similar manner. The concentration of the various ions present in the coatings was determined by dissolving the coating in 1M HCl and analysing the solution using a Thermo IRIS Advantage Inductively Coupled Plasma Optical Emission Spectroscopy (ICP-OES).

2.3.2 *In vitro* Ion Release Studies

The study which compares CoBlast HA surface to a plasma spray HA coating (**Chapter 4**), calcium (Ca) and phosphorus (P) release from the HA surfaces into buffer were analysed using ICP-OES. Tris buffer was prepared by preparing 50 mM tris (hydroxmethyl) aminomethane and adjusting the pH to 7.4 using 50 mM HCl. Samples were placed in 20 ml tris buffer (pH 7.4) and incubated in a shaking

incubator at 37 °C and removed after time-points, 1, 2 and 3 days (n=3) for elemental analysis using ICP-OES.

For the substituted apatite coatings (**Chapters 5** and **6**), the coated coupons were placed in 20 ml PBS and incubated under physiological conditions (pH 7.4, 37 ºC and agitated at 150 rpm, n=3). The coated coupons were withdrawn from the PBS solution after day 1 and placed into fresh PBS (20 ml) and returned to incubation. This was repeated for the remaining time points. The ion release at each time point was determined using ICP-OES.

2.3.3 Physical Analysis

SEM analysis was performed using an FEI Quanta 200 Focused Ion Beam and Scanning Electron Microscope in backscattered electron mode. The high voltage was set at 10kV and an approximate working distance of 20 mm was used. Gravimetric analysis of the surface treatments deposited on Ti was used to determine the coating mass using an Ohaus DV314C analytical balance by measuring the sample before and after an acid wash (ultrasonic treatment in 20 ml 1M HCl for 10 minutes). Coating thickness was measured using a PosiTector 6000 N thickness gauge (DeFelsko, NY, USA). An average of six readings was used to determine each value. The surface roughness in nanometers (Ra, nm) and microns (Ra, µm) was measured using different profilometers. The surface roughness (Ra, nm) of the coatings was determined using a Veeco Dektak 8 Advanced Development Profiler. Measurements were taken across 5 positions of each sample in a quincunx manner at a scan length of 1000 µm over a 30 seconds time period. A 12.5 mm diameter diamond tipped stylus was employed at a force of 15 mg. The surface roughness (Ra, µm) was also

determined using a Talsurf 10 surface profilometer (Talyor Hobson, UK) on 3 random points on each sample.

2.3.4 Mechanical Analysis

The ASTM F1147 tensile test is recommended for tension testing the calcium phosphate (CaP) coatings on metal substrates, and can provide information on the adhesive strength of coatings under uniaxial stress (ASTM Standard, 2011). The test pieces used were as specified per ASTM F1147 with a substrate cross-sectional area of 5.07 cm^2 upon which the coating was applied. Adhesive FM 1000 with a thickness of 0.25 mm was placed on the coated side of the test piece. A blank piece was placed on top. Care was taken to ensure the adhesive was aligned in the centre of the surface coating. A constant force of 20 psi was applied to the assembly. The assembly was cured in an oven at 176 °C for 2-3 hours. Once cured, the assembly was removed from the oven and allowed to cool in air. Any excess glue was removed from the edges with care taken not to affect the integrity of the coating. The specimen assembly was placed in the grips of the tensile tester (Lo-Cap 2000, Tinius Olsen, UK) ensuring the long axis of the assembly coincides with the direction of the load. A tensile load was applied to each assembly at a cross head speed of 0.25 cm/min. The maximum load applied was recorded and the failing stress in MPa of adhesive bond area was determined.

2.3.5 Bioactivity Study in Stimulated Body Fluid

Simulated body fluid (SBF) was prepared according to Ohtsuki *et al.* (Ohtsuki *et al.*, 1991). The different agents were added in the exact sequence as listed in Table 2.2 and the pH was adjusted to 7.4 at 25 ºC. Samples were added to 20 ml SBF with the

coated side down as outlined by Kokubo *et al.* (Kokubo *et al.*, 2006). Samples were incubated at 37 ºC. The incubation time periods were 1, 3, 7, 14 and 30 days. At each time point, the sample was removed from the SBF and rinsed with deionised water and dried in a desiccator overnight. Samples were analysed for chemical composition, coating mass, XRD, FTIR, SEM and adhesion testing.

Table 2.2: Reagents for preparation of SBF (pH 7.4, 37 °C, 1l).

Order	Reagent	Amount
1	NaCl	7.996 g
2	$NaHCO_3$	0.350 g
3	KCl	0.224 g
4	$K_2HPO_4 \cdot 3H_2O$	0.228 g
5	$MgCl_2 \cdot 6H_2O$	0.305 g
6	1 M HCl	40 ml
7	$CaCl_2$	0.278 g
8	Na_2SO_4	0.071 g
9	$(CH_2OH)_3CNH_2$	6.057 g
10	1 M HCl	pH adjusted to 7.4

2.4 *In Vitro* Cell Culture Assessment

Prior to cell culture analysis, each sample set was steam autoclaved at 121 °C for 20 minutes. MG-63 cells derived from an osteosarcoma of a 14-year-old male were used to assess cell viability. Cells were cultured in the MEM media supplemented with 10% foetal calf serum and antibiotic/antimycotic (penicillin G sodium 100 U/ml, streptomycin 100 µg/ml, amphotericin B 0.25 µg/ml) in 75 cm^3 tissue culture flasks. Cells were maintained in a humidified atmosphere with 5% CO_2 at 37 °C and were sub-cultured when they reached confluence using 0.25% Trypsin EDTA solution to provide adequate numbers of cells for the various *in vitro* culture studies undertaken.

2.4.1 Cell Viability

MG-63 cell attachment to the various treated and untreated Ti substrates was determined after 4 hours in culture using a commercial MTT assay and employing a modified Mosmann method (Mosmann, 1983). Cells were seeded onto the samples at a concentration of $1x10^5$ cells/$cm^2$and allowed to adhere during incubation at 37 °C in 5% CO_2 for 4 hours. The MTT assay reagent was prepared as a 5 mg/ml stock solution in PBS, sterilised by filtration, and stored in the dark. An aliquot of the MTT stock solution (10% of total volume) was added to each well of a six well plate containing the samples. After 3 hour incubation at 37 °C in 5% CO_2, 200 µl of dimethyl sulphoxide was added to dissolve the formazan crystals. The solution was agitated for 15 minutes on a shaker to ensure adequate dissolution. The optical density of the formazan solutions was read by spectrophotometry using an ELISA plate reader (Tecan Sunrise, Tecan Austria) at 570 nm with the background absorbance value measured at 650 nm. The absorbance values recorded were determined to be proportional to the number of cells attached to the surface in each case. All data reported are expressed as mean ± standard deviation (SD). Sample numbers between 3-5 were used.

2.4.2 Cell Morphology

MG-63 cells were seeded onto each of the above substrates at a cell density of $5 x10^5$ cells/cm^2 in 6-well plates and were incubated for 24 hours. After cell culture, the samples were gently rinsed with PBS to remove any unattached cells and fixed in a modified Karnovsky's fixative (2% paraformaldehyde/ 2% glutaraldehyde in PBS) for 1 hour. The samples were then rinsed in PBS and post-fixed in 1% osmium tetroxide and rinsed three times with PBS. The specimens were dehydrated by

rinsing in an alcohol series (20, 30, 50, 70, 80, 90 and 95% ethanol), and finally rinsing 3 times in 100% ethanol. The samples were then were chemically dried in hexamethyldisilizane (HMDS) overnight. A 50 nm layer of gold-palladium was deposited onto the substrates using a Polaron E5000 SEM Sputter Coating Unit. The sputtering conditions used included a set voltage of 1.4 kV, with a plasma current of 18 mA (argon gas), a deposition time of 2 minutes at a vacuum pressure of 0.05 Torr. The samples were then analysed using the Jeol JSM 5510 SEM and subsequently using a FEI Quanta 200 Focused Ion Beam and SEM in backscatter electron mode.

2.5 Microbiology Assessment using *S. aureus* as the Bacterial Challenge

This is divided into antimicrobial and anticolonising studies using *S. aureus* (ATCC 1448) as the bacterial challenge**.**

2.5.1 Antimicrobial Studies using *S. aureus*

Antimicrobial testing consisted of two test methods. A modification of the ASTM standard E2149-01 protocol was used to determine the antibacterial effect of permanent, non-leaching surfaces (ASTM Standard, 2010; Murata, 2007). A second test also based on the E2149-01 standard was employed to assess the potential antimicrobial impact of eluted ions from the sample surfaces.

Growth of the *S. aureus* challenge organism was achieved by the aseptic inoculation of a discrete colony from the surface of LB agar, into 30 ml of fresh LB liquid media

and allowed to grow overnight at 37 ^{o}C in a shaking incubator at 180 rpm, to provide adequate oxygenation for abundant cell growth. Typically, overnight cultures achieved a cell density of 10^{8}-10^{9} CFU/ml, which was subsequently diluted with sterile PBS buffer to provide a standardised microbial challenge load of approximately 1 x 10^{6} CFU/ml.

2.5.1.1 Antimicrobial Activity of the Surface Ion using S. aureus

The activity of the coatings was performed on coupons following deposition (air-cleaned) and also on coupons following 30-day incubation in PBS buffer (pH 7.4, 37 ºC and 150 rpm). Coupons for assessment were sterilised by immersion in 70% ethanol and allowed to dry at a 45^{o} angle in sterile 12 well titre plates in a LAF hood. Once dry, 2 ml aliquots of the microbial suspension containing 1 x 10^{6} CFU/ml were added to each coupon containing well and the plates incubated at 37 ^{o}C in a shaking incubator at 200 rpm for 1 hour.

2.5.1.2 Antimicrobial Activity of the Released Ion using S. aureus

Coupons for assessment via the leach test were sterilised as previously described and 2 ml of freshly prepared, sterile PBS (pH 7.4) added to each coupon containing well to provide a medium for ion release. Plates were subsequently placed in a shaking incubator (150 rpm) at 37 ^{o}C for the required length of the trial period, (1, 8 and 16 days). The test volume of 2 ml was maintained during extended trial periods by making appropriate additions of PBS during the incubation period. At the end of the test period PBS containing leached ions was aseptically removed from each well. In a clean, sterile 12 well plate, 0.5 ml of the microbial challenge (2 x 10^{6} CFU/ml) was

mixed with 0.5 ml of respective leachate and the plates incubated at 37 ^{o}C, shaking at 150 rpm for a period of 1 hour.

2.5.1.3 Quantification of Antimicrobial Impacts

0.1 ml of each test sample (from leach and non leach test) was aseptically transferred to a 1.5 ml microcentrifuge tube containing 0.9 ml of sterile PBS to achieve a 10^{-1} dilution. For each sample coating, tests were conducted in triplicate. Each 1 ml solution was vortexed for 5 seconds to achieve thorough mixing and 0.1 ml was again transferred to a fresh 0.9 ml of PBS and thoroughly mixed to provide a 10^{-2} dilution. The serial dilution procedure above was repeated to produce 10^{-3} and 10^{-4} dilutions. To enumerate the microbial content of a sample, sterile, solid LB agar plates were divided into four quadrants i.e. 10^{-1}-10^{-4}. Subsequently 3 discrete 10 µl drops from a single dilution sample were added within the respective quadrant. Once dot plating of dilutions 10^{-1} to 10^{-4} had been conducted the drops were allowed to diffuse into the media by air drying in the fume hood. Dried plates were subsequently incubated overnight (in an inverted position) in a 37 ^{o}C incubator for a maximum period of 14 hours. Colonies present on the plates were enumerated and used to calculate the potential antimicrobial impact of the apatite coating and leached ion by comparison with control samples (HA coating). The results are presented as % kill (Eq 2.1) (CFU data are presented in **Appendix II** and **III**).

$$\%Kill = \frac{CFU_{HA} - CFU_{Sample}}{CFU_{HA}} x100 \qquad \text{(Eq 2.1)}$$

2.5.2 Anticolonising Studies using *S. aureus*

To investigate the potential anticolonising efficacy of the respective sample coatings, a quantitative assessment of biofilm formation was carried out at various points over a 14 day period. The approach used was based upon the previously reported method of Chae and Schraft (Chae and Schraft, 2000).

S. auerus cultivation and coupon sterilisation was carried out as previously described. To facilitate bacterial attachment and biofilm initiation, 100 µl of undiluted *S. aureus* culture (10^8-10^9 CFU/ml) was aseptically spotted onto the surface of each sample coupon in discrete wells. Plates were then incubated at 37 ^oC for 3 hours without shaking. Post incubation, coupons were gently rinsed with 10 ml sterile PBS in the laminar air flow hood to remove planktonic cells, before being placed in plate wells containing 2 ml of sterile LB media, with the coating surface facing upward. After 24 hours, and at 48 hour intervals thereafter, coupons were aseptically removed from plates, rinsed with 10 ml of sterile PBS and placed in fresh plate wells again with 2 ml LB media. At time points 1, 7 and 14 days, coupons were aseptically removed from wells and rinsed with 10 ml of sterile PBS to wash off planktonic cells. Attached organisms were then collected by swabbing the coupon surface 100 times with a sterile cotton bud, which was subsequently placed in 2 ml of sterile PBS and vortexed vigorously for 10 seconds to remove collected cells. Serial dilutions (10^{-1}-10^{-4}) of the microbial colonies of the test samples were prepared and dot plating procedure performed, as previously described. Enumeration of resultant colony growth associated with the respective coating surfaces, relative to the HA experimental control, were used to determine the % biofilm inhibition of the apatite coatings (CFU data are presented in **Appendix II** and **III**).

$$\%Biofilm \cdot Inhibition = \frac{CFU_{HA} - CFU_{Sample}}{CFU_{HA}} x100 \quad \text{(Eq 2.2)}$$

2.5.3 Fluorescence Microscopy and Biofilm Staining Studies

A qualitative approach based on acridine orange staining and fluorescence microscopy (Leica DM300 microscope with Leica EL6000 fluorescent light source, Leica Microsystems, Germany) imaging of coupon associated biofilms was also performed. The imaging approach sought to establish the validity of the quantitative data generated and to provide *in situ* visualisation of the impact of apatite coating on biofilm formation by *S. aureus.* Sample preparation involved the removal of respective coupons after 1, 7 and 14 days incubation in LB and rinsing with 10 ml of sterile PBS. Coupons were subjected to drying and heat fixing of biofilm in an oven at 105 ^{o}C for 3 minutes. A staining solution of acridine orange dye was prepared by dissolving 2 mg/ml of the dye in deionised water. A 1:100 dilution in de-ionised water was then performed and the resulting 20 μg/ml working solution was sterilised by passage through a 0.45 μm syringe filter. Two millilitres of the 20 μg/ml acridine orange stain was added to plate wells containing the heat fixed coupons, and incubated at room temperature in the dark for 5 minutes to allow nucleic acid and stain interactions sufficient time to occur. Coupons were subsequently removed from the solution and rinsed with sterile PBS, air dried and stored in the dark at room temperature.

2.6 Microbiology Assessment using Clinical Isolates as the Bacterial Challenge

Similar methods to **Section 2.5** were used. However, in this study clinical isolate organisms *MRSA* (BH1CC), *MSSA* (BH48) and *S. epidermis* (BH1457) are the bacterial challenges and different recovery methods were used.

2.6.1 Antimicrobial Studies using Clinical Isolates

The antimicrobial behaviour of the samples was assessed using a modified ASTM standard E2149-01 protocol, which was used to determine the antibacterial effect of the released ions from the sample surfaces (ASTM Standard, 2010). A second test also based on this ASTM standard was used to assess the activity of antimicrobial agents immobilised on the surfaces. The modified methods have been detailed previously (O'Sullivan *et al.,* 2010).

Standard overnight cultures of the clinical isolate organisms *MRSA* (BH1CC), *MSSA* (BH48) and *S. epidermis* (BH1457) were prepared in 30 ml of fresh BHI broth and allowed to grow overnight at 37 °C in a shaking incubator at 150 rpm when typical cell density values of 10^8–10^9 CFU/ml in BHI broth were reached. The cultures were subsequently diluted with an appropriate volume of sterile PBS buffer to provide a standardised microbial challenge load of approximately $1x10^6$ CFU/ml.

Coated coupons were sterilised using 70% ethanol and were then placed in 2 ml sterile PBS in a 12-well plate and incubated for 7, 14 or 30 days (pH 7.4, 150 rpm, 37 °C). The test volume of 2 ml was maintained during extended trial periods by

making appropriate additions of PBS during the incubation period. At the end of the test period, PBS containing leached ions (leachate) was aseptically removed from each well. In a clean, sterile 12-well plate, 0.5 ml of the microbial challenge was mixed with 0.5 ml of respective leachate and the plates were incubated at 37 °C, followed by agitation at 150 rpm for a period of 1 hour (n=3) to assess the efficacy of the leachate at each timepoint. The amount of viable bacterial cells present in the above test samples were quantified using a standard dot plate counting of serial culture dilutions on BHI agar (O'Sullivan *et al.,* 2010). The results were presented as % kill determined from Eq 2.1.

The antimicrobial activity of the immobilised ion on the coating surface was assessed before (day 0) and after an incubation period of 7, 14 or 30 days in 2 ml PBS. The coated coupons were removed from the PBS at each time point and sterilised using 70% ethanol. Once dried the coupons were challenged by incubation with 2 ml aliquots of the clinical isolate suspension containing approximately 1 x10^6 CFU/ml for 1 hour (37 °C, 150 rpm, n=3). The dot plating procedure of the serial dilutions on BHI agar was performed to quantify the number of living cells present in the samples (O'Sullivan *et al.,* 2010). The results were presented as % kill (Eq 2.1).

2.6.2 Anticolonising Studies using Clinical Isolates

Further anticolonising tests were performed using the clinical isolates *MRSA*, *MSSA* and *S. epidermis* in BHI broth to investigate the potential to inhibit biofilm growth on the sample surface. The same anticolonising test procedure was performed as described earlier with similar wash procedures adhered to. However, a simpler

ultrasonic method was used in this case to collect the attached bacterial cells from the coupon surface. After incubation in BHI broth at day 1, 7, 14 and 30 days, the coupons were removed and washed with 10 ml sterile PBS. The washed coupons were then placed in a sterile vial containing 5 ml PBS and ultrasonicated for 10 minutes. Enumeration of the attached bacterial cells was again conducted using serial dilutions (10^1 to 10^4) of the microbial colonies and the dot plating procedure. Data was presented as % biofilm inhibition for each of the apatite coatings with respect to the HA control (Eq 2.2).

2.7 *In Vivo* Assessment

The *in vivo* model and analysis in this study was based on previous studies (Adams *et al.*, 2008, Antoci *et al.*, 2008; Van Wijngaerden *et al.*, 1999). The species chosen for the *in vivo* study were nude mice. Four coated Ti (V) K-wires (0.8 mm x 8 mm dimensions) were surgically implanted subcutaneously into each mouse with 12 mice studied per material type. An inoculum of bacteria was introduced and the mice were sacrificed after 2 days. The implants were removed and the % biofilm inhibition was determined. SEM analysis was performed on the K-wires post incubation for presence of bacteria colonisation (1 implant from each mouse). Blood samples were collected to indicate possible systemic infection and the presence of key inflammatory markers.

2.7.1 Bacterial Challenge

S. aureus ATCC 1448 was cultivated in 5 ml of tryptone soya broth (TSB) supplemented with dextrose (1.5%) and incubated with agitation (250 rpm) at 37°C

for 16 hours. Bacterial cells were harvested by centrifugation (1200 rpm for 4 minutes), washed once and re-suspended in sterile saline. The suspension was diluted to a concentration of 1.5 x 10^8 CFU/ml as determined by adjusting the suspension to 0.5 McFarland using a densitometer. After further adjusting the suspension to 4 x 10^7 CFU, ten-fold serial dilutions were made to obtain a suspension containing approximately 4 x 10^5 CFU/ml of *S. aureus*, prior to inoculation of 250 µl into the host.

Each nude mouse (approximately 22 g) was anesthetised through inhalation of nitrous oxide, oxygen and isofluorane in a closed tank. The sterilised catheter needle (loaded with the coated implants) pieced a hole in the back of the mouse and was used to create a channel subcutaneously to all four limbs. The implants were deployed at the intended site using a wire through the needle. Through the same point of entry 250 µl of 4 x 10^5 CFU/ml inoculum was introduced. Upon exiting cyanoacrylate (vetbond) was used to seal the incision. Each mouse was placed back in containment and the procedure was repeated for the remaining mice. One coating type was used per mouse and the coating type was assigned to each mouse by random sampling.

After two days of husbandry, the mice were euthanised by placing each animal in a closed tank containing CO_2. Cardiac puncture was performed to obtain blood samples for blood culture and free radical analysis. Two 1 ml aliquots of whole blood were collected in a sterile tube containing EDTA as an anticoagulant.

2.7.2 Anticolonising Activity

To estimate the number of non-attached bacteria, each retrieved implant was rolled onto a Columbia blood agar plate, incubated at 37ºC for 24 to 48 hours and colonies counted. To quantify adherent bacteria, the K-wire was transferred into 2 ml of TSB, sonicated for 7 minutes, and vortexed for 3 minutes. One hundred microlitres of this solution was plated on tryptone soya agar (TSA), incubated at 37 ºC for 24 to 48 hours and colonies counted. Ten-fold serial dilutions were made and plated on TSA, incubated as above, and colonies counted (Adams *et al.*, 2008, Antoci *et al.*, 2008). The CFU data from the diluted samples was used to determine the % biofilm inhibition. The % biofilm inhibition was determined for 5% wt and 12% wt AgA relative to the HA control. It was noted that some samples following explantation did not show CFU on the agar plates on which the samples were rolled. This suggests that the inoculum did not reach the biomaterial's surface resulting in successful colonisation. To avoid discrepancies in the results, samples that showed <100 CFU on the rolled agar plate were omitted from the results. SEM images were taken of the samples to investigate bacteria attachment. Samples were prepared using the fixation method as outlined in **Section 2.4.2.**

2.7.3 Blood Cultures

Quantitative whole-blood culture was performed using a pour plate method described previously by Wain *et al.* (Wain *et al.*, 1998). Briefly, a 1 ml aliquot of blood was mixed with 19 ml of molten (50 °C) Columbia agar in a sterile Petri dish, allowed to set, and then incubated at 37 °C. Colonies were enumerated after 2 to 4 days and expressed as CFU/ml.

2.7.4 Chemiluminesence Test

Initially, reagents pholasin (10 mg/l), adjuvant K, formyl-methionyl-leucyl-phenylalanine (fMLP) (10 μmol/l) and phorbol 12-myristate 13-acetate (PMA) (10 μmol/l) were reconstituted as recommended by the manufacturers' instructions and added to appropriate wells of a white 96 well plate (n=4). Whole blood samples were diluted 100 fold in blood dilution buffer to give a concentration of $1.6x10^7$cells/ml. Approximately 10 μl of the cell suspension was added to each well, incubated at 37 ^oC for 40 minutes, throughout which chemiluminescence was measured using a luminometric plate reader (FLUOstar OPTIMA, BMG LABTECH, UK), after which fMLP was added to each well by automated injector to stimulate activation of the leukocyte surface. Following that peak in activation, PMA was injected (70 minutes) to stimulate extracellular leukocyte degranulation. Controls were included, which consisted of identical incubations as described previously in the absence of material, to deduce the amount of cell activation inherent in the assay materials and procedures. In addition, incubations in the absence of both cells and material were performed to confirm the absence of background luminescence from pholasin and verified that increases in the observed chemiluminescence were a function of the excitement of pholasin by leukocyte secreted ROS.

2.8 Statistical Analysis

In **Chapters 3-7**, statistical analysis was performed using IBM SPSS 19 software. For two group comparison, a 2 sample independent t-test was performed whereas a statistical one way analysis of variance (ANOVA) was performed on three or more groups to determine statistical differences between samples ($p<0.05$). Post-hoc

analysis used included Dunnett's test and Tukey honest significant difference (HSD) test. In Chapter 6, equivalent non parametric tests were conducted. Non parametric tests performed included Mann-Whitney U test for two group comparisons (p values <0.05 was significant) and Kruskal-Wallis test was conducted for three or more group comparisons. Where a significant difference of $p<0.05$ was obtained (Kruskal-Wallis test), Dunn's test was performed. Details of statistical analysis performed and significant levels identified are given in each chapter.

2.9 Other Analysis

In **Chapter 3**, various powders were analysed for chemical and elemental analysis as described above. In addition, particle size analysis was performed using a laser light technique (Mastersizer S, UK).

Chapter 3

3.0 Physicochemical and Biological Characterisation of CoBlast HA Surface

Results and discussions published in *Coatings* (2011), 1(1): 53-71.

Abstract:

Hydroxyapatite (HA) coating of hard tissue implants is widely employed for its biocompatible and osteoconductive properties as well as its improved mechanical properties. Plasma technology is the principal deposition process for coating HA on bioactive metals for this application. However, thermal decomposition of HA can occur during the plasma deposition process, resulting in coating variability in terms of purity, uniformity and crystallinity, which can lead to implant failure caused by aseptic loosening. In this study, CoBlast, a novel blasting process has been used to successfully modify a titanium (Ti) (V) substrate with a HA treatment using a dopant/abrasive regime. The impact of a series of apatitic abrasives under the trade name MCD, was investigated to determine the effect of abrasive particle size on the surface properties of both microblast (abrasive only) and CoBlast (HA/abrasive) treatments. The resultant HA treated substrates were compared to substrates treated with abrasive only (microblast) and an untreated Ti. The HA powder, apatitic abrasives and the treated substrates were characterised for chemical composition, coating coverage, crystallinity and topography including surface roughness. The results show that the surface roughness of the HA blasted modification was affected by the particle size of the apatitic abrasives used. The CoBlast process did not alter the chemistry of the crystalline HA during deposition. Cell proliferation on the HA surface was also assessed, which demonstrated enhanced osteoblast cell viability compared to the microblast and blank Ti. This study demonstrates the ability of the CoBlast process to deposit HA coatings with a range of surface properties onto Ti substrates. The ability of the CoBlast technology to offer diversity in modifying surface topography offers exciting new prospects in tailoring the properties of medical devices for applications ranging from dental to orthopaedic settings.

3.1 Introduction

HA, a proven bioceramic for coating medical device implants is widely known, not only for its biocompatible and osteoconductive properties, but also for its increased mechanical properties when applied to bioinert metals for orthopaedic use, as previously mentioned in **Chapter 1** (Borsari *et al.,* 2005; Oh *et al.,* 2005; Stoch *et al.,* 2005; Lu *et al.,* 2004). Implant surface modifications are often required in order to prescribe a particular surface roughness and increase surface area for osteoblast attachment, as well as to enhance the bioactive and osteoconductive properties of the underlying substrate. Such surface treatment methods include sand- or grit-blasting using abrasives, chemical treatments and deposition of calcium phosphate (CaP) coatings (Gil *et al.,* 2007; Nakada *et al.,* 2007; Stoch *et al.,* 2005; Oh *et al.,* 2005; Stoch *et al.,* 2001; Lu *et al.,* 2004; Abron *et al.,* 2001; Wennerberg *et al.,* 1997).

Abrasive blasting involves impacting the implant metal surface with abrasive particles under pressure to roughen the surface. Roughening orthopaedic and dental implants utilising alumina (Al_2O_3) abrasives is a common practice to enhance implant osteointegration *in vivo* (Abron *et al.,* 2001; Wennerberg *et al.,* 1997). However, the use of apatite abrasives are often preferred as it enhances bone formation (Nakada *et al.,* 2007; Mano *et al.,* 2002). It has been shown that this technique can be effective in depositing a thin layer of CaP on the surface being roughened (Mano *et al.,* 2002; Ishikawa *et al.,* 1997). A number of other HA coating deposition techniques have been employed to confer a bioactive layer onto metallic and other inert substrates including plasma spraying, which is one of the most common types of coating process for the generation of CaP thin films (Li *et al.,*

2009; Heimann and Wirth, 2006; Oh *et al.,* 2005; Lu *et al.,* 2004; Gross and Berndt, 1998; Gross *et al.,* 1998; Weng *et al.,* 1997; Chen *et al.,* 1994). Other deposition techniques include PLD, RF magnetron sputtering, sol-gel immersion and electrophoresis as summarised in Table 1.3. However, there are a number of problems associated with these deposition techniques as outlined in **Section 1.6** (expensive, time consuming, crystallinity, reproducibility etc.).

More recently, a novel approach using the blasting technique CoBlast has been shown to deposit HA and substituted apatites onto Ti substrates (O'Hare *et al.,* 2010; O'Sullivan *et al.,* 2010; O'Neill *et al.,* 2009). The CoBlast technique is based on the convergent flow of an abrasive and a dopant stream onto the implant surface which can effectively impregnate the metal with the dopant material (**Section 1.6.1)**. HA coatings prepared using the CoBlast technique demonstrated enhanced osteoblast attachment *in vitro* and early stage lamellar bone growth *in vivo* compared to microblast and untreated Ti surfaces (O'Hare *et al.,* 2010). The established research showed that less than 10 μm thick coatings were applied with this technique employing alumina as the abrasive and that there was no evidence of alumina being incorporated into the modified surface (O'Hare *et al.,* 2010). Previous studies using the CoBlast technique used slightly different processing conditions.

In this study, a series of apatitic abrasives (sintered CaP) under the trade name MCD, were used in both the microblast and the CoBlast (dopant/abrasive regime) techniques to modify Ti surfaces. These MCD abrasives included MCD-106, MCD-180 and MCD-425 which corresponds to the grade of MCD with d(90) particle size values of 106, 180 and 425 microns respectively. The controls used included those

prepared with the abrasive only (microblast) roughening technique and also an untreated Ti substrate (blank Ti). Chemical composition and coating coverage of these substrates were examined with a view to determining the effect of abrasive particle size on the properties of the modified surfaces. The osteoblast cell viability was assessed using MG-63 cells on surfaces modified using the CoBlast and microblast surface modification approaches and also on a blank Ti sample.

3.2 Materials and Methods

Materials and methods used for work carried out in this chapter are outlined in **Chapter 2**. The various powders (HA, MCD-106, MCD-180 and MCD-425) used in this section were characterised for median particle size using laser light technique (n=3 samples), elemental and chemical composition (EDX and FTIR) and crystallinity (powder X-ray diffraction (PXRD)). HA coatings were deposited onto Ti substrates using MCD apatitic abrasives of various particle size and the modified surfaces were subsequently analysed for elemental and chemical composition (EDX, FTIR), crystallinity (XRD), surface morphology (SEM), surface roughness (Taylor Hobson profilometer (n=3 samples)), coating thickness (PosiTector thickness gauge (n=3 samples), coating mass (gravimetric analysis before and after acid etching the surface (n=3 samples)). Sample modifications prepared using CoBlast HA/MCD-106 and microblast MCD-106 and the blank Ti were evaluated for cytotoxicity and osteoconductivity using cell culture analysis at days 1 and 5 (MTT assay (n=4 samples)) and SEM image analysis of the cultured cells on HA surfaces.

Statistical analysis was performed on the surface roughness and the MTT data. One way analysis of variance (ANOVA) was performed to determine if significant differences existed between samples ($p<0.05$). Where a significant difference was obtained, multiple comparisons of surface response were performed using Tukey's post-hoc analysis (surface roughness (Ra)) and Dunnett's test in the case of samples compared to the HA control (MTT assay). Significant levels of $p<0.05$ and 0.001 were observed for statistical analysis using the Tukey's post-hoc analysis.

3.3 Results

3.3.1 Chemical Characterisation of HA and MCD Abrasive Powders

The particle size of the HA and MCD abrasives were measured using a laser light technique (Mastersizer S), Table 3.1.

Table 3.1: Median particle size analysis and EDX analysis of the powders (n=3 samples). Median particle size values are reported as ±2 x standard deviations (2SD).

Powder	Median particle size (μm)	O % atm	P % atm	Ca % atm	Ca/P ratio
HA	40 (±8)	71	11	18	1.66
MCD-106	44 (±4)	72	10	18	1.76
MCD-180	124 (±12)	73	10	17	1.73
MCD-425	355 (±12)	77	10	13	1.29

The median particle size (d(0.5)) increased in the following order: HA<MCD-106<MCD-180<MCD-425. The various powders were analysed for their chemical composition using energy dispersive X-ray (EDX) analysis, Table 3.1. The calcium

phosphate powders (HA and MCD abrasives) were found to be composed of oxygen (O), phosphorous (P) and calcium (Ca). The Ca/P ratio for stoichiometric HA was found to be similar to the previously reported value of 1.67 (Kim *et al.,* 1998). The increase in Ca/P ratio for MCD-106 and MCD-180 as seen in Table 3.1, suggests the presence of impurities. However, the Ca deficient nature for MCD-425 results in a reduced Ca/P ratio (1.29).

Relative crystallinity of each powder was investigated using PXRD, (Figure 3.1). HA was found to be highly crystalline with well defined narrow peaks. The main characteristic peaks associated with HA can be assigned to the 002, 102, 210, 211, 112, 300 and 202 reflections corresponding to 25.9°, 28.1°, 28.9°, 31.9°, 32.2°, 33.1° and 34.1°, as previously reported (Kim *et al.,* 1998).

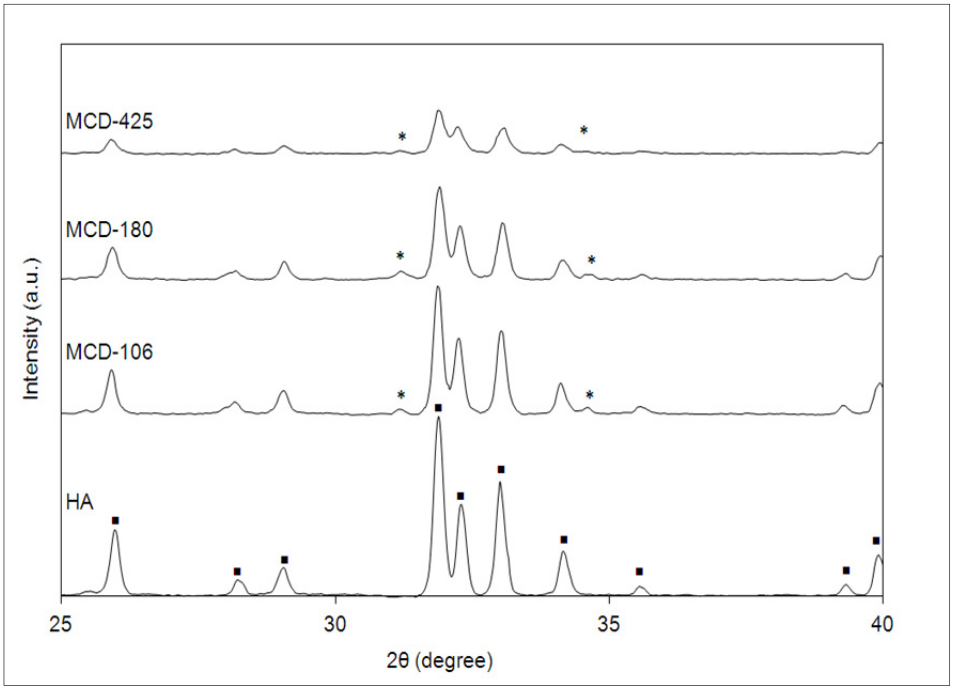

Figure 3.1: PXRD spectra of the powders (■ denotes HA peaks and * represents TCP).

The resulting PXRD patterns for the MCD apatite series indicate a lower crystallinity relative to the HA powder. A small peak present at 31.0° and 34.4° was attributed to the TCP phase (Fathi *et al.,* 2008). Also in the MCD-425 pattern, peaks are poorly resolved with low intensity relative to the other apatites, demonstrating the more amorphous nature of this material (Fathi *et al.,* 2008; Kim *et al.,* 1998).

The Fourier transform infrared spectrometer (FTIR) spectra of the powders in the range 1600-450 cm^{-1} are presented in Figure 3.2. The most intense peaks observed for the crystalline HA powder are those attributable to vibrations of the PO_4^{3-} groups; the ν_1 and ν_3 phosphate bands in the region of 900-1200 cm^{-1} and ν_4 absorption bands in the region of 500-700 cm^{-1}, which are used to characterise apatite structure. The peak at 962 cm^{-1} is assigned to the ν_1 symmetric P-O stretching vibration of the PO_4^{3-} and the ν_3 asymmetric P-O stretching mode are indexed at 1090 and 1045 cm^{-1}. The bands at 601 and 571 cm^{-1} are assigned to ν_4 vibration mode of the phosphate group, which occupies two crystal lattice sites (O-P-O bending mode) according to previous studies (Varma and Babu, 2005). The HA adsorption bands of the ν_1 and ν_4 of the PO_4^{3-} groups determined here are those of stoichiometric HA (Hong *et al.,* 2007). The bands at 631 and 474 cm^{-1} correspond to the vibrations of OH^- groups in the structure (Varma and Babu, 2005). The MCD series showed similar finger-print bonds for calcium phosphate bonds but with broader definition, which is representative of the increased amorphous content of these CaP materials (Pleshko *et al.,* 1991).

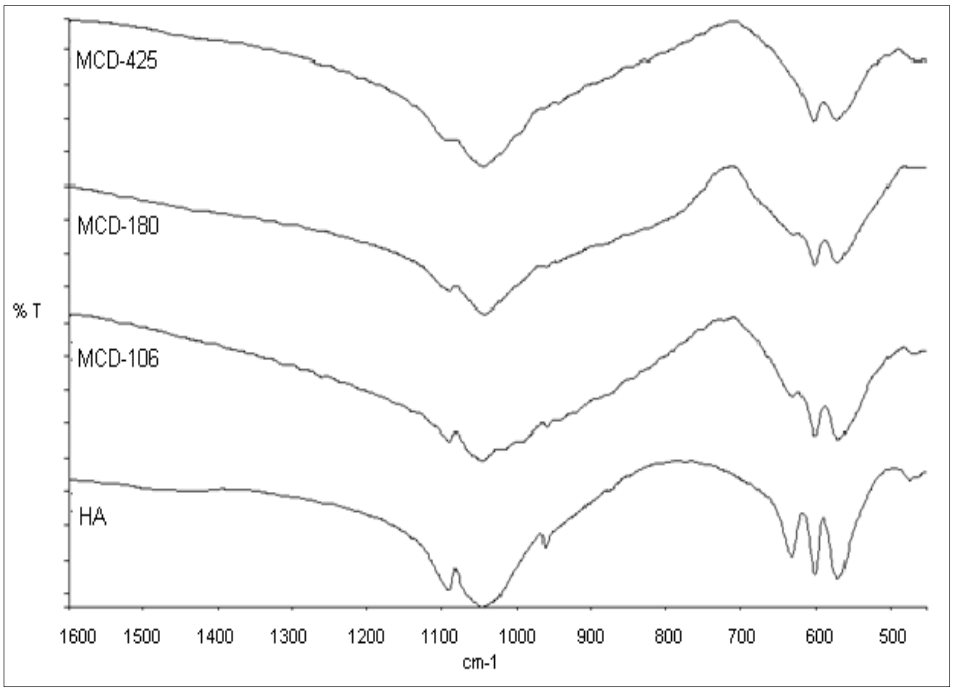

Figure 3.2: FTIR spectra of the various apatite powders.

3.3.2 Characterisation of the Modified Titanium Substrates

Ti (V) was used as the base substrate and the untreated Ti surface was determined to contain 23% O and 77% Ti using EDX analysis. The chemical composition of the microblast surfaces (abrasive blast only, no dopant) are presented in Table 3.2 and were analysed for O, Ca, P and Ti only.

The % atm Ti determined reflects the exposure of the underlying substrate and can be used to represent the degree of coverage resulting from apatite materials. A high Ti level represents a thin or patchy coating and conversely, a low Ti concentration signifies a thicker coating. The EDX results reveal that after a wash treatment, the MCD microblast surfaces show a reduction in Ti concentrations to 21-27% atm, and the presence of Ca and P which are the main constituents of the MCD abrasive. This illustrates that a thin coating of Ca/P material has been blasted onto the surface and

successfully deposited as a stable layer onto the Ti surface. The Ca/P values obtained for the microblast samples treated with the MCD series of the abrasives ranged between 1.53 and 1.57 which is consistent with similar grit blasted studies (Mano *et al.,* 2002).

Table 3.2: EDX analysis, coating thickness (PosiTector thickness gauge) and coating mass of the modified surfaces (n=3 samples).

Modification	Identification	O % atm	P % atm	Ca % atm	Ti % atm	Ca/P	Coating Thickness (μm) (±2SD)	Coating Mass (mg/cm^2) (±2SD)
Blank	Ti	23	-	-	77	-	0	-
Microblast	MCD-106	59	8	12	21	1.56	3±1	-
	MCD-180	56	6	10	27	1.53	3±1	-
	MCD-425	55	7	11	27	1.57	3±2	-
CoBlast	HA/MCD-106	63	13	21	2	1.59	6±3	0.48±0.4
	HA/MCD-180	67	12	18	3	1.53	6±1	0.44±0.4
	HA/MCD-425	65	12	20	5	1.61	7±3	0.44±0.3

The chemical composition of the CoBlast surfaces (blasting with both abrasive and dopant) on Ti are also presented in Table 3.2. For CoBlast coatings, the levels of O, P, Ca and Ti obtained were determined to be in the range of 63-67%, 12-13%, 18-21% and 2-5% atm, respectively. The reduced level of Ti detected in these samples, compared to the Ti substrate and microblast surfaces, is indicative of a high degree of coating coverage across all CoBlast samples. The Ca/P values were found to display a ratio of between 1.53 and 1.61, which are relatively close to the value for stoichiometric HA (Kim *et al.,* 1998). The % atm Ti, determined using EDX analysis, was observed to increase as the MCD series particle size order increased,

indicating a decrease in the thickness of the deposited layer, as outlined in Table 3.2. This suggests that the smaller the particle size of the MCD abrasive the more HA was deposited, although the coating thickness determined using the PosiTector thickness gauge, and the coating mass values were found to be similar. The coating thickness of all the CoBlast samples was <10 microns which is in agreement with a previous study which used Al_2O_3 as the abrasive (O'Neill *et al.,* 2009).

The SEM image of the untreated Ti substrate can be seen in Figure 3.3 (a) which has similar topography to that observed in a previous study (Abron *et al.,* 2001). This image reveals a very smooth surface and the morphology of a machined metal. The SEM images of the microblast MCD-106 surfaces, as well as the corresponding CoBlast HA/MCD-106 surfaces, are presented in Figure 3.3 (b) and (c), respectively (More images can be seen as supporting information in Appendix I). As expected, the microblast process was observed to roughen the untreated Ti surface. Examination of the CoBlast surfaces suggests that the co-introduction of the HA with the abrasive appears to have in-filled some of the surface features that are evident on the microblast surface and also shows the presence of coarser deposits.

(a)

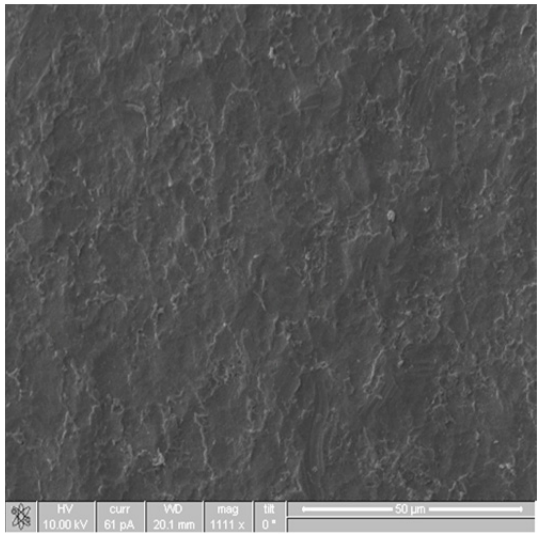

(b)

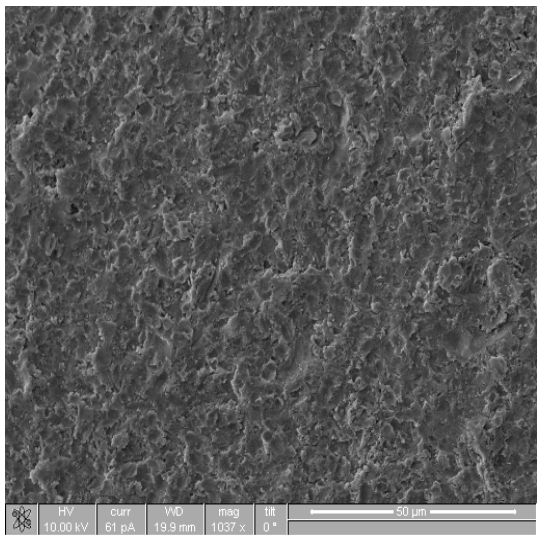

(c)

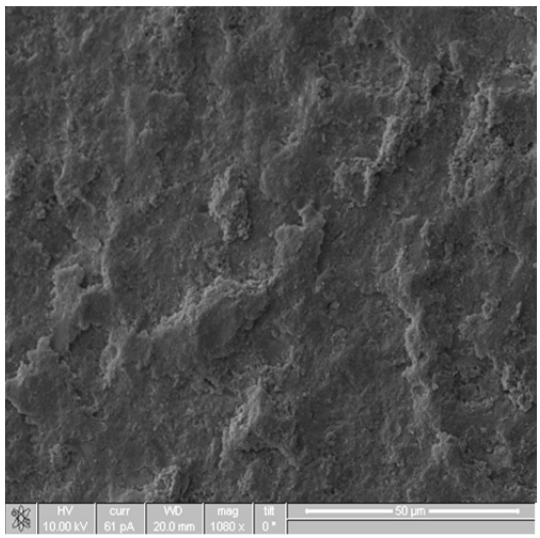

Figure 3.3: SEM images (x1000 magnification): (a) untreated titanium; (b) microblast MCD-106; (c) CoBlast HA/MCD-106.

The surface roughness was measured using a stylus method and the results obtained are given in Figure 3.4. The arithmetical mean roughness (R_a) was used as a measure of the surface roughness, which tended to increase as the particle size of the abrasive increased. Significant differences were observed between the surface treated and the untreated Ti. The average surface roughness of the blank Ti (0.4 μm) increased to 0.5, 0.8, 1.4 μm when MCD-106, MCD-180 and MCD-425, respectively were employed for microblast treatments. It has been previously reported that an increase in surface roughness was observed with the introduction of HA with the Al_2O_3 abrasive using the CoBlast technique and the same trend was observed here on the introduction of HA with the MCD abrasives (O'Hare *et al.,* 2010).

Statistical significant differences were noted between all samples analysed ($p<0.05$) using one way ANOVA and multiple comparisons between all samples were analysed using Tukey's post-hoc test. All treatments were observed to be significantly rougher compared to untreated Ti with the exception of the microblast surface using MCD-106. Microblast treatment prepared using MCD-425 was found to be statistically rougher compared to all microblast surfaces examined in addition to the blank Ti ($p<0.001$). The introduction of HA to MCD-425 resulted in a significant increase in surface roughness compared to all surfaces analysed ($p <0.001$) with the exception of the microblast treatment using the same abrasive (MCD-425). There were statistically differences between the CoBlast HA surfaces using abrasives MCD-106 and MCD-180.

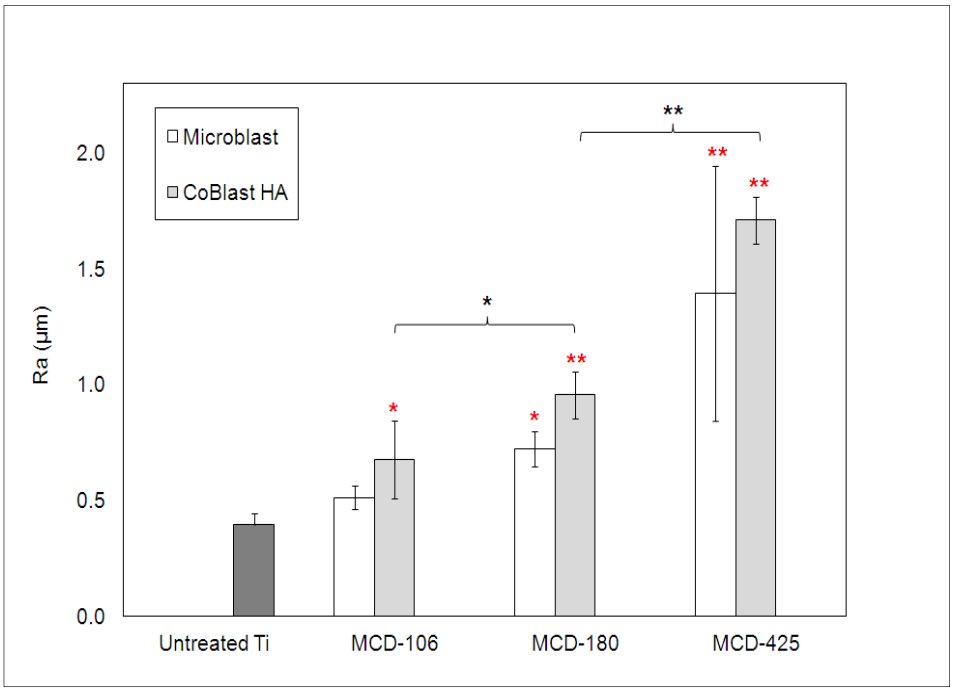

Figure 3.4: Surface roughness (R_a) of the various modifications (n=3 samples ±2SD). Statistical significance was determined using Tukey's post-hoc analysis (* denotes $p < 0.05$ and ** ascribes $p < 0.001$ between the sample and the untreated Ti whereas * denotes $p < 0.05$ and ** ascribes $p < 0.001$ between the CoBlast samples indicated).

Figure 3.5 shows the XRD pattern of the CoBlast HA coated substrates. Due to the thin nature of the deposited material and the interference of the background Ti metal, detailed analysis of the XRD profiles was not possible. However, for the CoBlast substrates, the peaks detected clearly correspond to that of HA powder employed. The additional 2θ peaks observed at 35.3° and 38.5° were assigned to the Ti substrate. No evidence of the TCP phase was detected (31.0° and 34.4°), which suggests that no compositional or crystallographic changes occurred to the HA powder during the blasting process, with negligible uptake of the abrasive, which is in keeping with previous studies (O'Hare *et al.,* 2010).

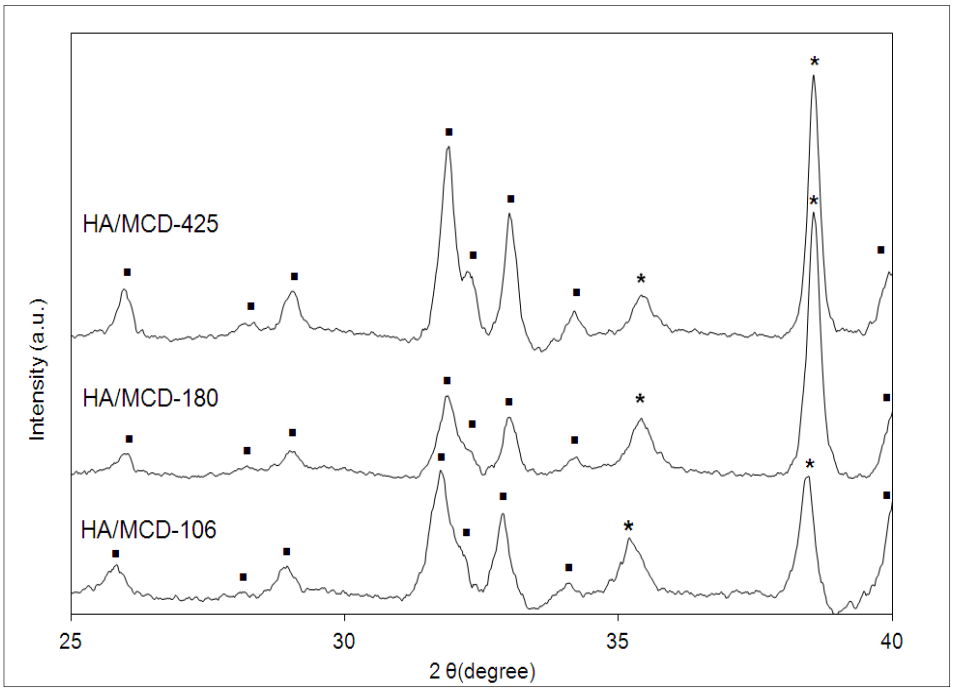

Figure 3.5: XRD of the CoBlast HA modifications (■ denotes HA peaks;*denotes Ti peaks).

Figure 3.6 shows the FTIR spectrum in the range 1600-450 cm^{-1} for the HA coated substrates. The FTIR spectra for all CoBlast HA coatings irrespective of the abrasive used are very similar and display the characteristic features of the HA powder used, as discussed earlier. There was no evidence of hydration (broad banding at 3450 cm^{-1}), further demonstrating a pure HA coating has been deposited. Also, the position of the characteristic peak at 962 cm^{-1} represents a highly ordered, non-carbonated apatite and indicates a highly crystalline material (Hong *et al.,* 2007). The banding assignments are in agreement with those of the HA powder as seen in Figure 3.2 suggesting that the chemistry is retained during the deposition process. This also supports the XRD analysis discussed above, which suggests that there has been minimal uptake of the abrasive powders during sample preparation.

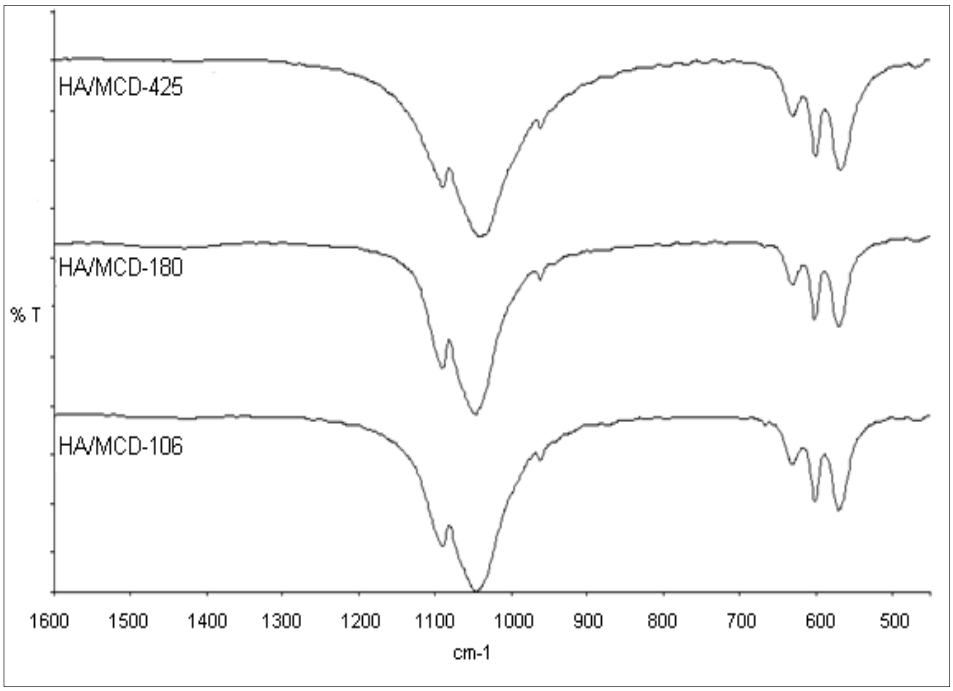

Figure 3.6: FTIR analysis of the CoBlast HA surface modifications.

3.3.3 Cell Culture Analysis

3.3.3.1 Cell Proliferation and Cytotoxicity

Cytocompatibility of the modified surfaces was determined via an MTT assay and the osteoblast proliferation results are presented in Figure 3.7. Microblast and CoBlast surfaces prepared using the MCD-106 abrasive were selected for comparison. There was no significant difference in the cell viability between samples analysed at day 1. However, at day 5 a significant difference ($p<0.05$) between samples was noted using the one-way ANOVA. Comparison between groups at day 5 using Dunnett's test indicated that there was a significant difference between the CoBlast surface and both the blank Ti and the microblast surface ($p<0.01$) whereas the difference between the blank Ti and microblast surfaces was not significantly different ($p>0.05$). No evidence of cytotoxicity was observed using MG63 cells on any of the samples evaluated.

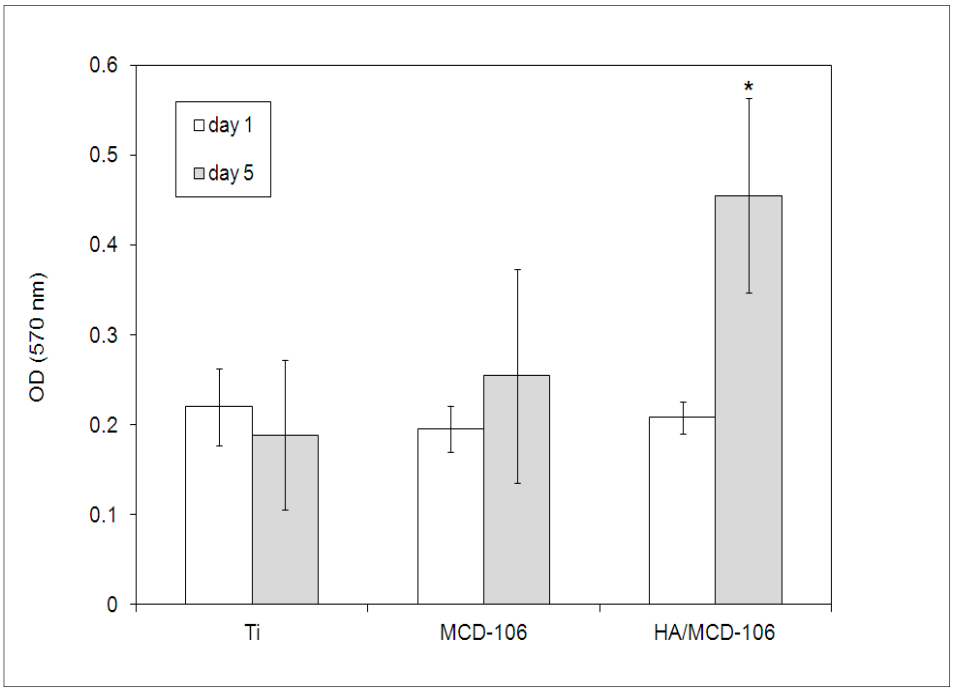

Figure 3.7: MTT assay data for MG-63 cells on modified Ti surfaces over 5 days *in vitro* (*ascribes statistical difference between the CoBlast (HA/MCD-106) surface and the blank Ti and the CoBlast (HA/MCD-106) and the microblast (MCD-106) surface at day 5 ($p<0.01$) determined using Dunnett's test) (n=4 samples ±SD).

3.3.3.2 Cell Morphology

Figure 3.8 shows various images of MG63 cells that were cultured on the untreated Ti substrates (Figure 3.8 (a)), microblast MCD 106 surface (Figure 3.8 (b)) and CoBlast HA/MCD-106 (Figure 3.8 (c)) after 24 hours. Cells attached well to the untreated Ti surfaces and displayed a fibroblastic morphology synonymous with that of this osteoblastic cell line. The cells are typically polarised in one direction with the average cell length measuring roughly 76±30 μm (n=15) (Figure 3.8 (a)). Furthermore, lamellipodia and filopodia extensions (cytoskeletal organisation) from the main body of cells onto the surface are observed. The presence of these processes suggest good cell-substrate interactions where the cell is actively probing for specific

topographical features and connects the cell to the substrate (via filopodia) from the lamellipodia, which is the protrusion of their leading edge indicative of cell spreading and migration. However, the presence of numerous spherical cells indicates that not all cells are actively involved in spreading and migration. The cells cultured on microblast surface (Figure 3.8 (b)) display morphologies similar to that observed on the untreated Ti surfaces.

Figure 3.8 (c) shows an image of MG-63 cells cultured on the CoBlast after 24 hours, it can be seen that these differed from those of the untreated and microblast Ti in terms of morphology where they had a polygonal shape rather than a polarised fibroblastic morphology indicating increased cell spreading. The cells also tended to align to the surface features created by the addition of the bioactive layer, which was earlier observed to increase the surface roughness (Figure 3.4). An abundance of lamellipodia and filopodia were present on the CoBlast surface. The addition of a HA coat to the Ti surface, resulted in a higher order of cell spreading and cell focal adhesion attachment compared to the microblast surface (Figure 3.8 (b)).

(a)

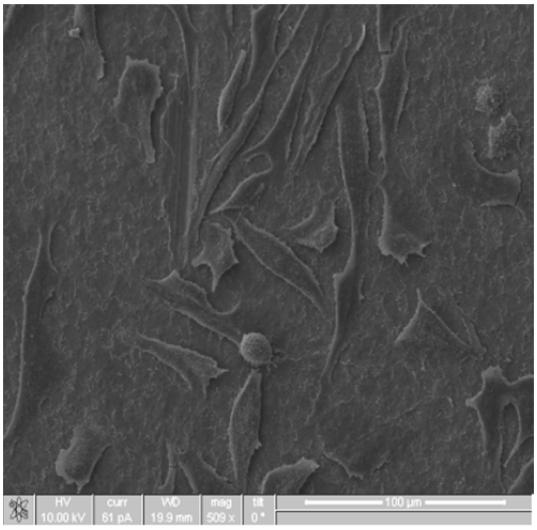

(b)

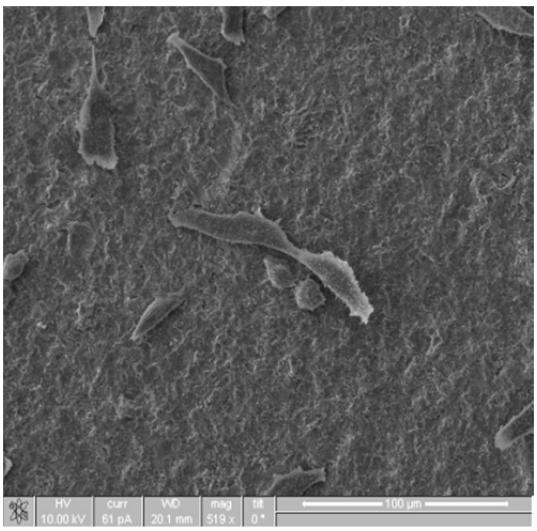

(c)

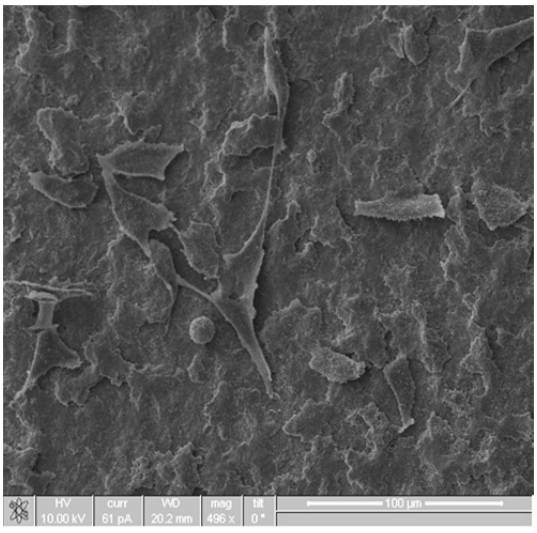

Figure 3.8: MG-63 osteoblasts cultured for 24 hours on (a) untreated Ti and (b) microblast MCD 106 treatment and (c) HA/MCD-106 surfaces (CoBlast treatment) (x 500 magnification).

3.4 Discussion

Implants with rougher surfaces result in a higher removal torque force and demonstrate excellent osteointegration when compared to those with smoother surfaces (Wennerberg *et al.,* 1997). As seen in this study, microblasting offers increased roughening of machined Ti substrates as expected and the use of MCD abrasives results in the deposition of a thin coating layer of calcium phosphate. Furthermore, the roughness of the microblast process can be tuned between 0.5-1.4 μm depending on the particle size of the apatite abrasive employed (Figure 3.4). This is consistent with previously studies (Abron *et al.,* 2001; Wennerberg *et al.,* 1997). Unfortunately, the coatings deposited using this microblast process have demonstrated poor adhesion to the metal and have not been widely employed as final surface treatments for this reason (O'Hare *et al.,* 2010).

For the CoBlast samples, the tribochemical bonding which results from surface roughening, activation and subsequent bonding of the powder to the substrate has been shown to improve the HA bonding to the Ti (O'Hare *et al.,* 2010; O'Neill *et al.,* 2009). The deposition of HA via the CoBlast process combines the benefits of increased roughness and enhanced deposition of a bioceramic coating, the bioactive property of which can improve osteointegration compared to the microblast surfaces (Figure 3.4 and Table 3.2). The surface treatment effect was also dependant on the particle size of the abrasive, with the larger particle size producing greater surface erosion and a rougher topography resulting in reduced coating thickness as evidenced by an increase in % atm Ti (EDX analysis).

In literature, HA coatings deposited using the standard high temperature plasma spray deposition technique have been reported to contain a variety of crystalline phases and the presence of altered chemical functionality (Chen *et al.,* 1994). This can lead to the formation of intermediates such as calcium oxide (CaO), octa-hydroxyapatite (OHA), α-tricalcium phosphate (α-TCP), β-tricalcium phosphate (β-TCP) and tetra-calcium phosphate (TTCP) (Gross and Brendt, 1998; Gross *et al.,* 1998). The presence of these impurities in a HA modified surface can decrease the crystallinity and subsequently make it more prone to dissolution. The increased solubility of these phases can eventually lead to the poor apposition of bone and compromise the mechanical stability of the implant (Heimann and Wirth, 2006). This can occur when the coating itself delaminates over time due to poor bonding strength of the HA onto the underlying surface or as the coating itself resorbs into the surrounding environment (Mohammadi *et al.,* 2008).

CoBlast demonstrated the ability to deposit a well adhered HA coating with no major evidence of contamination with additional CaP phases. This is in contrast to the variety of crystalline phases and the presence of altered chemical functionality produced during the standard high temperature plasma spray deposition process. The XRD and FTIR analysis does not suggest formation of any such impurities within the CoBlast samples indicating that the HA coating on the CoBlast samples has retained the same properties as the starting crystalline HA powder employed (Figures 3.1, 3.2, 3.5 and 3.6). Therefore, it is anticipated that HA modified surfaces prepared using CoBlast should not exhibit the problems associated with the presence of impurities observed for HA modified surfaces deposited using standard high temperature plasma spray as outlined above.

Osteoblasts are the key cells involved in the osteoconduction process. The success of the implantation is strongly influenced by how well the first phase of the attachment and adhesion of these cells will occur, which will then lead to the subsequent proliferation and osteogenic differentiation upon contact with the implant surface. CoBlast surfaces deposited using alumina abrasives have exhibited excellent osteoblast attachment and proliferation *in vitro* compared to their respective controls (O'Hare *et al.,* 2010; O'Neill *et al*., 2009). Here the introduction of the bioactive HA layer through the CoBlast process using apatitic abrasives was shown to offer significantly higher levels of cell viability after 5 days compared to the untreated Ti and microblast surfaces which is attributed the combination of surface topography (increased surface roughness) and bioactive surface chemistry. It was noted that the cell proliferation on the modified surfaces were all roughly comparable at 24 hours.

Surface modification techniques are extremely important for evoking desired cellular responses through tailoring the implants surface properties. The osteointegration process is greatly enhanced by these modifications, which in turn increases the longterm success of the implant. As previously mentioned, HA is well known for its osteoconductive properties and its ability to influence cell adhesion and interaction at the implant-host interface. It is generally accepted that alongside chemical compatibility, the three dimensional surface topography (shape, size and surface texture) of the implant also influences early tissue response. The cells appeared to follow the contours of the MCD blasted surface where they would sit in the defects on the surface and align themselves along grooves or dents in a process referred to as 'contact guidance'. An increase in the surface roughness (determined to be 0.4, 0.5 and 0.7 μm for the blank Ti, microblast MCD-106 and the CoBlast HA/MCD-106,

samples respectively) of the samples coincided with enhanced cell contact with the CoBlast substrate. This has important consequences as contact guidance effect has commonly been associated with increased cell proliferation and differentiation (Anselme, 2000).

Research has proven that early controlled osteoblast alignment was demonstrated on patterned substrates (Pukett *et al.,* 2008). Therefore, due to the patterned nature of the HA surface after CoBlast treatment, a more favourable surface resulted for cell spreading which subsequently lead to increased cell viability compared to the microblast and blank Ti surfaces. *In vivo* evaluation of CoBlast substrates prepared using an alumina abrasive have already demonstrated early stage lamellar bone growth (O'Hare *et al.,* 2010), however this study demonstrates the capacity to enhance bone-implant contact *in vivo* by employing differing grades of MCD abrasive in the CoBlast process to achieve greater control over surface topography. Further *in vitro* evaluations such as dissolution studies and bioactive studies in stimulated body fluid must be investigated to support these capabilities.

3.5 Conclusions

Detailed surface studies have shown that the combination of an apatite abrasive and a HA dopant in the CoBlast process produces surfaces with a combination of optimised apatite chemistry and controlled surface structure. The CoBlast process has the ability to retain the chemistry of the starting HA material. This offers advantages over conventional high temperature plasma processing which alters the HA material from its desired chemical, structural and dissolution requirements for its

use as an *in vivo* implant material. The study also shows that employing MCD abrasives offer an alternative to alumina for deposition using CoBlast process. *In vitro* studies clearly show that increased roughness of treated surfaces favours enhanced cell viability and the CoBlast process offers the ability to tailor the surface texture to produce an optimised surface for osteointegration of a HA modified implant. Enhanced cell viability was observed for CoBlast modified surfaces compared to the microblast surface. The ability of the CoBlast technology to offer diversity in modifying surface topography is clearly shown in this and previous studies and represents foundation work, which supported by bioactivity studies and *in vivo* trials, offers exciting new prospects in tailoring the properties of medical devices for applications ranging from dental to orthopaedic settings.

Chapter 4

4.0 A Comparison of CoBlast and Plasma Sprayed HA Coating Stability Following SBF Immersion

Results and discussion submitted to Surface Coatings and Technology

Abstract:

Hydroxyapatite (HA) coatings were applied to titanium substrates using either a blasting technique known as CoBlast or the traditional plasma spray method. The coatings were compared after incubation in simulating body fluid (SBF) using standard *in vitro* techniques and the results were interpreted in view of chemical, mechanical and biological properties of the coatings. The data strongly suggests that the presence of additional phases in the plasma coating limits the chemical, structural and mechanical stability of the surface. The CoBlast surface was shown to produce a more uniform and crystalline structure that produced excellent coating adhesion, lower dissolution and higher levels of mechanical and chemical stability in SBF and which resulted in higher levels of osteoblast proliferation *in vitro.*

4.1 Introduction

HA is widely used and well established as a biocompatible coating on metallic implants (Tanzer *et al.*, 2001; Furlong and Osborn, 1991; Geesink, 1989). Numerous studies have clearly shown that the presence of a HA coating on hard tissue implants encourages osteoblast proliferation (Rosa *et al.*, 2003; Massaro *et al.,* 2001), facilitates early bone fixation (Vani Vasudev *et al.*, 2004; Burr *et al.*, 1993) and provides positive outcomes during clinical trials (Hansson *et al.*, 2008; Oliver *et al.*, 2005; Cross and Parish, 2005; Geesink, 2002).

At present, HA deposition is dominated by plasma spraying and most orthopaedic companies offer some version of plasma HA. Despite the clinical success seen to date (Oliver *et al.*, 2005; Cross and Parish, 2005; Røkkum *et al*., 1999; Dorr *et al*., 1998), significant issues exist which can limit the effectiveness of plasma deposited coatings (Gross *et al*., 2004; Geesink*.,* 2002; LeGeros *et al.,* 1991). In particular, the plasma HA adhesion can be adversely affected by coating quality (Sun *et al.*, 2001). This is generally reflected in significant variations in mechanical (Dalton and Cook, 1995), structural (Xue *et al.*, 2004) and chemical properties (Heimann, 2006) of the coatings. Despite these problems being well known for some time (Chang and Khor, 1996; Søballe and Overgaard, 1996) these issues still persist. Furthermore, the compatibility of plasma processing with the trend towards porous three dimensional surface finishes is questionable, as the thick plasma coatings have a tendency to in-fill and block the pores (Hayashi *et al.*, 1994).

This has led to numerous attempts at producing an alternative HA surface deposition technique which would retain the benefits of the HA material without compromising the uniformity of the coating. Electrochemical deposition (Wang *et al.*, 2006) has been one of the more successful approaches and Stryker Orthopaedic (New Jersey, USA) have launched a number of products using this coating approach (Hansson *et al.*, 2008). However, these processes are based on wet chemical processing with all the inherent complications and difficulties therein associated. Other researchers have investigated dry processes for depositing HA (Ishikawa *et al.*, 1997). Apatitic grit blasting with sintered apatites and CoBlast process, which combines both abrasive and dopant (HA) (O'Sullivan *et al.*, 2011; O'Hare *et al.*, 2010) have also been discussed earlier in **Section 1.6.1.**

In this Chapter, HA coating surfaces deposited by the CoBlast technology are compared to a standard industrial plasma HA coating using *in vitro* responses. The chemical stability, mechanical adhesion and bioactivity of the HA coatings are examined over time in simulated body fluid and the results used to elucidate *in vitro* cell proliferation results. The surface changes are discussed with reference to detailed surface characterisation studies.

4.2 Materials and Methods

Various analytical techniques were employed to determine the surface properties of the two HA surfaces (CoBlast and plasma sprayed surfaces): elemental and chemical composition (EDX (n=3 samples); XRD, FTIR) physical analysis: coating mass (gravimetric analysis (n=3 samples); surface roughness (Ra, n=3 samples); surface

topography (SEM); ion release (ICP-OES) and mechanical analysis (ASTM F1147 (adhesion test), n=3 samples). The surface roughness in nanometers and microns was measured using different profilometers (Veeco Dektak 8 Advanced Development Profiler, n=3 samples) and Talsurf 10 surface profilometer (Taylor Hobson, n=3 samples). *In vitro* ion release studies were performed as outlined in **Section 2.3.2**. Surfaces were incubated for 1, 3, 7, 14 and 30 days in SBF to determine the bioactivity of the two HA surfaces (n=3 samples) (**Section 2.3.5**). Surface analysis (EDX, XRD, FTIR, SEM) were performed on the surfaces following SBF immersion. The ASTM F1147 tensile test was also performed on the surfaces post incubation in SBF (ASTM Standard, 2011). Cell proliferation and cytotoxicity studies at day 1 and 5 using a MTT assay (n=4 samples) and cell morphology of the cultured osteoblasts on the surfaces were executed.

A statistical one-way analysis of variance (ANOVA) was performed to determine statistically significant differences between the sample types ($p<0.05$). Where significant differences were found, Dunnett's test was used to compare the sample data to those of the untreated Ti samples (MTT assay) and multiple comparisons between all samples were analysed using Tukey's post-hoc test (surface roughness (AFM)). Comparison between the CoBlast HA and plasma HA surfaces was performed using the independent 2-sample t-test (tensile bond strength), with significance level of $p<0.05$ noted.

4.3 Results

4.3.1 Surface Characterisation

Chemical analysis of the untreated titanium (Ti), CoBlast HA coated Ti and plasma HA coated Ti was carried out via EDX and the results are shown in Table 4.1. For both the CoBlast and the plasma HA surfaces, the surfaces contained high levels of calcium (Ca), phosphorous (P) and oxygen (O), which are typical of an apatite rich surface. Titanium was detected on the CoBlast but not on the plasma HA surface, indicating that a thicker coating was applied using the plasma process. Ca/P ratios were obtained for these processes which are close to stoichiometric HA (1.67) (Kim *et al.*, 1998).

Table 4.1: Chemical composition using EDX analysis (% atm) and surface characteristics of the HA modifications (n=3 samples). Coating thickness, coating mass and surface roughness values are reported ±2SD.

Modification	O	P	Ca	Ti	Ca/P	Coating Thicknesss (μm)	Coating Mass (mg/cm^2)	Surface Roughness	
								Ra (nm) Veeco Dektak 8	Ra (μm) Taylor Robson
Blank Ti	23	-	-	77	-	0	-	155±4	0.39±0.05
CoBlast HA	66	11	16	7	1.56	7±2	0.53±0.2	546±110	1.24±0.20
Plasma HA	72	11	17	0	1.63	65±6	11.0±0.4	965±86	>5

The coating thickness and the coating mass per unit area results given in Table 4.1 confirmed the EDX analysis of the surfaces, which indicated that the plasma HA coating was thicker than the CoBlast HA coating and these values are broadly in agreement with previous studies of CoBlast HA surfaces (O'Sullivan *et al.*, 2011; O'Hare *et al.*, 2010). The plasma samples were found to exhibit higher levels of

surface roughness (micron features and nano features) compared to the CoBlast samples, which in turn were rougher than the untreated Ti (Veeco Dektak (nm) and Taylor Robson (μm) data). Multiple comparisons between groups (AFM data) revealed statistical differences between all samples ($p<0.001$) using the Tukey's post-hoc analysis.

The release profile of Ca and P ions from the HA coated surfaces are given in Figure 4.1.

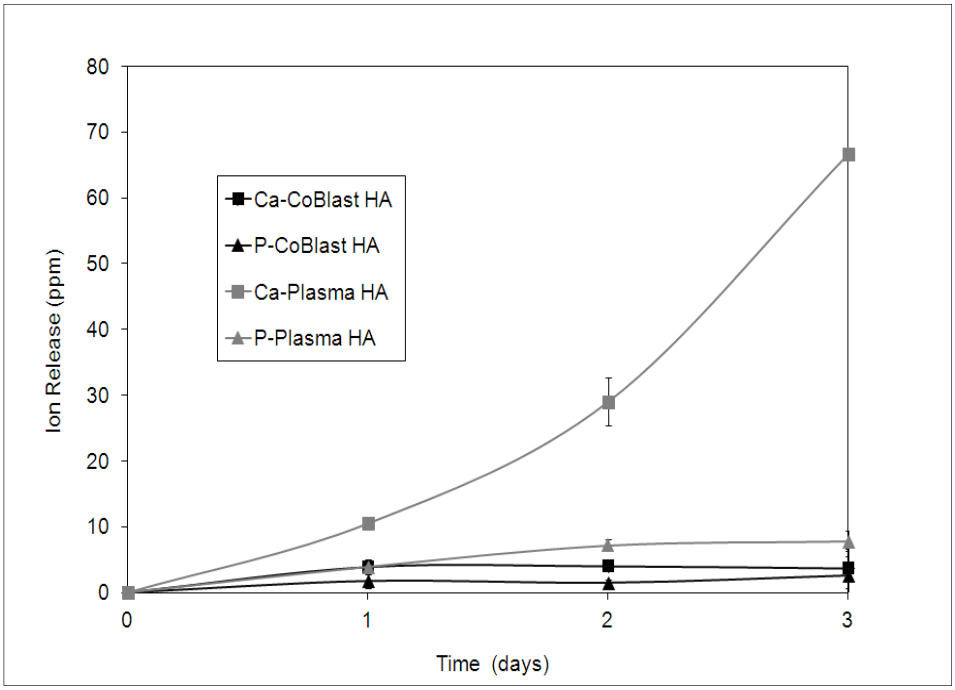

Figure 4.1: Ca and P ion release in tris-HCl buffer (37 °C, pH 7.4, 150 rpm, n=3 samples ±2SD).

The CoBlast surface was observed to release a lower concentration of Ca and P ions from its surface compared to the plasma sample, in agreement with previous studies (Tan *et al*., 2012). At day 1, 11 ppm Ca ions were released from the plasma HA

surface which was seen to increase to 67 ppm at day 3. However, at day 1 maximum Ca release was observed from the CoBlast surface (4 ppm). Low levels of P ions were released (<8 ppm) from the plasma and CoBlast surface (<4 ppm) throughout the analysis period.

4.3.1 Bioactivity Study

The surface analysis of the HA modifications before and after incubation in SBF are presented in Figures 4.2-4.9. The Ti and Ca/P levels were monitored using EDX analysis over a 30 day period following incubation in SBF (Figure 4.2).

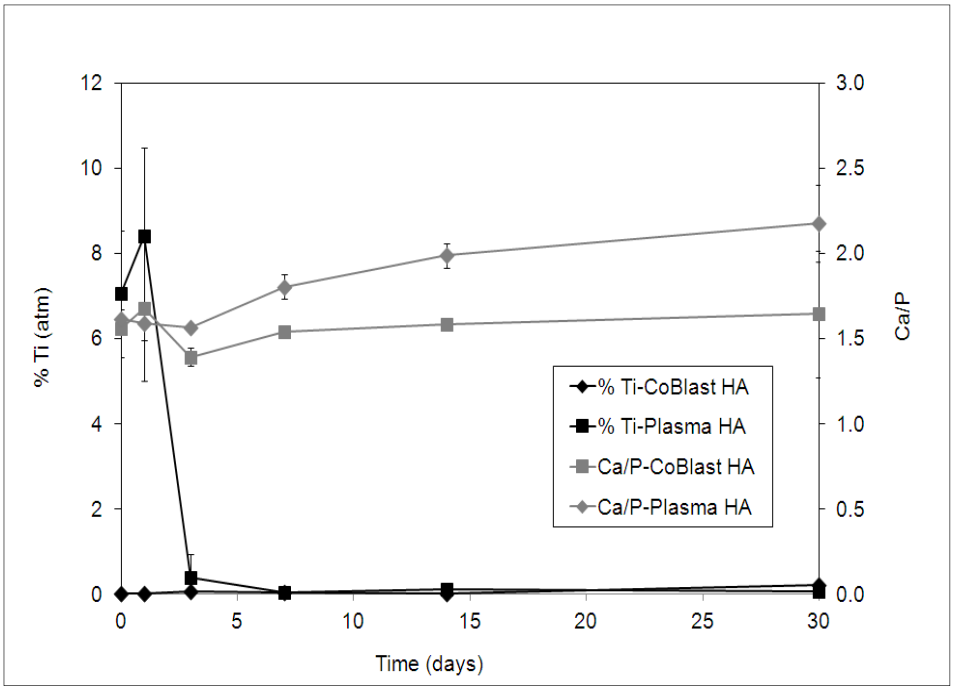

Figure 4.2: Ti levels (primary y-axis) and Ca/P (secondary y-axis) of the HA modifications following incubation in SBF solution (n=3 samples ±2SD).

Titanium was not detected for the plasma sample suggesting that the thick apatite coating remained on the surface over the 30 day period. The Ca/P levels for the

plasma sample were seen to increase to 2.18 at day 30 indicating a sizeable change from the initial stoichiometric HA chemistry. The CoBlast surface which was a thinner coat to begin with, following incubation in SBF the Ti % atm was observed to increase at day 1 and then decrease to 0.4 % atm Ti at day 3 with no Ti detected thereafter. The Ca/P ratios for the CoBlast surface ranged between 1.4 to 1.7 over the 30 days, remaining close to the pure HA value. An increase in coating mass was observed for the plasma HA coating at day 1 whereas the coating mass remained unchanged for the CoBlast HA, Figure 4.3. The coating mass was observed to increase between day 7 and 14 for both HA surfaces. However, there was a noticeable difference between the coating mass of the CoBlast HA surface and the plasma HA surface with an increased mass noted in the case of the latter following incubation in SBF.

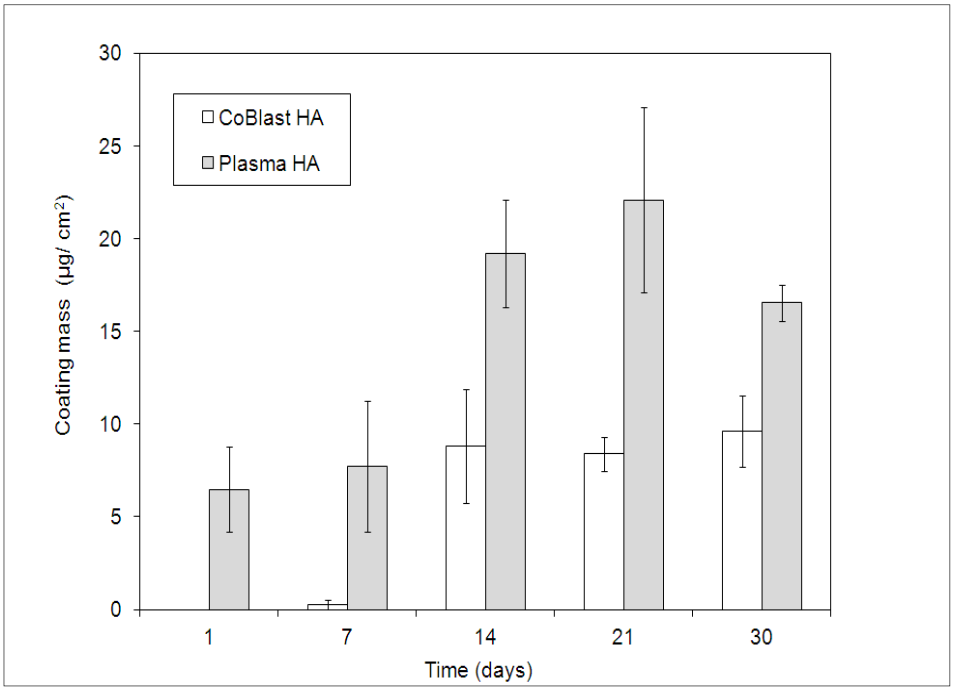

Figure 4.3: Mass of SBF deposit per unit surface area with SBF soakage time (n=3 samples ±2SD).

The crystal structure of the HA modified surfaces was also investigated using XRD (Figure 4.4).

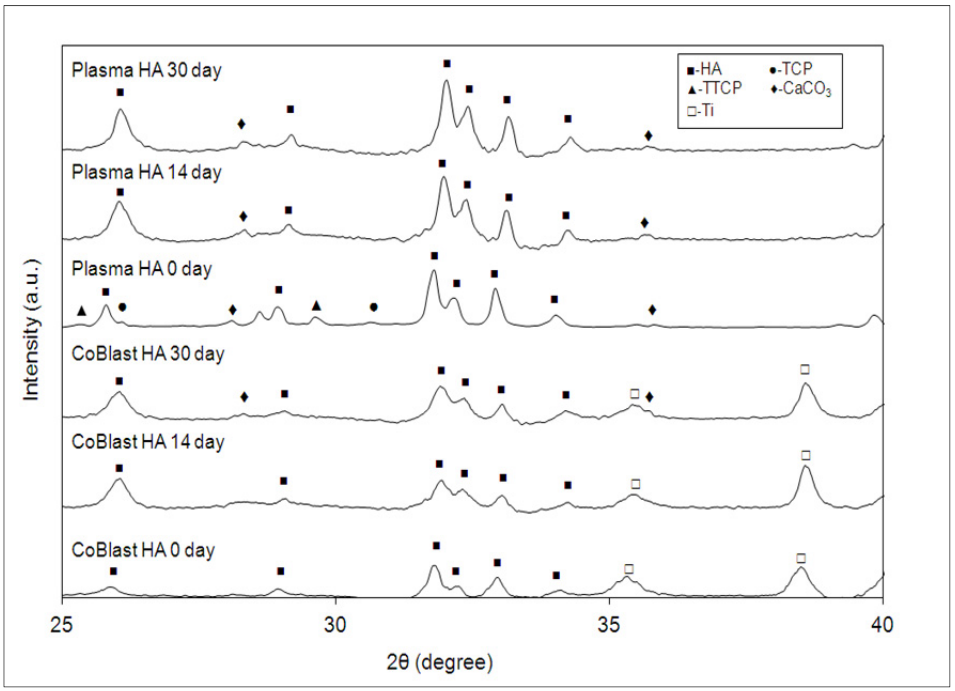

Figure 4.4: XRD spectra of HA coated surfaces before (day 0) and after incubation in SBF over a 30 day period.

As shown in Figure 4.4, prior to SBF soakage both samples produce data consistent with the deposition of HA (day 0). The five strongest lines in the XRD pattern are 002, 211, 112, 300 and 202 reflections from HA corresponding to approximately 25.9, 28.9, 31.9, 32.2, 34.1° 2θ. The CoBlast HA sample also contains a number of additional peaks which can be attributed to the Ti substrate and a higher degree of signal to noise, indicating that the coating is quite thin. On the contrary, the plasma sample is largely devoid of Ti features and is dominated by the HA peaks, as would be expected from a thick coating. Impurities such as tricalcium phosphate (TCP), tetracalcium phosphate (TTCP) and calcium carbonate ($CaCO_3$) were detected in the

plasma HA coating analysed (Li *et al.*, 2009; Fathi *et al.*; 2008; Gross *et al.*, 1998) suggesting that a less pure HA coating was detected. Increasing SBF soakage time resulted in the disappearance of the TCP and TTCP phases and the sustained presence of $CaCO_3$ for the plasma HA surface. $CaCO_3$ peaks were observed on the CoBlast surface following maturation in SBF over a day 30 period.

The FTIR spectra of the CoBlast HA surface before and after immersion in SBF is presented in Figure 4.5.

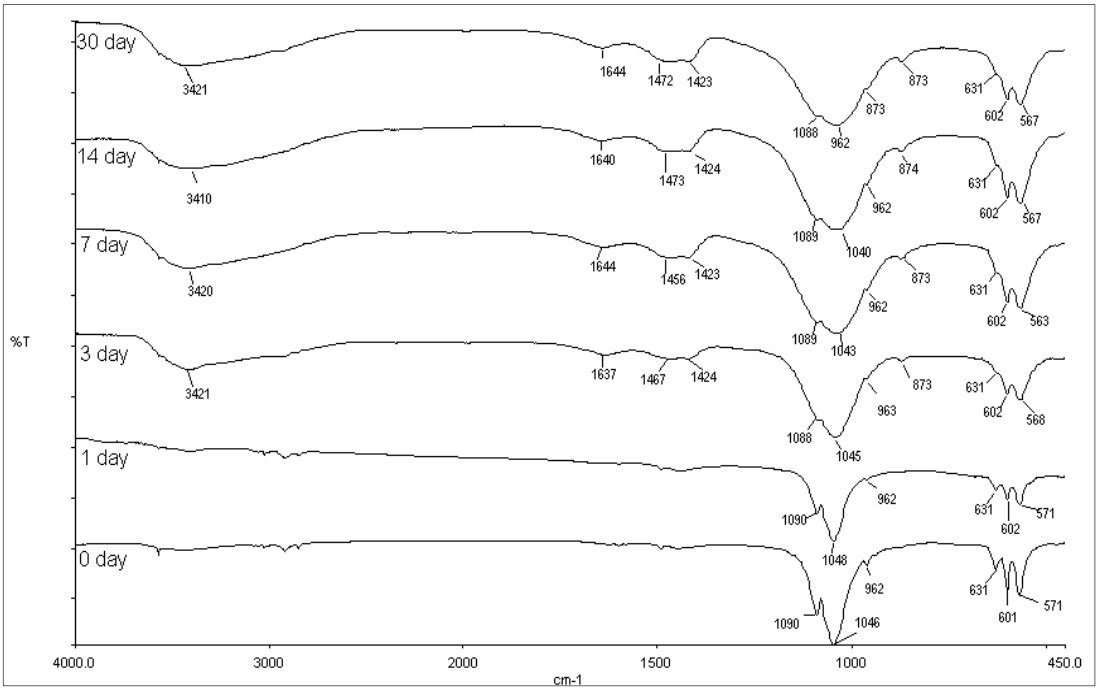

Figure 4.5: FTIR analysis of CoBlast HA surface before and following incubation in SBF over 30 day period.

These include the O-P-O bending vibrations (700 – 300 cm^{-1}), the P-O stretching vibrations (1200 – 900 cm^{-1}) and the O-H stretching vibrations (3571 cm^{-1} and 630 cm^{-1}) (Fathi *et al*., 2008). The resolved PO_4 bands (1200 – 900 cm^{-1}) indicate that crystalline HA was deposited. Also, the small peak present at 962 cm^{-1} was assigned

to the P-O symmetric stretching mode and represents a highly ordered, non-carbonated apatite and is indicative that the material is well crystallised (Hong *et al.*, 2007).

The FTIR spectra for the SBF immersed CoBlast HA coatings shows that the surface chemistry remains unchanged at day 1. However at day 3, the PO_4 modes exhibited a broad overlap from 880 cm^{-1} to 1250 cm^{-1} indicating a deviation of the phosphate ions from the tetrahedral configuration (Zhang *et al.*, 2003) in addition to changes of the O-P-O bending vibrations (700 – 400 cm^{-1}). Water was absorbed in the layer as indicated by the broad bands from 3700 to 2500 cm^{-1}, with the presence of structural OH groups (approximately 1640 cm^{-1}) in the apatite lattice can be seen in the spectrum from day 3 onwards (Weng *et al.*, 1997). Following maturation in SBF beyond day 3, the spectra shows the presence of prominent carbonate (CO_3^{2-}) bands (1423-1473 cm^{-1} and 873 cm^{-1}) had grown suggesting an obvious change in composition. This suggests the formation of a carbonated hydroxyapatite (CHA) at day 3, and the structural changes are in agreement with literature (Zhang *et al.*, 2003).

The FTIR spectra of the plasma HA before and after immersion in SBF is presented in Figure 4.6. The more amorphous character of the plasma HA coating was clearly evident with the broad nature of the PO_4 bands between 750 to 1300 cm^{-1}, which is a feature of the different phases present (TCP, TTCP) as well as the carbonate peaks present (1493-1433 cm^{-1}) (Figure 4.6). Structural changes characteristic of CHA growth are evident at day 1, with the increased broadness of the above PO_4 modes,

carbonate peaks (1493-1433 and 875 cm^{-1}) as reported by Zhang *et al.* and adsorbed water (3700 to 2500 cm^{-1} and 1650 cm^{-1}) (Zhang *et al.*, 2003).

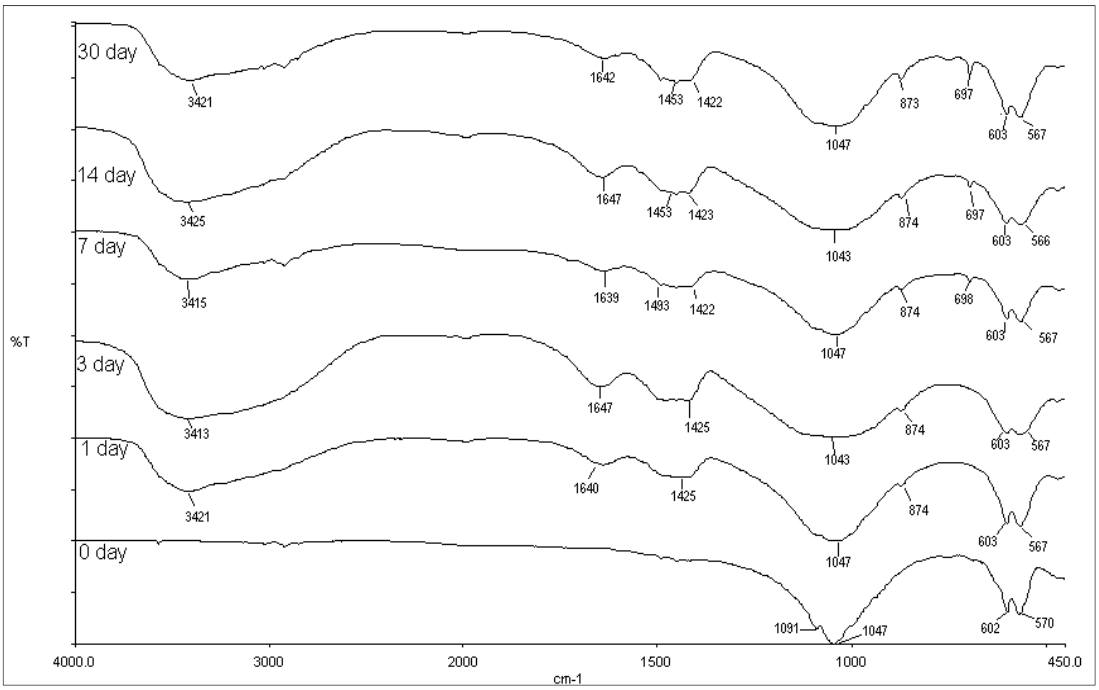

Figure 4.6: FTIR analysis of plasma HA surface before and following incubation in SBF over a 30 day period.

The SEM images provide evidence as to what was occurring at the surface during incubation in SBF. The images of the CoBlast surface before and after SBF immersion are shown in Figure 4.7 (a)-(f). The images of the plasma HA surface before and after SBF immersion are shown in Figure 4.8 (a)-(f).

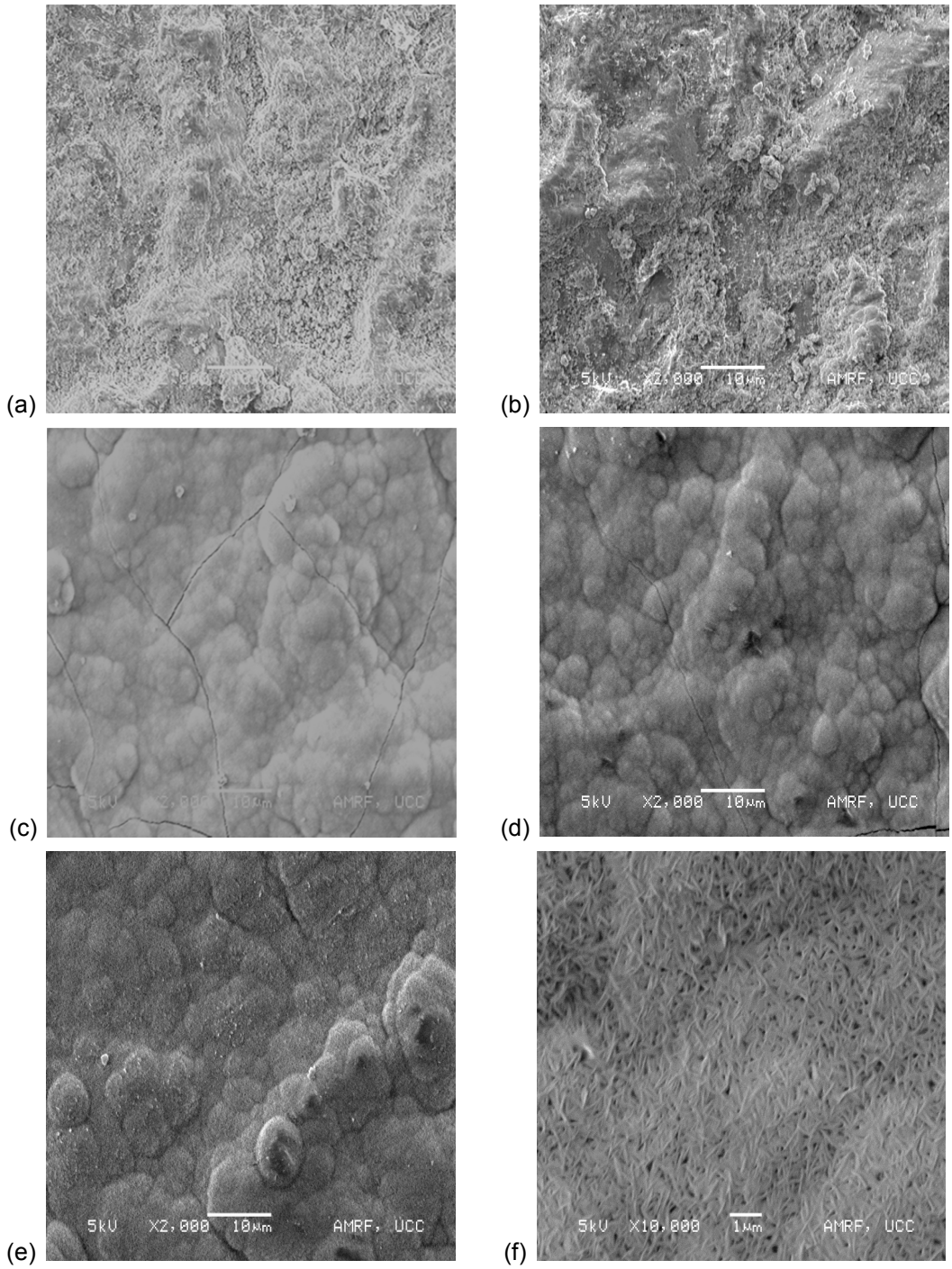

Figure 4.7: Images of CoBlast HA coating following incubation in SBF at (a) 0 day; (b) 1 day; (c) 3 days; (d) 7 days; (e) 14 days ((a)-(f) x2000 magnification); (f) 30 days x10000 magnification.

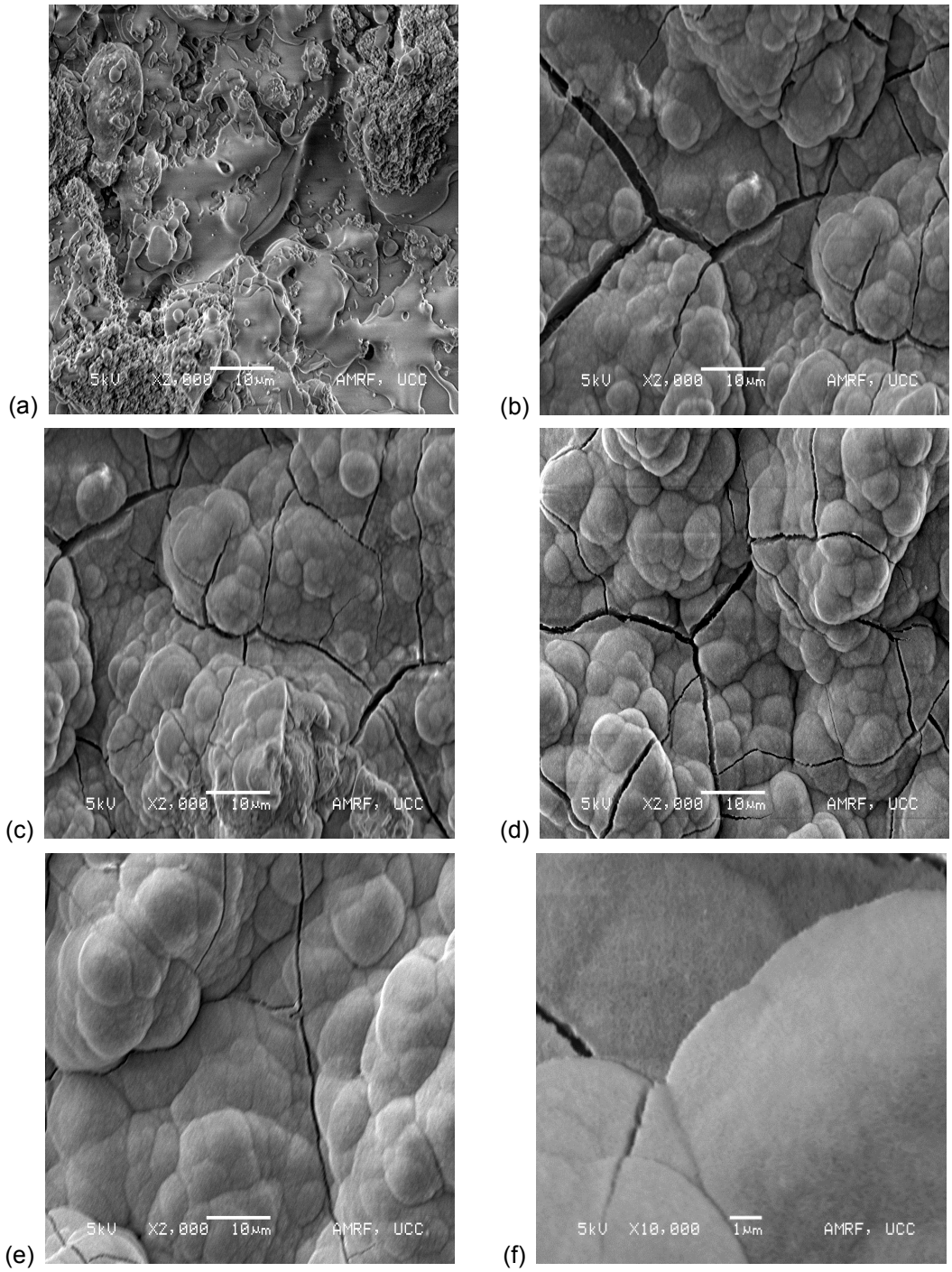

Figure 4.8: Plasma HA samples in SBF following incubation at (a) 0 day; (b) 1 day; (c) 3 days; (d) 7 days; (e) 14 days ((a)-(e) x2000 magnification); (f) 30 days x10000 magnification.

The CoBlast treatment results in a roughened, highly regular and uniform surface (Figure 4.7 (a)). At day 1 no evident change resulting in an altered coating morphology was observed. However, at day 3 nucleation of globular precipitates had occurred which completely changed the original morphology of the coating at day 0. This is the CHA layer that has formed through precipitation as indicated by FTIR results. In literature, it has been described as a dune-like layer, characterised by many cracks of tortoise–shell appearance that completely covers the surface (Weng *et al*., 1997). At days 7, 14 & 30, the globular surface features were still evident, which on closer investigation were found to possess a subtle texture of needle-like crystallites (Figure 4.7 (f)), which supports observations by Leeuwenburg *et al.* (Leeuwenburg *et al.*, 2006).

Figure 4.8 (a) reveals a typical HA plasma treated surface, which as expected, gives a rough morphology with large spherical agglomerates and typical deposits of bioceramic material evident on the surface. Nucleation had occurred rapidly after immersion in SBF and was evident on day 1. As the soaking time increases the granules become larger and evolved into a more dense dune-like layer as a result of increase apatite growth. Established research has observed similar findings (Gu *et al.*, 2003; Weng *et al.* 1997). Again, needle-like surface texture was observed under higher magnification (Figure 4.8 (f)). However, a smoother morphology of crystalline formation with nanopores after incubation in SBF was observed for the CoBlast surface compared to the globular surface of the plasma coating.

Mechanical adhesion testing of the HA coatings was undertaken as per the ASTM F1147 standard test method for tension testing of CaP and substrate coatings and the

results are presented in Figure 4.9 (ASTM Standard, 2011). The results reveal that the CoBlast HA coating had a significantly higher bond strength ($p<0.05$) compared to the plasma HA coatings at day 0. Following immersion in SBF, the bond strengths were seen to decrease with immersion time. However, significantly higher bond strength values were observed for the CoBlast HA surface compared to the plasma HA surface throughout the entire 30 days following submersion in SBF. A statistically significant decrease in the bond strength was observed for the plasma HA surface after submersion in SBF at 14 compared to day 0. Although the average CoBlast HA coating adhesion value also dropped at day 14, this was not deemed to be statistically significant ($p>0.05$).

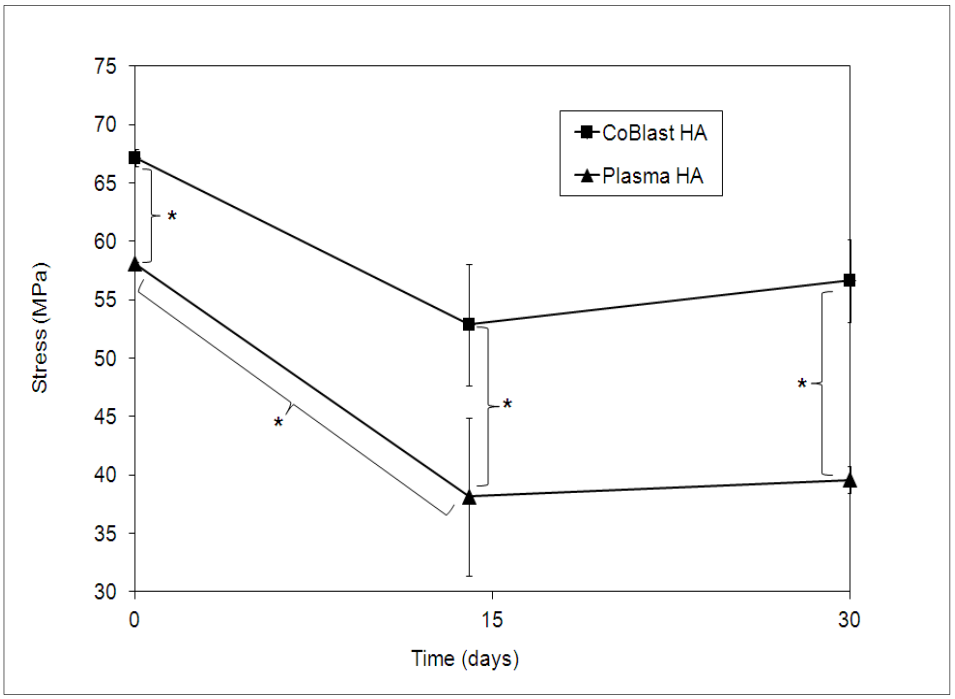

Figure 4.9: Tensile bond stress values of the HA modifications (ASTM F1147) (n=3 samples ±2SD) (* represents $p<0.05$ determined using independent 2-sample t-test).

4.3.3 Cell Culture Analysis

4.3.3.1 Cell Proliferation

MG-63 osteoblastic cell proliferation studies were carried out on the plasma and CoBlast HA surfaces and the results are presented in Figure 4.10. Cell proliferation data at day 1 were comparable. Statistically differences between samples were found only at day 5 ($p<0.05$) using one way ANOVA. At day 5, there was a significant increase in cell proliferation on the CoBlast HA coated substrate ($p<0.01$) compared to the untreated Ti, whereas no significant difference was observed between the plasma and the Ti sample (Dunnett's test). No evidence of cytotoxicity was observed using MG63 cells for any of the samples evaluated.

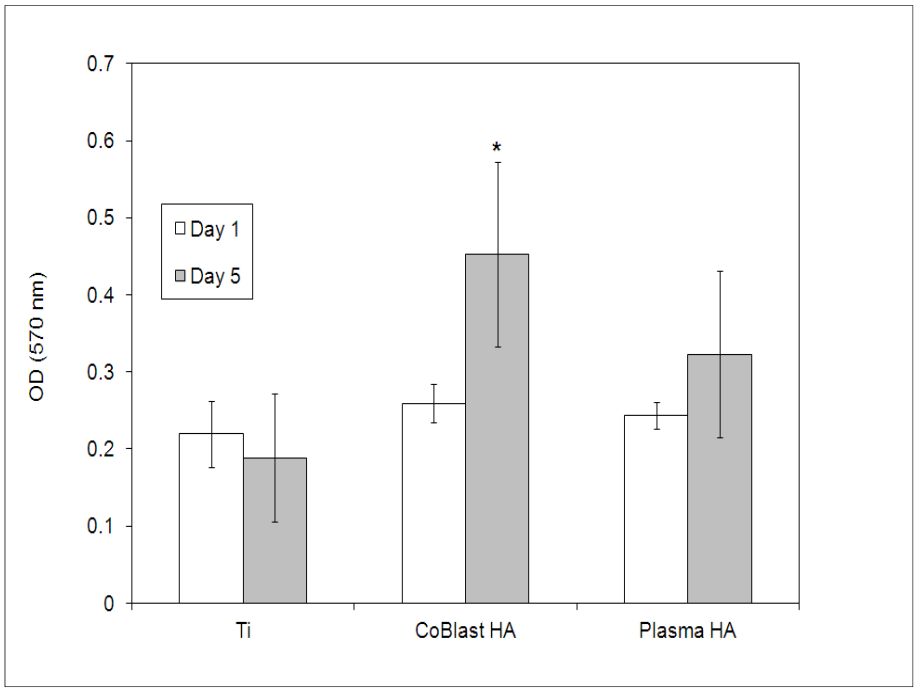

Figure 4.10: MTT assay data for MG-63 cells on modified Ti surfaces over 5 days *in vitro* (n=3 samples ±SD) (***** represents statistical significance between the CoBlast HA sample and the titanium control at day 5 ($p<0.01$) determined using Dunnett's test).

4.3.3.1 Cell Morphology

The morphology of the MG-63 cells on each surface was investigated using SEM imaging and typical results are presented in Figure 4.11. The cells on both HA surfaces exhibit polygonal shapes rather than a polarised fibroblastic morphology indicating increased cell spreading. In addition, there was also an abundance of lamellopodia and filopodia present on both HA surfaces signifying good cell adhesion. However, cells appeared to preferentially reside in the pits of the plasma HA surface where the optimal cell adhesions could be achieved.

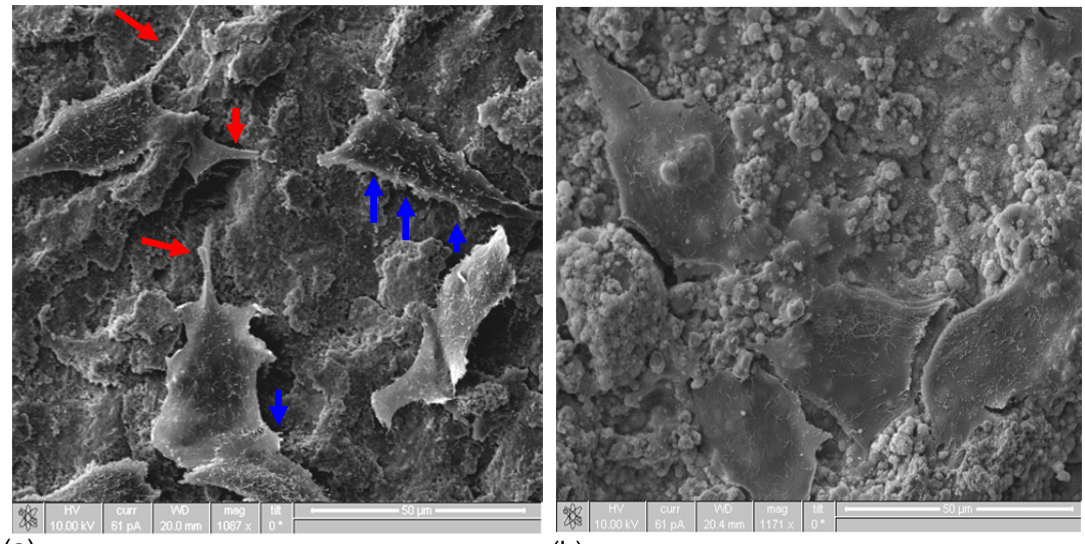

Figure 4.11: MG-63 osteoblasts cultured on (a) CoBlast HA surface x1000 magnification and (b) plasma HA surface x1000 magnification. Red arrows indicates the presence of lamellipodia and blue arrows highlights the presence of filopodia.

4.4 Discussion

From the results generated in this study, it is clear that the structure of the final HA coating and its behaviour in SBF is largely dependent on the processing method used

to apply it onto the surface. Surface analysis of the coated samples prepared herein indicates that both CoBlast and plasma spraying are effective mechanisms of creating a HA rich surface on Ti metal. In both cases, EDX clearly shows that the surface has been covered with a CaP layer. However, the morphology and uniformity of both coatings is considerably different. It is evident that a much thicker coating is applied with the plasma technique compared to the blasting method (Table 4.1). While analysis of the CoBlast samples produce results that are consistent with the presence of a thin and homogeneous HA surface, the plasma process was found to produce a thick deposit with significant variations in structure and chemistry. The impact of the high velocity spraying of molten HA powder onto an implant surface, which rapidly cools, is the formation of a dense coating with a morphology consisting of bioceramic deposits on the plasma surface (Campbell, 2003). Crystallographic examination clearly shows that the plasma process contains secondary CaP phases which can be attributed to the thermal degradation of the HA precursor during the deposition process, which is in agreement with the FTIR spectra (broad PO_4 bands between 750 to 1300 cm^{-1}). SEM image analysis reveals the morphology of the surfaces and provides evidence of a more uniform coating from the CoBlast treatment compared to a rougher and irregular HA surface deposited using the plasma spray method (Figures 4.7 (a) and 4.8 (a)). Controlling the deposition parameters of such high temperature methods of the plasma technology can be difficult to achieve. In contrast, the CoBlast process produces a more pure, crystalline HA layer on the Ti surface with no major evidence of contamination from additional CaP phases (supported by XRD and FTIR analyses).

The presence of impurities such as CaO, OCA, α-TCP, β-TCP and TTCP in a HA material have been reported to decrease the crystallinity and subsequently, increase dissolution rate (Gross and Berndt, 1998; Gross *et al.*, 1998; Zyman *et al.*, 1998). Ion release from the various coatings are given in Figure 4.1, and when combined with the disappearance of the TCP phases in the XRD analysis, the data clearly shows that the thicker plasma HA dissolves at a quicker rate and releases more Ca and P ions compared to the CoBlast coatings as a direct result of the presence of such impurities. There are a number of problems associated with increased solubility of the secondary impurity phases in plasma coatings as outlined in **Section 1.7** (reduced mechanical stability, delamination etc.) (Mohammadi *et al.*, 2007, Heimann and Wirth, 2006, LeGeros, 1991).

The bond strength of the HA coatings on the Ti implant material is very much critical as it has to withstand crevice and bone growth stress in addition to its load bearing activities. Consequences of poor adhesion strength may lead to wear debris accumulation resulting in inflammation, osteolysis and implant loosening (Long and Rack, 1998). The adhesive strength of the coatings under investigation was measured by tensile adhesion test which measures the combination of cohesive strength (within the coating) and adhesive strength (coating to substrate) (Yang and Chang, 2001). It has been reported that cohesive strength is dominated by coating properties such as crystallinity and microstructure (dense or porous) while the adhesive strength is affected by coating properties, residual stress and surface roughness (Yang and Chang, 2001). Amorphous coatings have a more brittle nature and exhibit less adhesion strength compared to the crystalline coatings (Clèries *et al*., 2000). In addition, Filiaggi reported that bond strength is dependent on coating thickness,

coatings of 240 µm had lower bond strength compared to coatings of 50 µm (Filiaggi *et al*., 1991). In comparison with measured values herein and literature values, the bond strength values determined suggest that the CoBlast HA coatings produces higher adhesion levels than industry standard plasma coatings (20-48 MPa) (Røkkum *et al*., 1999; Dorr *et al*., 1998) and also other deposition processes such as sol-gel, ion beam and spluttered coatings (25-30 MPa) (Chen *et al*., 2007a; Fujihara *et al*., 2004; Lee *et al*., 2002; Piveteau *et al*., 2000). The increased strength of the CoBlast surface can be attributed to a combination of highly crystalline HA deposition combined with direct tribochemical bonding of the bioceramic to the metal substrate (O'Hare *et al*., 2010) whereas a lower bond strength was obtained from the less crystalline and thicker nature of the plasma coating. However, these effects are only significant if they can be maintained over time in a biological environment.

It is well known that the formation of bone like or CHA layer plays an important role in establishing through bone-bonding interactions between the implant and living tissues promoting fast fixation and long term stability (Sun *et al.,* 2001; LeGeros, 1991). According to Kokubo *et al,* SBF has approximately the same ion concentration as that of the human blood plasma and the *in vitro* immersion of bioactive materials in SBF is thought to reproduce the *in vivo* surface structure changes. Therefore, bioactivity of biomaterials in SBF is an important factor to assess and provides a good model for monitoring biological responses *in vitro* (Kokubo *et al.*, 1990).

The SBF studies here clearly show that the plasma HA has an early onset of CHA formation (day 1) compared to the CoBlast HA surface (day 3) as demonstrated by

the FTIR and XRD analysis. The formation of the CHA layer is a complex process involving the release of both Ca and P ions through dissolution resulting in an increase in super-saturation in the localised area around the coating which correlates with increased Ca ion release from the plasma surface. The results presented are in agreement with literature, as the amorphous phases of plasma coatings increase the dissolution rate of the HA with the granular feature of the apatitic precipitation process observed between 6-12 hours in SBF (Weng *et al.*, 1997). The formation of a carbonated CaP layer plays an important role in bone fixation of the implant to the living tissue *in-vivo* (Sun *et al.* 2001; LeGeros et al., 1998; LeGeros and Craig, 1993). During the formation pores or microcracks in recessed regions of the coating may be observed. The presence of nanopores on the CoBlast surface was observed after incubation in SBF for 30 days, Figure 4.7 (f) while large fissures were evident in the plasma sample, Figure 4.8 (f). The increase in surface roughness as a result of dissolution is favourable for nuclei to anchor resulting in precipitation of bone-like apatite onto the HA surface (Sun *et al.* 2001; Weng *et al.*, 1997; LeGeros, 1991).

In comparison, there are very low levels of ions released from the CoBlast coating over the three days (<4 ppm) (Figure 4.1), however carbonate apatite was evident on the coating at day 3 (Figures 4.5-4.8). In addition, a lower deposition mass and a smoother morphology of the CHA resulted on the CoBlast surface compared to the plasma coating, further suggesting that the lower dissolution of ions from the CoBlast surface limited the CHA growth. The Ca/P ratios did not change from day 7 to day 30 for the CoBlast surface suggesting that the deposit maintained a relatively high phosphate content. In contrast, an increase in the Ca/P ratio was observed after

day 7 for the plasma surface suggesting that the deposit contains significant carbonate substitution for the phosphate within the apatite structure.

These variations in timing, chemistry and morphology suggest that perhaps there is a different mechanism for apatite growth for the crystalline CoBlast HA surface. LeGeros *et al.* described one model that is based on a dissolution and precipitate phenomenon, where the release of Ca^{2+} and other ions leads to the small interfacial region becoming highly saturated, thereby inducing precipitation of carbonated apatites, leading to re-crystallisation on the surface (LeGeros, 1991). Other models have been proposed that ion-exchange occurs at the interface between the physiological solution that transforms the HA surface into other CaP phases (Bertazzo *et al*., 2010; Ducheyne and Qui, 1999), which may subsequently lead to the formation of the CHA layer *in vivo* (Chen *et al*., 2004). These models support the observed changes in the plasma HA coating in SBF where the impurity phases rapidly dissolve and can thereby participate in the formation of the CHA layer. However, the low levels of ion elution, the Ca/P ratio and slow growth of apatite on the crystalline CoBlast surface suggests that the deposit may form through ion exchange at the surface. This *in vitro* study may indeed mimic the growth model put forward by Hench to describe how crystallised HA can cause the epitaxial growth of bone mineral towards it, eventually fusing in a cement-like matrix (Cao and Hench., 1996). This complex process of osteointegration is dependent on surface reaction which includes the chemical (composition and dissolution), biological (osteoblast cell attachment and proliferation) and mechanical (bond strengths) interactions between the implant and the host. Here it is suggested that relative dissolution rates are determined by the chemical composition and the crystallinity of the HA (Cao and

Hench, 1996). This response suggests the crystalline CoBlast offers a stable surface both *in vitro* and *in vivo* when compared to the rapid dissolution of the plasma surface. This rapid alteration of the plasma HA surface could therefore compromise the stability of the implant when compared to the more crystalline CoBlast surface.

This analysis is supported by the mechanical testing of the bond strength of the HA coatings following soakage in SBF. Obviously, the heterogeneous nature of the plasma coating (uniformity, crystallinity and thickness) and the increased degradation of the coating as a result of the rapid dissolution of the TCP and TTCP phases combined with the formation of the thicker carbonate apatite layer had a definite impact on the bonding strength of the plasma HA. The bond strength was seen to degrade concomitant with the process of chemical dissolution and the deposition of a thicker amorphous coating. As seen in the dissolution studies, the CoBlast HA surface was seen to offer minimal dissolution and delivered a different mechanism for the carbonate apatite formation and hence the bond strength of the CoBlast samples was higher than that of the plasma samples at each time point. This indicated that the CoBlast HA coating is more physically stable and less prone to biological demineralisation as proven by the later onset of CHA formation and this may be expected to have an impact *in vivo*.

It was observed in this study that cell proliferation on the modified surfaces were all approximately comparable at day 1, however after 5 days the CoBlast surface outperformed the plasma surface which may be attributed to a combination of surface structure and chemistry. The CoBlast sample was found to have significantly

higher levels of cell proliferation ($p<0.01$) when compared to the control surface after 5 days incubation.

It is well established that topography plays a major role in the alignment, adhesion and subsequent spreading of osteoblast cells across the surface, with rougher surfaces often reported to increase cell adhesion and proliferation. However, this was not seen here. The increased surface roughness of the plasma HA did not increase cell proliferation compared to the smoother CoBlast surface (Table 4.1 and Figure 4.10) After 24 hours, SEM imaging revealed significant MG-63 cell growth and proliferation on the surface of both the plasma and CoBlast HA samples demonstrating the cytocompatible nature of these surfaces. However, a more regular alignment was observed on the CoBlast surface compared to the more sunken cellular behaviour on the plasma surface (Figure 4.11). The increased viability on the smoother CoBlast HA surface may be attributed to the regular HA surface produced by the blasting technology coupled with a highly stable structure that facilitated proliferation. In contrast, the highly variable plasma process produced a surface that altered over time due to the dissolution and recrystallisation of the semi-crystalline and amorphous phases, as detected in the ion elution and SBF studies. This unstable and altering surface topography may have disrupted the growth and proliferation of the osteoblast cells. It has previously been shown that highly stable crystalline coatings offer superior outcomes *in vivo* (Dekker *et al*., 2005; Xue *et al.*, 2004).

Modifications are needed at varying degrees to modify the HA material to meet the desired chemical, structural and dissolution requirements for its use as an *in vivo* implant material without jeopardising the long term mechanical stability of the

implant. The importance of material formulation is fundamental so that the bioactive coating will confer adequate dissolution properties needed to induce the complex process of the osteointegration process and quality lamellar bone formation. In this study, the deposition process used is an important consideration as this will influence the chemistry and composition of the resultant HA coating which will then in-turn affect the stability of the implant.

4.5 Conclusions

The *in vitro* studies described herein have shown that the introduction of HA onto the surface produced highly cytocompatible and bioactive surfaces. The thermal plasma spray process produced a thicker, heterogeneous, amorphous HA coating with lower bond strength and lower *in vitro* stability when compared to the crystalline CoBlast HA surface. The presence of secondary crystalline phases in the plasma sample resulted in a rapid dissolution in SBF and thereby reduced the bond strength of the coating. The crystalline CoBlast surface was found to be much more stable and produced a different response profile in an SBF immersion trial with minimal dissolution and retention of excellent coating adhesion throughout. It is postulated that a different mechanism for apatite growth is at play in SBF for the CoBlast surface, however further studies are required to confirm this. Enhanced osteoblast proliferation was observed for CoBlast modified surfaces compared to the thicker and rougher plasma spray coating and this may be explained by the highly stable surface structure of the CoBlast HA which offers a more predictable and regular surface for cells to adhere to and proliferate upon.

Chapter 5

5.0 Deposition of Substituted Apatites with Anticolonising Properties onto Titanium Surfaces using CoBlast Technology

Results and discussion published in *Journal of Biomedical Materials Research B: Applied Biomaterials,* (2011), 95(1):141-149.

Abstract:

A series of substituted apatites have been deposited onto titanium (V) substrates using a novel ambient temperature blasting process. The potential of these deposited substituted apatites as non-colonising osteoconductive coatings has been evaluated *in vitro*. XPS, EDX and gravimetric analysis demonstrated that a high degree of coating incorporation was observed for each material. The modified surfaces were found to produce osteoblast proliferation comparable to, or better than, a hydroxyapatite (HA) finish. Promising levels of initial microbial inhibition were observed from all of the substituted surfaces, with the strontium (Sr) surface showing prolonged ability to reduce bacteria numbers over a 30 day period. Ion elution profiles have been characterised and linked to the microbial response and based on the results obtained, mechanisms of kill have been suggested. In this study, the presence of coated substrate surfaces was observed to be a significant contributing factor to the antimicrobial performance and the anticolonising activity. The silver substituted apatite (AgA) was observed to out-perform both the strontium (SrA) and zinc substituted apatites (ZnA) in terms of biofilm inhibition.

5.1 Introduction

Biomaterial-associated infections (BAI) pose great surgical problems, as revision surgery is not always easy and patients suffer severe discomfort (Schmidmaier *et al.,* 2006). Such infections are common in orthopaedic surgery where infection rates range from 0.5% to 5%, irrespective of the utilisation of strict hygienic protocols (aseptic and sterilisation procedures) and also the systemic administration of antibiotic prophylaxis (Hetrick and Schoenfisch, 2006; Virk and Osmon, 2001; Lidwell *et al.,* 1984). These infections are the result of bacterial adhesion and subsequent colonisation leading to the inevitable biofilm formation at the implantation site (Van de Belt *et al.,* 2001; Dougherty, 1988). The introduction of bacteria such as *Staphylococcus aureus* (*S. aureus*) and *Staphylococcus epidermidis* (*S. epidermidis*) onto implant surfaces before or during surgery have been highlighted as the main causes of such infections (An and Friedman, 1996). Therefore, there is a need for a bioceramic coating that will not only have osteointegrative properties but can also effectively resist bacterial colonisation.

With regards to this aim, substituted apatites which can deliver added functionality to the HA bioactive surfaces, through their antimicrobial impact are of major interest. Investigations into the use of ions such as silver (Ag) and zinc (Zn) incorporated into HA have shown positive antimicrobial effects (Zhou *et al.*; 2008; Kim *et al.,* 1998). Strontium ions (Sr), typically present in trace quantities in the mineral phase of bone, have been reported to have an antimicrobial effect *in vitro* (Lin *et al.,* 2008; Guida *et al.,* 2003). The presence of Zn and Sr has also been shown to increase the activity of osteoblast cells *in vitro* (Capuccini *et al.,* 2008;

Caverzasio, 2008; Ito *et al.,* 2002). Several proposed mechanisms have been reported for the antimicrobial mode of action for these metal ions, but results have been mixed and the mechanisms by which the surfaces produce an antibacterial effect has not been fully elucidated. Reported mechanisms include disruption of electron transport chain, inhibition of DNA replication, DNA cleavage, membranous disruption, reactive oxygen formation and enzyme inhibition (Applerot *et al.,* 2009; Park *et al.,* 2009; Feng *et al.,* 2000b; Kim *et al.,* 1998; Faigan *et al.,* 1986; Richards *et al.,* 1984; Yakabe *et al.,* 1980; Bragg and Rannie, 1975; Kasahara and Anraku, 1974).

In this study, CoBlast technology was used to deposit various substituted apatites as well as HA onto titanium (Ti) substrates. A range of *in vitro* tests were undertaken to determine if the dopant materials could produce a modified surface which possess simultaneously osteoconductive and anticolonising potential and the results were interpreted in view of detailed surface characterisation studies.

5.2 Materials and Methods

The materials and methods used in this chapter are outlined in **Chapter 2**. Surface characterisation techniques were employed to analyse the CoBlast surfaces (HA, AgA, SrA, ZnA). This included elemental composition (EDX (n=3 samples)), XPS (n=3)), ion concentration (ICP-OES of dissolved coatings in acid (n=3 samples)), SEM images of topography and surface roughness (Taylor Hobson (n=3 samples)). The *in vitro* ion release from the surfaces into PBS over 30 days were analysed using ICP-OES (n=3 samples). Cell culture tests were performed on the CoBlast surfaces

using the commercially available MTT assay which assessed cell viability at day 1 and 3 (n=4 samples). Information relating to the osteoblast cell viability and cytotoxicity are obtained. The antimicrobial efficacy and anticolonising performance of the coatings were also assessed using *S. aureus* (ATCC 1447) as the challenge organisms (CFU data are presented in **Appendix II**). The impact of the released ion into PBS over 30 days (n=3 samples) as well as the surface effects of the immobilised ion before and after incubation at 30 days was assessed (n=3 samples).

A statistical one-way analysis of variance (ANOVA) was performed to determine statistically significant differences between the sample types with a value of $p<0.05$ considered to be statistically significant. Following this, the Dunnett's test was applied, to compare values between all the sample data to the control HA sample (surface roughness data, MTT assay data, antimicrobial and anticolonising data). Two levels of significance was noted for the statistical analysis performed on the MTT data using the Dunnett's test ($p<0.01$ and 0.001). Multiple comparisons were performed between substituted sample types using the Tukey's post-hoc analysis (surface roughness data).

5.3 Results

5.3.1 Surface Characterisation

The XPS analysis of the HA coating revealed a surface rich in calcium (Ca), phosphorous (P) and oxygen (O), as shown in Table 5.1 and Table 5.2. The modified apatites presented with low dopant ion levels of less than 5% atm with the Ag

producing the lowest level of dopant ion incorporation and Zn producing the highest levels.

Table 5.1: Elemental composition of the coatings via XPS (% atm).

Coating	C	O	P	Ca	Ti	Ion
HA	17.1	53.9	10.0	15.5	0.6	N/A
AgA	11.3	57.7	13.9	15.6	0	Ag – 0.9
SrA	8.4	53.5	18.2	14.6	0	Sr – 1.9
ZnA	10.0	56.3	13.5	15.2	0	Zn – 3.6

Adventitious carbon was also present on all coatings analysed using XPS, as is common on apatite coatings. The XPS analysis was largely devoid of Ti signals, while low Ti levels were detected in the EDX analysis. This suggests that the low levels of Ti detected by EDX are due to high sampling depth (10 μm) of this method and not due to incomplete coverage of the surface by the apatite. This would suggest that the coating applied is less than 10 μm in thickness as reported elsewhere (O' Neill *et al.,* 2009). On the basis of the low levels of Ti in the EDX results, the Sr substituted materials appear to have a higher depth of surface treatment than the other materials.

Table 5.2: Elemental composition of coated samples via EDX (% atm).

Coating	O	P	Ca	Ti	Ion
HA	65.8	6.7	9.2	14.7	N/A
AgA	69	8.8	10.6	10.1	Ag – 0.6
SrA	68.4	13.0	15.6	1.6	Sr – 1.1
ZnA	68	11.0	12.7	4.5	Zn – 1.9

This is supported by gravimetric analysis which revealed a coating mass of between 0.32 and 1.6 mg/cm^2 per coupon, with the Sr substituted apatite coating exhibiting the greatest coating mass (Figure 5.1). The concentration of the dopant ions present in each coating was determined by dissolving the complete coating in acid and then determining the ionic concentrations using ICP analysis (Figure 5.2).

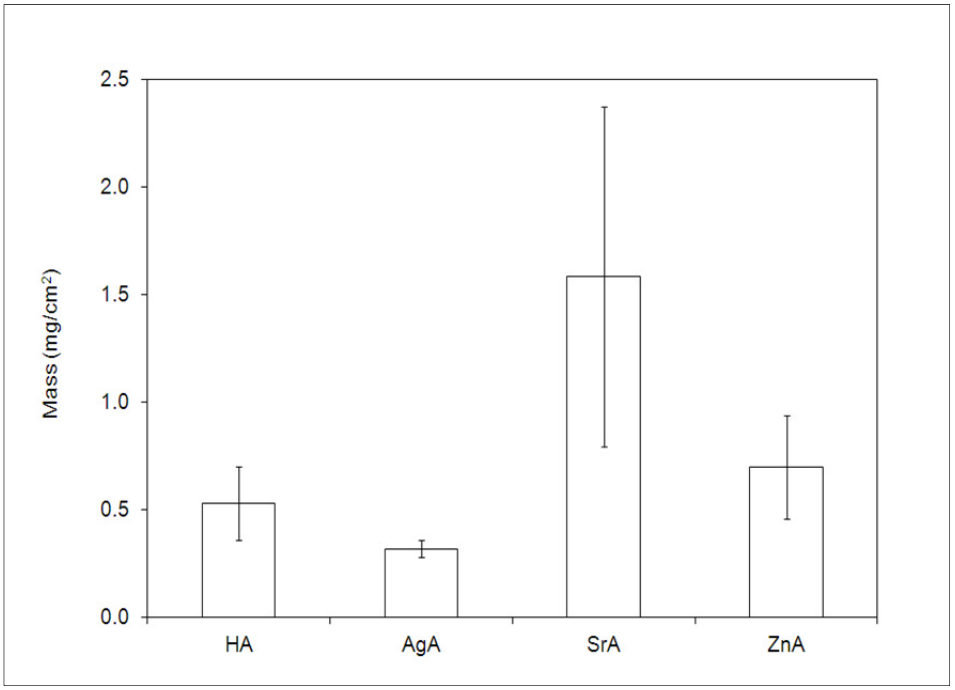

Figure 5.1: Coating mass of the various modifications (gravimetric analysis, n=3 samples ±2SD).

The combination of ICP ion levels, gravimetric analysis and low Ti readings in EDX suggests that the highest coating deposition rates were obtained for the Sr and Zn substituted materials, with lower levels of deposition being recorded for the HA and Ag substituted ceramics. This appears to correlate with the surface roughness values detected, with R_a values of 1.7, 2.2, 2.9 and 3.6 μm for HA, AgA, SrA and ZnA respectively (Table 5.3).

Table 5.3: Surface roughness analysis (Ra, n=3 samples).

Coating	Surface Roughness (μm) (±2SD)
Uncoated Ti	0.4±0.1
HA	1.7±0.3
AgA	2.2±0.3
SrA	2.9±0.3
ZnA	3.6±0.3

The surface roughness of SrA and ZnA were observed to be significantly greater compared to the HA ($p<0.01$) (Dunnett's test). In addition, there were significant differences ($p<0.01$) between all the substituted apatite surfaces using Tukey's post-hoc analysis. ICP was used to determine the concentration of ions released into PBS buffer from each coating. The % ion release was determined using the initial concentration of ions in the coating before elution (Figure 5.2) and the amount released in the elution samples over 30 days (Figure 5.3). As seen from Figure 5.3, low levels of ions were released over the 30 day period with ZnA producing the lowest level of dopant ion release.

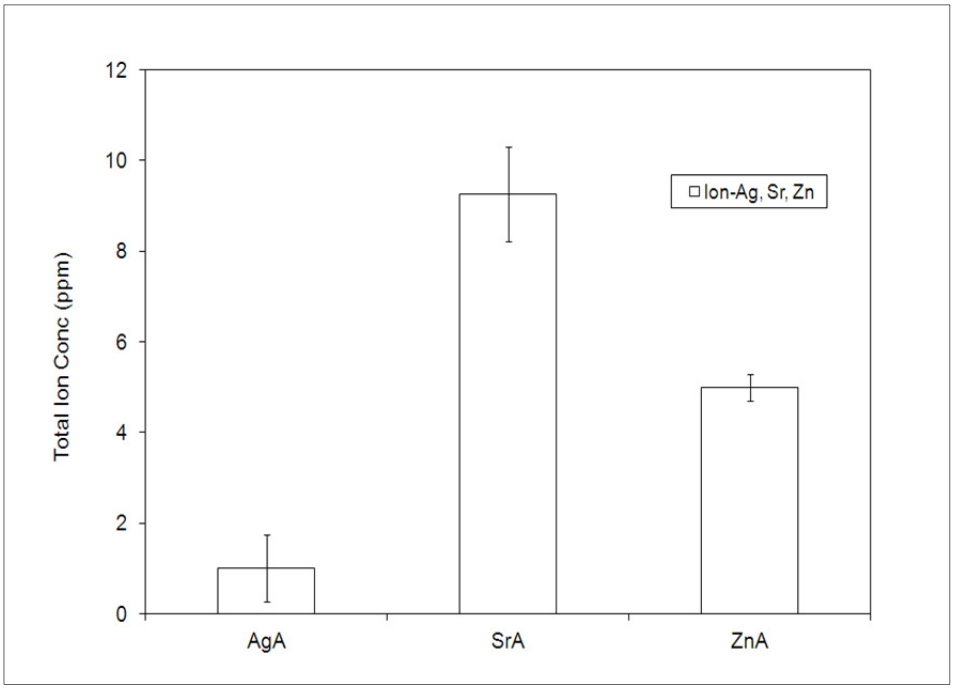

Figure 5.2: Concentration of dopant ion present in the coatings (ICP-OES analysis, n=3 samples ±2SD).

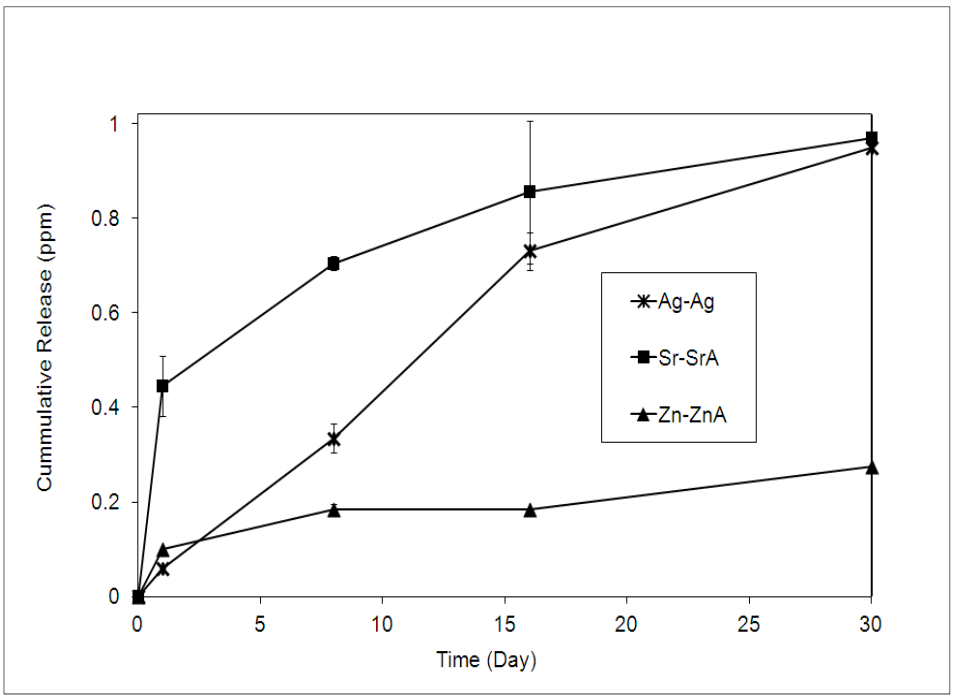

Figure 5.3: Cumulative ion release from the coatings over 30 days determined using ICP-OES (37 ºC, 150 rpm, n=3 samples ±2SD).

It was found that over 90% of the Sr and Zn still remained in the coatings at 30 days (Figure 5.4), whereas 90% of the Ag was released, which was found to have a direct impact on the antimicrobial properties of the treated surfaces.

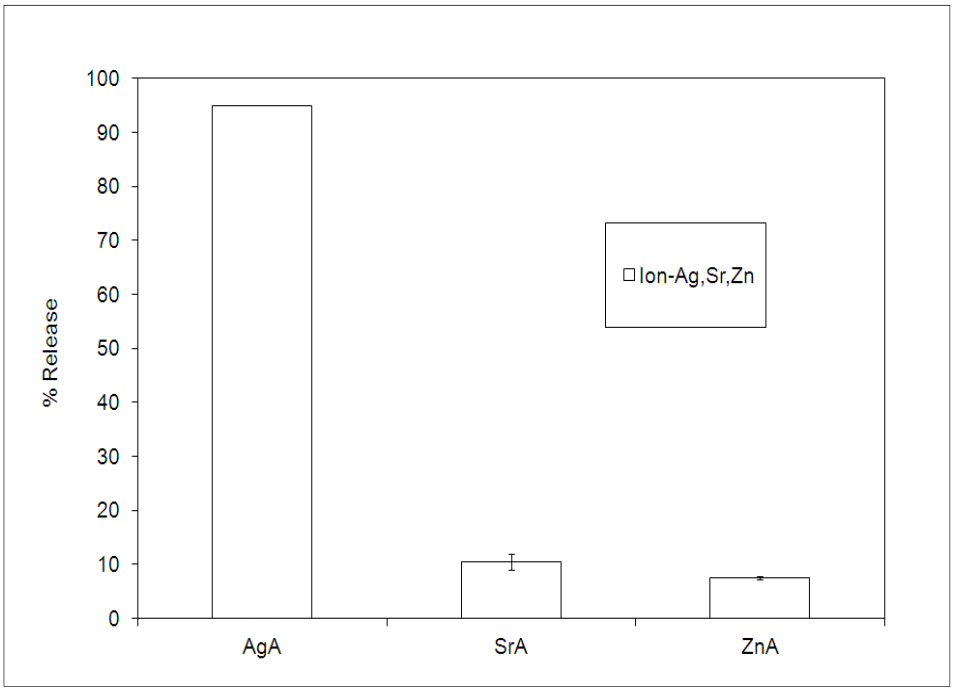

Figure 5.4: % Ion released from the various coatings over 30 days (37 ºC, 150 rpm, n=3 samples ±2SD).

5.3.2 Cell Proliferation and Cytotoxicity

The extent of osteoblast cell proliferation on the substituted apatite substrates is presented in Figure 5.5. Significant differences were noted between sample types at day 1 and 3 using one way ANOVA ($P<0.05$). After 1 day there was a significant increase in proliferative rates on the SrA surface ($p<0.01$) compared to the control HA surface. At day 3 there was also a significant increase in cell proliferation on both the SrA ($p<0.001$) and ZnA ($p<0.01$) surfaces in comparison to the control HA

surface, indicating that the surfaces possess osteoconductive potential. No evidence of cytotoxicity was observed using MG-63 cells on any of the samples evaluated.

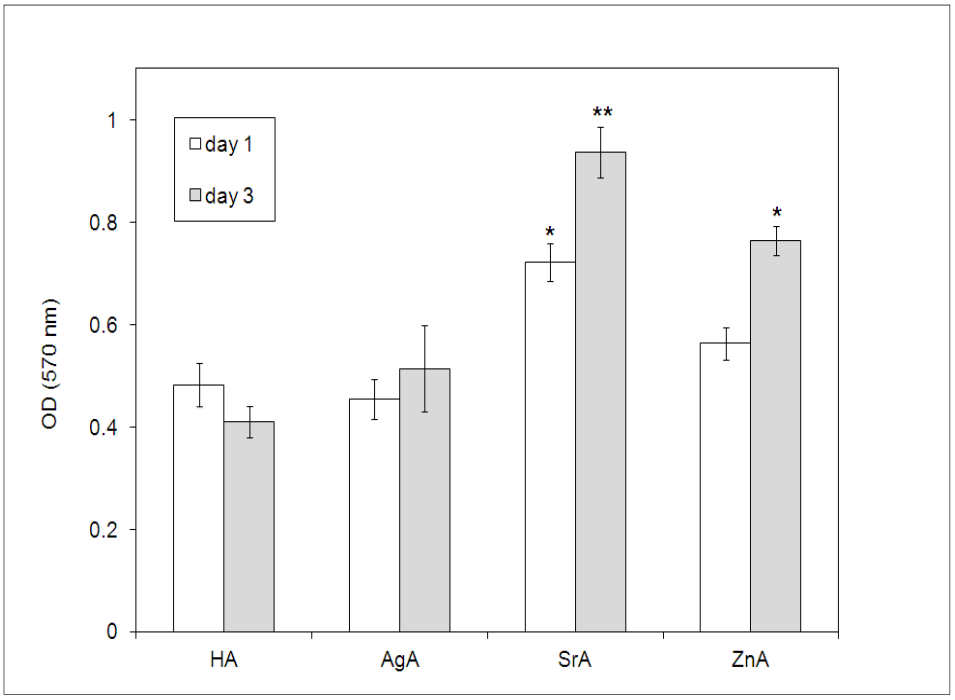

Figure 5.5: Optical density measurements for MG-63 cell proliferation after 1 and 3 days of incubation (n=4 samples ±SD) (* denotes statistical significance compared to the HA control ($p<0.01$) and ** represents statistical significance compared to the HA control ($p<0.001$) at respective time-points determined using Dunnett's test)

5.3.3 Antimicrobial Studies

The antimicrobial properties of the samples were determined for freshly prepared samples and for samples that were allowed to elute ions over 30 days. As can be seen from Figure 5.6, both AgA and SrA offer promising antimicrobial coatings with 57% and 49% kill respectively when freshly prepared. A significant difference was determined between sample types at day 0 ($p<0.05$ using one way ANOVA). The AgA surface was observed to have significant effect compared to HA control ($p<0.05$) prior to incubation (Dunnett's test). On the contrary, ZnA demonstrated

low antimicrobial performance (26% kill) against the Gram positive bacterium. After 30 days of incubation the antimicrobial surface activity of AgA had decreased to 9% bacteria cell reduction while the SrA activity remained unchanged (Figure 5.6). One way ANOVA revealed no statistical difference between samples at day 30 ($p>0.05$).

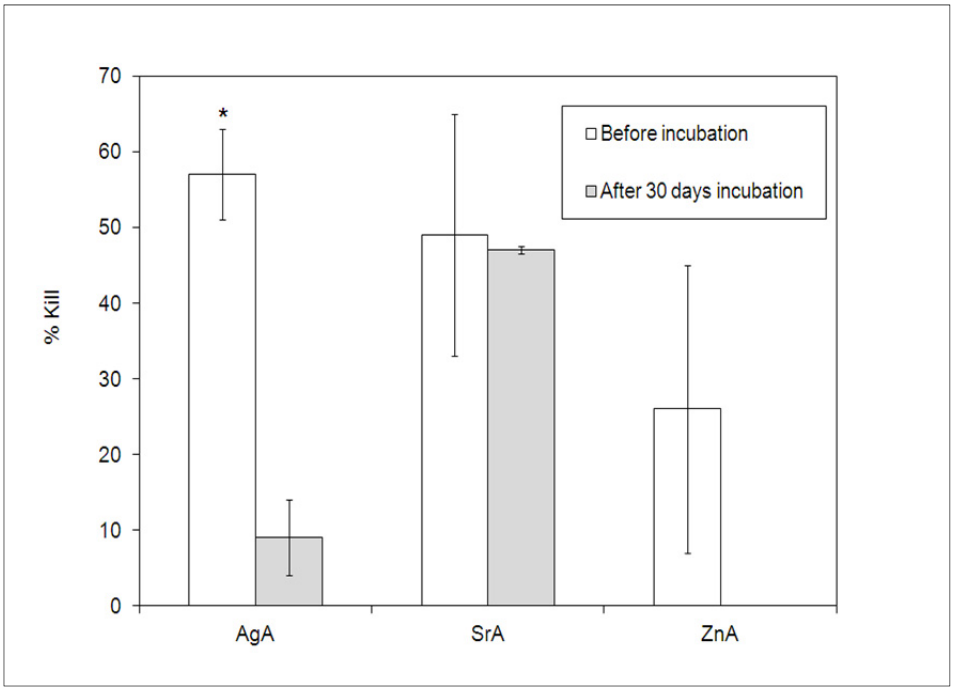

Figure 5.6: Antimicrobial activity of the coatings expressed as % kill using *S. aureus* as the bacterial challenge organism before and after elution at 30 days (n=3 sample ±SD) (* denotes statistical significance compared to HA control before incubation ($p<0.05$) determined using Dunnett's test).

As well as the antimicrobial properties of the coupons, the antimicrobial impact of the ions eluted from the coatings was also investigated by collecting the leachate and conducting a separate bacterial challenge and the results are displayed in Figure 5.7. In general, low antibacterial activity was observed for the leachate when compared

to results obtained from the non leach test. It was found that <26 % kill was obtained from the eluted ions irrespective of the surface under investigation.

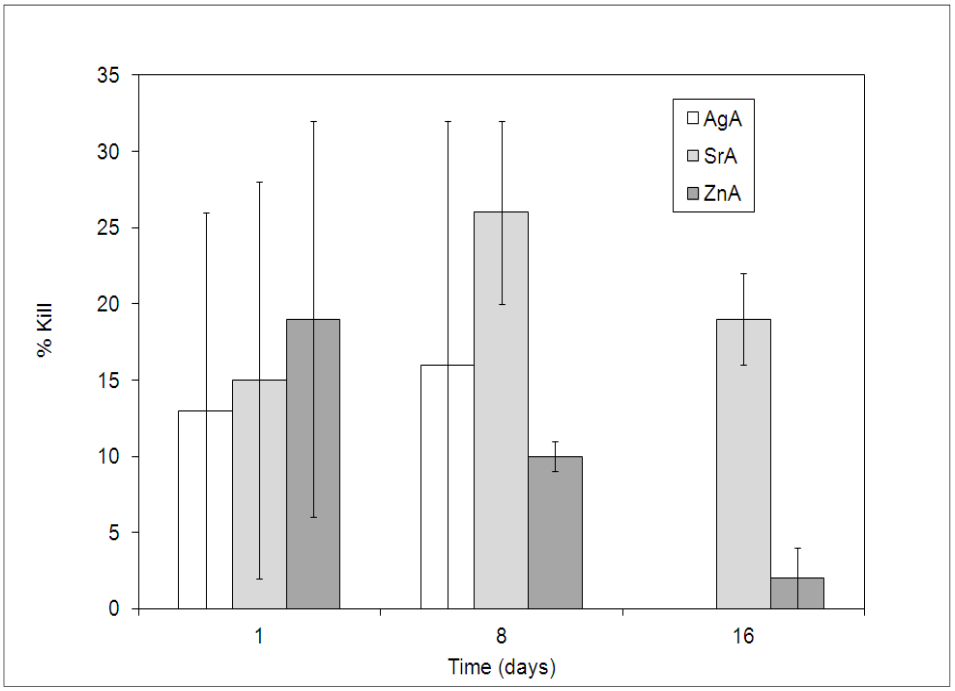

Figure 5.7: Antimicrobial activity of the released ion from the coatings expressed as % kill using *S. aureus* as the bacterium challenge (n=3 samples ±SD).

5.3.4 Anticolonising Studies

The ability of the surfaces to inhibit biofilm growth was also assessed over a 14 day period and the results are presented in Figure 5.8. All coatings produced a similar result at day 1 (32-42% biofilm inhibition). However, the Ag substituted apatite coating outperformed the other two surfaces at day 7 and 14. One way ANOVA revealed that there were no statistical differences between samples at day 1 and 30 ($p>0.05$). However, there was a significant reduction in bacterial numbers recovered from the AgA sample at day 7 compared to the control HA surface ($p<0.001$ using Dunnett's test).

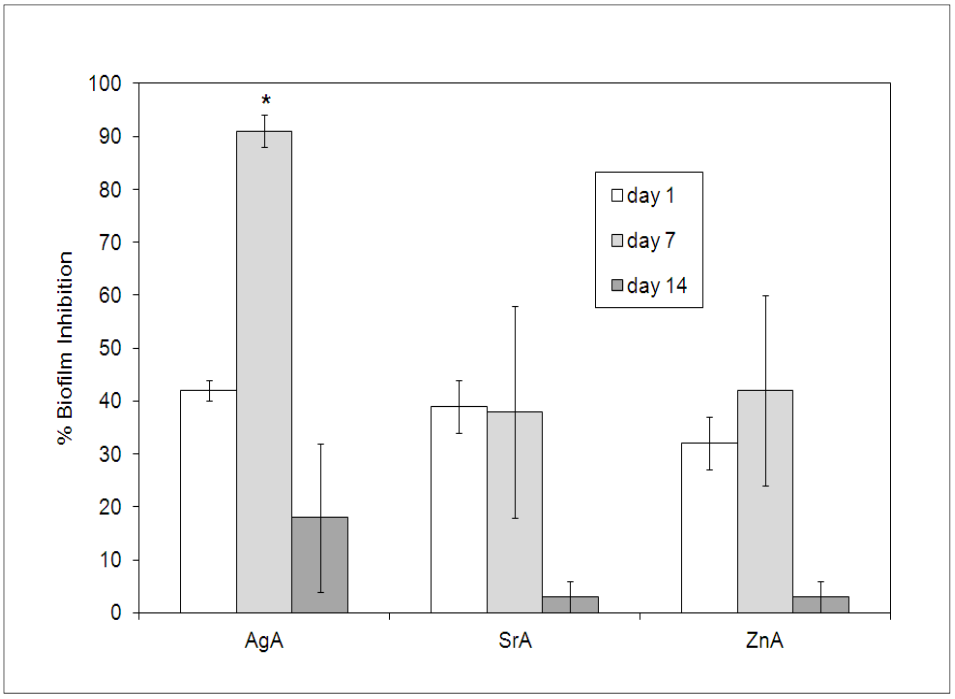

Figure 5.8: Anticolonising activity of the coatings expressed as % biofilm inhibition using *S. aureus* as the bacterium challenge (n=3 samples ±SD) (* denotes statistical significance between AgA surface and control HA surface at day 7 ($p<0.001$) determined using the Dunnett's test).

Fluorescent microscopy of the biofilm formation on the HA coated control and the AgA sample at day 7 can be seen in Figure 5.9. These images highlight the orange stained particles which represent the metabolically active bacterial cells on the surface. As can be seen, the AgA sample revealed reduced microbial colonisation compared to the HA coated control, as evidenced through dramatically reduced levels of viable bacterial cells on the Ag substituted surface.

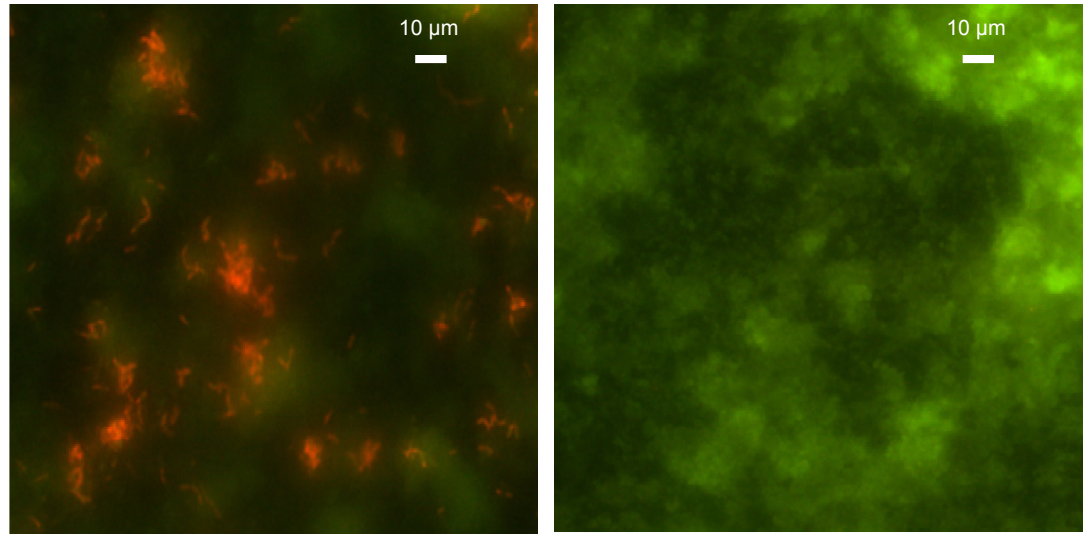

Figure 5.9: Fluorescent microscopy of biofilm formation at day 7 x400 magnification of (a) HA coated control coupon and (b) AgA coated titanium coupon. Orange fluorescence indicates cell attachments.

5.4 Discussion

Irrespective of which coatings are applied on hard tissue implants to enhance the osteointegration process, the hosts tissue cells (osteoblasts) and bacterial microorganisms compete for the implants surface in a process coined as "race to the surface" (Gristina, 1987). Bacteria capable of attaching to the implant surface, synthesise a matrix consisting largely of extracellular polysaccharides that encompasses the cells to form a biofilm which enables the bacteria to escape the effects of antibiotics therapy and host clearance. A colonised implant may rapidly result in chronic infection and the only successful treatment is removal of the infected implant (Van de Belt *et al.,* 2001). Inhibiting bacterial adhesion is regarded as the critical step in preventing implant associated infections thereby, promoting

tissue interactions with the implant (Jiranek *et al.,* 2006). This study strongly supports the potential future use of substituted apatites as orthopaedic and dental coatings which could combine excellent osteoconductive properties with the key function of infection prevention.

The CoBlast technique was used to deposit coating modifications of less than 10 μm resulted in this study. The combination of the ICP measurements, gravimetric analysis and low Ti readings in EDX suggests that the highest coating deposition rates were obtained for the Sr and Zn substituted materials, with lower levels of deposition being recorded for the HA and Ag substituted ceramics. Surface roughness is also a key parameter which governs cell attachment which leads to the subsequent cell proliferation stage. It has been reported that the CoBlast HA significantly increased the surface roughness of blank Ti which also demonstrated osteoblastic activity compared to an uncoated Ti surface (O'Hare *et al.,* 2010). In this study, it was found that the deposition of the substituted apatites significantly increased the surface roughness compared to the HA control with ZnA and SrA creating the greatest effect. This would suggest that the thicker and better coating coverage associated with both ZnA and SrA (EDX and gravimetric results) lead to increased surface roughness as more of the dopant was deposited.

The surfaces examined in this study were all shown to be cytocompatible with no evidence of cytotoxicity in the case of MG-63 osteoblast cells. The proliferation results (Figure 5.5) appear to agree with the findings of Capuccini *et al.,* who found that in comparison to a HA control surface there was an increase in osteoblast activity on strontium-substituted hydroxyapatite coatings on a Ti substrate

(Capuccini *et al.,* 2008). It has been suggested that Sr may affect cell replication by two possible mechanisms; through the triggering of mitogenic signalling pathways or the release of autocrine growth factors (Caverzasio, 2008). Ito *et al* have shown that the incorporation of Zn into implant materials may increase bone formation (Ito *et al.,* 2002). Low levels of Ag ions are known to be clinically safe, with systematic accumulation of 4-6 g required to produce cytotoxic effects in humans (Hardes *et al.,* 2007; Gosheger *et al.,* 2004). Exposure thresholds of 8.75 mmol/Kg/day of strontium produces toxic effects whereas no such data exists for Zn (D'Haese *et al.,* 2000). The ion elution data produced herein reveal low levels of ion release, <1 ppm, over the duration of the study, which would correlate with the lack of toxicity towards mammalian osteoblast cells observed *in vitro*.

Despite the absence of toxicity observed during the osteoblast proliferation study, the surfaces were found to have a significant toxic effect on bacterial cells which were in contact with the surface. While the ions eluted from the surface were found to have a low level of kill (Figure 5.7), the direct action of the modified surfaces on the bacteria produced measurable decreases in bacteria numbers for both the Ag and Sr substituted bioceramics (Figure 5.6). Zn was found to have minimal antimicrobial properties initially and after 30 days in solution had no measureable antibacterial effect against *S. aureus.*

In the case of the silver coatings, the antibacterial effect was found to diminish with time and the coatings had minimal antibacterial properties at day 30. The ion elution studies indicate that the low level of Ag ions (4%) remaining in the surface after 30 days elution is responsible for the reduced kill at this time point. Conversely, the

high levels of ions (90%) still present in the corresponding Sr substituted surface after 30 days would explain the retention of the antimicrobial properties of that surface over the 30 days of the trial.

It is interesting to note that the leachates were not found to perform as well as when the modified surfaces were in contact with the microbes. In part, this could be attributed to the fact that the concentration of the ions released within the test time periods examined (1, 8, 16 days) was low relative to the MIC of the challenge organism, *S. aureus*. The MIC for Ag and Zn has been reported to be 0.5 mg-10 mg/l and 200-500 ppb respectively, however no such data exists for Sr (Tapiero and Tew, 2005; Schierholz *et al.,* 1998). Indeed, Jung *et al.,* demonstrated that a Ag ion concentration of 0.2 ppm in solution is necessary to effect log reductions in a *S. aureus* test culture (Jung *et al.,* 2008). However, the ion release rates indicated in Figure 5.3 of this study, reveal that such a concentration would not accumulate in the coupon leachate until approximately 15 days of incubation.

On the basis of comparisons of the leaching and the non leach tests, the data presented herein suggests that the direct contact of microbes with the coating may be a significant contributing factor for the antibacterial activity of the samples, as the antimicrobial effect was significantly amplified by the presence of the substrate surfaces in the non leaching test. It has been reported that a dual antimicrobial mechanism exists for substituted apatites, where the antimicrobial action was not only attributed to the low release of ions but also from the generation of the free radicals from the apatite surface (Matsumoto *et al.,* 2009; Hu *et al.,* 2007). However, the mechanisms of kill may not be the same for each of the materials evaluated

herein and possible antimicrobial mechanisms are discussed below for each of the surfaces.

From the results obtained, the release of Ag ions from the AgA coating would appear to contribute to the antimicrobial response, which is in agreement with the literature (Kim *et al.,* 1998). However, the poor performance of the leachate in comparison to the potency of the direct contact with the surface (non-leach test) suggests other mechanisms of antimicrobial action may also be responsible for the activity of silver containing surfaces. It is important to note that high local concentrations of Ag ions at the surface of the coupon may be responsible for the higher potency observed during the non-leach studies compared to the leachate studies.

The mechanistic action of Sr ion is less well understood than that of Ag. Previous studies have shown antibacterial effects of Sr ions released from glass cements and also Sr containing hydroxyapatites (Liu *et al.,* 2008; Guida *et al.,* 2003). Little is currently known with respect to microbial resistance to Sr, as only a limited number of published studies on the *in vitro* or *in vivo* antibacterial applications of the ion are available (Liu *et al.,* 2008; Guida *et al.,* 2003). However, the results suggest a significant potential for SrA coatings to be further investigated/developed in antimicrobial applications given the sustained antibacterial impact observed in this study, when compared with AgA coatings. Moreover, the beneficial effect of Sr ions on osteoblast cells creates the possibility to produce a surface which inhibits microbial colonisation while simultaneously promoting osteointegration, thereby providing an optimal surface for orthopaedic and dental implant fixation. Poor antibacterial effects of Zn compounds against *S. aureus* have been previously

reported (Kim *et al.,* 1998) and in the current study, ZnA coatings were not found to have significant antimicrobial impact in both leach and non-leach antimicrobial tests.

The % biofilm inhibition attributed to the various coatings assessed over a 14 day period illustrated the anti-colonisation potential of the surfaces. The anticolonising results revealed that the AgA coating had the greatest impact in preventing microbial attachment compared to the other coatings. Both the SrA and ZnA coatings produced similar anticolonising performance, although the impact was less effective than AgA after day 1. Subsequent qualitative analyses by fluorescence microscopy indicated that the AgA coating effectively prevented *S. aureus* attachment, as opposed to inhibiting the proliferation of attached cells as indicated by less orange stained cells compared to the HA, Figure 5.9. These observations correlate well with the earlier non-leach test results, suggesting the importance of microbe coating surface interactions in the observed antibacterial impact.

It is generally accepted that the surface topography of the implants is one of the most important parameters that influence cellular reactions. In this study the surface composition played more of an important role in cellular adhesion and the subsequent proliferation was clearly evident in the MTT assay results. In addition, the less rougher surface of the control, HA sample, was observed to be more susceptible to colonisation in comparison to the rougher substituted apatite samples as seen in the % kill. Direct surface-bacteria interaction appears to control the colonisation process and is mediated through the impact of the dopant ion. This interaction appears to dominate the colonisation process irrespective of any surface topography or ion elution effects.

5.5 Conclusions

A series of substituted apatites (AgA, SrA, ZnA) were effectively deposited onto biomedical grade titanium metal. The study presented demonstrates that the surface treatments investigated offer the dual benefits of cytocompatible properties essential for bone integration with the added potential of microbial colonisation inhibition without cyctoxic effects. The direct contact of the microbes with the coating may be a significant contributing factor to the anticolonising activity of the samples, as it was shown that the antimicrobial effect was significantly amplified by the presence of the substrate surfaces. AgA was observed to out-perform both the SrA and ZnA in terms of biofilm inhibition. Further optimisation of the coating performance can be achieved through varying the loading of the dopant ion, tailoring the elution profile and controlling the surface morphology. These novel coatings possess new opportunities in orthopaedic and dental applications for impeding infection while enhancing osteointegration, thereby increasing the success rate and improved patient outcomes for hard tissue implants.

Chapter 6

6.0 Evaluation of Increased Ion Concentration on the Antimicrobial and Anticolonising Properties of Substituted Apatite Coatings

Abstract:

Biomaterial associated infections (BAI) pose a challenge for coatings on hard tissue implants. 12% wt apatitic powders substituted with silver (AgA), strontium (SrA) or a co-substituted silver-strontium (AgSrA) were deposited. A novel ambient temperature blasting process was used to deposit substituted apatites onto biomedical grade titanium (V) metal. The potential use of these coatings as an infection preventing strategy for application on hard tissue implants was assessed. Surface physicochemical properties were determined using EDX, ICP-OES and surface proliferometry in addition to surface cytocompatibility assessments using an MG-63 osteoblast cell line. The antibacterial potential of both the eluted and surface immobilised Ag ion to inhibit the growth of a number of clinically relevant strains was investigated. Strontium demonstrated enhanced osteoblast proliferation, however, a lower inhibition of biofilm (*S. aureus*) was observed at day 1 compared to the other surfaces. AgA exhibited sustained anticolonising activity over the 14 days with log reduction in CFU achieved. The effects of the co-substituted AgSrA did not show enhanced osteoconductive potential or anticolonising properties compared to the SrA and AgA surfaces, respectively. As a result of the promising anticolonising activity of the AgA, its impact against clinical isolates (*MRSA, MSSA* and *S. epidermis*) was also investigated. The results revealed that the AgA surface demonstrated good antibacterial activity (eluted and immobilised ion) against *MRSA* followed by *MSSA*, however only good anticolonising activity was observed at day 1 against *MRSA*. The AgA surface displayed poor impact against *S. epidermis* compared to the other clinical isolates examined. AgA demonstrates promising potential as a coating to combat biomaterial associated infections.

6.1 Introduction

Common clinical problems such as poor bone-implant integration and long term stabilisation result from the formation of BAI. Bacterial adherence to biomaterials appears to be a pivotal step in the pathogenesis of such infections as it results in the formation of a biofilm. Extensive research has been performed to develop surfaces for orthopaedic and dental applications, which inhibit bacterial attachment and subsequent biofilm formation. Moreover, much interest exits in antimicrobial bioceramic surfaces that enhance tissue integration and resist microbial colonisation.

Studies using antimicrobial ions such as silver (Ag), zinc (Zn), copper (Cu) and strontium (Sr), which were formulated into calcium phosphate (CaP) materials have shown positive *in vitro* results against different bacterial micro-organisms *(Staphylococcus aureus (S. aureus), Pseudomonas aeruginosa, Escherichia coli, Staphylococcus epidermis (S. epidermis))* (O'Sullivan *et al.,* 2010; Matsumoto *et al.,* 2009; Chen *et al.,* 2008; Lin *et al.,* 2008; Zhou *et al.,* 2008; Hu *et al.,* 2007). The release of Ag ions ensured excellent antibacterial activity (95% kill) from silver containing hydroxyapatite (HA) coating against *S. aureus* (Chen *et al.,* 2008) and similar findings were observed in other studies (O'Sullivan *et al.,* 2010). Recently, it has been reported that Ag loaded HA demonstrated good osteogenic properties with low toxicity *in vitro* (Roy *et al*., 2012; Sandukas *et al*., 2011; Ruan *et al.*, 2009). Antibacterial activity against MRSA *in vitro* (Ando *et al.*, 2010) and *in vivo* (Shimazaki *et al*., 2010) has also been reported. The redox nature of the Ag and Cu formulated into HA was responsible for producing radicals and together with released antibacterial ions were responsible for its antibacterial activity (Hu *et al.,*

2007). A synergistic effect was observed by Matsumato *et al.* when a co-substituted HA apatite consisting of AgZn or AgCu was used (Matsumoto *et al.,* 2009).

In **Chapter 5**, CoBlast was used to deposit a series of substituted apatites (5% wt AgA, ZnA and SrA) on Ti substrates. AgA was observed to outperform the other samples analysed while SrA demonstrated enhanced osteoblast proliferation. It was found that 5% wt AgA exhibited promising results in preventing microbial attachment over a 14 day period with 91% biofilm inhibition at day 7.

In this study, 12% wt AgA and SrA was assessed for improved performance compared to the lower substituted ion content (5% wt). Additionally, based on the promising results in earlier studies a co-substituted apatite incorporating Ag and Sr (AgSrA) at a concentration of 12% wt was also examined. A preliminary study was undertaken to investigate the anticolonising and osteoconductive potential of a series of apatite surfaces HA, AgA, SrA and AgSrA using a standard strain *S. aureus* (ATCC 1448) and MG-63 osteoblast cells, respectively. This was performed to define the best surface for subsequent microbial studies using clinical isolate strains relevant for orthopaedic applications. The efficacy of the chosen surface was examined using methicillin resistant *S. aureus* (*MRSA*), methicillin susceptible *S. aureus* (*MSSA*) and *S. epidermis*. The isolates used in this study were isolated from device-related infections by the clinical microbiology laboratory of Beaumont Hospital, Dublin, Ireland.

6.2 Materials and Methods

The materials and methods used in this chapter are summarised in **Chapter 2**. Surface characterisation techniques were employed to analyse the CoBlast surfaces (HA, AgA, SrA, AgSrA). This included elemental composition (EDX (n=3 samples), ion concentration (ICP-OES (n=3 samples), surface roughness (Taylor Hobson, (n=3 samples). The *in vitro* ion release from the surfaces into PBS over 30 days (days 1, 7, 14 and 30) were analysed using ICP-OES (n=3 samples). The MG-63 cell proliferation was determined by measuring the optical density (OD) after 1 and 4 days incubation to determine osteoblast cell viability as an indication of osteoconductivity and surface toxicity (n=3 samples). To investigate the anticolonising activity of the substituted apatite coatings, an initial quantitative assessment of biofilm formation on the coated coupons was carried out at day 1 and 14 after incubation in LB broth using *S. aureus* (ATCC 1448) as the bacterial challenge organism. Following this analysis, one CoBlast surface was chosen for further microbiological studies using clinical isolates as outlined in **Section 2.6**. The antimicrobial efficacy of the released ion into PBS at different time points (7, 14, 30 days) was assessed (n=3 samples). The antimicrobial effects of the surface immobilised ion before and after incubation at various time points (7, 14, 30 days) was assessed (n=3 samples). Finally, the anticolonising activity of the CoBlast surfaces at day 1 and 14 were assessed.

One way analysis of variance (ANOVA) was used to determine statistical differences between samples, with p values <0.01 deemed significant. Comparison

with HA was performed using Dunnett's test (surface roughness (Ra), anticolonising data using *S. aureus*). Tukey's post-hoc analysis was used to determine statistically significant differences between substituted apatite samples (surface roughness (Ra)). Kruskal-Wallis test was conducted to determine if there was a significant difference between samples. Where significant levels of $p<0.05$ were determined, Dunn's test was performed (MTT assay). Mann-Whitney U test was performed to compare two samples (antimicrobial activity and anticolonising data using the clinical isolates).

6.3 Results

6.3.1 Surface Characterisation

EDX analysis was carried out to determine the elemental composition of the coatings. The results obtained are presented in Table 6.1, which illustrates that the surfaces are composed largely of calcium (Ca), phosphorous (P) and oxygen (O). The underlying Ti substrate was not observed for the SrA and AgSrA coatings indicating that good coverage and a thick coating was deposited (10 μm). However, the Ti levels of AgA and the HA control was determined to be 9% atm and 20% atm respectively suggesting that the thinnest coating was obtained for AgA. The substituted ion concentrations in the coatings were determined to be 1 and 5 % atm for the AgA and SrA coatings respectively, whereas the AgSrA coating was composed of 1 % atm Ag and 3 % atm Sr. ICP-OES analysis of the coatings revealed similar trends. The levels of Sr ion present in SrA and AgSrA were observed to be higher than the Ag content in AgA and AgSrA. The surface roughness values obtained, outlined in Table 6.1, reveal that the substituted apatite coatings were

significantly rougher (2.0-2.3 μm) ($p<0.05$) compared to the HA control (1.2 μm) (Dunnett's test). However, there was no significant difference between the substituted apatite samples ($p>0.05$) (one way ANOVA).

Table 6.1: Surface characterisation of the coated samples including EDX, surface ion concentration, surface roughness and % ion release at day 30 (n=3 samples). Surface roughness, surface ion concentration and % ion release values are reported ±2SD.

	SEM-EDX (% atm)					Surface roughness	Ion (ppm)	% Ion Release at day 30
Coating	O	Ca	P	Ti	Ion	Ra (μm)	(ICP-OES)	(ICP-OES)
HA	65	12	15	9	N/A	1.2±0.2	N/A	-
AgA	64	7	8	20	1	2.2±0.5	7.0±0.4	17±5
SrA	68	12	15	0	5	2.0±1.0	55.0±22.9	6±3
AgSrA	68	13	15	0	1-Ag, 3-Sr	2.3±0.5	7.0±0.5 Ag, 30.0±0 Sr	16±1 Ag, 13±2 Sr

In vitro ion release in PBS over 30 days was quantified using ICP-OES (Figure 6.1). The total ion release at day 30 expressed as a percentage of total ion content present in the coated sample is listed in Table 6.1. There was a linear release of the Ag ion from the AgA coating from 0.3 ppm at day 1 to 1.2 ppm at day 30 (R^2=0.9922), which corresponded to 17% of the total Ag ion present in the coating being released. A lower % ion release was observed for the SrA coating with 6% Sr release at day 30 (3.4 ppm). Both the concentration of Sr and Ag ions from the AgSrA coating were seen to gradually increase from day 1 (0.3 ppm Ag, 1.8 ppm Sr) to day 30 (1.1 ppm Ag, 4 ppm Sr). The overall % ion release from the AgSrA coating at day 30 was determined to be 16% Ag and 13% Sr. Similar % Ag release was noted, with higher

% elution of Sr ions from the AgSrA surface when compared to the single doped samples (Table 6.1).

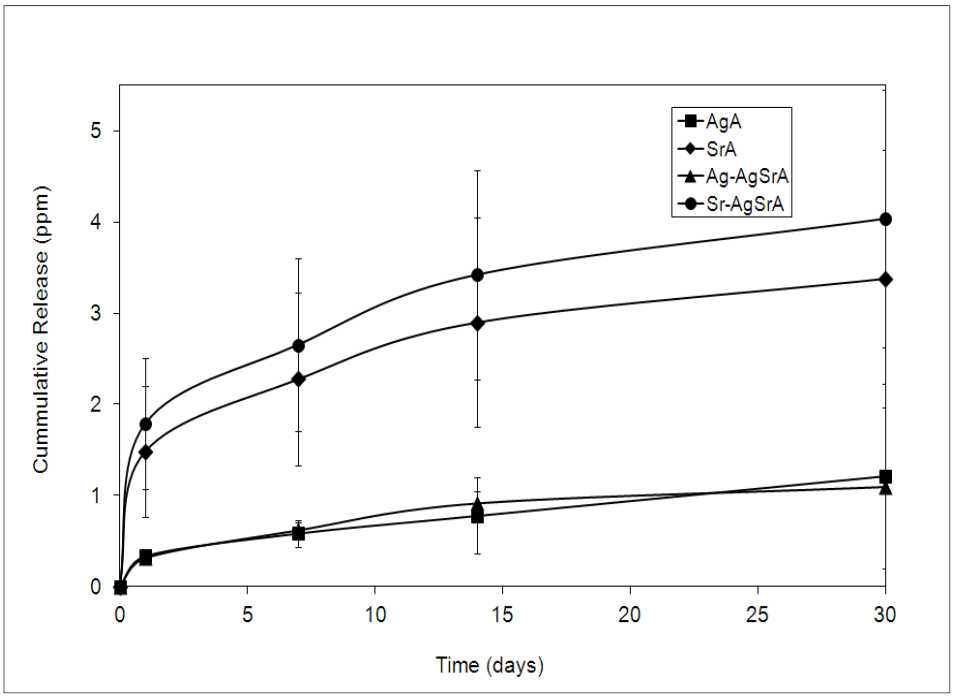

Figure 6.1: Ion release from the substituted apatite samples over 30 days as determined by ICP-OES (n=3 samples ±2SD).

6.3.2 Cell Proliferation and Cytotoxicity

Cytocompatibility of the modified surfaces was determined via a MTT assay and the osteoblast proliferation results are presented in Figure 6.2. Significant differences between samples for day 1 and 4 were noted using the Kruskal Wallis test ($p<0.05$). After day 1 and 4, SrA was seen to have a significant impact on cell viability ($p<0.01$) compared to the HA control surface indicating the osteoconductive potential of this coating (Dunn's test). At day 1 and 4, the cell proliferation results of the AgA and the AgSrA surfaces were comparable to the HA surface with no statistical differences noted ($p>0.05$) (Dunn's test). The combination of Ag with Sr

in the AgSrA coating resulted in decreased MG-63 cell proliferation on the surface compared to the SrA sample at day 1 and 4. Irrespective of these finding, cell proliferation was observed on all surfaces at day 4, however AgA and AgSrA did not match the performance of the well documented osteoconductive HA surface (Arinzeh et al., 2005; Borsari et al., 2005; Stoch et al., 2005). There was no evidence of cytotoxicity observed using MG-63 cells on any of the surfaces assessed.

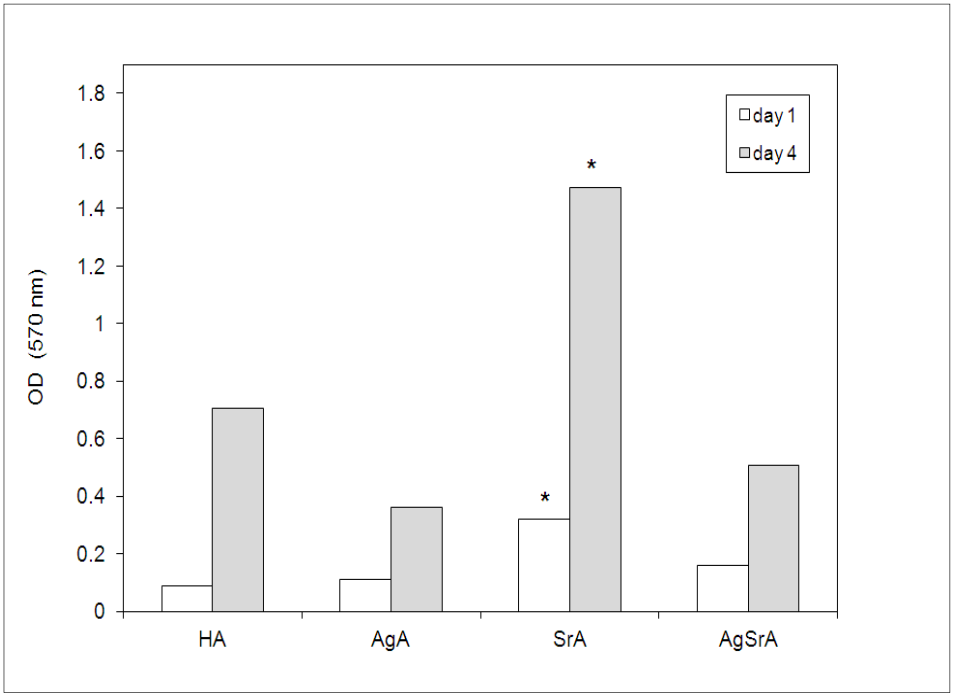

Figure 6.2: Optical density measurements of MG-63 osteoblast cells at day 1 and day 4 (n=3 samples with median values presented) (* denotes statistical significance compared to the HA control ($p<0.01$) using Dunn's test).

6.3.3 Preliminary Study to Ascertain the Best Anticolonising Coating Using a Standard Strain

The anticolonising behaviour of the 12% wt substituted apatite coatings at day 1 and 14 (Figure 6.3) was evaluated using *S. aureus* in order to select the 12% wt coating with the most promising anticolonisation potential for subsequent microbiology characterisation using clinical isolate strains (CFU data presented in **Appendix III**).

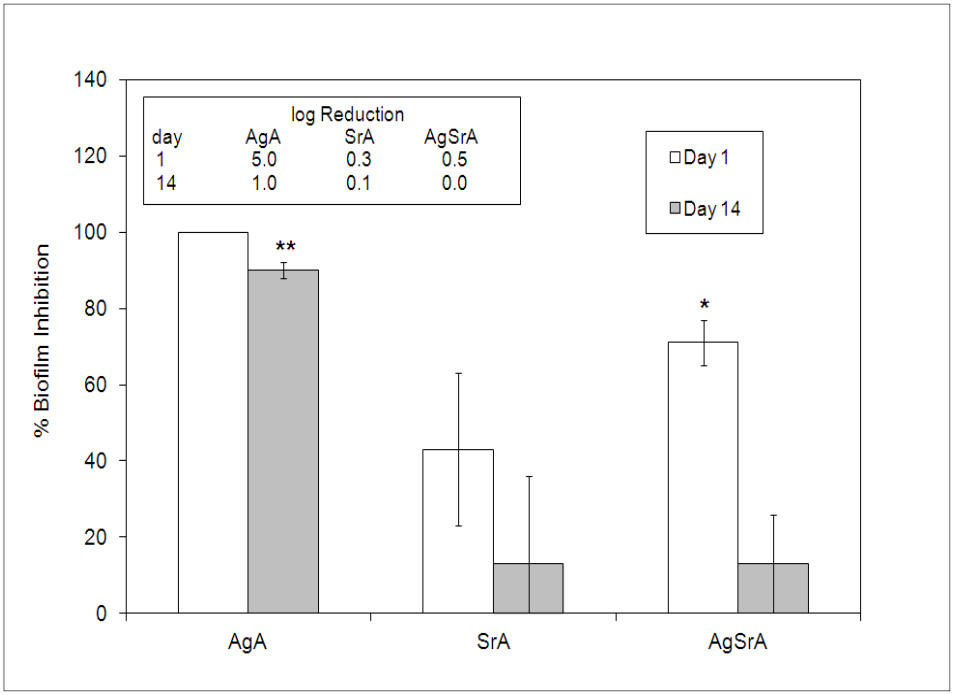

Figure 6.3: Anticolonising activity of the coatings using *S. aureus* as the challenge organism (ATCC 1448) at day 1 and 14 (n=3 samples ±SD) (* denotes statistical significance compared to the HA control ($p<0.05$) and ** represents statistical significance compared to the HA control ($p<0.01$) at respective time points using Dunnett's test). Inset, the log reduction in CFU is also presented.

AgA was found to demonstrate a 100% biofilm inhibition at day 1 and was statistically significant ($p<0.01$) at day 14 (90% biofilm inhibition) (Dunnett's test).

In addition, a significant anticolonising impact ($p<0.05$) was revealed for the AgSrA surface at day 1. As can be seen from Figure 6.3, the AgA coating was observed to give the best performance in preventing microbial attachment as indicated by the % biofilm inhibition data and the log reduction in CFU data over the time scale.

Despite the favourable impact on the viability of osteoblastic cells demonstrated by SrA, it exhibited the lowest anticolonising performance compared to the other surfaces analysed (0.3-0.1 log reduction in CFU). As a result of the promising osteoconductive potential of the 5% wt SrA and the anticolonising activity of the 5% AgA and SrA surfaces evaluated in a previous study (O'Sullivan *et al.*, 2010), a combination apatite AgSrA, was specifically investigated for improved performance in this study. As the Ag concentration and release profile of the AgSrA were similar to the AgA surface (Table 6.1 and Figure 6.1), it was expected to perform at least as well as AgA if not better due to the potential for a synergistic effect by incorporating Sr in the AgSrA coating. The AgSrA resulted in 71% biofilm inhibition at day 1 however, this was observed to decrease to 13% at day 14 and to perform better than SrA at day 1 only. The outcome from this study was that 12% wt AgA surface was chosen for subsequent antimicrobial and anticolonising studies using clinical isolate strains.

6.3.4 Antimicrobial Studies

In this study, the microbial impact (expressed as CFU, % kill and log kill) of the released Ag ion from the coupon surface as well as from the immobilised ion on the 12% wt AgA surface was investigated. The antibacterial effect of the released Ag ion towards the clinical isolates is given in Table 6.2.

Table 6.2: Antimicrobial activity of the released Ag ion from AgA coating using clinical isolates (*MRSA, MSSA, S. epidermis)* as the bacterial challenge organisms (n=3 samples with median values presented for CFU which was used to calculate the % kill and log kill).

		day 7			day 14			day 30		
Strain	Sample	CFU median	% kill	log kill	CFU median	% kill	log kill	CFU median	% kill	log kill
MRSA	HA	3.1E+06	-	-	7.0E+06	-	-	5.7E+06	-	-
	AgA	3.3E+04	99	2.0	2.5E+03	100	3.4	5.3E+05	91	1.0
MSSA	HA	8.3E+06	-	-	2.9E+07	-	-	1.5E+07	-	-
	AgA	5.1E+06	39	0.2	2.0E+06	93	1.2	4.0E+06	73	0.6
S. epidermis	HA	1.9E+07	-	-	1.7E+07	-	-	1.7E+07	-	-
	AgA	4.0E+06	79	0.7	1.0E+06	94	1.2	5.0E+06	71	0.5

The released Ag ion exhibited excellent antimicrobial activity against *MRSA* over the 30 days (91-100%), which corresponds to >1 log reduction in CFU observed over the time period. Statistical analysis revealed significant differences ($p<0.05$) between AgA and HA at day 7 and 30 (independent-sample Mann-Whitney U test). The susceptibility of *MSSA* ranged between 39-93% whereas the released Ag ion demonstrated a 71-94 % bactericidal effect against *S. epidermis*. A lower reduction in CFU (log kill) for the *MSSA* and *S. epidermis* isolates compared to the *MRSA* with maximum impact achieved at day 14 in both cases was observed.

The antibacterial activity of the Ag ion immobilised on the surface against the clinical isolates strains prior to and after incubation in PBS (7-30 days) is presented in Table 6.3. This analysis represents the bactericidal activity of the ions present on the surface which are in direct contact with the bacteria before and after ion elution. Before incubation in PBS, the impact of the AgA surface was determined to be 98%,

94% and 92% against *MRSA*, *MSSA* and *S. epidermis*, respectively, Table 6.3. Statistical analysis revealed significant surface impact at day 0 for AgA against MRSA ($p<0.05$) (Mann-Whitney U test). Following incubation, the surface effect of the residual Ag ion at day 14 maintained an excellent antibacterial effect (100%) against the *MRSA* cells, however this was seen to reduce to 73% kill at day 30. The impact of the AgA surface against *MSSA* and *S. epidermis* ranged between 88-94% over the 14-30 day incubation period which approximates to a log reduction in CFU values of 1.

Table 6.3: Antimicrobial activity of the immobilised ion in the AgA coating against clinical isolates (*MRSA, MSSA, S. epidermis* as the bacterial challenge organisms before (day 0) and after coupon incubation for 14 and 30 days (n=3 samples with median values presented for CFU which was used to calculate the % kill and log kill).

incubation		day 0			day 14			day 30		
Strain	Sample	CFU	% kill	log kill	CFU	% kill	log kill	CFU	% kill	log kill
MRSA	HA	2.8E+06	-	-	4.2E+06	-	-	1.5E+07	-	-
	AgA	6.4E+04	98	1.6	1.00E+00	100	6.6	4.0E+06	73	0.6
MSSA	HA	9.7E+06	-	-	1.8E+07	-	-	1.9E+07	-	-
	AgA	6.0E+05	94	1.2	1.0E+06	94	1.3	2.0E+06	89	1.0
S. epidermis	HA	8.9E+06	-	-	1.9E+07	-	-	1.9E+07	-	-
	AgA	7.5E+05	92	1.1	2.0E+06	89	1.0	2.33E+06	88	0.9

6.3.5 Anticolonising Studies

The anticolonising effect of the AgA coating against the clinical strains *MRSA* and *MSSA* is presented in Figure 6.4 (CFU data is presented in **Appendix III**). This analysis focuses on the combination of the immobilised surface ion and ion release

to prevent bacterial attachment. The AgA was seen to inhibit *MRSA* biofilm growth by 90% at day 1 which reduced to 54% at day 14. Whereas biofilm formation associated with *MSSA* growth was inhibited by 50% at day 1, no impact was observed at day 14. The AgA surface was not seen to demonstrate any inhibitory activity against *S. epidermis* attachment over the 14 days (0% biofilm inhibition). The only log reduction in bacteria attachment achieved was at day 1 against *MRSA,* however statistical analysis revealed no significant differences between samples at the different time points ($p>0.05$ using the Mann-Whitney U test).

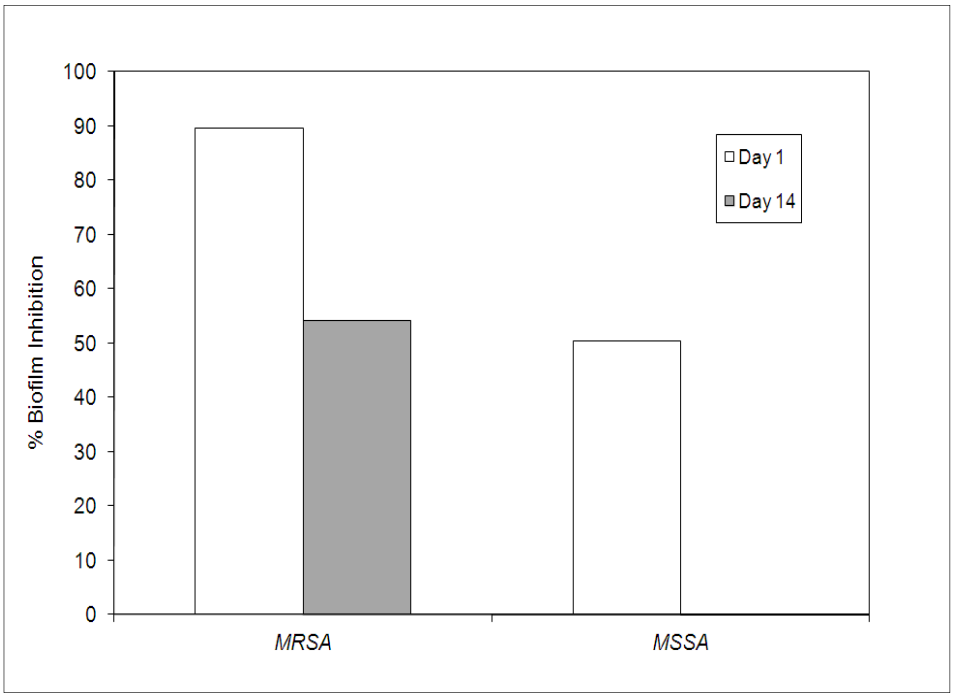

Figure 6.4: Anticolonising effect of the AgA coating using the clinical strains *MRSA* and *MSSA* as the bacteria challenges. *S. epidermis* is not presented here as it failed to inhibit biofilm formation (n=3 samples).

Fluorescent microscopy of the biofilm formation on the HA control and the AgA substrates at day 1 using the three clinical isolate strains can be seen in Figures 6.5-

6.7. The orange stained particles seen in these images indicate the presence of metabolic active bacterial cells. In the case of surfaces incubated with *MRSA* it can be seen that a reduced number of microbial colonies are attached to the AgA surface (Figure 6.5 (b)), compared to the control HA surface (Figure 6.5 (a)). Evidence of a reduction in metabolically active *MSSA* cells was observed on the AgA surface (Figure 6.6 (b)) compared to the HA control (Figure 6.6 (a)). However, this was not observed in the case of the *S. epidermis* strain Figure 6.7. These images suggest that AgA performed the best against *MRSA* which supports the findings as detailed in Figure 6.4.

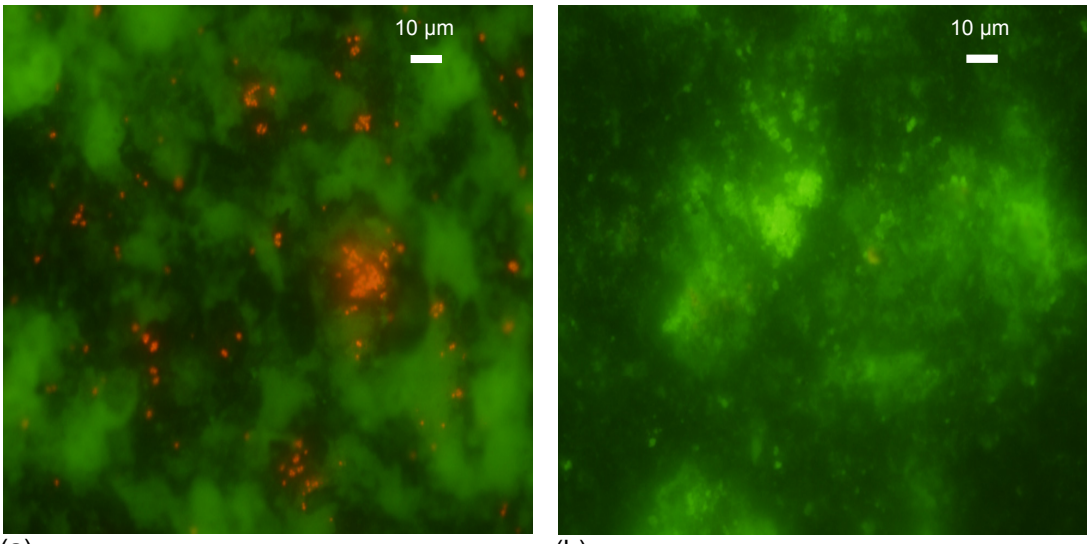

Figure 6.5: Fluorescent microscopy of biofilm formation at day 1 x400 magnification using *MRSA* as the bacterial challenge organism on the (a) control HA coating and (b) AgA coating.

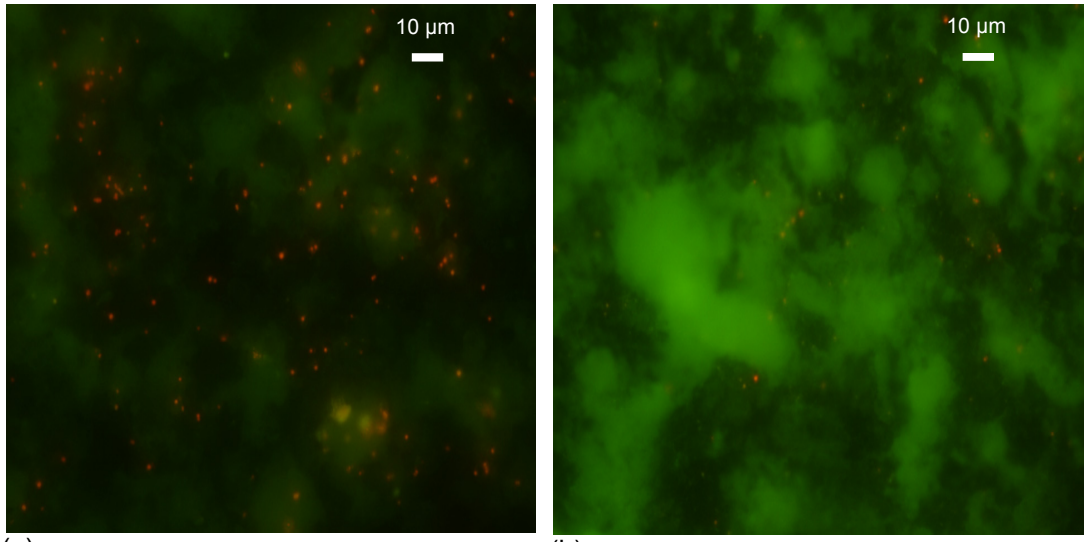

Figure 6.6: Fluorescent microscopy of biofilm formation at day 1 x400 magnification using *MSSA* as the bacterial challenge organism on the (a) control HA coating and (b) AgA coating.

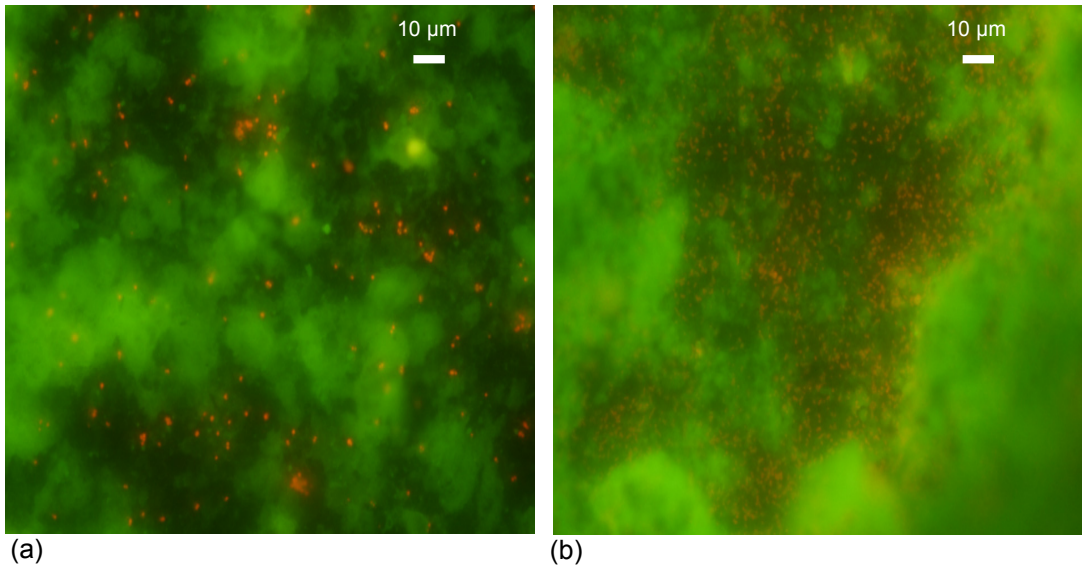

Figure 6.7: Fluorescent microscopy of biofilm formation at day 1 x400 magnification using *S. epidermis* as the bacterial challenge organism on the a) control HA coating and b) AgA coating.

6.4 Discussion

It is well established that biofilm formation, characterised by micro-colonies enveloped in a protective extracellular biopolymer matrix is often associated with implant infection. Such infections are caused by bacteria introduced from trauma, surgery, implant use, by direct colonisation from a proximal infection or via systemic circulation (Wu and Grainger, 2006; An and Friedman, 1996). Biofilm forming bacteria exhibit increased protection from the hosts defence mechanism and enhanced resistance to antibiotic treatment (Zilberman and Elsner, 2008; Hetrick and Schoenfisch, 2006; Rupp *et al.,* 1999; Van de Belt *et al*., 1999) which drastically leads to the failure in eradicating BAI. A large proportion of all BAI are caused by the gram positive staphylococcus genus, *S. aureus* and *S. epidermis* (Campoccina *et al.,* 2006; An and Friedman, 1996) with prevalence of methicillin resistant strains emerging (Van Houwelingen, 2012). It has been reported that out of 81% of *S. aureus* infections recorded, 61% of these were *MRSA* in origin. *S. epidermis* is the most frequently isolated species of coagulase negative staphylococcus (CNS) isolated form BAI (Rupp *et al.,* 1999).

To address this problem, this study examines the use of a coating system based on a CaP material loaded with metal ions, which has potential antibacterial and osteoconductive properties to overcome the limitations associated with current treatment regimes. This study further supports the findings from a previous study by O'Sullivan *et al.,* which investigated the use of 5% wt substituted apatites (AgA, ZnA, SrA) and concluded that AgA demonstrated promising anticolonising properties without compromising the osteocompatibility of the bioactive CaP surface

layer. The anticolonising activity of the substituted apatites was the result of the combined antibacterial properties of both the released and the immobilised ions on the coating surface (O'Sullivan *et al.,* 2010)

The 12% wt AgA demonstrated excellent inhibition of *S. aureus* attachment (>90%) over the 14 days and outperformed the other surfaces assessed in this study. It was also observed to be superior to the 5% wt AgA sample evaluated previously which only resulted in 18% biofilm inhibition at day 14. (O'Sullivan *et al.,* 2010). Even though, there was only 1.21 ppm of Ag released over the 30 days, the lowest increment released was 0.3 ppm, which is more than the minimum concentration (0.2 ppm) required to elicit a log reduction response to *S. aureus* (Jung *et al.,* 2008). In addition, 83% of the Ag ion had remained on the surface at day 30 for 12% AgA (Table 6.1) compared to only 10% for 5% wt AgA (O'Sullivan *et al.,* 2010). The difference in the initial concentration of Ag ions present in the coating between the 5% and 12% wt loadings (1 ppm and 7 ppm, respectively) greatly influenced the amount of ion released and the concentration of the Ag remaining on the surface following ion elution over a 30 day period. It is obvious, that the higher loading of the 12% wt AgA contributed to the enhanced anticolonising activity observed compared to the 5% wt AgA. The 12% wt AgA proved successful in preventing the growth of the *S. aureus* biofilm in the anticolonising studies performed. However, irrespective of the increased ion concentration (6-7 times more Ag and Sr for AgA and SrA) for the 12% wt apatites, comparable surface roughness values of 2.0-2.3 μm were observed for the 5% wt and 12% wt substituted apatites (O'Sullivan *et al.,* 2010).

While Ag possesses antibacterial properties for a broad spectrum of bacterial strains, it is relatively non-toxic to human cells (Alt *et al.,* 2004). The maximum amount of Ag that could be released in this study (7 ppm) is below the critical level of cyctotoxicity reported in literature (10 ppm) (Vik, 1985), and supports the findings in this study that demonstrated the cytocompatibility of the AgA coating. In a previous study by Ruan *et al.,* <1 ppm of Ag ions were released over 49 days and the research also demonstrated that that the osteoconductivity of the HA coating was not reduced with the addition of the Ag (Ruan *et al.,* 2009). A balance between osteocompatability and antimicrobial property was achieved with 2-4% wt Ag in a HA coating, however reduced osteoblast cell proliferation was observed when 6% wt Ag was incorporated into a HA coating (Roy *et al.,* 2012). There was no evidence of cytotoxicity observed using MG-63 cells on any of the surfaces assessed in this study, however SrA did demonstrate enhanced viability of osteoblastic cells compared to the other apatitic surfaces assessed. This is in agreement with previous studies using the 5% wt SrA (O'Sullivan *et al.,* 2010) and other research (Capuccini *et al.,* 2008). The 12% wt AgA was found to be cytocompatible with comparable levels of cell proliferation to the HA surface, however further *in vitro* and *in vivo* measures of osteoconductivity are required to elucidate it potential as an osteoconductive surface. This study highlights the importance of material optimisation in formulating implant coatings with comparable osteoconductive properties to HA and with an added anticolonising behaviour.

Established studies have reported an enhanced antibacterial activity when the bioceramic was loaded with two metal ions such as AgCu or AgZn (Matsumoto, 2010) and Sr and fluoride (F) (Guida *et al.,* 2003). Despite the potential for

synergistic behaviour in the combined AgSrA coating, it did not perform as well as the single substituted apatites. Enhanced anticolonising behaviour was observed at day 1 only for the AgSrA surface with no significant difference in osteoblast cell viability compared with that of AgA. Even though more Sr was present for the 12% wt SrA (4.5 times) which resulted in 3 times more Sr being eluted from the surface over the 30 days compared to the 5% wt SrA, poor anticolonising activity was observed for both loadings over the two week incubation period with *S. aureus* (43% and 3% biofilm inhibition for 12% and 5% wt respectively) (O'Sullivan *et al*., 2010). This would suggest that SrA was not as effective an antibacterial metal ion compared to Ag. It is obvious that the addition of the Sr undermined the performance of the Ag. There is very little understanding of the antibacterial mechanism of Sr only that the release of the ion (Sr^{2+}) is important for the antibacterial action (Lin *et al.*, 2008). The oxidative state of the poorly soluble Ag ions may have also contributed to this unexpected result as the antibacterial activity of Ag is dependent on the Ag cation (Ag^{+}) (Chen *et al.*, 2008; Chen *et al.*, 2006). If the silver is bound then it has no function (Hardes *et al.,* 2007). It is reported that the addition of metal ions change the overall structure of the CaP (Matsumoto *et al.,* 2009; Guida *et al.,* 2003) and perhaps this may have influenced the variability in performance observed for the samples. The combination of Sr and Ag in the coating may have affected not only the ion loading but also the distribution, solubility and release of the active metal ions from the surface. In a study by Lin *et al.,* they reported that the morphology, crystallinity and the antibacterial properties of HA were altered when half or all the Ca ions were substituted with Sr (Lin *et al.,* 2008). Further work would be required to elucidate this.

More recently, the antimicrobial action has been attributed to not only the low levels of Ag released but also from the formation of lethal free radicals as a result of the redox nature of silver on the surface (O'Sullivan *et al.*, 2010; Matsumoto *et al.,* 2009; Hu *et al.,* 2007). All these mechanisms contribute to the complete degeneration and ultimate death of the bacterial cells. To demonstrate antibacterial efficacy, a reduction of three or more orders of magnitude in the number of CFU is needed (Troitzsch *et al.,* 2009). From the antimicrobial studies, the bactericidal effect of the released Ag ion against *MRSA* was evident over the 30 days (91-100%), whereas the highest % kill was only achieved at day 14 only for *MSSA* and *S. epidermis* (93% and 94% respectively). *MRSA* was more susceptible to the released Ag ion compared to the other two clinical isolates with a log kill of 3.4 at day 14 whereas a 1 log reduction in CFU numbers was only achieved at day 14 for both *MSSA* and *S. epidermis*.

The surface impact of the immobilised Ag ion demonstrated the highest antimicrobial activity before incubation in the order of *MRSA* (98%), *MSSA* (94%) and *S. epidermis* (92%). Subsequent analysis of the surfaces after ion release revealed approximately 1 log kill against *MSSA* and *S. epidermis* with improved log kill observed against *MRSA* (1.6-6.6) up to day 14 but decreased to <1 log kill at day 30. The AgA surface performed the best at preventing *MRSA* attachment (90% biofilm inhibition) followed by *MSSA* which had only impact at day 1 (50% biofilm inhibition). However, the AgA surface did not exhibit inhibition of *S. epidermis* colonisation. The combined antimicrobial effect from the released ion and the immobilised ion, which demonstrated approximately 1 log kill over the 30 days (Table 6.2 and Table 6.3), was not effective in eradicating the biofilm growth

associated with this strain. *MSSA* demonstrated some biofilm inhibition at day 1 (45%) only. The combined results of the study suggest that MRSA was the most susceptible strain. A number of studies have reported the bactericidal effect of Ag loaded HA surfaces against *MRSA in vitro* which demonstrated higher impact compared to *S. aureus* strains (Yonekura *et al.,* 2011; Noda *et al.,* 2008).

However, the difference in the clinical isolate performance can be attributed to the nature of the strains and the different factors which impact on adherence to surfaces and biofilm development for each strain. It has been reported that biofilm producing staphylococcus adhere to implants in greater numbers than non producing strains (O'Gara and Humphreys, 2001; Rupp *et al.,* 1999). The images in Figure 6.6 (a), 6.7 (a) and 6.8 (a), clearly indicates the presence of bacterial attachment on the HA control and also on the AgA sample for *S. epidermis* (Figure 6.8 (b)). However, there are reduced numbers of active microorganisms *MRSA* and *MSSA* on the AgA surface (Figure 6.6 (b) and 6.7 (b) which supports the biofilm inhibition data. The adherence of *S. epidermis* to the implant surface involves the rapid attachment mediated by non-specific factors such as surface properties of the implant and also by specific adhesins (e.g. polysaccharide intercellular adhesion (PIA) and accumulation associated proteins (AaP)). On the other hand, the adherence of *MRSA* is more dependent on the presence of the host-tissue proteins (fibronectin and fibrinogen) (O'Neill *et al.,* 2009; O'Gara and Humphreys, 2001). The fact that the AgA has a higher surface roughness compared to the control may have affected the anticolonising behaviour of *S. epidermis*, as it is well established that rougher surfaces provide more favourable sites for *S. epidermis* colonisation (Sousa *et al.,* 2009).

Moreover, it has been reported that there is a processing window whereby 10 mg/l of Ag is the maximum toxic concentration for human cells (Vik *et al.,* 1985). As a result, an increase in Ag content in the coating could be incorporated into the surface to adequately reduce bacterial adhesion and biofilm formation as well as minimising cytotoxic risks. CoBlast offers an alternative process for depositing silver loaded apatitic powders as it does not alter the chemical composition of the starting material (O'Sullivan *et al*., 2011). CoBlast offers a number of advantages over the traditional deposition processes used to coat metals with Ag loaded apatitic powders included plasma, sol-gel and thermal techniques. The sol-gel technique used by Chen *et al.,* was a time consuming process where it was reported that a minimum of 6 days was required to produce the coatings (Chen *et al.,* 2007b). The magnetron co-spluttered process required an additional heat treatment step so as to increase the crystallinity of the coating (Chen *et al.,* 2006). Decomposition of the HA was reported during the thermal and plasma spraying processes (Roy *et al.*, 2012; Ruan *et al.*, 2009; Zheng *et al.*, 2009; Noda *et al.,* 2008; Chen *et al.*, 2008; Chen *et al.,* 2007b; Chen *et al.,* 2006). Secondary phases such as tricalcium phosphate (TCP), calcium oxide (CaO) and tetracalcium phosphate (TTCP) were all observed in the coating as a result of the high temperature deposition process of plasma spraying (Roy *et al*., 2012). Therefore, the antibacterial results here for the *S. aureus* related strains are promising and have important implications for the development of an antimicrobial strategy using metal ion based technology to control BAI.

6.5 Conclusions

Silver has been known to have a strong inhibitory and bactericidal effect as well as a broad spectrum of antimicrobial activities. This study offers an AgA surface as a strategy to treat and prevent infections associated with hard tissue implants at the site of implantation in order to deliver antibacterial effect against harmful bacteria while maintaining cytocompatibility. Together with an increase in the release of the Ag ion and the residual surface Ag, it is not surprising therefore, that the AgA surface exhibited superior performance compared to the 5% wt AgA coating. AgSrA demonstrated promising anticolonising activity at day 1, however the effect decreased at day 14. No improvement in the anticolonising behaviour was observed with SrA even with increasing the Sr ion content of the coating. More research is required to establish the mechanism. Optimisation of the AgA formulation is still required to enable more profound impact on clinical relevant strains whilst developing its osteoconductive potential. Considering the demand for an antibacterial implant, the AgA demonstrates a great potential to be used in an *in vivo* setting.

Chapter 7

7.0 *In Vivo* Evaluation of Silver Substituted Apatite Coatings to Combat Infection on Hard Tissue Implants

Abstract:

Biomaterial associated infections (BAI) remain a serious complication in orthopaedic surgery. In addressing this problem, it has been previously reported that CoBlast was used to deposit apatitic powders onto biomedical grade titanium (Ti) Kirshner wires (K-wires) including a silver (Ag) loaded powder. The coating demonstrated anticolonising activity and uncompromised the osteoblast cell viability compared to a standard hydroxyapatite (HA) coating in *in vitro* studies. In this study the use of Ag loaded apatite at two different loadings are evaluated as an infection preventative coating for hard tissue implants using an *in vivo* study nude mouse model. Two Ag containing apatitic powders loaded at concentrations of 5% wt and 12% wt were assessed and compared to a standard HA coating. Chemical composition and morphology of the surface were assessed using EDX and SEM. Assessment of bacterial adherence on coated K-wires following subcutaneous implantation in a nude mouse infection model for two days demonstrated that the 12% wt surface outperformed the 5% wt AgA coating. Inflammation and systemic responses were investigated. Lower inflammatory responses were activated with the insertion of the Ag loaded K-wires, in addition the infection remained localised at the implantation site over the two day study period. These results indicate that the AgA coating on the surface of orthopaedic implants demonstrate good biocompatibility whilst inhibiting bacterial adhesion and colonising of the implant surface.

7.1 Introduction

Staphylococci bacteria are a prevalent cause of BAI associated with prosthetic and indwelling medical devices such as orthopaedic implants. These infections are categorised as acute, subacute and late infections depending on the time of onset. Perioperative bacterial seeding has been highlighted as the main cause of acute and subacute infections detected twelve weeks to one year after the implant operation. However, the haematogenous transmission of bacteria has been reported as a possible cause of late infection which develops years after implantation (Gristina and Jolkin, 1993). These chronic infections are related to biofilm formation on the implant surface and bacterial adherence has been established as a critical step in the pathogenesis of BAI. Bacteria adherence is a complex multi-step process and was reviewed in **Chapter 1.** Biofilm formation poses a serious clinical complication as successful treatment often requires the removal of the contaminated implant coupled with extensive bone debridement, excision of infected tissues and bone and prolonged antibiotic treatment (Van Houwelingen, 2012).

In recent years, Ag coated medical devices for heart valves, cardiac catheters and urinary catheters have been proven to reduce BAI (Brutel de la Riviere, 2000; Karchmer *et al.*, 2000; Boswald *et al.*, 1999). Its properties and application are reviewed in **Chapter 1** and *in vitro* evaluation of its inclusion in CaP coatings for hard tissue applications are outlined in **Chapters 5** and **6**.

A number of techniques to deposit bioactive coating layers containing hydroxyapatite (HA) onto metallic and inert substrates for hard tissue implants have been investigated (Li *et al.*, 2009; Stoch *et al.*, 2005, Stoch, 2001). The drawbacks with these methods have also been reviewed in **Chapters 1, 3** and **4**.

A number of studies have demonstrated the efficacy of these bioceramic coatings with antimicrobial activity against a wide range of bacterial strains *in vitro* (O'Sullivan *et al.*, 2010; Matsumoto *et al.*, 2009; Chen *et al.*, 2008; Lin *et al.*, 2008; Hu *et al.*, 2007; Feng *et al.*, 1998), however few have examined the coating performance in an *in vivo* model. Various animals models are available to study osteomyelitic infections, which include the direct inoculation of bacterium localised at the site of implantation, precolonising the implant with bacteria prior to implantation, the intravenous administration of the inocula post implantation or a mixture of these methods. How the inoculums are introduced greatly influences the bacteria growth (Van Wijngaerden *et al.,* 1999). Studies investigating precolonised implant versus direct inoculation models have been investigated, mixed results have been reported (Sheehan *et al.,* 2004; Kadurugamuwa *et al.,* 2003). Comparing *in vitro* and *in vivo* results are often difficult due to the complexity of the factors affecting biofilm formation *in vivo* including the presence of matrix proteins on the implant surface and leukocytes, antibodies and other components of the host's defence system that aid in the scavenging of foreign bodies such as microbes (Kadurugamuwa *et al.,* 2003; Monzón *et al.,* 2002). Subcutaneous models have been effectively used in previous studies to evaluate the interaction between different

microbial strains and biomaterials (Monzón *et al.,* 2002; Monzón *et al.,* 2001) and is used here.

Such models were investigated to mimic contamination caused due to perioperative or late hematogeneous infection with repeatable results (Sheehan *et al.,* 2004; Goshedger *et al.,* 2004; Kadurugamuwa *et al.,* 2003, Monzón *et al.,* 2002, Gottenbos *et al.,* 2001, Van Wijngaerden *et al.,* 1999). However, many of these models were employed to investigate effective strategies for the prevention of BAI using antibiotics at the localised implantation site (Adams *et al.,* 2009; Monzón *et al.,* 2001; Van Wijngaerden *et al.,* 1999). Recently, Ag containing apatites have proven to be successful in exhibiting antibacterial activity with the added value of being cytocompatible with osteoblast cells *in vitro* (Roy *et al.,* 2012; O'Sullivan *et al.,* 2010; Ruan *et al.,* 2009). However, as previously stated only a few studies exist validating these observations *in vivo*. In a study by Shimazaki *et al.,* 3% wt silver containing HA deposited onto Ti using a thermal technique, exhibited significant kill against methicillin-resistant *Staphylococcus aureus* (*MRSA*) compared to a HA coating when evaluated in a subcutaneous rat model (Shimazaki *et al.,* 2010). In a second study, the same coating demonstrated low toxicity and good osteoconductivity 12 weeks after implantation into rat tibia (Yonekura *et al.,* 2011). In **Chapters 5** and **6**, silver substituted apatites (AgA), deposited using CoBlast showed excellent antimicrobial activity against *Staphylococcus aureus (S. aureus)* without cytotoxicity *in vitro* (O'Sullivan *et al.,* 2010).

In this study, the CoBlast deposition process was used to coat Ti K-wire implants with Ag substituted apatites (AgA). AgA powders with two silver loadings, 5% and 12% wt powders were investigated. In order to prove efficacy in preventing bacterial adhesion and biofilm formation *in vivo*, a simple infection model using immune deficient mice was used to evaluate the AgA surfaces. In this study a direct inoculation model with *S aureus* as the challenge organism was used. A low inoculum in the order of 10^3 colony-forming units (CFU), which has been shown to establish a stable infection resembling the case in a clinical situation was used (Kadurugamuwa *et al.,* 2003).

7.2 Materials and Methods

Materials and methods used in this study are summarised in **Chapter 2.** Ti K-wires (0.8 mm) were used as the implants and were coated with HA, 5 and 12% wt AgA. Implants were characterised using EDX analysis to determine elemental composition. As previously mentioned, the *in vivo* model and analysis in this study were based on established studies (Adams *et al.,* 2009, Antoci *et al.,* 2008; Van Wijngaerden *et al.,* 1999). An infection model (*S. aureus* ATCC 1448) using nude mice was used where implants were subcutaneously implanted for 2 days. After 2 days the implants were removed and the % biofilm incubated was determined. SEM images were taken of the samples. Blood cultures were taken to assess if a systemic infection was observed. Also, a chemiluminescence test was performed on blood samples taken to assess if an inflammatory response was noted. Also, the tissue samples at the localised site were qualitatively assessed for signs of cytotoxicity.

Statistical analysis (one way ANOVA) was performed on the biofilm data to determine if there was a statistical difference between samples.

7.3 Results

7.3.1 Surface Characterisation

Figure 7.1 shows the images of the coated implants which were used in this *in vivo* study compared to an uncoated Ti (V) control. These images clearly show a change in appearance of the wire after coating deposition.

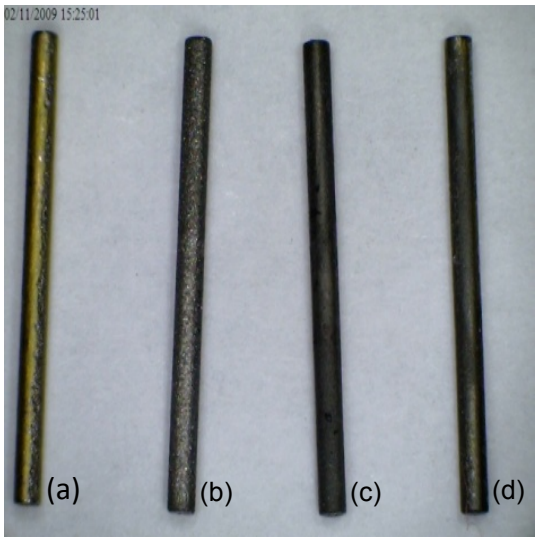

Figure 7.1: Images of the coated K-wires: (0.8 mm x 180 mm); a) uncoated Ti (V) control; b) HA coated sample; c) 5% wt AgA coated sample and d) 12% wt AgA coated sample.

EDX analysis was performed to determine the elemental compositions of the coated K-wires. The chemical composition of the bare Ti K-wire consists of 18% atm aluminum (Al), 79.6% atm Ti and 2.4% atm vanadium (V). The results obtained are presented in Table 7.1 which illustrates that the coated surfaces are composed of oxygen (O), phosphorous (P), calcium (Ca) (apatitic nature of the coatings) and the Ti from the underlying K-wire was also evident.

Table 7.1: EDX analysis of the coated implant surfaces.

Coating	O % atm	P % atm	Ca % atm	Ti % atm	Ion % atm
HA	76.0	7.0	8.0	10	-
5% wt AgA	74.8	7.2	8.2	8.5	0.6
12% wt AgA	72.0	10.1	11.9	6.6	1.2

The Ti levels which signifies the coating thickness ranged between 6.6-10% atm. Thus, the coating thickness was observed to follow the following order of HA < 5% wt AgA < 12% wt AgA. As expected, the 12% wt AgA surface contained a higher Ag content (1.2% atm) compared to the 5% wt AgA surface (0.6% atm). The SEM images of the uncoated and coated Ti (V) surfaces are presented in Figure 7.2. The introduction of the CoBlast surface exhibits higher levels of surface roughness than the bare metal. The images illustrate highly regular and uniform coatings. The process uses a combination of grit blasting to roughen the surface with the co-introduction of a second dopant (HA, 5% wt and 12% wt AgA) which fills in the abraded surface producing a tribochemical bonded surface. The EDX and SEM

analysis are typical results for the CoBlast surfaces (O'Sullivan *et al.*, 2011; O'Sullivan *et al.*, 2010).

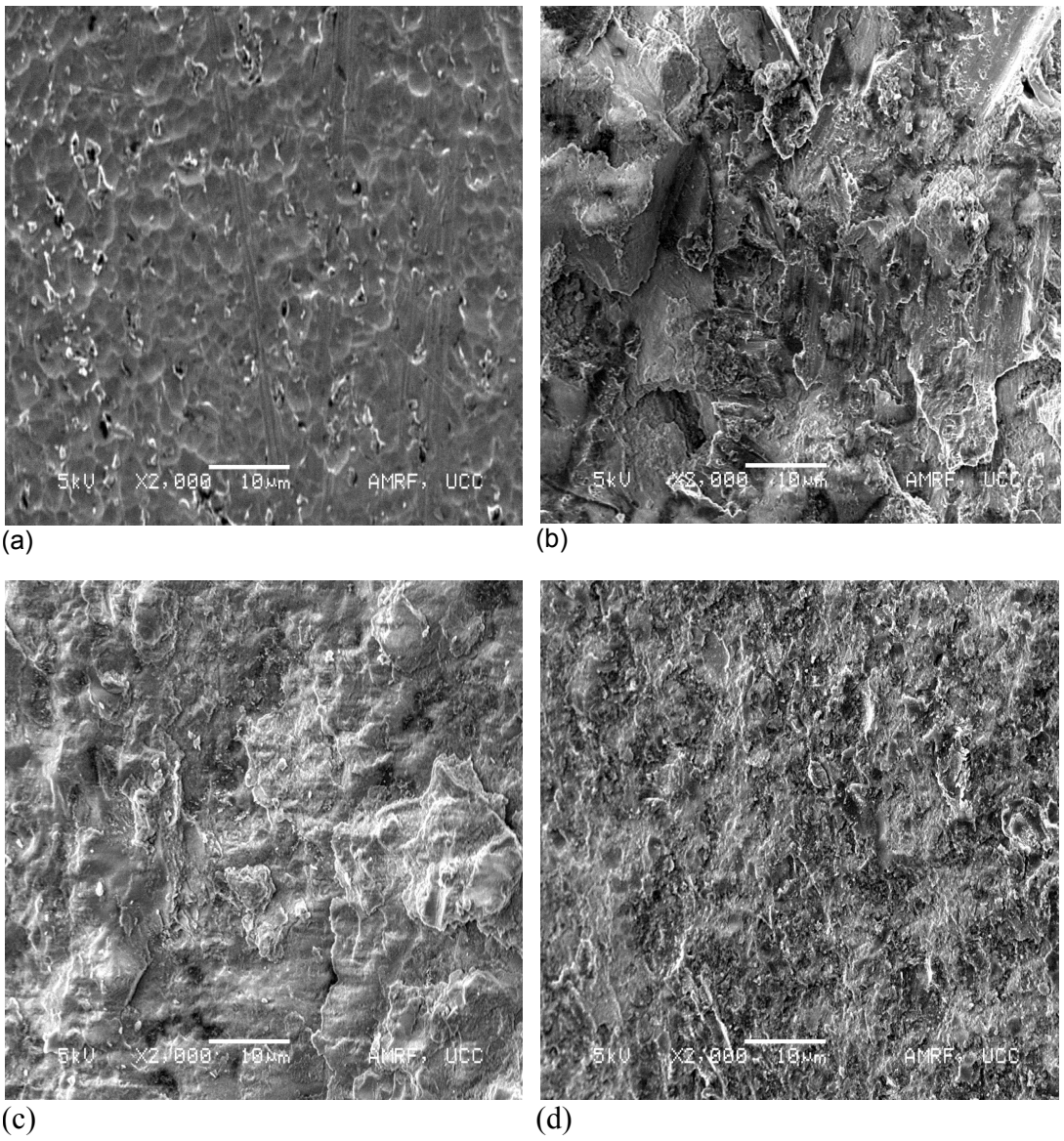

Figure 7.2: SEM images of (a) bare Ti; (b) HA; (c) 5% wt AgA and (d) 12% wt AgA.

7.3.2 Anticolonising Studies

Anticolonising activity of the coated implant surfaces was evaluated after removal of non-attached bacteria by rolling the explanted implants on blood agar plates. The

blood agar plates also confirmed whether the Ti rods were colonised by the bacteria *in vivo*. The presence of CFU indicated that the bacterial inoculum introduced successfully colonised the implant surface. The number of adherent bacteria was quantified by sonicating the explanted implants in buffer which were subsequently diluted in order to enumerate the CFU. Images of the bacteria cultured on the agar at each stage, after rolling, initial sonication and dilution for the various coated implants are given in Figure 7.3. It is evident that the concentration of the bacteria recovered decreased from the agar plates in the order of rolled>sonication>sonication and dilution.

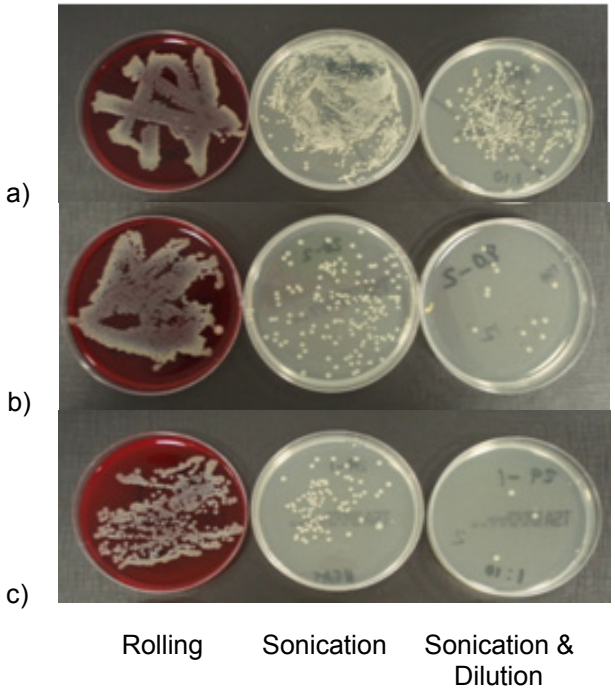

Figure 7.3: Images of bacteria cultured on agar plates for coated surfaces following explantation after 2 days: a) HA; b) 5% wt AgA and c) 12% wt AgA after rolling, after sonication and after sonication and dilution (rolled>sonication>sonication and dilution).

While many bacterial were visualised on the control plates (Figure 7.3 (a)), a lower number of bacteria were recovered from both the AgA surfaces, with 12% wt AgA demonstrating the greatest reduction in adherent bacteria (Figure 7.3 (c)). The number of adherent bacteria recovered were observed to decrease in the following order for all agar plates: HA>5% wt AgA>12% wt AgA. Qualitative analysis of the agar plates in Figure 7.3 highlights that the addition of Ag and the increase from 5 to 12% wt led to a decrease in adherent bacteria, demonstrating the potential use of the AgA coatings as anticolonising surfaces. The CFU data from the diluted samples was used to determine the % biofilm inhibition of the AgA coatings relative to the HA coated control. The % biofilm inhibition for the AgA samples is presented in Figure 7.4. The 12% AgA was seen to prevent 95% *S. aureus* attachment whereas the 5% AgA surface demonstrated an impact of 68% growth inhibition. The 5% wt AgA shows considerable variation in the % biofilm inhibition data suggesting that the lower silver content was not as effective at preventing bacterial attachment compared to the 12% wt AgA. It was noted from the compilation of CFU data in Figure 7.4 that a wide variation exists. However, a 1 log reduction in CFU was observed with the 12% wt AgA suggesting that this surface performed the best in this study.

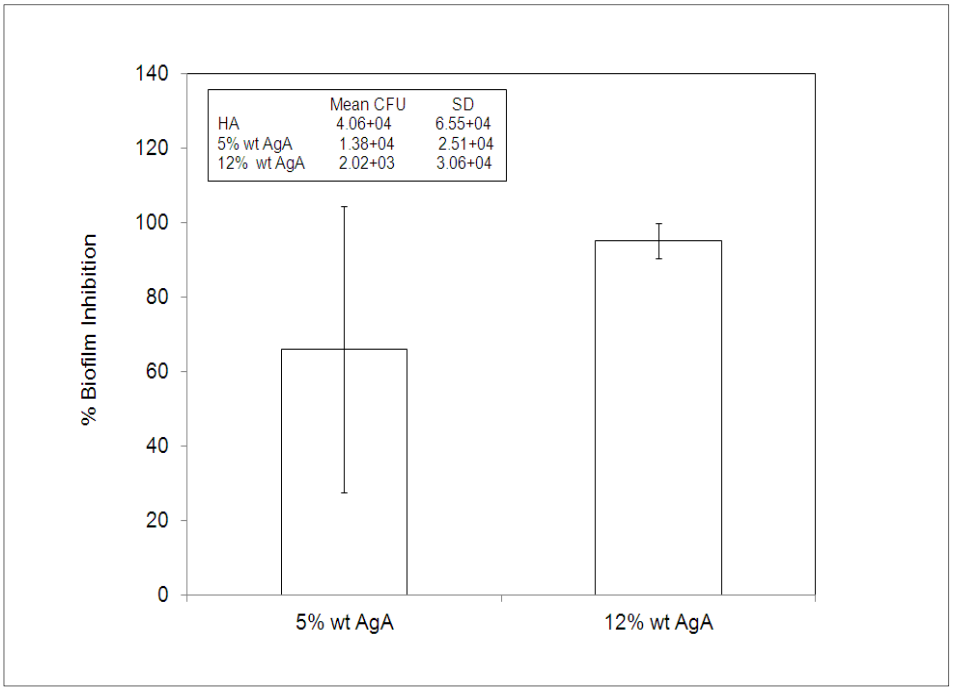

Figure 7.4: Biofilm inhibition data of 5% wt AgA and 12% wt AgA coated K-wires relative to the HA surface, evaluated in an *in vivo* model using *S. aureus* as the bacterium challenge. The insert presents the CFU data obtained.

The results obtained here were in agreement with the findings in Figure 7.3 and are further confirmed by the SEM images of the explanted surfaces (Figure 7.5). There was definite evidence of bacterial attachment on the control HA coated surface with the presence of the characteristic spherical shape of cocci whereas reduced bacterial contamination was observed on the 12% wt AgA. However, one way ANOVA revealed that there was no statistical difference between samples ($p>0.05$).

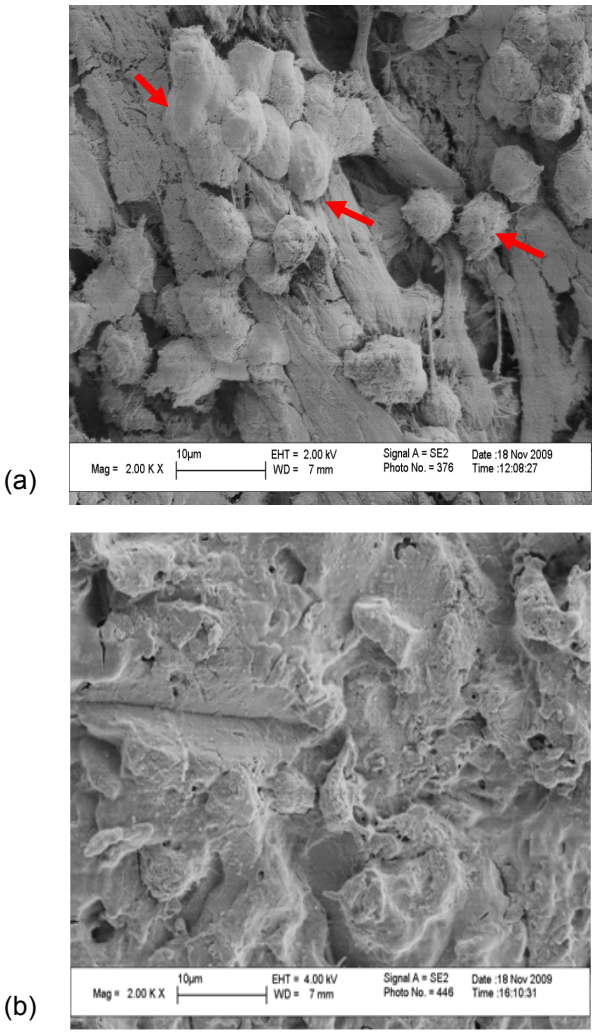

Figure 7.5: SEM images of the explanted K-wire following infection study: (a) control HA coating and (b) 12% wt AgA. Red arrows indicates the presence of *S. aureus* organism on the surface.

7.3.3 Blood Culture Test

The blood culture test was performed to determine whether a systemic infection resulted from the bacteria introduced at the localised implantation site. The test was performed using a commercially available agglutination test to simultaneously detect

the presence of fibrinogen affinity factor, protein A and polysaccharides of the bacteria. The test is positive if coloured particles form indicating the presence of the above antigens (Weist *et al.*, 2006) (Figure 7.6). The test was negative for the presence of coloured particles in the blood cultures indicating that there was no systemic infection obtained from the bacteria introduced at the localised implantation site for both the HA control and AgA samples (Figure 7.6).

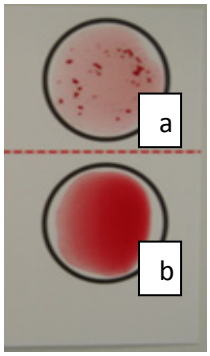

Figure 7.6: Image of a positive result (control (a)) and a negative result (12% wt sample (b)) for the agglutination test.

The images of the blood cultures are given in Figure 7.7 which clearly shows no presence of *S. aureus* cells however skin microflora was observed. This contamination was more than likely introduced during the surgery.

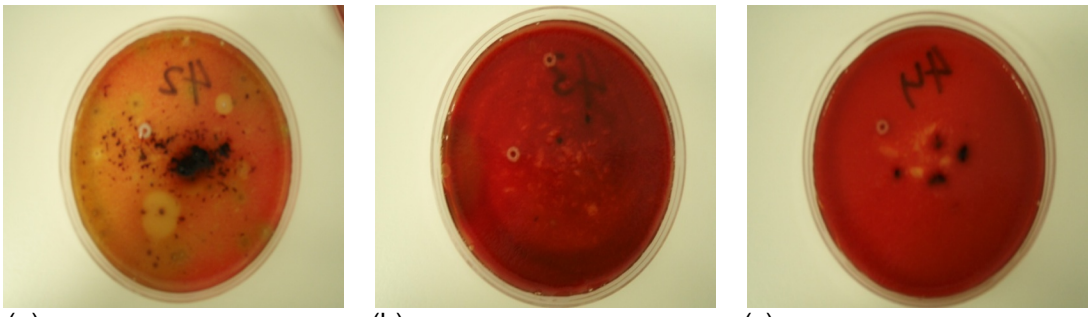

Figure 7.7: Images of Blood Cultures a) HA control; b) 5 wt AgA and c) 12% wt AgA.

7.3.4 Inflammatory Response

The chemiluminesent test measures the real time production of reactive oxygen species (ROS) produced during the degranulation and the respiratory burst of leucocytes which are key inflammatory markers (Rohn *et al.*, 1999). The release of ROS is accompanied by chemiluminescence or emission of light which can be monitored. The assay conducted analysed whole blood whereby the first step involves stimulation with N-formyl-methionyl-leucyl-phenylalanine (fMLP) and the second step is primed with phorbol-12-myristate-13-acetate **(**PMA). Exposure of neutrophils to chemoattractants such as fMLP results in marked increases in the surface expression of specific membrane-associated proteins resulting in chemotaxis, degranulation and generation of ROS (Prossnitz and Ye, 1997). PMA is a surface active agent which stimulates metabolic responses activated in neutrophils by particle ingestion thus it is responsible for inducing phagocytosis producing ROS (Antonini *et al*., 1994). fMLP and PMA stimulated chemiluminescence of whole blood samples recovered from the mice implanted with the different coated K-wires for 2 days was measured in this study (Figure 7.8).

The results are presented in Figure 7.8 which revealed that the control HA coating activated an acute response whereas the 12% wt AgA response followed the same profile but was less activated. The 5% wt AgA response initially less activated but with time obtains a similar level of luminescence to the HA control and is at all times higher than the 12% wt AgA.

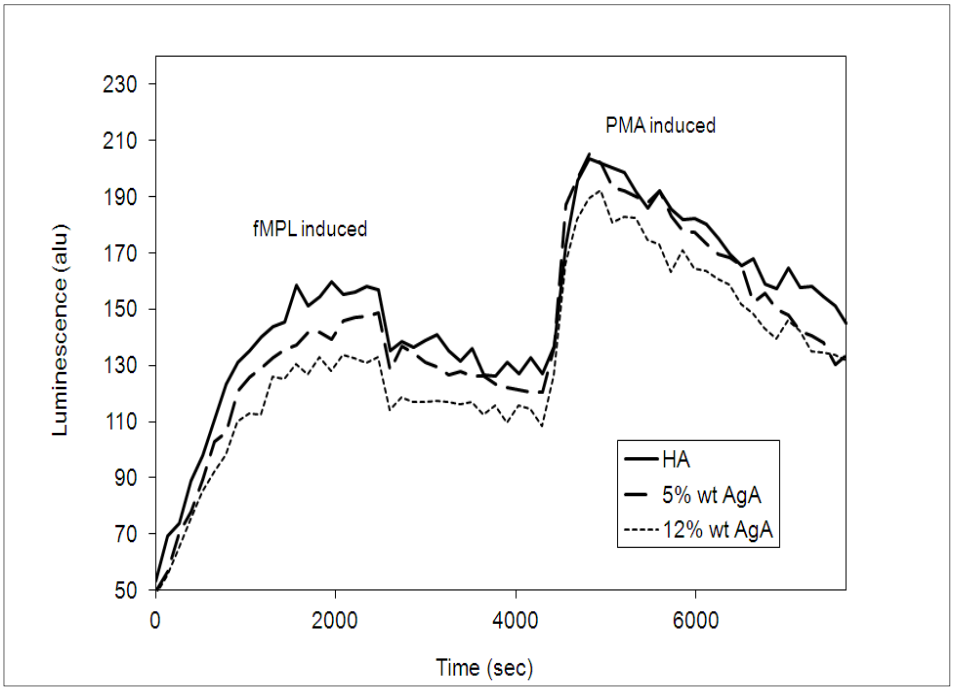

Figure 7.8: Chemiluminescence results from inducing inflammatory response using fMPL and PMA for blood samples from HA control, 5%wt AgA and 12% wt AgA.

7.4 Discussion

Previous studies have shown that the CoBlast process deposits micron thick, crystalline HA coats which have good adherence to the underlying Ti substrate without leading to the formation of unwanted calcium phosphate phases (O'Hare *et al*., 2010; O'Sullivan *et al*., 2010). In this study, the CoBlast deposition process was used to effectively coated a 3 dimensional (3D) implant and demonstrates potential use as an antimicrobial surface against *S. aureus* in a subcutaneous mouse model. The coating thickness can be indicated by the levels of Ti present using EDX analysis. There was reduced variation in Ti levels obtained for the 3D surfaces compared to previous results where coatings on flat 2 dimensional (2D) Ti surfaces

were evaluated. In previous studies, the Ti levels obtained included 9-14.7% atm for HA, 10.1% atm for 5% wt AgA and 20% atm Ti for 12% wt AgA (O'Sullivan *et al.*, 2010 and Table 6.1) whereas in this study comparative Ti levels were obtained for all surfaces (6.6-10% atm). More importantly, the Ag ion content on the 3D surfaces (0.6 % atm for 5% wt AgA and 1.2% atm for 12% AgA), which is responsible for the antimicrobial activity was consistent with previous studies on 2D surfaces (0.6 % atm for 5% wt AgA and 1% atm for 12% AgA) (O'Sullivan *et al.*, 2010 and Table 6.1). The highly regular and roughened morphology of the surfaces obtained from the CoBlast process are similar with a previous study where 2D substrates were used, **Chapters 5** and **6** (O'Sullivan *et al.*, 2011).

Depending on the method of inoculation, biofilm growth was observed as quickly as one hour following bacteria introduction (Kadurugamuwa *et al.*, 2003). Sheehan *et al.* also investigated the impact of a Ag coated K-wire after 2 days in a rat model and concluded that 2 days was sufficient for biofilm formation (Sheehan *et al.*, 2004). It has also been shown that the Ag concentration in the substituted apatites greatly influenced the bactericidal activity of the coated surfaces as the 12% wt Ag content exhibited better performance compared to the 5% wt loading (O'Sullivan *et al.*, 2010). In this study similar findings were observed for the *in vivo* study compared to previous *in vitro* studies, **Chapters 5** and **6** (O'Sullivan *et al.*, 2010). To determine whether the bacteria colonised the various rods *in vivo*, the rods were rolled on the agar plates. A reduced number of bacteria colonies were evident on the 12% wt AgA surface compared to the other coated rods. Analogous to previous studies, % biofilm inhibition was used to determine the impact the surface against bacterial colonisation

(O Sullivan *et al.*, 2010; Adams *et al.*, 2009). In this study, 95% biofilm inhibition, equivalent to 1 log reduction was achieved for the anticolonising behavior of 12% wt AgA surface compared to 68% for the 5% wt AgA (Figure 7.4). SEM analysis supported that few bacteria managed to colonise the 12% wt AgA surface compared to the other surfaces (Figure 7.5 (c)). The qualitative representation of the agar plates for the rolled, neat and diluted samples obtained following the processing of the explanted samples further support the reduced number of adherent bacteria of the 12% wt AgA compared to the other samples (Figure 7.3). It was established in an earlier study that the anticolonising activity of AgA was attributed to a synergistic effect of the immobilised Ag ion and to a lesser extent the released ion, **Chapter 5**. It was reported that there was 40% and 90% biofilm inhibition was observed for the 5% wt AgA (day 1 and day 7). At day 1, there was 6% Ag ions released which was responsible for a poor bactericidal effect (13% kill) however, the immobilised silver ion contributed to 57% kill. The increased Ag ion content of the 12% wt AgA had an obvious effect on preventing the bacterial attachment compared to the 5% wt AgA. It was reported in **Chapter 6** that there was 100% and 90% biofilm inhibition determined at day 1 and 14 for 12% wt AgA. Similar concentrations of the Ag ion was released for both 5% and 12% surfaces (1 ppm over 30 days) however, 83% of Ag still remained on the 12% wt AgA surface following elution at day 30 compared to only 10% for the 5% AgA surface. Based on the *in vitro* results, it can be ascertained that a similar mode of action accounts for the bactericidal activity of the AgA surfaces in the *in vivo* trial whereby the immobilised ion plays a dominant role and the released Ag ion elicits a minor effect in comparison.

Biocompatibility is an important characteristic of biomaterial coatings which represents that the implants surface must not evoke an inflammatory response. Such a response could jeopardise the successful osteointegration of the implant surface with bone tissue. The process of acute inflammation is initiated by cells already present in all tissues (macrophages, neutrophils), which at the onset of infection, undergo activation and release inflammatory mediators responsible for the clinical signs of inflammation (redness, bruising, swelling, pain). These phagocytic cells when challenged with specific chemicals such as fMLP and PMA, release ROS which is accompanied by the emission of light known as chemiluminescence. Therefore, measurement of chemiluminescence is an effective tool in examining phagocytic functions (Rohn *et al.*, 1999; Prossnitz and Ye, 1997; Antonini *et al.*, 1994). The chemiluminescent test was determined to be lower for the 12% wt AgA compared to the other surfaces in this study, suggesting that the AgA samples induced a lower inflammatory response due to its bactericidal action of the AgA coating which was responsible for reducing the number of microbes present.

Systemic infection was not detected for the three test groups, indicating that the infection had not spread but was confined to the site of surgery. This is supported by previous studies (Kadurugamuwa *et al.*, 2003; Monzón *et al.*, 2001). Systemisation of implant induced infections is a serious complication which can lead to septicaemia and malfunction of the device (Wu and Grainger, 2006; Kadurugamuwa *et al.*, 2003). This further illustrates the need for an antimicrobial surface to combat early stage infection at the localised site. Cytotoxic effects seem to be dose dependent so careful consideration must be given to the formulation of surfaces (Hardes *et al.*,

2007). It is well reported that Ag ions have a bactericidal activity at concentrations as low as 35 ppb without toxic effects to mammalian cells (Pratten *et al.*, 2004), with a Ag ion concentration as high as 10 mg/L required to have toxic effects on mammalian cells (Vik *et al.*, 1985). Cytocompatability was also assessed using MG-63 cells i*n vitro* and revealed that the 5% wt and 12% wt AgA did not compromise the osteoblast cell viability compared to the HA surface. No black particles were observed around the tissue suggesting that initial qualitative analysis, revealed no toxicity however toxicology analysis would be required to verify this.

As previously reported, several models have been reported for the study of orthopaedic prosthetic infections. Theoretically in an effort to mimic human conditions as closely as possible larger animals such as sheep or dogs should be used. However, there are a lot of expense, handling difficulties and housing larger animals. Small animals have been extensively used for studying bacterial infections at the implant site to investigate antimicrobial surfaces and antibiotic effectiveness (Balaban *et al.*, 2004). Common problems associated *in vivo* models have been the variation in infection rates and repeatability which was more than likely due to host immune activity, distribution, homogeneity and propagation time of the bacteria cells (Balaban *et al.*, 2004, Sheehan *et al.*, 2004). As previously mentioned, the host's defence system can aid in the scavenging of foreign bodies such as microbes. In this study, immunosuppressed nude mice were chosen so that the immune system (T cells and B cells) would not interfere with the antimicrobial action of the coatings in combating the infection. The choice of direct inoculation was chosen due to ease and simple means of administration of the inoculum as oppose to the extra steps involved

in pre-colonising the implants with bacteria. However, it was noted that infection rates were variable from the retrieved samples (CFU data in Figure 7.4). In an attempt not to overload each animal with 4 inoculations at each implant site, one inoculum was introduced. However, variation in the distribution of bacteria was observed. To overcome this constraint, only samples that showed TMTC in the rolled sample were enumerated. To address this limitation in future studies, precolonised implants could be used to improve the reproducibility of a stable infection as seen in other studies (Kadurugamuwa *et al.,* 2003).

In order to prove efficacy in the use of this antimicrobial surface on hard tissue

implants, further work should involve an osteomyelitis model incorporating an intramedullary implant. Vital information about the role of AgA surfaces in a prevention strategy as well as the osteointegrative properties of the surface would be determined. In addition, the use of AgA in this study proves an attractive alternative to the typical antibiotic loaded cements and prophylactic treatment which have poor susceptibility to the increasing number of antibiotic resistant bacteria that are prevalent. A 6 hour post implantation 'decisive period' has been identified during which prevention of bacteria adherence is critical to the long term success of the implant (Hendrick and Schoenfisch, 2006). Therefore, the AgA surface in this early adhesion study has not only demonstrated effectiveness against bacteria colonisation but is clinically relevant as the method employed mimics the perioperative infection process.

7.5 Conclusions

The pathogenesis of prosthetic device infections is complex process in which bacterial adherence to biomaterials and elaboration of biofilm are critical. The *in vivo* findings here were analogous to those obtained previous *in vitro* studies detailed in **Chapter 5** and **6**. CoBlast technology was effective in depositing apatitic materials on the 3D substrates. A localised infection was delivered to the site of implantation which was responsible for the bacterial colonisation of the surfaces. Following a two day *in vivo* evaluation, the 12% wt AgA was observed to outperform the lower Ag content surface as confirmed by qualitative analysis of biofilm inhibition, SEM images and activated inflammatory response.

Chapter 8

8.0 General Discussion

The general discussion is structured to address the questions outlined in the objectives of this study (**Section 1.7**):

8.1 Ultimate aim: Added Value and Key Benefits of CoBlast Technology

- CoBlast can produce a high quality surface with the ability to deposit the 'as received' powders without altering the chemical composition of the starting materials as demonstrated in **Chapter 3**. The utilisation of CoBlast, with its advantage of room temperature processing holds considerable potential for depositing and delivering therapeutic molecules. The work undertaken in this thesis has shown the ability of the CoBlast process to deposit apatite coatings on 2D.substrates in **Chapters 3-6** and 3D surfaces demonstrated in **Chapter 7**.
- A definite tailoring of surface composition and topography can be made through the use of the abrasive and dopant selected as highlighted in **Chapter 3**.
- A crystalline HA layer can be deposited onto biomedical metals as demonstrated in **Chapters 3** and **4**. This has the potential to induce the early formation of lamellar bone *in vivo* for long term stability.

- In **Chapter 5** and **6**, the deposition of SrA coatings have shown osteoconductive potential and can outperform the gold standard HA as a coating on hard tissue implants.
- AgA surfaces deposited using the CoBlast process offer promising results as an anticolonising, cytocompatible surface in addition to possessing osteoconductive potential. Furthermore, the AgA surface holds particular promise as a preventative surface against perioperative infections.

8.2 Objective 1: Evaluations of HA Coatings Deposited using CoBlast Technology in *in vitro* studies

The novel deposition process, CoBlast was seen to effectively modify Ti (V) substrates with a micron thick HA layer with increased surface roughness (Ra<0.6-1.8 μm). CoBlast did not alter the chemistry of the crystalline HA powder resulting in a highly crystalline HA layer deposited. From an *in vitro* perspective, the CoBlast HA had increased cell proliferation responses supporting a previous *in vivo* study which demonstrated enhanced lamellar bone growth on CoBlast surface compared to its microblasted surface (O'Hare *et al*., 2010). The surface roughness of the resultant HA surface produced can be altered depending on the particle size of the abrasive used with the potential to enhance the osteointegration process. The implications of the preliminary studies undertaken in **Chapter 3** demonstrates the ability of CoBlast to tailor surface properties that could positively influence the long-term success of HA coating implants in the dental and orthopeadic arena. As seen in **Chapter 4,** the industry standard plasma process does alter the chemical composition of crystalline HA on deposition producing a thicker (65 μm) and rougher coating (Ra>5 μm)

compared to CoBlast. Multi-crystalline phases can result from the thermal decomposition of the material when thermally processed using plasma technology. This leads to the formation of intermediates (α-TCP, β-TCP and TTCP) which lowers the crystallinity of the HA coating which was observed via XRD and FTIR analyses of the plasma coating. The formation of these intermediates resulted in a faster dissolution process compared to the more crystalline HA coating produced by CoBlast. This has a knock-on effect on the biological activity on the different HA surfaces with enhanced cell proliferation observed on the stable CoBlast HA compared to the more resorbable plasma HA. Plasma HA does exhibit enhanced bioactivity in the SBF study in **Chapter 4**, where the presence of multiple CaP phases trigger a rapid formation of CHA, which is the proposed mechanism for the chemical bonding of the implant to bone. The bioactivity of the plasma sprayed HA surface will promote early osteointegration, however the long term stability will also be influenced by the dissolution behavior of the coating as well as the mechanical integrity of this layer. Clinical trials have shown that such resorbable characteristics of plasma HA can result in delamination and surface cracking leading to aseptic loosening (Gross *et al.,* 2004). On the other hand, the more stable CoBlast HA surface (lower dissolution rate) induces a slower formation of the CHA layer. A different bone bonding mechanism is proposed for the CoBlast surface, which involves the modification of the crystalline HA into a less crystalline phase through ion-exchange coinciding with a late onset of the carbonate apatite being formed. The thin HA coating deposited by CoBlast may incorporate more of the bulk properties of the Ti metal leading to enhanced tensile bond strength compared to the thicker coating of plasma sprayed HA. The more stable HA surface produced by CoBlast which subsequently led to a lower level of surface CHA, also had a positive effect on

the mechanical bond strength compared to the plasma surface. The surface chemical reactions of HA coatings with SBF is an important consideration for the understanding of the surfaces *in vivo* and this SBF *in vitro* study further supports work performed understanding the performance of these two HA surfaces *in vivo.* The deposition process used is an important consideration as this will influence the chemistry and composition of the resultant HA coating which will in-turn affect the mechanical interlocking of the implant to bone. As a result, CoBlast is an attractive coating technology for depositing HA surfaces that induce lamellar bone growth and possess long-term stability and fixation) which may be attributed to key properties (crystalline coating, good coating adhesion, stability) when compared to plasma spraying approaches.

8.3 Objective 2: Evaluation of Substituted Apatites Containing Antimicrobial Metals as an Infection Preventing Strategy in *In Vitro* Studies

The two major factors limiting the survival of the hard tissue implants are aseptic loosening and BAI. The deposition of a high quality HA layer using CoBlast technology will reduce the risk of aseptic loosening as already discussed. BAI are the result of bacterial adhesion to a biomaterials surface. Upon implantation a competition exists whereby microbes and osteoblasts ‘race to the surface’ of the implant. For a successful implant, tissue integration occurs prior to bacterial adhesion, thereby preventing colonisation However, once bacteria adhere onto an implants surface, biofilm can form within 24 hour post implantation (Figure 1.3). A 6 hr post implantation ‘decisive period’ has been identified during which prevention

of bacterial adhesion is crucial for long term success of an implant (Hetrick and Schoenfisch, 2006; Poelstra *et al*., 2002). However, the use of bioceramics with bactericidal agents as coatings, in particular AgA, has demonstrated anticolonising behaviour against *S. aureus* and clinical strains *MRSA* in addition to possessing osteoconductive properties with no cytotoxicity effect (**Chapters 5 & 6**). CoBlast was effective in depositing substituted apatites (AgA, SrA, ZnA, AgSrA) onto Ti (V) metal with surface roughness of 2.0-3.6 μm. Enhanced osteoblast cell proliferation was observed with 5% and 12% wt SrA compared to the other samples investigated (HA, AgA, ZnA). Five percent and 12% wt AgA was observed to superior antimicrobial properties when compared to the other apatites investigated using *S. aureus* as the antibacterial challenge. The anticolonising behaviour of the 5% wt substituted apatites was proposed to be strongly related to the surface action of the immobilised antibacterial metal ion with a contributory action from the low levels of ions released from the surface. Even with increased surface roughness of the substituted apatites, the surface composition (antibacterial metals ion content) played a significant role not only in cellular adhesion and proliferation but also in preventing attachment of microbes. The colonisation of substituted apatite coatings appears to be controlled by the microbe-surface interaction irrespective of the surface topography. The anticolonising behaviour of AgA was also linked to the amount of the Ag ion present on the surface. However, the behaviour of the 12% wt AgA against three clinical isolates (*MRSA, MSSA* and *S. epidermis*) exhibited best performance against *MRSA* followed by *MSSA* only at day 1, with no impact evident against *S. epidermis*. This was more than likely due to the fact that the adhesion of the bacterium type *S. epidermis* is more influenced by surface roughness than *MRSA* and *MSSA* (Sousa *et al*., 2009). *S. aureus* is the most common source of BAI with

MRSA being the most prevalent form of methicillin-resistant bacteria found on infected hard tissue implants. Good initial kill against these two strains demonstrates potential use of the AgA surface as an effective surface to combat infection especially in the first 24 h post implantation. Other technologies (plasma and sol-gel) have been shown to be capable of depositing Ag loaded apatites, however the same drawbacks as outlined in Table 1.3, can be observed. More reliability (lower SD obtained with the antimicrobial and anticolonising results) was seen with the higher content of AgA present compared to 5% wt. *In vitro* results demonstrate the potential use of AgA as an osteoviable surface with effective anticolonising activity against clinical isolates. In addition SrA also demonstrated enhanced osteoconductive potential compared to the other substituted apatites analysed but also to the gold standard HA coating.

8.4 Objective 3: Evaluation of AgA as an Infection Preventing Surface in an *In Vivo* Model

CoBlast was effective in depositing AgA onto 3D K-wire substrates with a visible increase in surface roughness observed compared to blank Ti. Two Ag containing apatitic powders loaded at a concentration of 5% wt and 12% wt were assessed in a 2 day *in vivo* infection model using the same strain of *S. aureus* as in **Chapter 7** in nude mice. A reduced number of bacterial colonies were evident in the 12% wt AgA surface compared to the other coated rods. The results showed that 12% wt surface was observed to outperform the 5% wt AgA (% biofilm inhibition, images of agar plates and SEM images). A localised infection was contained at the site of implantation with lower levels of inflammatory responses activated with the

insertion of the Ag loaded implants compared to the HA surfaces. In conjunction with these findings, no initial signs of cyctoxicity were observed, suggesting that the AgA surface exhibited no toxic effect towards the tissue but was lethal to the microbes present but further toxicological studies to confirm this would be required. Irrespective of these differences between the *in vitro* and *in vivo* studies, good correlation was observed in relation to the anticolonising data (% biofilm inhibition). It is difficult to ignore the variation in infection rates obtained due to colonisation of microbes on the implant surfaces at day 2. Despite this, the *in vivo* study employed a model that replicated the perioperative process and demonstrated effectiveness against bacterial colonisation. To overcome this, precolonised implants could be used to improve the reproducibility of a stable infection as an alternative to the procedure used in this study. More effectively, an infection model that also uses a precolonised implant inserted into the intramedullary canal of a rabbit could be used to evaluate the infection prevention and osteointegration properties of the surface.

8.5 Conclusions

In summary, the major findings of this thesis are as follows:

- CoBlast is indeed effective in depositing apatite bioceramics onto biomedical metals. A definite tailoring of surface composition and topography can be made through the choice of abrasive and dopant selected. A high quality crystalline and stable layer of HA can be deposited without any impurities present as a direct result of the coating process. The crystalline HA follows a different chemical bioactivity mechanism compared to the less pure HA

coating deposited using plasma spraying methods. A more mechanically stable bond was observed between the CoBlast HA and the underlying Ti metal than that of the plasma HA before and after CHA formation.

- This room temperature process with its ability to retain the chemistry of the starting material is an attractive process in areas of tailored surface modification, deposition of bioactive materials and offers the potential to deliver drugs from coating surfaces. As the plasma process occurs at high temperature it limits the co-deposition of therapeutic drugs and biologics which may enhance the efficacy of the HA surface. The high temperatures employed can destroy the active agents or render them irreversibly inactive. Thus, CoBlast offers a versatile route to modify the surfaces of hard tissue implants to deliver optimum integration of hard tissue implants
- The uniform, highly crystalline, defect free, thin film coating associated with CoBlast HA is advantageous compared to the thick thermal sprayed HA coatings. CoBlast offers as an alternative to the traditional methods of coating HA implants.
- Substituted apatites can be deposited to add functionality to HA coatings. SrA was observed to enhance the cell viability of osteoblasts. AgA was observed to outperform all other apatites with respect to its anticolonising activity against *S. aureus* and *MRSA* without cytotoxicity.
- *In vivo* results demonstrated that AgA surface can be used to combat infections at the localised site thus preventing early stage infection without causing inflammatory and initial cytotoxic responses. However further *in vivo* trials would need to be performed to evaluate the osteointegration of AgA surface. A

dual *in vivo* model which investigates the osteointegration process and also the anticolonising behaviour would give beneficial results.

- *The use* of substituted apatites potentially can be used to produce positive patient outcomes and reduce the economic burden of revision surgery due to aseptic loosening and BAI.

8.8 Limitations of the Work Performed

- Some surface techniques proved difficult to analyse CoBlast surfaces, in particular, those executed using reflective mode due to surface roughness (Zygo white-light interferometer) or thin coatings analysis (reflective and transmission mode of XRD).
- Due to the limit of available samples produced for this study, sample size of 3-5 were used for analysis.
- The CoBlast technology was continuously being improved through advancements in research and development work, as a result, the nozzle arrangement in-addition to the abrasives used was frequently updated as part of the standard process set-up.
- A smaller preliminary study performed prior to the larger animal study which mimicked the proposed procedure would have elucidated the potential use of precolonised K-wire implants.

8.7 Future Work

Based on the conclusions of this thesis, the following work has been suggested and other avenues explored for applications using CoBlast technology:

- *In vivo* trials using precolonised implants to assess the anticolonising behaviour of AgA. Also, there is a need to investigate the osteointegration of AgA using an animal model.
- Optimisation of materials is key. Increasing Ag loading in order to identify the limit to maximise AgA activity, whilst minimising cytotoxicity to human cells. It would also be interesting to investigate if enhancing the crystalline properties of the substituted apatites would improve the osteoconductive potential of these materials. A pre-blend of AgA and SrA powders may improve the osteoconductive potential of AgA and the anticolonising properties of SrA.
- Optimisation of process conditions to tailor-make surface properties such as pretreating the surface with MCD-425 followed by a CoBlast treatment using HA/MCD-106. A surface with increased roughness and HA coating would result.
- A study which investigates the anticolonising behaviour of the substituted apatites so as to gain an insight into their mode of action and further investigate the hypothesis that metal ions produce a redox reaction on the surface which produces ROS capable of killing microbes. Further investigation the co-doped AgSrA surface so as to understand why the results obtained were not as expected are warranted.

- CoBlast can deposit onto metals however, nitinol and CoCr are other important metals commonly used. Other biomaterials are also used as key components of hard tissue implants such as polyethylene which is used as a liner in acetabular cups. It would be interesting to investigate if CoBlast can be used to deposit on other material substrates.
- Since CoBlast is a blasting technology which uses materials, could a pre-blend of HA and antibiotics be deposited. Also, could proteins such as BMP's be deposited using CoBlast technology. Other therapeutic avenues could be explored such as the use of bisphosphonates to prevent osteointegration for trauma pins etc.
- Coat metals with an-allergic materials so that these surfaces could be incorporated into individuals who are allergic to the underlying surface, thus preventing exposure to the allergen *in vivo*.
- Also, recently new infection preventing strategies are emerging such as tethering of antibiotics and AmPs so as to have a permanent coating (non-leaching) of these active agents on the surface.

References

Abron, A., Hopfensperger, M., Thompson, J. and Cooper, L.F. (2001). "Evaluation of a predictive model for implant surface topography effects on early osseointegration in the rat tibia model." *Journal of Prosthetic Dentistry* **85**(1): 40-46.

Abu-Amer, Y., Darwech, I. and Clohisy, J.C. (2007). "Aseptic loosening of total joint replacements: mechanisms underlying osteolysis and potential therapies." *Arthritis Research & Therapy* **9**(Suppl 1): S6.

Adams, C.S., Antoci, V.J., Harrison, G., Patal, P, Freeman, T.A., Shapiro, I.M., Parvizi, J, Hickok, N.J., Radin, S. and Ducheyne, P. (2009). "Controlled release of vancomycin from thin sol gel films on implant surfaces successfully controls osteomyelitis." *Journal of Orthopaedic Research* **27**(6): 701-709.

Ahmed, I., Ready, D., Wilson, M. and Knowles, J.C. (2006). "Antimicrobial effect of silver-doped phosphate-based glasses." *Journal of Biomedical Materials Research Part A* **79**(3): 618-626.

Albrektsson, T. and Johansson, C. (2001). "Osteoinduction, osteoconduction and osseointegration." *European Spine Journal* **10**: S96-S101.

Alt, V., Bechert, T., Steinrücke, P., Wagener, M., Seidel, P., Dingeldein, E., Domann, E.and Schnettler, R. (2004). "An in vitro assessment of the antibacterial properties and cytotoxicity of nanoparticulate silver bone cement." *Biomaterials* **25**(18): 4383-4391.

Amyes, S.G.B. and Gemmell, C.G. (1997). "Antibiotic resistance: proceedings of a symposium held on 12 July 1996 at the University of Southampton." *Journal of Medical Microbiology* **46**: 436-470.

An, Y.H. and Friedman, R.J. (1996). "Prevention of sepsis in total joint arthroplasty." *Journal of Hospital Infection* **33**(2): 93-108.

Ando, Y., Miyamoto, H., Noda, I., Sakurai, N., Akiyama, T., Yonekura, Y., Shimazaki, T., Miyazaki, M., Mawatari, M. and Hotokebuchi, T. (2010). "Calcium phosphate coating containing silver shows high antibacterial activity and low cytotoxicity and inhibits bacterial adhesion." *Materials Science and Engineering*: C **30**(1): 175-180.

Anselme, K. (2000). "Osteoblast adhesion on biomaterials." *Biomaterials* **21**(7): 667-681.

Anselme, K. and Bigerelle, M. (2005). "Topography effects of pure titanium substrates on human osteoblast long-term adhesion." *Acta Biomaterialia* **1**(2): 211-222.

Anselme, K., Linez, P., Bigerelle, M., Le Maguer, D., Le Maguer, A., Hardouin, P., Hildebrand, H.F., Lost, A. and Leroy, J.M. (2000). "The relative influence of the topography and chemistry of TiAl6V4 surfaces on osteoblastic cell behaviour." *Biomaterials* **21**(15): 1567-1577.

Antoci, V.J., Adams, C.S., Parvizi, J., Davidson, H.M., Composto, R.J., Freeman, T.A., Wickstrom, E., Ducheyne, P., Jungkind, D., Shapiro, I.M., and Hickok, N.J. (2008). "The inhibition of Staphylococcus epidermidis biofilm formation by vancomycin-modified titanium alloy and implications for the treatment of periprosthetic infection." *Biomaterials* **29**(35): 4684-4690.

Antonini, J.M., Van Dyke K., Ye, Z., Di Matteo,M and Reasor, M.J. (1994) Introduction of luminol-dependent chemiluminesence as a method to study silica inflammation in the issue and phagocytic cells of rat lung." *Environmental Health Perspectives* **102**(10): 37-42.

Applerot, G., Lipovsky, A., Dror, R., Perkas, N., Nitzan, Y., Lubart, R. and Gedanken, A. (2009). "Enhanced antibacterial activity of nanocrystalline ZnO due to increased ROS-mediated cell injury." *Advanced Functional Materials* **19**(6): 842-852.

Arinzeh, T.L., Tran, T., Mcalary, J. and Daculsi, G. (2005). "Comparative study of biphasic calcium phosphate ceramics for human mesenchymal stem-cell-induced bone formation." *Biomaterials* **26**(17): 3631-3638.

ASTM Standard E2149, 2001 (2010). *American Test Standard Test Method for determining antimicrobial activity of immobilized antimicrobial agents under dynamic contact conditions.* ASTM international, West Conshohocken, Pennsylvania, US.

ASTM Standard F11479, 2005 (2011). *American Test Standard Test Method for tension testing of calcium phosphate and metallic coatings*. ASTM international, West Conshohocken, Pennsylvania, US.

Aubin, J.E. (2001). "Regulation of osteoblast formation and function." *Revision in Endocrine and Metabolic Disorders* **2**(1): 81-94.

Balaban, N., Gov, Y., Giacometti, A., Cirioni, O., Ghiselli, R. Mocchegiani, F., Orlando, F., D"Amato, G., Saba, V., Scalise, G., Bernes, S. and Mor, A. (2004). "A chimeric peptide composed of a dermaseptin derivative and an RNA III-inhibiting peptide prevents graft-associated infections by antibiotic-resistant staphylococci." *American Society for Microbiology* **48**(7): 2544-2550.

Baron, R., Neff, L., Louvard, D. and Courtoy, P.J. (1985). "Cell-mediated extracellular acidification and bone resorption: evidence for a low pH in resorbing lacunae and localization of a 100-kD lysosomal membrane protein at the osteoclast ruffled border." *Journal of Cell Biology* **101**(6): 2210-22.

Barrère, F., van Blitterswijk, C. A. and de Groot, K. (2006). "Bone regeneration: molecular and cellular interactions with calcium phosphate ceramics." *International Journal of Nanomedicine* **1**(3): 317–332.

Baujard-Lamotte, L., Noinville, S., Goubard, F., Marque, P. and Pauthe, E. (2008). "Kinetics of conformational changes of fibronectin adsorbed onto model surfaces." *Colloids and surfaces B: Biointerfaces* **63**(1): 129-137.

Bendall, S.P., Gaies, M., Frondoza, C., Jinnah, R.H. and Hungerford, D.S. (1998). "Effect of particulate bioactive glass on human synoviocyte cultures." *Journal of Biomedical Materials Research* **41**(3): 392–397.

Berry, J.A, Biedlingmaier, J.F. and Whelan, P.J. (2000). "In vitro resistance to bacterial biofilm formation on coated fluoroplastic tympanostomy tubes." Otolaryngology - *Head and Neck Surgery* **123**(3): 246-251.

Bertazzo, S., Zambuzzi, W.F., Campos,D.D., Ogeda, T.L., Ferreira, C.V. and Bertran, C.A. (2010). "Hydroxyapatite surface solubility and effect on cell adhesion." *Colloids and Surface B: Biointerface* **78**(2): 177-84.

Bertinetti, L., Tampieri, A., Landi, E., Martra, G. and Coluccia, S. (2006). "Punctual investigation of surface sites of HA and magnesium-HA." *Journal of the European Ceramic Society* **26**(6): 987-991.

Best, S.M., Porter, A.E., Thian, E.S. and Huang J. (2008). "Bioceramics: Past, present and for the future." *Journal of the European Ceramic Society* **28**(7): 1319-1327.

Bigerelle, M. and Anselme K. (2005). "Statistical correlation between cell adhesion and proliferation on biocompatible metallic materials." *Journal of Biomedical Materials Research A* **72**(1): 36-46.

Bonfield, W.I. (1988) ed. *In*: Paipetis S.A., (ed.) *Engineering Applications of New Composites*. Oxford: Omega Scientific: pp. 17–21.

Borsari, V., Giavaresi, G., Fini, M., Torricelli, P., Salito, A., Chiesa, R., Chiusoli, L., Volpert, A., Rimondini, L. and Giardino, R. (2005). "Physical characterization of different-roughness titanium surfaces, with and without hydroxyapatite coating, and their effect on human osteoblast-like cells." *Journal of Biomedical Materials Research B: Applied Biomaterials* **75**(2): 359-368.

Boswald, M., Mende, K., Bernschneider, W., Bonakdar, S., Ruder, H., Kissler, H., Sieber, E., and Guggenbichler, J. P. (1999). "Biocompatibility testing of a new silver impregnated catheter in vivo." *Infection* **27**(1): S38-42.

Boyan, B.D., Hummert, T.W., Dean, D.D. and Schwartz, Z. (1996). "Role of material surfaces in regulating bone and cartilage cell response." *Biomaterials* **17**(2): 137-146.

Boyan, B.D., Lossdörfer, S., Wang, L., Zhao, G., Lohmann, C.H., Cochran, D.L. and Schwartz, Z. (2003). "Osteoblasts generate an osteogenic microenvironment when grown on surfaces with rough microtopographies." *European Cells Materials* **24(**6):22-27.

Bragg, P.D., and Rainnie, D.J. (1975). "The effect of silver ions on the respiratory chain of Escherichia coli." *Canadian Journal of Microbiology* **20**(6): 883-889.

Brohede, U., Forsgren, J., Roos, S., Mihranyan, A., Engqvist, H. and Strømme, M. (2009). "Multifunctional implant coatings providing possibilities for fast antibiotics loading with subsequent slow release. *Journal of Materials Science: Materials in Medicine* **20**(9): 1859-1867.

Brunski, J.B. (1999). "In vivo bone response to biomechanical loading at the bone/dental-implant interface." *Advances in Dental Research* **13**(1): 99-119.

Brutel de la Riviere, A., Dossche, K.M., Birnbaum, D.E, and Hacker, R. (2000). "First clinical experience with a mechanical valve with silver coating." *Journal of Heart and Valve Disease* **9**(1): 123-129.

British Standards Institution (1994) BS EN 552:1994. "Sterilization of medical devices. Validation and routine control of sterilization by irradiation". London: BSI.

Burr, D. B., Mori, S., Boyd, R. D., Sun, T. C., Blaha, J.D., Lane, L. and Parr J. (1993). "Histomorphometric assessment of the mechanisms for rapid ingrowth of bone to HA/TCP coated implants." *Journal of Biomedical Materials Research* **27**(5): 645-653.

Campbell, A.A. (2003). "Bioceramics for implant coatings." *Materials Today* **6**(11): 26-30.

Campoccia, D., Montanaro, L. and Arciola, C.R. (2006). "The significance of infection related to orthopedic devices and issues of antibiotic resistance." *Biomaterials* **27**(11): 2331-2339.

Cao, W. and Hench, L.L. (1996). "Bioactive materials." *Ceramics International* **22**(6): 493-507.

Capuccini, C., Torricelli, P., Sima, F., Boanini, E., Ristoscu, C., Bracci, B., Socol, G., Fini, M., Mihailescu, I.N. and Bigi, A. (2008). "Strontium-substituted hydroxyapatite coatings synthesized by pulsed-laser deposition: In vitro osteoblast and osteoclast response." *Acta Biomaterialia* **4**(6): 1885-1893.

Carlson, R.P., Taffs, R., Davison, W.M. and Stewart, P.S. (2008). "Anti-biofilm properties of chitosan coated surfaces." *Journal of Biomaterials Science: Polymer Edition*. **19**(8): 1035-1046.

Caverzasio, J. (2008). "Strontium ranelate promotes osteoblastic cell replication through at least two different mechanisms." *Bone* **42**(6): 1131-1136.

Chae, M.S. and Schraft, H. (2000). "Comparative evaluation of adhesion and biofilm formation of different Listeria monocytogenes strains." *International Journal of Food Microbiology* **62**(1-2): 103-11.

Chai, F., Hornez, J.C., Blanchemain, N., Neut, C., Descamps, M. and Hildebrand, H.F. (2007). "Antibacterial activation of Hydroxyapatite (HA) with controlled porosity by different antibiotics." *Biomolecular Engineering* **24**(5): 510-514.

Chang, M.K., Raggatt, L.J., Alexander, K.A., Kuliwaba, J.S., Fazzalari, N.L., Schroder, K., Maylin, E.R., Ripoll, V.M., Hume, D.A. and Pettit, A.R. (2008). "Osteal tissue macrophages are intercalated throughout human and mouse bone lining tissues and regulate osteoblast function in vitro and in vivo." *Journal of Immunology* **181**(2): 1232-44.

Chang, P. and Khor K.A. (1996). "Addressing processing problems associated with plasma spraying hydroxyapatite coatings." *Biomaterials* **17**(5): 537-544.

Chen, W, Liu Y., Courtney H.S., Bettenga, M., Agrawal, C.M., Bumgardner, J.D. and Ong J.L. (2006). "In vitro anti-bacterial and biological properties of magnetron co-sputtered silver-containing hydroxyapatite coating." *Biomaterials* **27**(32): 5512-5517.

Chen, M., Liu, D., You, C., Yang, X. and Cui, Z. (2007a). "Interfacial characteristic of graded hydroxyapatite and titanium thin film by magnetron sputtering." *Surface and Coating Technology* **201**(9-11): 5688–5691.

Chen, W., Oh, S., Ong, A.P., Oh, N., Liu, Y., Courtney, H.S., Appleford, M. and Ong, J.L. (2007b). "Antibacterial and osteogenic properties of silver-containing hydroxyapatite coatings produced using a sol gel process." *Journal of Biomedical Materials Research A* **82**(4): 899-906.

Chen, J., Wolke, J.G.C., and De Groot, K. (1994). "Microstructure and crystallinity in hydroxyapatite coatings." *Biomaterials* **15**(5): 396-399.

Chen, Q.Z., Wong, C.T., Lu, W.W., Cheung, K.M.C., Leong, J.C.Y. and Luk, K.D.K. (2004). "Strengthening mechanisms of bone bonding to crystalline hydroxyapatite in vivo." *Biomaterials* **25**(18):4243-4254.

Chen, Y., Zheng, X., Xie,Y., Ding, C., Ruan, H. and Fan, C.,(2008). "Antibacterial and cytotoxic properties of plasma sprayed silver-containing HA coatings." *Journal of Materials Science: Materials in Medicine* **19**(12): 3603-3609.

Cho, S.A. and Park, K.T. (2003). "The removal torque of titanium screw inserted in rabbit tibia treated by dual acid etching." *Biomaterials* **24**(20): 3611–3617.

Chung, R.J., Hsieh, Huang ,M.F., Perng C.W., Wen L.H. and Chin, T.S. (2006). "Antimicrobial effects and human gingival biocompatibility of hydroxyapatite sol gel coatings." *Journal of Biomedical Materials Research Part B: Applied Biomaterials* **76**(1): 169-178.

Clèries, L., Martínez, E., Fernández-Pradas, J.M., Sardin, G., Esteve, J. and Morenz J.L. (2000). "Mechanical properties of calcium phosphate coatings deposited by laser ablation", *Biomaterials* **21**(9): 967-971.

Crist, B.V. (1999). The Elements and Native Oxides (for Ag-A). In *PDF Handbooks of Monochromatic XPS Spectra*. California (USA): XPS International, LLC.

Cross, M.J. and Parish, E.N. (2005). "A hydroxyapatite-coated total knee replacement: prospective analysis of 1000 patients." *Journal of Bone and Joint Surgery British* **87**(8): 1073-1076.

Dailey, L., Jekel, N., Fink, L., Gessler, T., Schmehl, T., Wittmar, M., Kissel, T. and Seeger, W. (2006). "Investigation of the proinflammatory potential of biodegradable nanoparticle drug delivery systems in the lung." *Toxicology Applied Pharmacology* **215**(1): 100-108.

Dalton, J.E. and Cook, S.D. (1995). "In vivo mechanical and histological characteristics of HA-coated implants vary with coating vendor." *Journal of Biomedical Materials Research* **29**(2): 239-245.

Darouiche, R. (2004). "Treatment of infections associated with surgical implants." *England Journal Medicine* **350**(14): 1422-1429.

Dekker, R.J., de Bruijn, J. D., Stigter, M., Barrere, F., Layrolle, P. and van Blitterswijk,.C.A. (2005). "Bone tissue engineering on amorphous carbonated apatite and crystalline octacalium phosphate-coated titanium discs." *Biomaterials* **26**(25): 5231-5239.

D'Haese, P.C, Schrooten, I., Goodman, W.G., Cabrera, W.E., Lamberts, L.V., Elseviers, M.M., Couttenye, M-.M. and De Broe, M.E. (2000). "Increased bone strontium levels in hemodialysis patients with osteomalacia." *Kidney Internationa*, **57**(3): 1107-1114.

D'Lima, D.D., Walker, R.H. and Colwell, Jr. C.W. (1999). "Omnifit-HA stem in total hip arthroplasty." *Clinical Orthopedic Related Research* **363**: 163-169.

Donnelly, W.J., Kobayashi, A., Freeman, M.A.R., Chin, T.W., Yeo, H., West, M. and Scott, G. (1997). "Radiological and survival comparison of four fixation of a proximal femoral stem", *Journal of Bone and Joint Surgery* **79B**(3): 351-360.

Dorozhkin, S.V. (2010). "Calcium orthophosphates as bioceramics: State of the art." *Journal of Functional Biomaterials* **1**(1): 22-107.

Dorozhkin, S.V. (1999). "Inorganic Chemistry of the Dissolution Phenomenon: The Dissolution Mechanism of Calcium Apatites at the Atomic(Ionic) Level." Comments on Inorganic Chemistry: *A Journal of Critical Discussion of the Current Literature* **20**(4-6): 285-299.

Dorozhkin, S.V. (1997). "Surface reactions of apatite dissolution." *Journal of Colloid and Interface Science* **191**(2): 489–497.

Dorr, L.D., Wan, Z., Song, M. and Ranawat, A. (1998). "Bilateral total hip arthroplasty comparing hydroxyapatite coating to porous coated fixation." *Journal of Arthroplasty* **13**(7): 729 -736.

Dougherty, S. (1988). "Pathobiology of infection on prosthetic devices." *Reviews of Infections Disease* **10**(6): 1102-1117.

Ducheyne, P. and Qiu, Q. (1999). "Bioactive ceramics: the effect of surface reactivity on bone formation and bone cell function." *Biomaterials* **20**(23-24): 2287-2303.

Ducheyne, P., Radin, S., Heughebaert, M. and Heughebaert, J.C. (1990). "Calcium phosphate ceramic coatings on porous titanium: effect of structure and composition on electrophoretic deposition, vacuum sintering and in vitro dissolution." *Biomaterials* **11**(4): 244-254.

Dumbleton, J. and Manley, M.T. (2004). "Hydroxyapatite-coated prostheses in total hip and knee arthroplasty." *Journal of Bone and Joint Surgery* **86**(11): 2526-2540.

Edupuganti, O.P., Antoci V.J., King, S.B., Jose, B., Adams, C.S., Parvizi, J., Shapiro, I.M., Zeiger, A.R., Hickok, N.J. and Wickstrom, E. (2007). "Covalent bonding of vancomycin to Ti6Al4V alloy pins provides long-term inhibition of Staphylococcus aureus colonization." *Bioorganic & Medicinal Chemistry Letters* **17**(10): 2692-2696.

Eggeler, G., Hornbogen, E., Yawny, A., Heckmann, A., Wagner, M. (2004). "Structural and functional fatigue of NiTi shape memory alloys." *Materials Science and Engineering:A* **378**(1-2): 24–33

Elmengaard, B., Bechtold, J.E. and Søballe, K. (2005). "In vivo effects of RGD-coated titanium implants inserted in two bone-gap models." *Journal of Biomedical Materials Research A* **75**(2): 249–255.

Faber, C., Stallmann, H.P., Lyaruu, D.M., De Blieck, J.M.A, Bervoets, T.J.M., Van Nieuw Amerongen, A. and Wuisman, P.I.J.M. (2003). "Release of antimicrobial peptide Dhvar-5 from polymethylmethacrylate beads." *Journal of Antimicrobial Chemotherapy* **51**(6): 1359-1364.

Fagian, M.M., Da Silva, L.P. and Vercesi, A.E. (1986). "Inhibition of oxidative phosphorylation by Ca2+ or Sr2+: a competition with Mg2+ for the formation of adenine nucleotide complexes." *Biochimica et biophysica acta* **852**(2-3): 262-268.

Fathi, M.H., Hanifi, A. and Mortazavi, V. (2008). "Preparation and bioactivity evaluation of bone-like hydroxyapatite nanopowder." *Journal of Materials Processing Technology* **202**(1-3): 536-542.

FDA. (1992). "Calcium phosphate (Ca-P) coating draft guidance for preparation of FDA submissions for orthopedic and dental endosseous implants." Washington, DC: Food and Drug Administration: pp. 1–14.

Feng, C.F., Khor, K.A., Kweh, S.W.K., Cheang, P. (2000a). "Thermally induced crystallization of amorphous calcium phosphate in plasma-spheroidised hydroxyapatite powders." *Materials Letters* **46**(4): 229–233.

Feng, Q.L., Kim, T.N., Wu, J., Park, E.S., Kim, J.O., Lim, D.Y. and Cui F. Z. (1998). "Antibacterial effects of Ag-HAp thin films on alumina substrates." *Thin Solid Films* **335**(1-2): 214-219.

Feng, Q.L., Wu, J., Chen, G.Q., Cui, F.Z., Kim, T.N. and Kim, J.O. (2000b). "A mechanistic study of the antibacterial effect of silver ions on Escherichia coli and Staphylococcus aureus." *Journal of Biomedical Materials Research* **52**(4): 662-668.

Ferreira, L. and Zumbuehl A. (2009). "Non-leaching surfaces capable of killing microorganisms on contact." *Journal of Materials Chemistry* **19**: 7796-7806

Ferreira, L., Langer, R.S., Loose, C.R., O'Shaughnessy, W.S., Zumbuehl, A. and Stephanopolous, G. (2008). "Medical Devices and coatings with non-leaching antimicrobial peptited", US patent **EP20070751170**.

Filiaggi, M.J., Coombs, N.A. and Pilliar, R.M. (1991). "Characterization of the interface in the plasma-sprayed HA coating/Ti-6Al-4V implant system." *Journal of Biomedical Materials Research* **25**(10): 1211-1229.

Fujihara, T., Tsukamoto, M., Abe, N., Miyake, S., Ohji,T. and Akedo, J. (2004). "Hydroxyapatite film formed by beam irradiation." *Vacuum* **73**(3-4): 629–633.

Furlong, R.J. and Osborn, J.F. (1991). "Fixation of hip prostheses by hydroxyapatite ceramic coatings." *Journal Bone and Joint Surgery* **73B**(5): 741- 745.

Gabriel, M., Nazmi, K., Veerman, E.C., Amerongen, A.V.N. and Zentner, A. (2006). "Preparation of LL-37-grafted titanium surfaces with bactericidal activity." *Bioconjugate Chemistry* **17**(2): 548-550.

Galliani, S., Viot ,M., Cremieux, A. and Van der Auwera, P. (1994). "Early adhesion of bacteremic strains of Staphylococcus epidermidis to polystyrene: influence of hydrophobicity, slime production, plasma, albumin, fibrinogen, and fibronectin." *Journal of Laboratory and Clinical Medicine* **123**(5): 685-692.

Garcia, A.J, Vega, M.D. and Boettiger, D. (1999). "Modulation of cell proliferation and differentiation through substrate-dependent changes in fibronectin conformation." *Molecular Biology of the Cell* **10**(3): 785-798.

Gbureck, U., Masten, A., Probst, J. and Thull, R. (2003). "Tribochemical structuring and coating of implant metal surfaces with titanium oxide and hydroxyapatite layers." *Material Science Engineering C* **23**(3): 461-465.

Geesink, R.G. T. (2002). "Osteoconductive coatings for total joint arthroplasty." *Clinical Orthopaedics & Related Research* **395**: 53-65.

Geesink, R.G.T. (1989). "Experimental and clinical experience with hydroxyapatite-coated hip implants." *Orthopedics* **12**(9): 1239-1242.

Geetha, M. Singh, A.K., Asokamani, R. and Gogia, A.K. (2009). "Ti based *Biomaterials* the ultimate choice for orthopaedic implants - A review." *Progress in Materials Science* **54**(3): 397-425.

Gil, F.J., Planell, J.A., Padros, A. and Aparicio, C. (2007). "The effect of shot blasting and heat treatment on the fatigue behavior of titanium for dental implant applications." *Dental Materials* **23**(4): 486-491.

Ginalska, G., Kowalczuk, D. and Osinska, M. (2005). "A chemical method of gentamicin bonding to gelatine-sealed prosthetic vascular grafts." *International Journal of Pharmaceutics* **288**(1): 131-140.

Ginebra M.P., Traykova T. and Planell J.A. (2006). "Calcium phosphate cements as bone drug delivery systems: A review." *Journal of Controlled Release* **113**(2): 102-110.

Gold, H.S, and Moellering, R.C. (1996). "Antimicrobial-drug resistance." *The New England Journal of Medicine* **335**(19): 1445-1453.

Gosain, A.K., Song, L., Riordan, P., Amarante, M.T., Nagy, P.G., Wilson, C.R., Toth, J.M., Ricci, J.L. (2002). "A 1-year study of osteoinduction in hydroxyapatite-derived biomaterials in an adult sheep model: part I." *Plastic Reconstruction Surgery* **109**(2): 619-630.

Gosheger, G., Hardes, J., Ahrens, H., Streitburger, A., Buerger, H., Erren, M., Gunsel, A., Kemper, F.H., Winkelmann, W. and Von Eiff, C. (2004). "Silver-coated megaendoprostheses in a rabbit model--an analysis of the infection rate and toxicological side effects." *Biomaterials* **25**(24): 5547-5556.

Gottenbos, B. Klatter, F., Van Der Mei, H.C., Busscher, H.J. and Nieuwenhuis, P. (2001). "Late hematogenous infection of subcutaneous implants in rats." *Clinical and Diagnostic Laboratory Immunology* **8**(5): 980-983.

Gottenbos, B., Van Der Mei, H.C. and Busscher, H. J. (2000). "Initial adhesion and surface growth of Staphylococcus epidermidis and Pseudomonas aeruginosa on biomedical polymers." *Journal of Biomedical Materials Research* **50**(2): 208-214.

Gristina, A.G. (1987). "Biomaterial-centered infection: microbial adhesion versus tissue integration." *Science* **237**(4822): 1588-1595.

Gristina, A.G. and Costerton, J.W. (1985). "Bacterial adherence to biomaterials and tissue. The significance of its role in clinical sepsis." *Journal of Bone and Joint Surgery* **67**(2): 264-273.

Gristina A.G. and Kolkin, J. (1983). "Current concepts review. Total joint replacement and sepsis." *The Journal of Bone & Joint Surgery* **65**(1): 128-134.

Grizon, F., Aguado, E., Huré, G., Baslé, M.F. and Chappard, D. (2002). "Enhanced bone integration of implants with increased surface roughness: a long term study in the sheep." *Journal of Dentistry* **30**(5-6): 195-203.

Gross, K.A. and Berndt, C.C. (1998). "Thermal processing of hydroxyapatite for coating production." *Journal of Biomedical Materials Research* **39**(4): 580-587.

Gross, K.A., Berndt, C.C. and Herman, H. (1998). "Amorphous phase formation in plasma-sprayed hydroxyapatite coatings." *Journal of Biomedical Materials in Research* **39**(3): 407-414.

Gross, K.A., Walsh, W. and Swarts E. (2004). "Analysis of Retrieved hydroxyapatite-Coated Hip Prostheses." *Journal of Thermal Spray Technology* **13**(2): 190-197.

Grzesik, W.J. and Robey P.G. (1994). "Bone matrix RGD glycoproteins: immunolocalization and interaction with human primary osteoblastic bone cells in vitro." *Journal of Bone Mineral Research* **9**(4): 487-496.

Gu, Y.W, Khor, K.A. and Cheang, P. (2003). "In vitro studies of plasma-sprayed hydroxyapatite/Ti-6Al-4V composite coatings in simulated body fluid (SBF)." *Biomaterials* **24**(9): 1603-1611.

Guida, A., Towler, M.R., Wall, J.G., Hill, R.G. and Eramo, S. (2003). "Preliminary work on the antibacterial effect of strontium in glass ionomer cements." *Journal of Materials Science Letters* **22**(20): 1401-1403.

Gunnigle, J.R. (2011). "The case for prolotherapy –The opening argument." *Journal of Prolotherapy* **3**(4): 741-743.

Habraken, W.J, Wolke, J.G. and Jansen, J.A. (2007). "Ceramic composites as matrices and scaffolds for drug delivery in tissue engineering." *Advanced Drug Delivery Reviews* **59**(4-5): 234-248.

Hansson, U., Ryd, L. and Toksvig-Larsen, S. (2008). "A randomised RSA study of Peri-Apatite™ HA coating of a total knee prosthesis." *The Knee* **15**(3): 211-216.

Hardes, J., Ahrens, H., Gebert, C., Streitbuerger, A., Buerger, H., Erren, M., Gunsel, A., Wedemeyer, C., Saxler, G., Winkelmann, W. and Gosheger, G. (2007). "Lack of toxicological side-effects in silver-coated megaprostheses in humans." *Biomaterials* **28**(18): 2869-2875.

Hardouin, P., Anselme, K., Flautre, B., Bianchi, F., Bascoulenguet, G. and Bouxin, B. (2000). "Tissue engineering and skeletal diseases." *International Bone Spine* **67**(5): 419-424.

Harkes, G., Dankert, J. and Feijen, J. (1992). "Growth of uropathogenic Escherichia coli strains at solid surfaces." *Journal of Biomaterials Science Polymer Edition* **3**(5): 403-418.

Hayashi, K., Inadome, T., Tsurnura, H., Nakashima, Y. and SuEioka, Y. (1994). "Effect of surface roughness of hydroxyapatite-coated titanium on the bone-implant interface shear strength." *Biomaterials* **15**(14): 1187-1191.

Heimann, R.B. and Wirth, R. (2006). "Formation and transformation of amorphous calcium phosphates on titanium alloy surfaces during atmospheric plasma spraying and their subsequent in vitro performance." *Biomaterials* **27**(6): 823-831.

Heimann, R.B., (2006). "Thermal spraying of biomaterials." *Surface and Coating Technology* **20**(5): 2012-2019.

Hench, L.L. (1998). "Bioceramics." *Journal of American Ceramic Society* **81**(7): 1705-1728.

Hench, L.L. and Polak, J.M. (2002). "Third-generation biomedical materials." *Science* **295**(5557): 1014-1017.

Hench, L.L. and Wilson, J. (Ed.). (1993) An introduction to bioceramics. London: World Scientific Publishing Company: pp. 1.

Hendriks, J.G.E, Van Horn, J.R, Van Der Mei, H.C. and Busscher, H.J. (2004). "Backgrounds of antibiotic-loaded bone cement and prosthesis-related infection." *Biomaterials* **25**(3): 545-556.

Hetrick, E.M., and Schoenfisch, M.H. (2006). "Reducing implant-related infections: active release strategies." *Chemical Society Reviews* **35**(9): 780-789.

Hile, D.D., Sonis, S.T., Doherty, S.A., Tian, X.Y, Zhang, Q., Jee, W.S.S. and Trantolo, D.J. (2005). "Dimensional Stability of the Alveolar Ridge After Implantation of a Bioabsorbable Bone Graft Substitute: A Radiographic and Histomorphometric Study in Rats." *Journal of Oral Implantology* **31**(2): 68-76.

Hilpert, K., Elliott, M., Jenssen, H., Kindrachuk, J., Fjell, C.D., Koerner, J., Winkler, D.F.H., Weaver, L.L., Henklein, P., Ulrich, A.S., Chiang, S.H.Y., Farmer, S.W., Pante, N., Volkmer, R. and Hancock, R.E.W. (2009). "Screening and characterization of surface-tethered cationic peptides for antimicrobial activity." *Chemical Biology* **16**(1): 58-69.

Hing, K.A., Best, S.M., Tanner, E.K., Bonfield, W. and Revell, P.A. (2004). "Mediation of bone ingrowth in porous hydroxyapatite bone graft substitutes." *Journal of Biomedical Materials Research Part A* **68A**(1): 187-200.

Hong, Z.; Luan, L. Paik, S.E.; Deng, B.; Ellis, D.E.; Ketterson, J.B. Mello, A.; Eon, J.G., Terra, J. and Rossi, A. (2007). "Crystalline hydroxyapatite thin films produced at room temperature - An opposing radio frequency magnetron sputtering approach." *Thin Solid Films* **515**(17): 6773-6780.

Hu, C., Guo, J., Qu, J., and Hu, X. (2007). "Efficient destruction of bacteria with Ti (V) and anti-bacterial ions in co-substituted hydroxyapatite films." *Applied Catalysis B: Environmental* **73**(3-4): 345-353.

Hu, Y.C. and Zhong, J.P. (2009). "Osteostimulation of bioglass." *Chinese Medical Journal* **122**(19): 2386–2389.

Hu, S., Chang, J. Liu, M. and Ning, C. (2009). "Study on antibacterial effect of 45S5 Bioglass." *Journal of Material Science in Materials in Medicine* **20**(1): 281–286.

Huiskes, R. (1993). "Failed innovation in total hip replacement: Diagnosis and proposals for a cure." *Acta Orthopaedica* **64**(6): 699-716.

Huo, M.H., Stockton, K.G., Mont, M.A. and Parvizi, J. (2010). "What"s new in total hip arthroplasty." *The Journal of Bone and Joint Surgery* **92**(18): 2959-2972.

Ignatius, A.A., Betz, O., Augat, P. and Claes, L.E. (2001). "In vivo investigations on composites made of resorbable ceramics and poly(lactide) used as bone graft substitutes." *Journal of Biomedical Materials in Research* **58**(6): 701-709.

Ishikawa, K., Miyamoto, Y., Nagayama, M. and Asaoka, K. (1997). "Blast coating method: new method of coating titanium surface with hydroxyapatite at room temperature." *Journal of Biomedical Material Research* **38**(2): 129-134.

Isiklar, Z.U., Darouiche, R.O., Landon, G.C. and Beck, T. (1996). "Efficacy of antibiotics alone for orthopaedic device related infections." *Clinical Orthopaedics and Related Research* **332**: 184-189.

ISO Standard 13779-1(2008). "International Organisation of Standards, Implants for surgery: Coating for hydroxyapatite ceramics." pp. 1–8.

Ito, A., Kawamura, H., Otsuka, M., Ikeuchi, M., Ohgushi, H., Ishikawa, K., Onuma, K., Kanzaki, N., Sogo, Y. and Ichinose, N. (2002). "Zinc-releasing calcium phosphate for stimulating bone formation." *Materials Science and Engineering*: C **22**(1): 21-25.

Jäger M., Zilkens C., Zanger K. and Krauspe, R. (2007). "Significance of nano- and microtopography for cell-surface interactions in orthopaedic implants." *Journal of Biomedical Biotechnology* **2007**(8): 1-19.

Jiranek, W.A., Hanssen, A.D. and Greenwald, A.S. (2006). "Antibiotic-loaded bone cement for infection prophylaxis in total joint replacement." Journal of Bone and Joint Surgery **88**(11): 2487-2500.

Jones, J.R., Ehrenfried, L.M. and Hench, L.L. (2006). "Optimising bioactive glass scaffolds for bone tissue engineering." *Biomaterials* **27**(7): 964–973.

Jose, B., Antoci, V., Zeiger, A.R., Wickstrom, E. and Hickok, N.J. (2005). "Vancomycin Covalently Bonded to Titanium Beads Kills Staphylococcus aureus." *Chemistry and Biology* **12**(9): 1041-1048.

Jung, W.K., Koo, H.C., Kim, K.W., Shin, S., Kim, S.H., and Park, Y.H. (2008). "Antibacterial activity and mechanism of action of the silver ion on Staphylococcus aureus and Escherichia coli." *Applied and Environmental Microbiology* **74**(7): 2171-2178.

Kadurugamuwa, J.L., Sin, L., Albert, E., Yu, J., Francis, K., DeBoer, M., Rubin, M., Bellinger-Kawahara, C., Parr, T.R. and Contag, P.R. (2004). "Direct continuous method for monitoring biofilm infection in a mouse model." *Infectious Immunology* **71**(2): 882-890.

Kapanen, A., Ryhänen, J., Danilov, A. and Tuukkanen, J. (2001). "Effect of nickel-titanium shape memory metal alloy on bone formation." *Biomaterials* **22**(18): 2475-2480.

Karchmer, T.B., Giannetta, E.T., Muto, C.A., Strain, B.A. and Farr, B.M. (2000). "A randomized crossover study ofsilver-coated urinary catheters in hospitalized patients." *Archives of Internal Medicine* **160**(21): 3294-3298.

Kasahara, M. and Anraku, Y. (1974). "Succinate- and NADH oxidase systems of Escherichia coli membrane vesicles: mechanism of Sselective inhibition of the systems by zinc ions." *Journal of Biochemistry* **76**(5): 967-976.

Katto, M., Kurosawa, K., Yokotani, A., Kubodera, S., Kameyama, A., Higashiguchi, T., Nakayama, T. and Tsukamoto, M. (2005). "Poly-crystallized hydroxyapatite coating deposited by pulsed laser deposition method at room temperature."*Applied Surface Science* **248**(1-4): 365-368.

Keselowsky, B.G., Collard, D.M. and García, A.J. (2004). "Surface chemistry modulates focal adhesion composition and signaling through changes in integrin binding." *Biomaterials* **25**(28): 5947-5954.

Khor, K.A., Gu, Y.W., Quek, C.H. and Cheang, P. (2003). "Plasma spraying of functionally graded hydroxyapatite/Ti-6Al-4V coatings." *Surface and Coatings Technology* **168**(2-3): 195-201.

Kim, T.N.; Feng, Q.L.; Kim, J.O.; Wu, J.; Wang, H.; Chen, G.C. and Cui, F.Z. (1998). "Antimicrobial effects of metal ions (Ag+, Cu2+, Zn2+) in hydroxyapatite." *Journal of Materials Science: Materials in Medicine* **9**(1-4): 129-134.

Kinnari, T.J., Peltonen, L.I., Kuusela, P., Kivilahti ,J., Könönen, M. and Jero J. (2005). "Bacterial adherence to titanium surface coated with human serum albumin." *Otology Neurotology* **26**(3): 380-384.

Kirby, G.T.S., White, L. J., Rahman, C.V., Cox, H.C., Qutachi, O., Rose, F.R.A. J., Hutmacher, D.W., Shakesheff, K.M. and Woodruff , M.A. (2011). "PLGA-Based Microparticles for the Sustained Release of BMP-2", *Polymers* **3**(1): 571-586.

Knaack, D., Goad, M.E., Aiolova, M., Rey, C., Tofighi, A., Chakravarthy, P. and Lee, D.D. (1998). "Resorbable calcium phosphate bone substitute." *Journal of Biomedical Materials Research* **43**(4): 399-409.

Koch, C.F, Johnson, S., Kumar, D., Jelinek, M., Chrisey, D.B., Doraiswamy, A., Jin, C., Narayan, R.J. and Mihailescu, I.N. (2007). "Pulsed laser deposition of hydroxyapatite thin films." *Materials Science and Engineering: C* **27**(3): 484-494.

Kokubo, T. and Takadama, H. (2006). "How useful is SBF in predicting in vivo bone bioactivity?." *Biomaterials* **27**(15): 2907-2915.

Kroese-Deutman, H.C., van den Dolder, J., Spauwen, P.H. Jansen, J.A. (2005). "Influence of RGD-loaded titanium implants on bone formation in vivo." *Tissue Engineering* **11**(11-12): 1867-75.

Kumta, P.N., Sfeir, C., Lee, D.H., Olton, D. and Choi D. (2005). "Nanostructured calcium phosphates for biomedical applications: novel synthesis and characterization." *Acta Biomaterialia* **1**(1): 65-83.

Landi, E., Celotti, G., Logroscino, G. and Tampieri, A. (2003). "Carbonated hydroxyapatite as bone substitute." *Journal of the European Ceramic Society* **23**(15): 2931-2937.

Lee, I.S., Whang ,C.N., Kim, H.E., Park, J.C., Song, J.H., Kim, S.R. (2002). "Various Ca/P ratios of thin calcium phosphate films." *Materials Science and Engineering C* **22**(1): 15–20.

Leeuwenburgh, S.C., Wolke, J.G., Lommen, L, Pooters, T, Schoonman, J. and Jansen, J.A. (2006). "Mechanical properties of porous, electrosprayed calcium phosphate coatings." *Journal of Biomedical Materials Research Part A* **78**(3): 558-569.

LeGeros, R.Z. (2001). "Formation and transformation of calcium phosphates: relevance to vascular calcification." *Z Kardiol* **90**: 116-124.

LeGeros, R.Z. and Craig, R.G. (1993). "Strategies to affect bone remodeling: osteointegration." *Journal of Bone and Mineral Research* **8**(S2): S583-96.

LeGeros, R.Z. Kim,Y.E and Kijkowska, R. (1998). "HA/ACP ratios in calcium phosphate coatings on dental and orthopedic implants:effect on properties. In: Legeros Rz, LeGeros J.P eds. *Bioceramics*." London: World Scientific Publishers: pp. 181-184.

LeGeros, RZ., Daculsi, G., Orly, I. and Gregoire, M. (1991). "*The bone-biomaterial interface*." Toronto: University of Toronto.

Levine, B. (2008). "A new era in porous metals: applications in orthopaedics." *Advanced Engineering Materials* **10**(9): 788-792.

Li, H., Li, Z.X., Li, H., Wu, Y.Z. and Wei, Q. (2009). "Characterization of plasma sprayed hydroxyapatite/ZrO2 graded coating." *Materials & Design* **30**(9): 3920-3924.

Lidwell, O.M., Lowbury, E.J., Whyte, W., Blower, R., Stanley, S. and Low, D. (1984). "Infection and sepsis after operations for total hip or knee-joint replacement: Influence of ultraclean air, prophylactic antibiotics and other factors." *Journal of Hygiene* **93**(3): 505-529.

Liu, W. and Chang, J. (2009). "In vitro evaluation of gentamicin release from a bioactive tricalcium silicate bone cement", *Materials Science and Engineering: C* **29**(8): 2486–2492.

Lin, Y., Yang, Z., Cheng, J. and Wang, L. (2008). "Synthesis, characterization and antibacterial property of strontium half and totally substituted hydroxyapatite nanoparticles." *Journal of Wuhan University of Technology Materials Science Edition* **23**(4): 475-479.

Lombardi, A.J., Berend, K.R. and Mallory, T.H. (2006). "Hydroxyapatite-coated titanium porous plasma Sspray tapered stem: Experience at 15 to 18 years." *Clinical Orthopaedics and Related Research* **453**: 81-85.

Long, J.D., Xu, S., Cai, J.W., Jiang, N., Lu, J.H., Ostrikov, K.N. and Diong, C.H. (2002). "Structure, bonding state and in vitro study of Ca-P-Ti film deposited on Ti6Al4V by RF magnetron sputtering." Materials *Science and Engineering: C* **20**(1-2): 175-180.

Long, M. and Rack, H.J. (1998). "Titanium alloys in total joint replacement-a materials science perspective." *Biomaterials* **19**(18): 1621-1639.

Lu, J., Descamps, M., Dejou, J., Koubi, G., Hardouin, P., Lemaitre, J. and Proust, J.P. (2002). "The biodegradation mechanism of calcium phosphate biomaterials in bone." *Journal of Biomedical Materials Research* **63**(4): 408-412.

Lu, Y.P., Li, M.S., Li, S.T., Wang, Z.G. and Zhu, R.F. (2004). "Plasma-sprayed hydroxyapatite+titania composite bond coat for hydroxyapatite coating on titanium substrate." *Biomaterials* **25**(18): 4393-4403.

Lucke, M., Schmidmaier, G., Sadoni, S., Wildemann, B., Schiller, R., Haas, N.P. and Raschke, M. (2003). "Gentamicin coating of metallic implants reduces implant-related osteomyelitis in rats." *Bone* **32**(5): 521-531.

Mano, T., Ueyama, Y., Ishikawa, K., Matsumura, T. and Suzuki, K. (2002). "Initial tissue response to a titanium implant coated with apatite at room temperature using a blast coating method." *Biomaterials* **23**(9): 1931-1926.

Marcacci, M., Kon, E., Moukhachev, V., Lavroukov, A., Kutepov, S., Quarto, R., Mastrogiacomo, M. and Cancedda, R. (2007). "Stem cells associated with macroporous bioceramics for long bone repair: 6- to 7-Year outcome of a pilot clinical study." *Tissue Engineering* **13**(5): 947-955.

Martini, F.H. (2005). (7th ed.) *Fundamentals of Anatomy & Physiology*. San Francisco: Benjamin Cummings. pp. 180-201.

Massaro, C., Baker, M. A., Cosentino, F., Ramires, P. A., Klose, S. and Milella, E. (2001). "Surface and biological evaluation of hydroxyapatite-based coatings on titanium deposited by different techniques." *Journal of Biomedical Materials Research* **58**(6): 651-757.

Matsumoto, N., Sato, K., Yoshida, K., Hashimoto, K. and Toda, Y. (2009). "Preparation and characterization of beta-tricalcium phosphate co-doped with monovalent and divalent antibacterial metal ions." *Acta Biomaterialia* **5**(8): 3157-3164.

Mavropoulos, E., Rossi, A.M., Da Rocha, N.C.C., Soares, G.A., Moreira, J.C. and Moure, G.T. (2003). "Dissolution of calcium-deficient hydroxyapatite synthesized at different conditions." *Materials Characterization* **50**(2-3): 203-207.

Maxian, S.H., Zawadsky, J.P. and Dunn, M.G. (1993). "In vitro evaluation of amorphous calcium phosphate and poorly crystallized hydroxyapatite coatings on titanium implants." *Journal of Biomedical Materials Research* **27**(1): 111-117.

McKee, M.D., Pedraza, C.E. and Kaartinen, M.T. (2011). "Osteopontin and wound healing in bone." *Cells Tissues Organs* **194**(2-4): 313-319.

Milović, N.M., Wang, J., Lewis, K., Klibanov, A.M. (2005). "Immobilized N-alkylated polyethylenimine avidly kills bacteria by rupturing cell membranes with no resistance developed." *Biotechnology and Bioengineering* **90**(6): 715-722.

Mohammadi, Z., Ziaei-Moayyed, A.A. and Mesgar, A.M. (2008). "In vitro dissolution of plasma-sprayed hydroxyapatite coatings with different characteristics: experimental study and modeling." *Biomedical Materials* **3**(1): 015006.

Mohammadi, Z., Ziaei-Moayyed, A.A., Sheikh-Mehdi, M. A. (2007). "Adhesive and cohesive properties by indentation method of plasma-sprayed Hydroxyapatite coatings." *Applied Surface Science* **253**(11): 4960-4965.

Monzón, M., García-Alvarez, F.,Laclériga, A. and Amorena, B. (2002). "Evaluation of four experimental osteomyelitis infection models by using precolonized implants and bacterial suspensions", *Acta Orthopaedica Scandinavica* **73**(1):11-9.

Monzón, M., García-Alvarez, F., Laclériga, A., Gracia, E., Leiva, J., Oteiza, C. and Amorena, B. (2001). "A simple infection model using pre-colonized implants to reproduce rat chronic Staphylococcus aureus osteomyelitis and study antibiotic treatment." *Journal of Orthopaedic Research* **19**(5): 820-826.

Mosmann, T. (1983). "Rapid colorimetric assay for cellular growth and survival: Application to proliferation and cytotoxicity assays." *Journal of Immunology Methods* **65**(1-2): 55-63.

Muralithran, G. and Ramesh, S. (2000). "Effects of sintering temperature on the properties of hydroxyapatite." *Ceramics International* **26**(1): 221-230.

Murata, H. Koepsel, R.R, Matyjaszewski, K. and Russell, A.J. (2007). "Permanent, non-leaching antibacterial surfaces: How high density cationic surfaces kill bacterial cells." *Biomaterials* **28**(32): 4870-4879.

Nagaoka, S. and Kawakami, H. (1995). "Inhibition of bacterial adhesion and biofilm formation by a heparinized hydrophilic polymer." *ASAIO Journal* **41**(3): M365.

Nair, L.S and Laurencin, C.T. (2007). "Biodegradable polymers as biomaterials." *Progress in Polymer Science* **32**(8-9): 762–798.

Nakada, H., Sakae, T., Legeros, R.Z., Legeros, J.P., Suwa, T., Numata,Y. and Kobayashi, K. (2007). "Early tissue response to Mmodified implant surfaces using back scattered imaging." *Implant Dentistry* **16**(3): 281-289.

Narayanan, R., Seshadri, S.K., Kwon, T.Y. and Kim, K.H. (2008). "Calcium phosphate-based coatings on titanium and its alloys." *Journal of Biomedical Material Research B: Applied Biomaterials* **85**B(1): 279-299.

Navarro, M., Ginebra, M., Planell, J., Barrias, C.C. and Barbosa, M.A. (2005). "In vitro degradation behavior of a novel bioresorbable composite material based on PLA and a soluble CaP glass." *Acta Biomaterialia* **1**(4): 411-419.

Navarro, M., Ginebra, M., Planell, J., Zeppetelli, S. and Ambrosio, L. (2004). "Development and cell response of a new biodegradable composite scaffold for guided bone regeneration." *Journal of Materials Science: Materials in Medicine* **15**(4): 419-422.

Navarro, M., Michiardi, A, Castaño, O. and Planell, J.A. (2008). "Biomaterials in orthopaedics." *Journal of Royal Society Interface* **5**(27): 1137-1158.

Nelea, V., Morosanu, C., Iliescu, M. and Mihailescu, I.N. (2003). "Microstructure and mechanical properties of hydroxyapatite thin films grown by RF magnetron sputtering." *Surface and Coatings Technology* **173**(1-2): 315-322.

Niinomi, M. (2002). "Recent metallic materials for biomedical applications." *Metallurgical and Materials Transactions A* **33**(3): 477-486.

Noda, I., Miyaji, F., Ando, Y., Miyamoto, H., Shimazaki, T., Yonekura, Y., Miyazaki, M., Mawatari, M. and Hotokebuchi, T. (2009). "Development of novel thermal sprayed antibacterial coating and evaluation of release

properties of silver ions." *Journal of Biomedical Materials Research B: Applied Biomaterials* **89**(2): 456-465.

O"Gara, J. P. and Humphreys, H. (2001). "Staphylococcus epidermidis biofilms: Importance and implications." *Journal of Medical Microbiology* **50**(7): 582-587.

O'Hare, P, Meenan, B.J.B., George A., Byrne, G., Dowling, D. and Hunt, J.A. (2010). "In vitro and In vivo response of hydroxyapatite surfaces deposited via a novel co-incident microblasting technique for improved orthopaedic implant performance" *Biomaterials* **31**(3): 515-522.

O'Neill, L, O"Sullivan, C, O"Hare, P, Sexton, L, Keady, F. and O"Donoghue, J. (2009). "Deposition of substituted apatites onto titanium surfaces using a novel blasting process". *Surface and Coatings Technology* **204**(4): 484-488.

Oh I.H., Nomura, N. and Chiba, A. (2005). "Microstructures and bond strengths of plasma-sprayed hydroxyapatite coatings on porous titanium substrates." *Journal of Materials Science Materials in Medicine* **16**(7): 635-640.

Ohtsuki, C., Kushitani, H., Kokubo, T., Kotani, S. and Yamamuro, T. (1991). "Apatite formation on the surface of ceravital-type glass-ceramic in the body." *Journal of Biomedical Materials Research* **25**(11): 1363-1370.

Okazaki, Y. and Gotoh, E. (2005). "Comparison of metal release from various metallic biomaterials in vitro." *Biomaterials* **26**(1): 11-21.

Oktar, F.N., Genc, Y., Goller, G., Erkmen, E.Z., Ozyegin, L.S., Toykan, D., Demirkiran, H. and Haybat, H. (2004). "Sintering of synthetic hydroxyapatite compacts." *Key Engineering Materials* **264-268**: 2087-2090.

Oliver, M.C., Keast-Butler, O.D., Hinves, B.L. and Shepperd, J.A. (2005). "A hydroxyapatitecoated Insall-Burstein II total knee replacement: 11-year results." *Journal of Bone and Joint Surgery British* **87**(4): 478-82.

Ong, J.L and Chan, D.C. (2000). "Hydroxyapatite and their use as coatings in dental implants: a review." *Critical Review of Biomedical Engineering* **28**(5-6): 667-707.

O'Donoghue., J. and O'Neill, L. (2009). "Turning convention On its head using abrasion for material deposition" *The Shot Peener* **23**(4) 4-6.

O'Sullivan C., O"Hare P., Byrne G., O"Neill L., Ryan K.B. and Crean A.M. (2011). "A modified surface on titanium deposited by a blasting process." *Coatings* **1**(1): 53-71.

O'Sullivan, C., O"Hare, P., O'Leary, N.D., Crean, A.M., Ryan, K., Dobson, A.D. and O'Neill, L.D. (2010). "Deposition of substituted apatites with anticolonizing properties onto titanium surfaces using a novel blasting process." *Journal of Biomedical Materials Research B: Applied Biomaterials* **95**(1): 141-149.

Overgaard, S., Bromose, U., Lind, M., Bünger, C. and Søballe, K. (1999). "The influence of crystallinity of the hydroxyapatite coating on the fixation of implants." Mechanical and histomorphometric results." *The Journal Bone Joint Surgery British Volume* **81**(4): 725-731.

Park, P.B. and Bronino, J.D. (2003) *Biomaterials: Principles and Application*. Florida: CRC Press.

Park, H.J., Kim, J.Y., Kim, J., Lee, J.H., Hahn, J.S., Gu, M.B. and Yoon, J. (2009). "Silver-ion-mediated reactive oxygen species generation affecting bactericidal activity." *Water Research* **43**(4): 1027-1032.

Parvizi, J., Bender, B., Saleh, K.J., Brown, T.E., Schmalzried, T.P. and Mihalko, W.M. (2009). "Resistant organisms in infected total knee arthroplasty: occurrence, prevention, and treatment regimens." *Instructional Course Lecture* **58**: 271-278.

Peitl Filho, O., LaTorre, G.P. and Hench, L.L. (1996). "Effect of crystallization on apatite-layer formation of bioactive glass 45S5." *Journal of Biomedical Material Research* **30**(4): 509-514.

Peraire, C., Arias, J.L., Bernal, D., Pou, J., León, B., Arañó, A. and Roth, W. (2006). "Biological stability and osteoconductivity in rabbit tibia of pulsed laser

deposited hydroxylapatite coatings." *Journal of Biomedical Materials Research A* **77**(2): 370-379.

Pereira, M.M., Clark, A.E. and Hench, L.L. (1994). "Calcium phosphate formation on sol-gel-derived bioactive glasses in vitro." *Journal of Biomedical Materials Research* **28**(6): 693-698.

Pettit, A.K., Chang M.K., Hume, D.A., Raggatt, L.J. (2008). "Osteal macrophages: A new twist on coupling during bone dynamics." *Bone* **43**(6): 976–982.

Pham, H., Luo, P., Génin, F. and Dash, A. (2002). "Synthesis and characterization of hydroxyapatite-ciprofloxacin delivery systems by precipitation and spray drying technique." *AAPS Pharmacology Science Technology* **3**(1): 1-9.

Piveteau, L.D., Gasser, B., Schlapbach, L. (2000). "Evaluating mechanicaladhesion of sol–gel titanium dioxide coatings containing calcium phosphate for metal implant application." *Biomaterials* **21**(21): 2193–2201.

Pleshko, N., Boskey, A. and Mendelsohn, R. (1991). "Novel infrared spectroscopic method for the determination of crystallinity of hydroxyapatite minerals." *Biophysical Journal* **60**(4): 786-793.

Poelstra, K.A., Barekzi, N.A., Rediske, A.M., Felts, A.G., Slunt, J.B., Grainger, D.W. (2002). "Prophylactic treatment of gram-positive and gram-negative abdominal implant infections using locally delivered polyclonal antibodies." *Journal of Biomedical Materials Research* **60**(1): 206-15.

Powles, J.W., Spencer, R.F. and Lovering, A.M. (1998). "Gentamicin release from old cement during revision hip arthroplasty." *Journal of Bone and Joint Surgery* **80-B**(4): 607-610.

Pratten, J., Nazhat, S.N., Blaker, J.J. and Boccaccini, A.R. (2004). "In vitro attachment of Staphylococcus epidermidis to surgical sutures with and without Ag-containing bioactive glass coating." *Journal of Biomaterials Applications* **19**(1): 47-58.

Price, J.S., Tencer, A.F., Arm, D.M. and Bohach, G.A. (1996). "Controlled release of antibiotics from coated orthopedic implants." *Journal of Biomedical Materials Research* **30**(3): 281-286.

Prossnitz, E. R. and Ye, R.D. (1997). "The N-formyl peptide receptor: A model for the study of chemoattractant receptor structure and function." *Pharmacology and therapeutics* **74**(1): 73-102.

Puckett, S., Paret, R. and Webster, T.J. (2008). "Nano rough micron patterned titanium for directing osteoblast morphology and adhesion." *International Journal of Nanomedicine* **3**(2): 229-241.

Raggatt, L.J. and Partridge N.C. (2010). "Cellular and molecular mechanisms of bone remodeling", *Journal of Biological Chemistry* **285**(33): 25103-25108.

Raggatt, L.J., Chang, M.K., Alexander, K.A., Maylin, E.R., Walsh, N.C., Gravallese, E. M., Hume, D.A. and Pettit, A.R. (2008). "Osteomacs: Osteoclast precursors during inflammatory bone disease but regulators of physiologic bone remodeling." *Bone* **43**(6): 976-982.

Ravaglioli, A. and Krajewski, A. (1992). *Bioceramics, Materials, Properties and Applications.* London: Chapman & Hall.

Redey, S.A., Nardin, M., Bernache-Assolant, D., Rey, C., Delannoy, P., Sedel, L. and Marie, P. J. (2000). "Behavior of human osteoblastic cells on stoichiometric hydroxyapatite and type A carbonate apatite: Role of surface energy." *Journal of Biomedical Materials Research* **50**(3): 353-364.

Rezwan, K., Chen, Q.Z., Blaker, J.J. and Boccaccini, A.R. (2006). "Biodegradable and bioactive porous polymer/inorganic composite scaffolds for bone tissue engineering." *Biomaterials* **27**(18): 3413-3431.

Richards, R., Odelola, H. and Anderson, B. (1984). "Effect of silver on whole cells and spheroplasts of a silver resistant Pseudomonas aeruginosa." *Microbios* **39**(157-158): 151-157.

Roche (2012). "The bone remodelling cycle"[image online] Available at: <http://www.roche.com/pages/facets/11/ostedefe.htm> [Accessed 01 June 2012].

Roach, P., Farrar, D. and Perry, C.C. (2005). "Interpretation of Protein Adsorption: Surface-Induced Conformational Changes." *Journal of the American Chemical Society* **127**(22): 8168-8173.

Rohn, T.T., Nelson, L.K., Sipes, K.M., Swain, S.D., Jutila, K.L. and Quinn, M.T. (1999). "Priming of human neutrophils by peroxynitrite: potential role in enhancement of the local inflammatory response." *Journal of Leukocyte Biology* **65**(1): 59-70.

Røkkum, M., Brandt, M., Rye, K., Hetland, K.R., Waage, S. and Reigstad, A. (1999). "Polyethylene wear, osteolysis and acetabular loosening with a HA-coated. A follow-up of 94 consecutive arthroplasties." *Journal of Bone and Joint Surgery: British Volume* **81**(4): 582-529

Rosa, A.L., Beloti, M.M. and Van Noort, R. (2003). "Osteoblastic differentiation of cultured rat bone marrow cells on hydroxyapatite with different surface topography." *Dental Materials* **19**(8): 768-772.

Rossi, S., Azghani, A.O. and Omri, A. (2004). "Antimicrobial efficacy of a new antibiotic-loaded poly(hydroxybutyric-co-hydroxyvaleric acid) controlled release system." *Journal of Antimicrobial Chemotherapy* **54**(6): 1013-1018.

Rouahi, M., Champion, E., Gallet, O., Jada, A. and Anselme, K. (2006). "Physico-chemical characteristics and protein adsorption potential of hydroxyapatite particles: Influence on in vitro biocompatibility of ceramics after sintering." *Colloids and Surfaces B: Biointerfaces* **47**(1): 10-19.

Roy, M., Fielding, G., Beyenal, H., Bandyopadhyay, A. and Bose, S. (2012). "Mechanical, in vitro antimicrobial and biological properties of plasma sprayed silver-doped hydroxyapatite coating"*ACS Applied Materials Interfaces* **4**(3) 1341-1349.

Ruan, H.J., Fan, C.Y., Zheng, X.B., Zhang ,Y. and Chen, Y. (2009). "In vitro antibacterial and osteogenic properties of plasma sprayed silver-containing hydroxyapatite coating." *Chinese Science Bulletin* **54**(23): 4438-4445.

Rupp, F., Scheideler, L., Rehbein, D., Axmann, D. and Geis-Gerstorfer, J. (2004). "Roughness induced dynamic changes of wettability of acid etched titanium implant modifications." *Biomaterials* **25**(7-8): 1429-38.

Rupp, M.E., Ulphani, J.S., Fey, P.D. and Mack, D. (1999). "Characterization of Staphylococcus epidermidis polysaccharide intercellular adhesin/hemagglutinin in the pathogenesis of intravascular catheter-associated infection in a rat model." *Infectious Immunology* **67**(5): 2656-2659.

Russell, J.C. (2009). "Bacteria, biofilms, and devices: The possible protective role of phosphorylcholine materials." *Journal of Endourology* **14**(1): 39-42.

Ruszczak, Z. and Friess, W. (2003). "Collagen as a carrier for on-site delivery of antibacterial drugs." *Advanced Drug Delivery Reviews* **55**(12): 1679-1698.

Ryan, G., Pandit, A. and Apatsidis, D.P. (2006). "Fabrication methods of porous metals for use in orthopaedic applications." *Biomaterials* **27**(13): 2651-2670.

Saikia, K.C., Bhattacharya, T.D., Bhuyan, S.K., Talukdar, D.J., Saikia, S.P. and Jitesh, P. (2008). "Calcium phosphate ceramics as bone graft substitutes in filling bone tumor defects." *Indian Journal of Orthopedic* **42**(2): 169–172.

Sampathkumaran, U., De Guire, M.R. and Wang, R. (2001). "Hydroxyapatite coatings on titanium." *Advanced Engineering Materials* **3**(6): 401-405.

Sandukas, S., Yamamoto, A. and Rabiei, A. (2011). "Osteoblast adhesion to functionally graded hydroxyapatite coatings doped with silver." *Journal of Biomedical Materials Research Part A* **97**(4): 490-497.

Schierholz, J.M, Lucas, L.J., Rump, A. and Pulverer, G. (1998). "Efficacy of silver-coated medical devices." *Journal of Hospital Infection* **40**(4): 257-262.

Schmidmaier, G., Lucke, M., Wildemann, B., Haas, N.P. and Raschke, M. (2006). "Prophylaxis and treatment of implant-related infections by antibiotic-coated implants: a review." *Injury* **37**(2): S105-S112.

Schuh, A., Holzwarth, U., Kachler, W., Göske, J. and Zeiler, G. (2004). "Surface characterization of Al2O3-blasted titanium implants in total hip arthroplast." *Der Orthopäde* **33**(8): 905-910.

Schwartz, Z. and Boyan, B.D. (1994). "Underlying mechanisms at the bone-biomaterial interface." *Journal of Cellular Biochemistry* **56**(3): 340-347.

Schwartz, Z., Kieswetter, K., Dean, D.D. and Boyan, B.D. (1997). "Underlying mechanisms at the bone-surface interface during regeneration." *Journal of Periodontal Research* **32**(1): 166-171.

Sheehan, E., McKenna, J., Mulhall, K.J., Marks, P. and McCormack, D. (2004). "Adhesion of Staphylococcus to orthopaedic metals, an in vivo study." *Journal of Orthopaedic Research* **22**(1): 39-43.

Shi, X., Wang, Y., Ren, L., Gong, Y. and Wang, D.A. (2009). "Enhancing alendronate Release from a novel PLGA/hydroxyapatite microspheric system for bone repairing applications." *Pharmaceutical Research* **26**(2): 422-430.

Shigeta, M., Tanaka, T., Koike, N., Yamakawa, N. and Usui, M. (2006). "Suppression of fibroblast and bacterial adhesion by MPC coating on acrylic intraocular lenses." *Journal of Cataract Refractive Surgery* **32**(5): 859-66.

Shimazaki, T., Miyamoto, H., Ando, Y., Noda, I., Yonekura, Y., Kawano, S., Miyazaki, M., Mawatari, M. and Hotokebuchi, T. (2010). "In vivo antibacterial and silver-releasing properties of novel thermal sprayed silver-containing hydroxyapatite coating." *Journal of Biomedical Materials Research B: Applied Biomaterials* **92**(2): 386-389.

Siebers, M.C., Walboomers, X.F. and Leeuwenburgh, S.C. (2004). "Electrostatic spray deposition(ESD) of calcium phosphate coatings, an in vitro study with osteoblast-like cells." *Biomaterials* **25**(11): 2019–2027.

Søballe, K. and Overgaard, S. (1996). "The current status of hydroxyapatite coating of prostheses." *Journal of Bone and Joint Surgery* **78B**(5): 689-690.

Sousa, C., Teixeira,P. and Oliveira, R. (2009)"Influence of surface properties on the adhesion of Staphylococcus epidermidis to acrylic and silicone." *International Journal of Biomaterials* **7**(1): 801-807.

Springer, B.D, Lee, G.C., Osmon, D., Haidukewych, G.J., Hanssen, A.D. and Jacofsky, D.J. (2004). "Systemic safety of high-dose antibiotic-loaded cement spacers after resection of an infected total knee arthroplasty." *Clinical Orthopaedics and Related Research* **427**: 47-51.

Stewart, M., Welter, J.F., Goldberg, V. M. (2004). "Effect of hydroxyapatite/tricalcium-phosphate coating on osseointegration of plasma-sprayed titanium alloy implants", *Clinical Orthopaedics and Related Research* **69**(1): 1-10.

Stigter, M., Bezemer, J., De Groot, K. and Layrolle, P. (2004). "Incorporation of different antibiotics into carbonated hydroxyapatite coatings on titanium implants, release and antibiotic efficacy." *Journal of Controlled Release* **99**(1): 127-137.

Stigter, M., De Groot, K. and Layrolle, P. (2002). "Incorporation of tobramycin into biomimetic hydroxyapatite coating on titanium." *Biomaterials* **23**(2): 4143-4153.

Stoch, A., Brozek, A., Kmita, G., Stoch, J., Jastrzebski, W. and Rakowska, A. (2001). "Electrophoretic coating of hydroxyapatite on titanium implants." *Journal of Molecular Structure* **596**(1-3): 191-200.

Stoch, A., Jastrze, B.W., Dlugon, E., Lejda, W., Trybalska, B., Stoch, G.J. and Adamczyk, A. (2005). "Sol-gel derived hydroxyapatite coatings on titanium and its alloy Ti6Al4V." *Journal of Molecular Structure* **744-747**: 633-640.

Sumner, D.R., Turner, T.M., Igloria, R., Urban, R.M. and Galante J.O. (1998). "Functional adaptation and ingrowth of bone vary as a function of hip implant stiffness". *Journal of Biomechanics* **31**(10): 909-917.

Sun, L., Berndt, C. C., Gross, K. A. and Kucuk, A. (2001). "Material fundamentals and clinical performance of plasma-sprayed hydroxyapatite coatings." *Journal of Biomedical Materials Research* **58**(8): 570-592.

Sundback, C.A., Shyu, J.Y., Wang, Y., Faquin, W.C., Langer, R.S.,Vacanti, J.P. and Hadlock, T.A. (2005). "Biocompatibility analysis of poly(glycerol sebacate) as a nerve guide material." *Biomaterials* **26**(27): 5454–5464.

Talib R.J. and Toff, T.M. (2004). "Plasma-sprayed coating of hydroxyapatite on metal implants." *Medicine Journal of Malaysia* **56**: 153.

Tampieri, A., Celotti, G. and Landi, E. (2005). "From biomimetic apatites to biologically inspired composites." *Analytical and Bioanalytical Chemistry* **381**(3): 568-576.

Tan, F., Naciri, M. and Al-Rubeai, M. (2011). "Osteoconductivity and Growth Factor Production by MG63 Osteoblastic Cells on Bioglass-Coated Orthopedic Implants", *Biotechnology and Bioengineering* **108**(2): 454-464.

Tan, F., Naciri, M., Dowling, D. and Al-Rubeai, M. (2012). "In vitro and in vivo bioactivity of CoBlast hydroxyapatite coating and the effect of impaction on its osteoconductivity." *Biotechnolology Advances* **30**(1): 352-362.

Tanzer, M., Kantor, S., Rosenthall, L. and Bobyn, D.J. (2001). "Femoral remodeling after porous-coated total hip arthroplasty with and without hydroxyapatite - tricalcium phosphate coating." *The Journal of Arthroplasty* **16**(5): 552-558.

Tapiero, H. and Tew, K.D. (2003). "Trace elements in human physiology and pathology: zinc and metallothioneins." *Biomedical Pharmacotherapy* **57**(9): 399-411.

Teller, M., Gopp, U., Neumann, H.G. and Kühn, K.D. (2007). "Release of gentamicin from bone regenerative materials: an in vitro study." *Journal of Biomedical Materials Research Part B: Applied Biomaterials* **81B**(1): 23-29.

Thompson, I.D. and Hench, L.L. (1998). "Mechanical properties of bioactive glasses, glass-ceramics and composites." Proceedings of the Institution of Mechanical Engineers, Part H: *Journal of Engineering in Medicine* **212**(2): 127-136.

Troitzsch, D., Borutzky,U. and Junghannß U. (2009). "Detection of antimicrobial efficacy in silver-coated medical device." *Hygenic Medicine* **34**(3): 80-85.

Tsui, Y.C., Doyle, C. and Clyne, T.W. (1998). "Plasma sprayed hydroxyapatite coatings on titanium substrates. Part 1: Mechanical properties and residual stress levels." *Biomaterials* **19**(22): 2015-2029.

Tzoris, A., Hall, E.A.H., Besselink, G. and Bergveld, P. (2003). "Testing the durability of polymyxin B immobilization on a polymer showing antimicrobial activity: A novel approach with the ion-step method." *Analytical Letters* **36**(9): 1781-1803.

Ulrich, S.D., Seyler, T.M., Bennett, D., Delanois, R.E. Saleh, K.J., Thongtrangan, I., Kuskowski, M., Cheng, E.Y., Sharkey, P.F., Parvizi, J., Stiehl, J.B. and Mont, M.A. (2008). "Total hip arthroplasties: what are the reasons for revision?" *International Orthopaedics* **32**(5): 597-604.

Vacheethasanee, K. and Marchant, R.E. (2000). Nonspecific Staphylococcus epidermis adhesion. In Y. H. An and R. J. Friedman ed. 2000. *Handbook of Bacterial Adhesion: Principles, Methods, and Applications*. NJ: Humana Press, Totowa: pp.73–90.

Vallejo, R., de Leon-Casasola, O. and Benyamin, R. (2004). "Opioid therapy and immunosuppression: A review." *American Journal of Therapeutics* **11**(5): 354-365.

Van de Belt, H., Neut, D., Schenk, W., Horn, J., Van der Mei, H. and Busscher, H. (2001). "Infection of orthopaedic implants and the use of antibiotic-loaded bone cement." *Acta Orthopaedica Scandinavia* **72**(6): 557-571.

Van de Belt, H., Neut, D., Uges, D.R., Schenk, W., Van Horn, J.R., Van der Mei, H.C. and Busscher, H.J. (2000). "Surface roughness, porosity and wettability of gentamicin-loaded bone cements and their antibiotic release." *Biomaterials* **21**(19): 1981-1987.

Van de Belt, H., Neut, D., Van Horn, J. R, Van der Mei, H.C., Schenk,,W. and Busscher, H. J. (1999). "Antibiotic resistance - to treat or not to treat? *Nature Medicine* **5**: 358-359.

Van Houwelingen, A.P., Garbuz, D.S., Masri, B.A. and Duncan, C.P. (2012). "Methicillin-resistant infection after hip and knee replacement: Reason to change practice?" *Journal of Orthopaedics Trauma and Rehabilitation* **16**(1): 9-12.

Van Loosdrecht, M.C., Lyklema, J., Norde, W. and Zehnder, A.J. (1990). "Influence of interfaces on microbial activity." *Microbiology and Molecular Biology Reviews* **54**(1): 75-87.

Van Wijngaerden, E., Peetermans, W.E., Vandersmissen, J., Van Lierde, S., Bobbaers, H. and Van Eldere, J. (1999). "Foreign body infection: a new rat model for prophylaxis and treatment." *Journal of Antimicrobacteial Chemotherapy* **44**(5): 669-674.

Vani Vasudev, D., Ricci, J.L. Sabatino, C., Li, P. and Parsons J.R. (2004). "In vivo evaluation of a biomimetic apatite coating grown on titanium surfaces." *Journal of Biomedical Materials Research A* **69**(4): 629-636.

Varma, H.K. and Babu, S.S. (2005). "Synthesis of calcium phosphate bioceramics by citrate gel pyrolysis method." *Ceramic International* **31**(1): 109-114.

Verrier, S., Blaker, J.J., Maquet, V., Hench, L.L. and Boccaccini, A.R. (2004). "PDLLA/Bioglass composites for soft-tissue and hard-tissue engineering: an in vitro cell biology assessment." *Biomaterials* **25**(15): 3013-3021.

Vik, H., Andersen, K.J., Julshamn, K. and Todnem, K. (1985). "Neuropathy caused by silver absorption from arthroplasty cement." *Lancet* **325**(8433): 872.

Virk, A. and Osmon, D.R. (2001). "Prosthetic joint infection." *Current Treatment Options in Infectious Diseases* **3**(4): 287-301.

Wain, J., Diep, T.S., Ho, V.A., Walsh, A.M., Tuyet-Hoa, N.T., Parry, C.A. and White, N.J. (1998). "Quantitation of bacteria in blood of typhoid fever patients and relationship between counts and clinical features,

transmissibility, and antibiotic resistance." *Journal of Clinical Microbiology* **36**(6): 1683-1687.

Wang, C., Duan, Y., Markovic, B., Barbara, J., Howlett, C.R., Zhang, X., Zreiqat, H. (2004). "Phenotypic expression of bone-related genes in osteoblasts grown on calcium phosphate ceramics with different phase compositions." *Biomaterials* **25**(13): 2507-2514.

Wang, H., Eliaz, N., Xiang Z., Hsu, H.P., Spector M. and Hobbs, L.W. (2006). "Early bone apposition in vivo on plasma-sprayed and electrochemically deposited hydroxyapatite coatings on titanium alloy." *Biomaterials* **27**(23): 4192-4203.

Wang, C., Ma, J., Cheng, W. and Zhang, R. (2002). "Thick hydroxyapatite coatings by electrophoretic deposition." *Materials Letters* **57**(1): 99-105.

Wang, X., Wang, G., Liang, J., Cheng, J., Ma, W. and Zhao, Y. (2009). "Staphylococcus aureus adhesion to different implant surface coatings: An in vitro study." *Surface and Coatings Technology* **203**(22): 3454-3458.

Webb, K., Vlady, H. and Tresco, P. A. (2000). "Relationships among cell attachment, spreading, cytoskeletal organization, and migration rate for anchorage-dependent cells on model surfaces." *Journal of Biomedical Materials Research* **49**(3): 362-368.

Weist, K., Cimbal, A.K., Lecke, C., Kampf, G., Rüden, H. and Vonberg, R.P. (2006). "Evaluation of six agglutination tests for Staphylococcus aureus identification depending upon local prevalence of meticillin-resistant S. aureus (MRSA)." *Journal of Medical Microbiology* **55**(3): 283-290.

Weng, J., Liu, Q., Wolke, J.G., Zhang, X. and De Groot, K. (1997). "Formation and characteristics of the apatite layer on plasma-sprayed hydroxyapatite coatings in simulated body fluid." *Biomaterials* **18**(15): 1027-1035.

Weng, W., Zhang, S., Cheng, K., Qu, H., Du, P., Shen, G., Yuan, J. and Han, G. (2003). "Sol gel preparation of bioactive apatite films." *Surface and Coatings Technology* **167**(2-3): 292-296.

Wennerberg, A., Ektessabi, A., Albrektsson, T., Johansson, C. and Andersson, B.A. (1997). "1-year follow-up of implants of differing surface roughness placed in rabbit bone." *International Journal of Oral and Maxillofacial Implant* **12**(4): 486-494.

Williams, D. (1999) *The Williams Dictionary of Biomaterials*. Liverpool (UK): Liverpool University Press.

Williams, D. (2009). "On the nature of biomaterials." *Biomaterials* **30**(30): 5897-5909.

Wu, P. and Grainger, D. (2006). "Drug/device combinations for local drug therapies and infection prophylaxis." *Biomaterials* **27**(11): 2450-2467.

Xin, R., Leng, Y., Chen, J. and Zhang, Q. (2005). "A comparative study of calcium phosphate formation on bioceramics in vitro and in vivo." *Biomaterials* **26**(33): 6477-6486.

Xu, Q. and Czernuszka, J.T. (2008). "Controlled release of amoxicillin from hydroxyapatite-coated poly(lactic-co-glycolic acid) microspheres." *Journal of Controlled Release* **127**(2): 146-153.

Xue, W., Liu, X. and Zheng, X. and Ding, C.J. (2005). "Effect of hydroxyapatite coating crystallinity on dissolution and osseointegration in vivo." *Journal of Biomedical Materials Research A* **74**(4): 553-561.

Xue, W., Tao, S., Liu, X., Zheng, X. and Ding, C. (2004). "In vivo evaluation of plasma sprayed hydroxyapatite coatings having different crystallinity." *Biomaterials* **25**(3): 415-421.

Xynos, I.D., Edgar, A. J., Buttery, L. D.K., Hench, L. L., Polak,, J.M. (2001). "Gene-expression profiling of human osteoblasts following treatment with the ionic products of Bioglass® 45S5 dissolution." *Journal of Biomedical Materials Research* **55**(2): 151-157.

Yakabe, Y., Sano, T., Ushio, H. and Yasunaga, T. (1980). "Kinetic studies of the interaction between silver ion and deoxyribonucleic acid." *Chemistry Letters* **9**(21): 373-376.

Yang, Y. and Chang, E. (2001)"Influence of residual stress on bonding strength and fracture of plasma-sprayed hydroxyapatite coatings on Ti–6Al–4V substrate", *Biomaterials* **22**(13): 1827-1836.

Yang, Y., Cavin, R. and Ong, J.L. (2003). "Protein adsorption on titanium surfaces and their effect on osteoblast attachment." *Journal of Biomedical Materials Research Part A* **67A**(1): 1552-4965.

Yang, Y., Kim, K.H. and Ong, J.L. (2005). "A review on calcium phosphate coatings produced using a sputtering process-an alternative to plasma spraying." *Biomaterials* **26**(3): 327-337.

Yang, Y., Lee, T.M., Yang, C.W., Chen, L.R., Wu, M.C. and Lui, T.S. (2007). "In vitro and in vivo biological responses of plasma-sprayed hydroxyapatite coatings with posthydrothermal treatment." *Journal of Biomedical Materials Research A* **83**(2): 263-271.

Yonekura, Y., Miyamoto, H., Shimazak, T., Ando, Y., Noda, I., Mawatari, M. and Hotokebuchi, T. (2011). "Osteoconductivity of thermal-sprayed silver-containing hydroxyapatite coating in the rat tibia." *Journal of Bone Joint Surgery British* **93**(5): 644-649.

Yuan, H., Zou, P., Yang, Z., Zhang, X., De Bruijn, J.D. and De Groot K. (1998). "Bone morphogenetic protein and ceramic-induced osteogenesis." *Journal of Material Science Materials in Medicine* **9**(12): 717-721.

Zasloff, M. (2002). "Antimicrobial peptides of multicellular organisms." *Nature* **415**(6870): 389-395.

Zhang, Q., Chen, J., Feng, J., Cao, Y., Deng, C. and Zhang, X. (2003). "Dissolution and mineralization behaviors of HA coatings." *Biomaterials* **24**(26): 4741-4748.

Zhao, G., Schwartz, Z., Wieland, M., Rupp, F., Geis-Gerstorfer, J., Cochran, D.l. and Boyan, B.D. (2005). "High surface energy enhances cell response to titanium substrate microstructure." *Journal of Biomedical Materials Research Part A* **74**(1): 49-58.

Zheng, X., Chen., Xie Y., Ji H., Huang, J. and Ding C. (2009). "Antibacterial Property and Biocompatibility of Plasma Sprayed Hydroxyapatite/Silver Composite Coatings." *Journal of Thermal Spray Technology* **18**(3): 463.

Zhou, G., Li, Y., Xiao, W., Zhang, L., Zuo, Y., Xue, J. and Jansen, J.A. (2008). "Synthesis, characterization, and antibacterial activities of a novel nanohydroxyapatite/zinc oxide complex." *Journal of Biomedical Materials Research Part A* **85**(4): 929-937.

Zhou, J., Zhang, X., Chen, J., Zeng, S. and Groot, K. (1993). "High temperature characteristics of synthetic hydroxyapatite. *Journal of Materials Science: Materials in Medicine* **4**(1): 83-85.

Zhu, X., Chen, J., Scheideler, L., Reichl, R. and Geis-Gerstorfer, J. (2004). "Effects of topography and composition of titanium surface oxides on osteoblast responses." *Biomaterials* **25**(18): 4087-4103.

Zilberman, M and Elsner, J.J. (2008). "Antibiotic-eluting medical devices for various applications." *Journal of Controlled Release* **130**(3): 202-215.

Zyman, Z., Ivanov, I., Glushko, V., Dedukh, N. and Malyshkina, S. (1998). "Inorganic phase composition of remineralisation in porous CaP ceramics." *Biomaterials* **19**(14): 1269-1273.

Appendix I

Further Analysis on HA surfaces (Chapter 3)

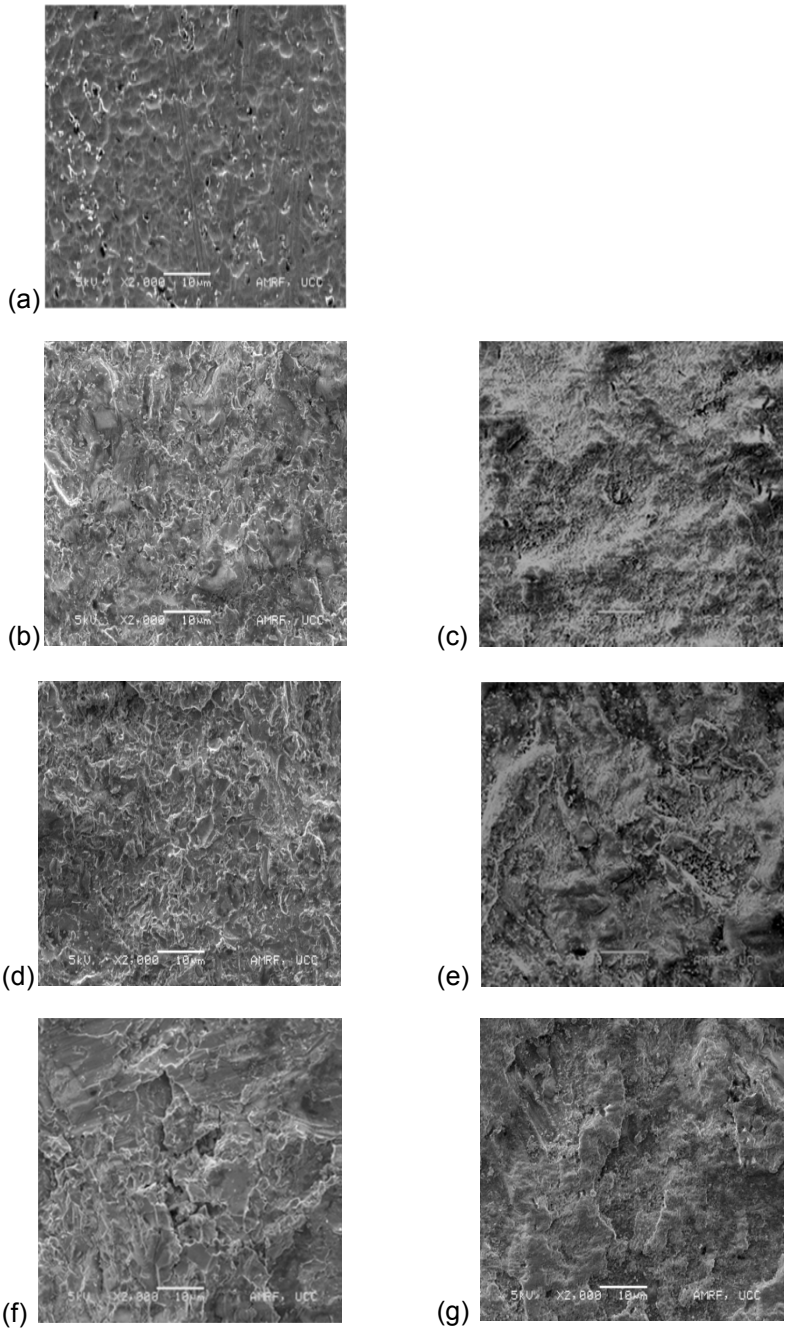

Figure I-1. SEM images (x2000 magnification): (a) titanium; (b) microblast MCD 106; (c) CoBlast HA/MCD-106;(d) microblast MCD-180; (e) CoBlast HA/MCD-180; (f) microblast MCD-425; (g) CoBlast HA/MCD-425.

Appendix II

Further Analysis on 5% wt Substituted Apatite (Chapter 5)

Table II-1: Median particle size (d(0.5)) analysis of the powers. Water contact angle and ion concentration (% wt using EDX analysis) of the various CoBlast surfaces (n=3 samples).

Coating	d(0.5) of the powders (μm) (±2SD)	Water contact angle (°) of the coating (±2SD)	Ion (%wt) EDX of the coatings
Uncoated Ti		68±9	-
HA	33±3	18±6	-
AgA	14±3	0	Ag-3
SrA	14±3	0	Sr-4
ZnA	10±1	0	Zn-5

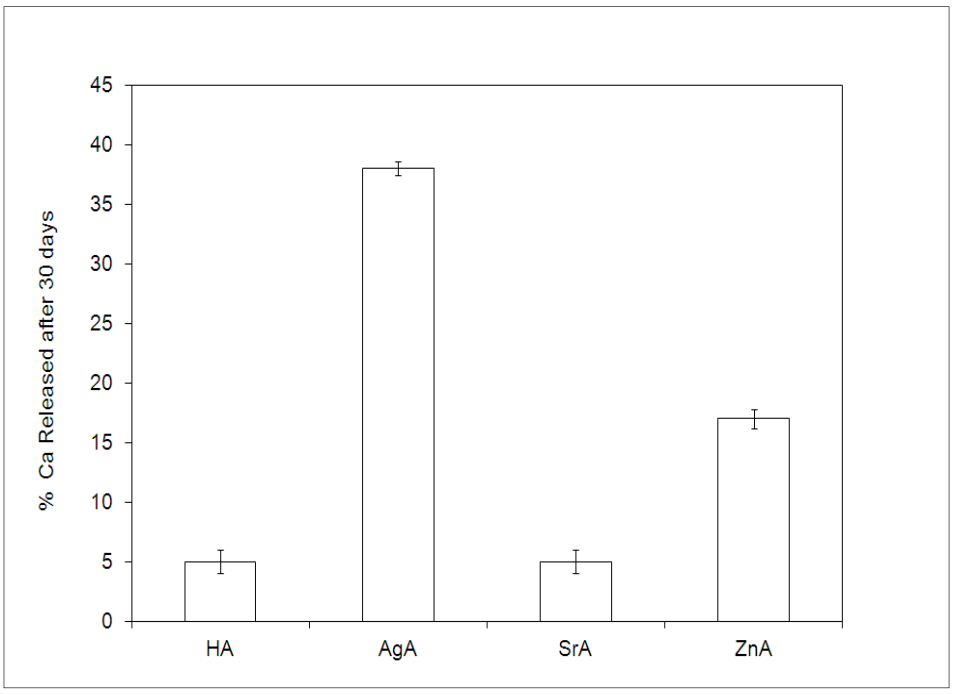

Figure II-1: % Ca released from the coating after 30 days incubation in buffer.

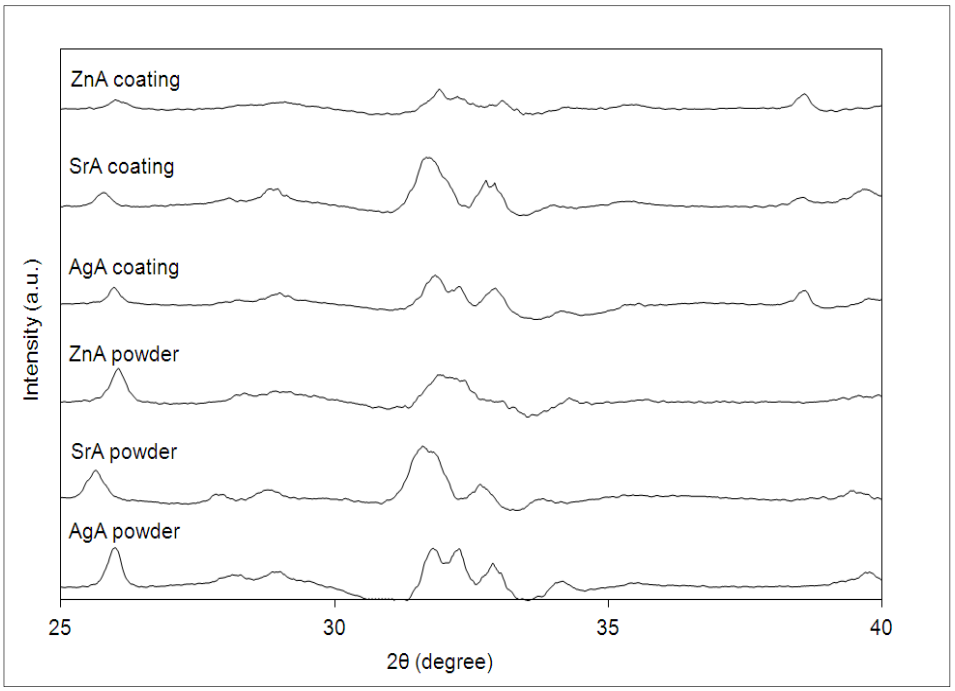

Figure II-2: XRD analysis of 5% wt substituted apatite powders and coatings.

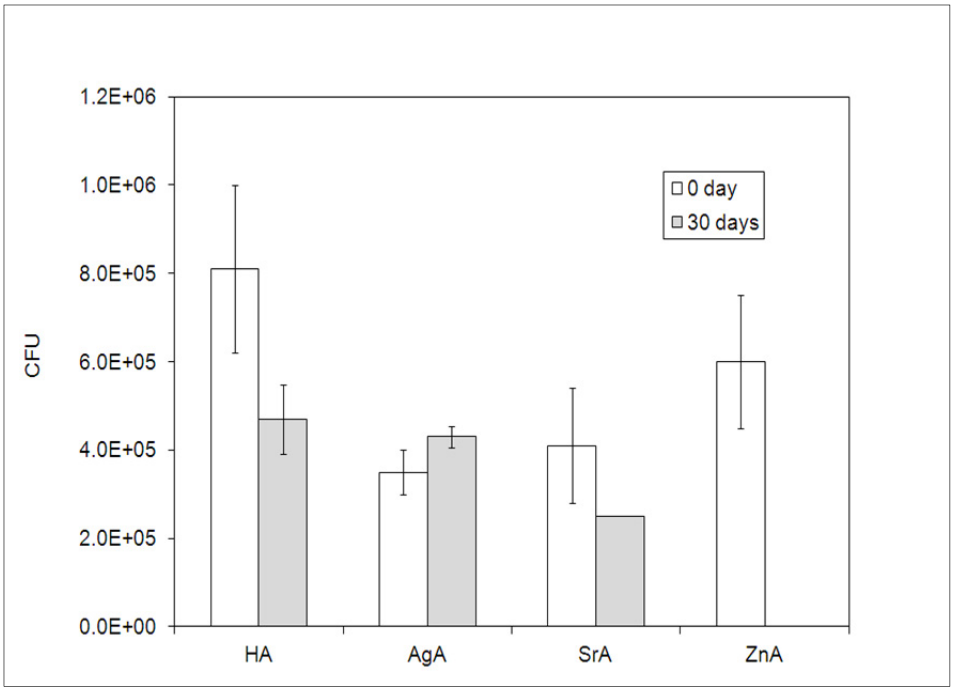

Figure II-3: Antimicrobial activity expressed as CFU of the immobilised surface ion of the various coatings using *S. aureus* as the bacterial challenge organism (n=3 samples ±SD).

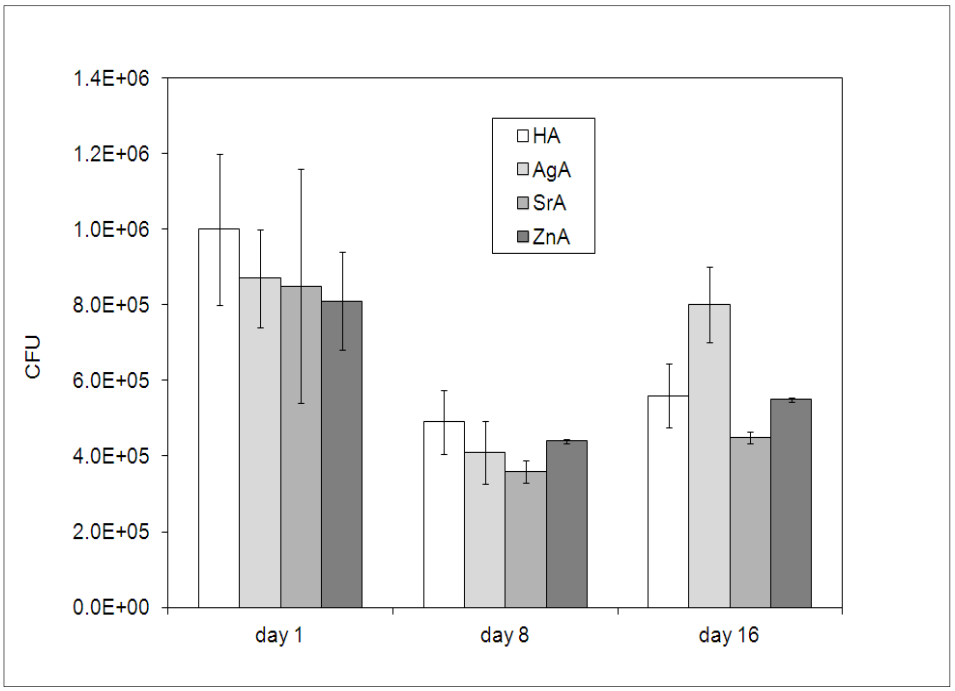

Figure II-4: Antimicrobial activity expressed as CFU of the released ion from the coating using *S. aureus* as the bacterial challenge organism (n=3 samples ±SD).

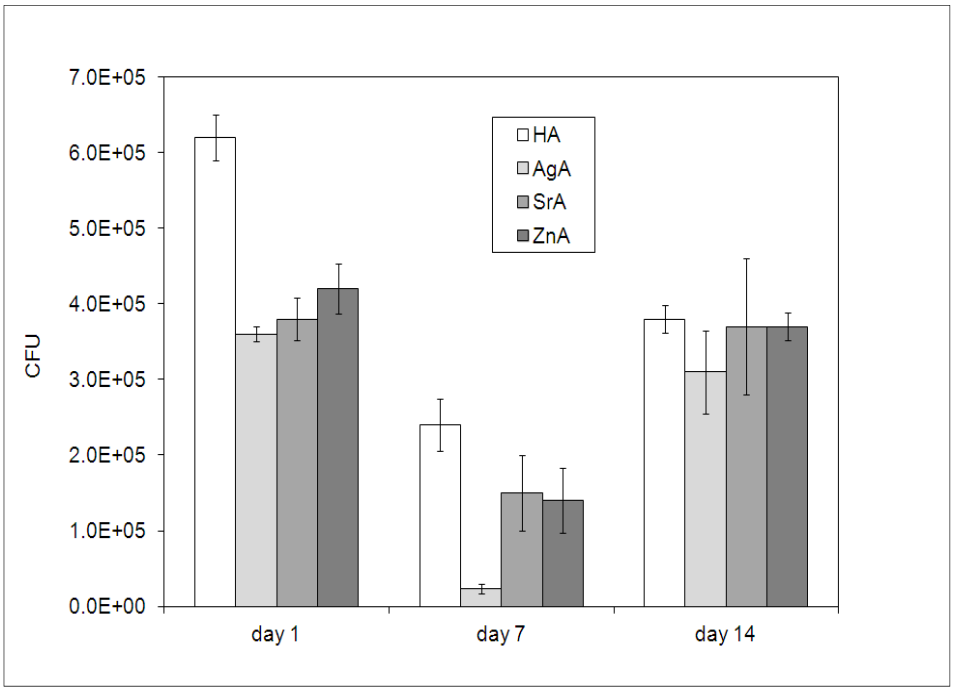

Figure II-5: Anticolonising activity expressed as CFU of the released ion from the coating using *S. aureus* as the bacterial challenge organism (n=3 samples ±SD).

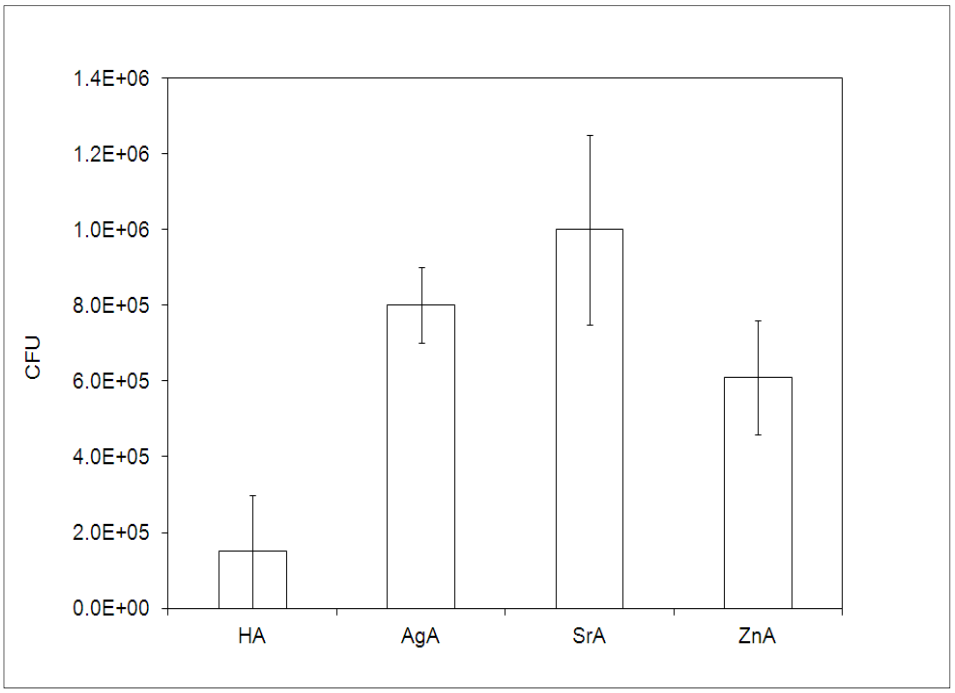

Figure II-6: Antimicrobial activity expressed as CFU of the immobilised surface ion of the various coatings at day 0 using *Pseudomonas aeruginosa* as the bacterial challenge organism (n=3 samples ±SD).

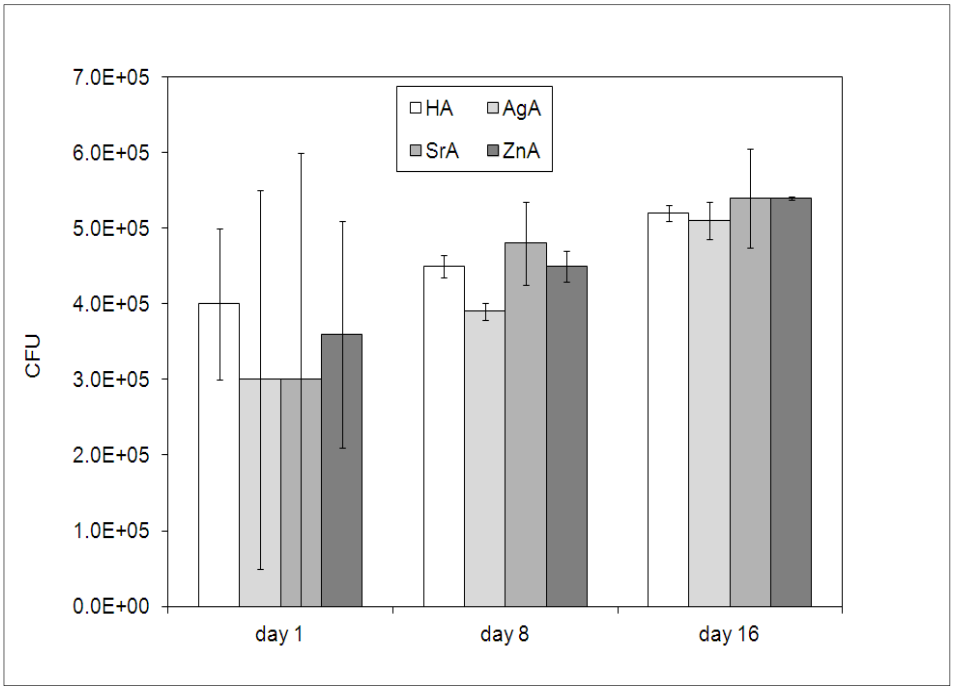

Figure II-7: Antimicrobial activity expressed as CFU of the released ion from the various coatings using *Pseudomonas aeruginosa* as the bacterial challenge organism (n=3 samples ±SD).

Table II-2: Antimicrobial effect (% kill) of the elutions from the various coatings using *Pseudomona aeruginosa* as the bacterium challenge (% kill ±SD)

Time (Day)	AgA		SrA		ZnA	
1	25	(±25)	35	(±3)	10	(±2)
8	13	(±62)	0	-	0	-
16	2	(±75)	0	-	0	-

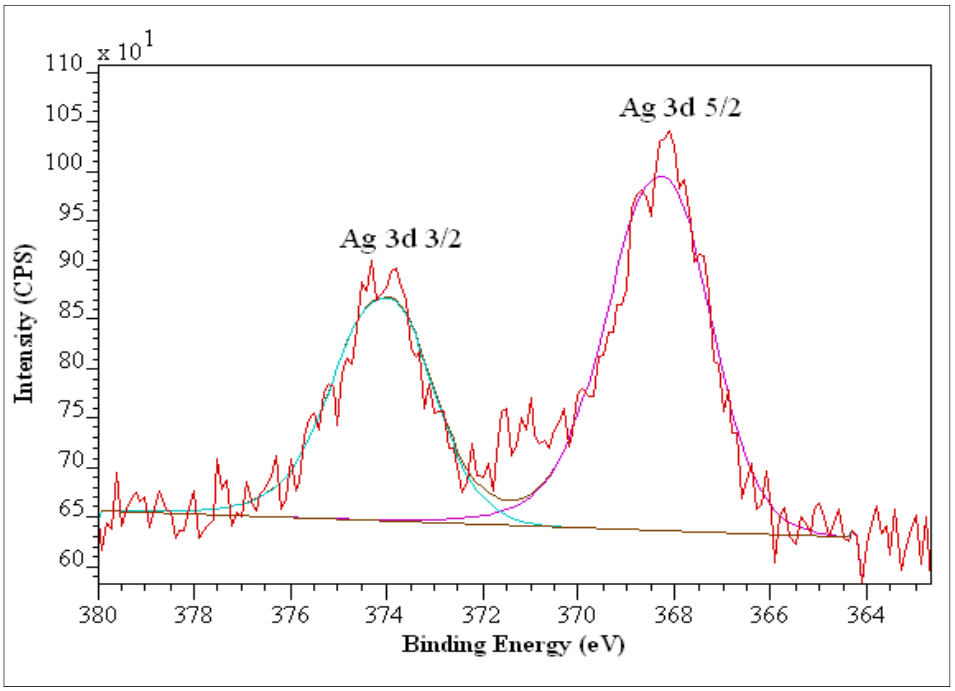

Figure II-8: High resolution XPS spectrum of the AgAP Ag 3d core level

In order to study the dopants further, curve fitting of the high resolution XPS 3d level of the silver sample was carried out, Figure II-. Using the C 1s core level (C-C at 285 eV) to charge correct the position of the Ag 3d level, the centroid of the Ag 3d 5/2 level was determined to be 368.2 eV. This is in good agreement with the literature values for elemental Ag (Christ, 1999). If an oxide were present, a decrease in the binding energy of 0.6 – 1.0 eV would be expected, which was clearly not the case in this study. This indicates that the Ag dopant is carried by the apatite, but is not part of the ionic bonding of the crystal structure.

(a)

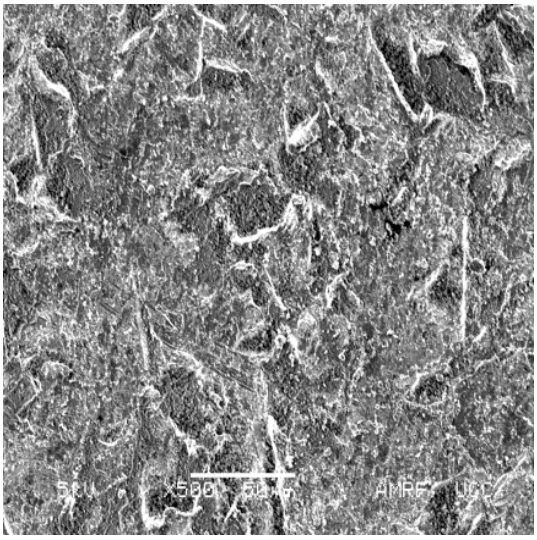

(b)

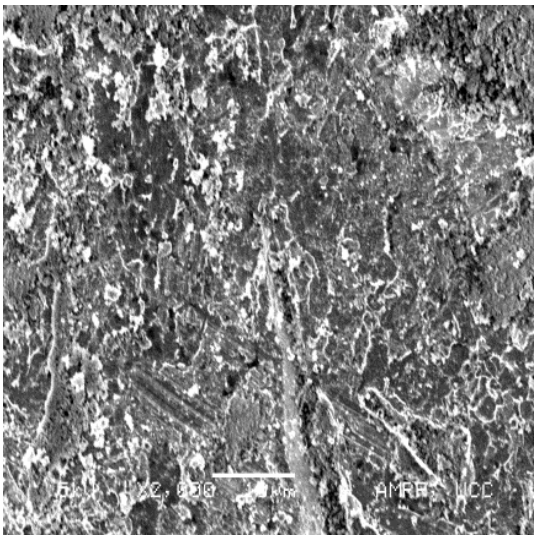

(c)

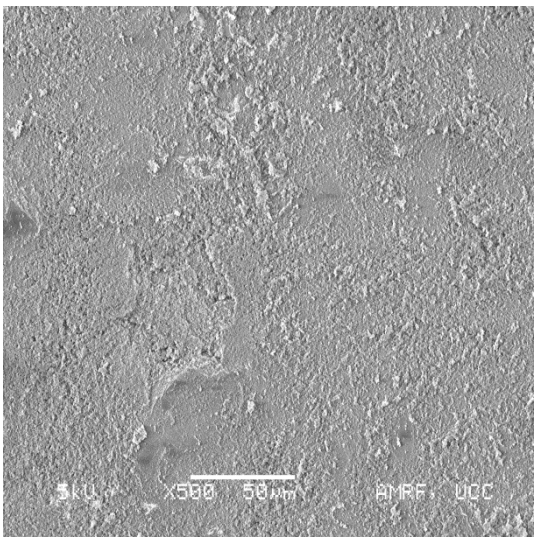

Figure II-9: SEM images: (a) 5% wt AgA (x500 magnification); (b) 5% wt SrA (x2000 magnification) and (c) 5% wt ZnA (x500 magnification).

Appendix III

Further Analysis on 12% wt Substituted Apatites (Chapter 6)

Table III-1: Median particle size (d(0.5)) analysis of the powers and various analysis on the coatings (coating mass, coating mass after washing treatment, water contact angle and % wt ion present) (n=3 samples).

Coating	d(0.5) powders (μm) (±2SD)	Coating mass (mg/cm^2) (±2SD)	Coating mass loss after IPA wash for 15 minutes (±2SD)	Water contact angle (°) of the coating (±2SD)	% wt ion present in the coating (EDX)
Uncoated Ti	-	-	-	8±20	-
HA	-	-	-	64±12	-
AgA	7±1	2.2±0.5	0.26±0.57	0	4-Ag
SrA	6±2	2.5±1.0	0.40±0.5	0	16-Sr
ZnA	6±2	3.0±0.6	0.65±0.3	0	10-Zn
AgSrA	8±2	2.5±0.6	0.5±0.2	8±20	5-Ag 11-Sr

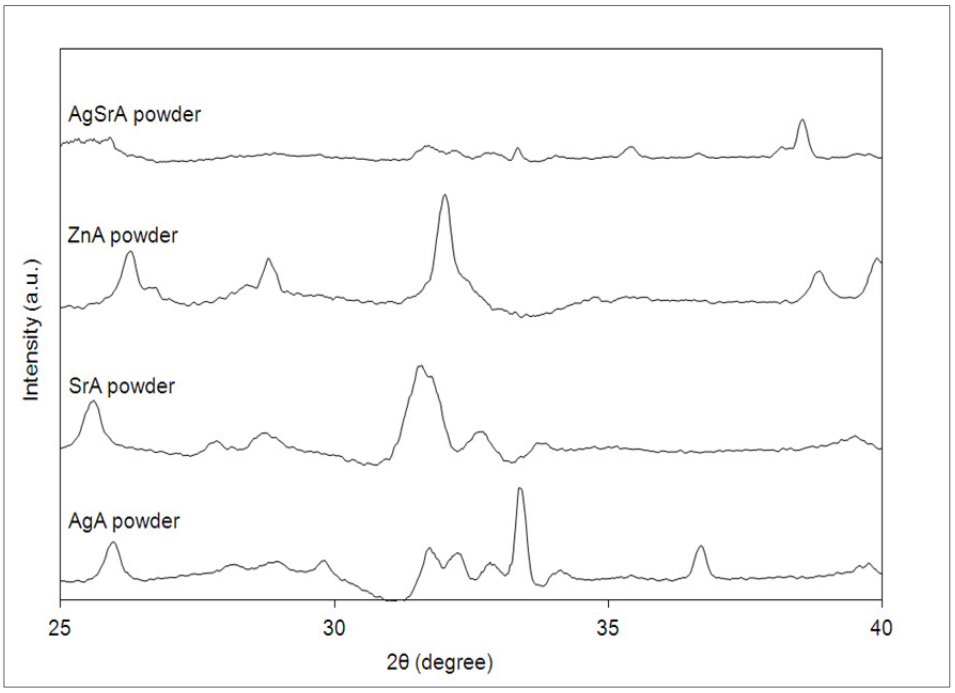

Figure III-1: XRD Analysis of 5% wt substituted apatite powders and coatings

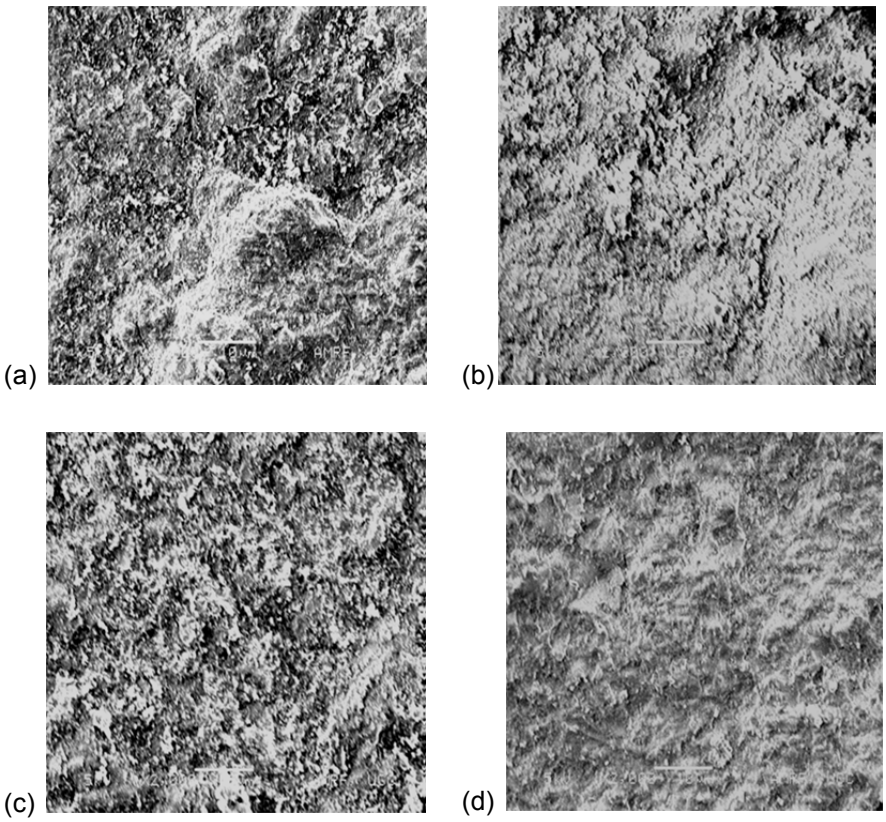

Figure III-2. SEM images of 12% wt substituted apatite coatings: (a) AgA (x2000 magnification); (b) SrA ; (c) ZnA and (d) AgSrA.

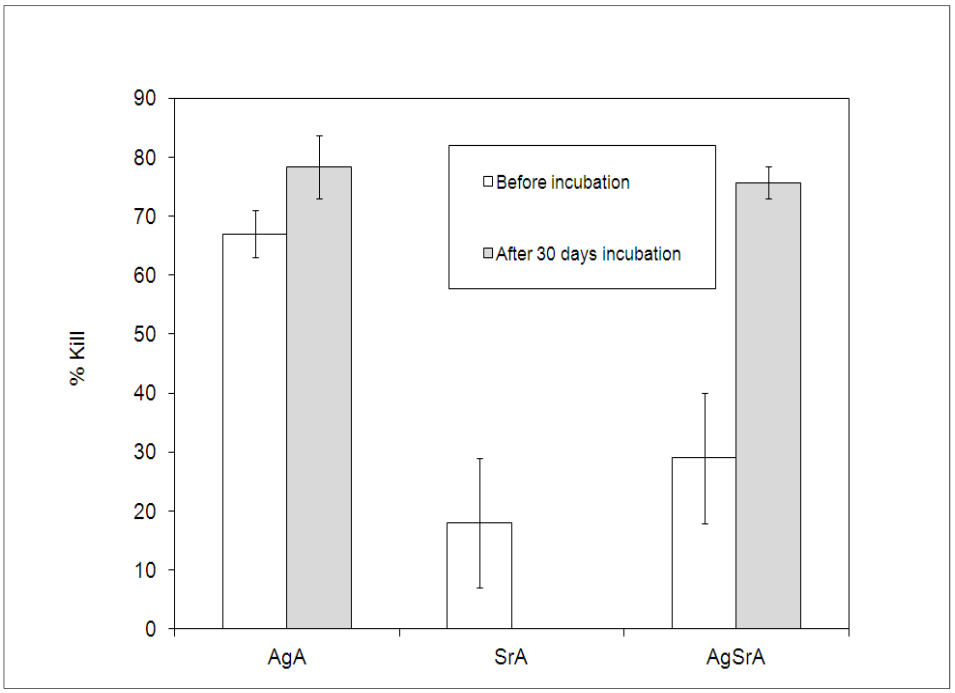

Figure III-3: Antimicrobial activity expressed as % kill of the immobilised surface ion of the various coatings (12% wt substituted apatites) using *S. aureus* as the bacterial challenge organism (n=3 samples ±SD).

Table III-2: Antimicrobial activity of the immobilised ion expressed as CFU of the coatings using *S. aureus* as the challenge organism (ATCC 1448) at day 0 and day 30 (n=3 samples ±SD).

	day 0		day 30	
Sample	CFU	SD	CFU	SD
HA	1.1E+06	2.3E+05	3.7E+06	3.0E+05
AgA	3.6E+05	4.2E+04	8.0E+05	2.0E+05
SrA	9.0E+05	1.3E+05	4.9E+06	1.1E+06
AgSrA	7.8E+05	1.3E+05	9.0E+05	1.0E+05

Table III-3: Anticolonising activity (CFU) of the coatings using *S. aureus* as the challenge organism (ATCC 1448) at day 1 and day 14 (n=3 samples ±SD)

	day 1		day 14	
Sample	CFU	SD	CFU	SD
HA	4.1E+05	6.7E+04	4.3E+05	9.4E+04
AgA	0.0E+00	0.0E+00	4.4E+04	7.4E+04
SrA	2.3E+05	8.0E+04	3.8E+05	1.0E+05
AgSrA	1.2E+05	2.3E+04	5.1E+05	7.4E+04

Table III-4: Anticolonising effect of the AgA coating using the clinical strains *MRSA, MSSA* and *S.epidermis* as the bacteria challenges.

		day 1		day 14	
	Sample	CFU	log Reduction	CFU	log Reduction
MRSA	HA	2.2E+06		8.7E+05	
	AgA	2.3E+05	1.0	4.0E+05	0.3
MSSA	HA	1.7E+07		1.6E+07	
	AgA	8.6E+06	0.3	4.6E+06	0.0
S.epidermis	HA	3.7E+06		2.0E+06	
	AgA	1.0E+07	0.0	6.0E+06	0.0

Appendix IV

Preliminary Study Prior to the *In Vivo* Work (Chapter 7)

Table IV-1: Preliminary work performed to determine the % biofilm using *S. aureus* as the bacterial challenge in an *in vitro* study

Coating	CFU (±SD)	% Biofilm Inhibtion day 1
HA K-wire	$2.13x10^5 \pm 1.52x10^5$	-
5% wt K-wire	$2.05x10^5 \pm 1.91x10^5$	0
12% wt K-wire	$2.5x10^4 \pm 7.1x10^3$	88±3

Note: Two nude mice were injected with 1 x 10^4 CFU of *S. aureus* (ATCC 1448) and survived for two days. The dose was increased to that used in the *in vivo* trials.

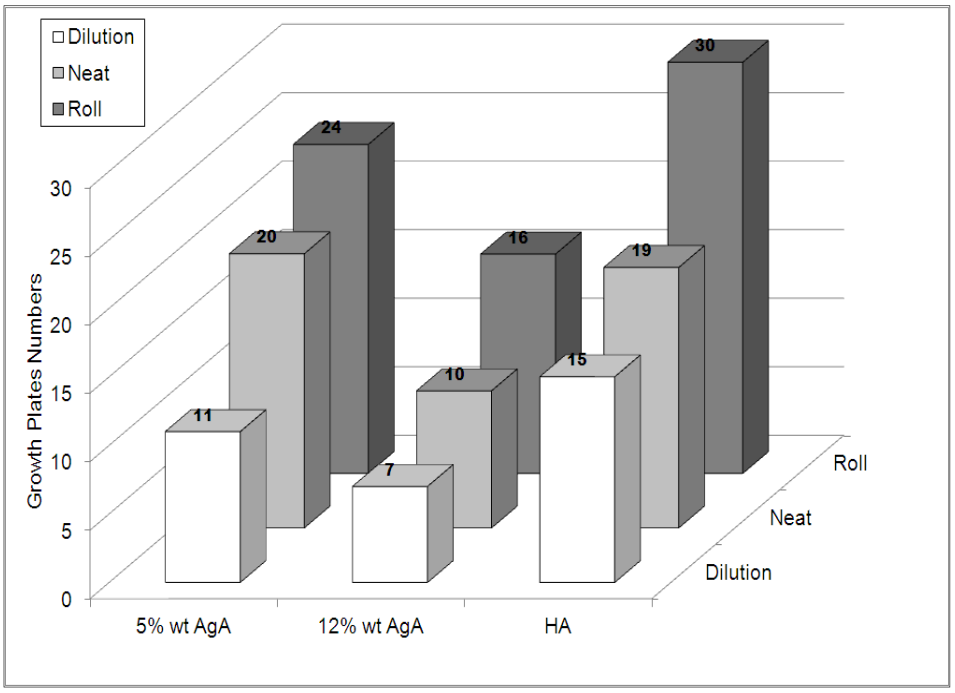

Figure IV-1: Scoring of growth plate numbers [1,0] (addition the number of agar plates that showed any *S. aureus* growth on the plates excluding plates that had no colonies).

Table IV-2: Scoring of the agar plates following explantation of the K-wires

Sample	Numbers	Roll	Neat	Dilution
	TMTC	13	4	0
	Zeros	14	19	26
5% wt AgA	Scoring [1,0]	24	20	11
	TMTC	5	1	0
	Zeros	23	30	32
12% wt AgA	Scoring [1,0]	16	10	7
	TMTC	13	6	1
	Zeros	9	20	23
HA	Scoring [1,0]	30	19	15

Appendix V

Drug Studies

Table V-1: Studies Performed

Studies	Drugs	Outcome
Deposition of HA mixed with 10% wt/wt antibiotics onto Ti using CoBlast Technology	Gentamicin, Vancomycin, Tobraymycin	Burst release and all drugs eluted after 15 mins
Deposition of HA loaded antibiotics (drug loaded into the HA pores) onto Ti using CoBlast Technology	Gentamicin	Burst release and drugs eluted after 1-2 hours
Deposition of HA mixed with HA/PLGA-drug (HA coating on a PLGA-loaded microspheres) onto Ti using CoBlast Technology	Gentamicin	Too dilute
Tethering drugs onto a CoBlast HA surface	Bisphosphonates Tetracycline	Drugs binded to the HA surface, elution of tetracycline from the surface was over 5 hours
PLGA films on a CoBlast HA/drug surface as a controlled release system	Gentamicin	Release was over a 24 hour period.

Appendix VI

Publications

Coatings **2011**, *1*, 53-71; doi:10.3390/coatings1010053

OPEN ACCESS

coatings

ISSN 2079-6412
www.mdpi.com/journal/coatings/

Article

A Modified Surface on Titanium Deposited by a Blasting Process

Caroline O'Sullivan [1,2,*], Peter O'Hare [3], Greg Byrne [4], Liam O'Neill [5], Katie B. Ryan [1] and Abina M. Crean [1]

[1] School of Pharmacy, Cavanagh Building, University College Cork, Cork, Ireland; E-Mails: katie.ryan@ucc.ie (K.B.R.); a.crean@ucc.ie (A.M.C.)
[2] Department of Chemical and Process Engineering, Cork Institute of Technology, Bishopstown, Cork, Ireland
[3] The Nanotechnology and Integrated BioEngineering Centre, University of Ulster at Jordanstown, Newtownabbey, Co Antrim, BT37 OQB, Northern Ireland; E-Mail: p.ohare@ulster.ac.uk
[4] School of Electrical, Electronic & Mechanical Engineering, University College Dublin, Belfield, Dublin 4, Ireland; E-Mail: gregory.byrne@ucd.ie
[5] Research & Development, EnBIO, Carrigtohill, Cork, Ireland; E-Mail: liam.oneill@enbiomaterials.com

* Author to whom correspondence should be addressed; E-Mail: caroline.osullivan@cit.ie; Tel.: +353-(0)21-490-1667; Fax: +353-(0)21-490-1656.

Received: 16 July 2011; in revised form: 23 August 2011 / Accepted: 1 September 2011 / Published: 13 September 2011

Abstract: Hydroxyapatite (HA) coating of hard tissue implants is widely employed for its biocompatible and osteoconductive properties as well as its improved mechanical properties. Plasma technology is the principal deposition process for coating HA on bioactive metals for this application. However, thermal decomposition of HA can occur during the plasma deposition process, resulting in coating variability in terms of purity, uniformity and crystallinity, which can lead to implant failure caused by aseptic loosening. In this study, CoBlast^{TM}, a novel blasting process has been used to successfully modify a titanium (V) substrate with a HA treatment using a dopant/abrasive regime. The impact of a series of apatitic abrasives under the trade name MCD, was investigated to determine the effect of abrasive particle size on the surface properties of both microblast (abrasive only) and CoBlast (HA/abrasive) treatments. The resultant HA treated substrates were compared

to substrates treated with abrasive only (microblasted) and an untreated Ti. The HA powder, apatitic abrasives and the treated substrates were characterized for chemical composition, coating coverage, crystallinity and topography including surface roughness. The results show that the surface roughness of the HA blasted modification was affected by the particle size of the apatitic abrasives used. The CoBlast process did not alter the chemistry of the crystalline HA during deposition. Cell proliferation on the HA surface was also assessed, which demonstrated enhanced osteo-viability compared to the microblast and blank Ti. This study demonstrates the ability of the CoBlast process to deposit HA coatings with a range of surface properties onto Ti substrates. The ability of the CoBlast technology to offer diversity in modifying surface topography offers exciting new prospects in tailoring the properties of medical devices for applications ranging from dental to orthopedic settings.

Keywords: hydroxyapatite; grit blasting; CoBlast; hard tissue implants

1. Introduction

Hydroxyapatite (HA), $Ca_{10}(PO_4)_6(OH)_2$, a proven bioceramic for coating medical device implants is widely known, not only for its biocompatible and osteoconductive properties, but also for its increased mechanical properties when applied to bio-inert metals for orthopedic use [1-4]. Implant surface modifications are often required in order to prescribe a particular surface roughness and increase surface area for osteoblast attachment, as well as to enhance the bioactive and osteoconductive properties of the underlying substrate. Such surface treatment methods include sand- or grit-blasting using abrasives, chemical treatments and deposition of calcium phosphate (CaP) coatings [2-8].

Abrasive blasting involves impacting the implant metal surface with abrasive particles under pressure to roughen the surface. Roughening orthopedic and dental implants utilizing alumina (Al_2O_3) abrasives is a common practice to enhance implant osteointegration *in vivo* [5,6]. However, the use of apatite abrasives are often preferred as it enhances bone formation [7,18]. It has been shown that this technique can be effective in depositing a thin layer of CaP on the surface being roughened [18-20]. A number of other HA coating deposition techniques have been employed to confer a bioactive layer onto metallic and other inert substrates including plasma spraying, which is one of the most common types of coating process for the generation of CaP thin films [3,4,9-14] and alternative deposition processes including pulsed laser deposition (PLD) [15], radio frequency (RF) magnetron sputtering [16], sol-gel immersion techniques, and electrophoretic deposition [17].

More recently, a novel approach CoBlast has been shown as an alternative process to deposit HA and substituted apatites onto titanium (Ti) substrates [21-23]. The CoBlast technique is based on the convergent flow of an abrasive and a dopant stream onto the implant surface which can effectively impregnate the metal with the dopant material. The CoBlast approach manipulates the ability of abrasive blasting to achieve surface roughening and bioactive layer deposition. The impregnation of the dopant material onto the surface results from a combination of the mechanical interlocking and tribo-chemical bond formation between the bioceramic material and the underlying metal

substrate [21]. HA coatings prepared using the CoBlast technique demonstrated enhanced osteoblast attachment *in vitro* and early stage lamellar bone growth *in vivo* compared to microblasted and untreated Ti surfaces [21]. Additionally, a series of substituted apatites (AgA, SrA, ZnA) were effectively deposited using the CoBlast technique and these modifications offered the dual benefits of osteoconductive properties essential for bone integration with the added potential of microbial colonization inhibition without cytotoxic effects [23]. The established research showed that <10 μm thick coatings were applied with this technique employing alumina as the abrasive and that there was no evidence of alumina being incorporated into the modified surface [21].

The objective of this study is to demonstrate the use of apatitic abrasives in the treatment of Ti substrates using both the CoBlast technique (dopant/abrasive regime) and a control microblast surface (abrasive only). The chemical, topological and osteo-viability advantages of treated Ti substrates was characterised. The effect of abrasive particle size on the properties and performance of the CoBlast and microblast modified surfaces was also investigated. A series of apatitic abrasives (sintered CaP under the trade name MCD) with differing mean particle size values were employed for both techniques.

2. Results and Discussion

2.1. Chemical Characterization of HA and MCD Abrasive Powders

The particle size of the HA and MCD abrasives were measured using a laser light technique (Mastersizer S), Table 1. The average particle size (d (0.5)) increased in the following order: HA < MCD-106 < MCD-180 < MCD-425. The various powders were analyzed for their chemical composition using energy dispersive X-ray (EDX) analysis, Table 1.

Table 1. Mean particle size analysis and energy dispersive X-ray (EDX) analysis of the calcium phosphate powders (n = 3).

Powder	Mean particle Size (μm)	O % atm	Ca % atm	P % atm	Ca/P
HA	40 (±4)	71	18	11	1.66
MCD-106	44 (±2)	72	18	10	1.76
MCD-180	124 (±6)	73	17	10	1.73
MCD-425	355 (±6)	77	13	10	1.29

The calcium phosphate powders (HA and MCD abrasives) were found to be composed of O, P and Ca. The Ca/P ratio for stoichiometric HA was found to be similar to the previously reported value of 1.67 [25]. The increase in Ca/P ratio for MCD-106 and MCD-180, as seen in Table 1, may be explained by the presence of impurities such as tricalcium phosphate (TCP) phase as determined by powder X-ray diffraction (PXRD) analysis (Figure 1). However, the Ca deficient nature for the more amorphous MCD-425 results in a reduced Ca/P ratio (1.29).

Relative crystallinity of each powder was investigated using PXRD, (Figure 1). HA was found to be highly crystalline with well defined narrow peaks. The main characteristic peaks associated with HA can be assigned to the 002, 102, 210, 211, 112, 300 and 202 reflections corresponding to 25.9°, 28.1°, 28.9°, 31.9°, 32.2°, 33.1° and 34.1°, as previously reported [25]. The resulting PXRD patterns for the MCD apatite series indicate a lower crystallinity relative to the HA powder. The small peak present at 31° and 34.4° was attributed to the TCP phase [26]. Also in the MCD-425 pattern, peaks are poorly resolved with low intensity relative to the other apatites, demonstrating the more amorphous nature of this material [25,26].

Figure 1. Powder X-ray diffraction (PXRD) spectra of the powders (■ denotes HA peaks and * represents tricalcium phosphate (TCP)).

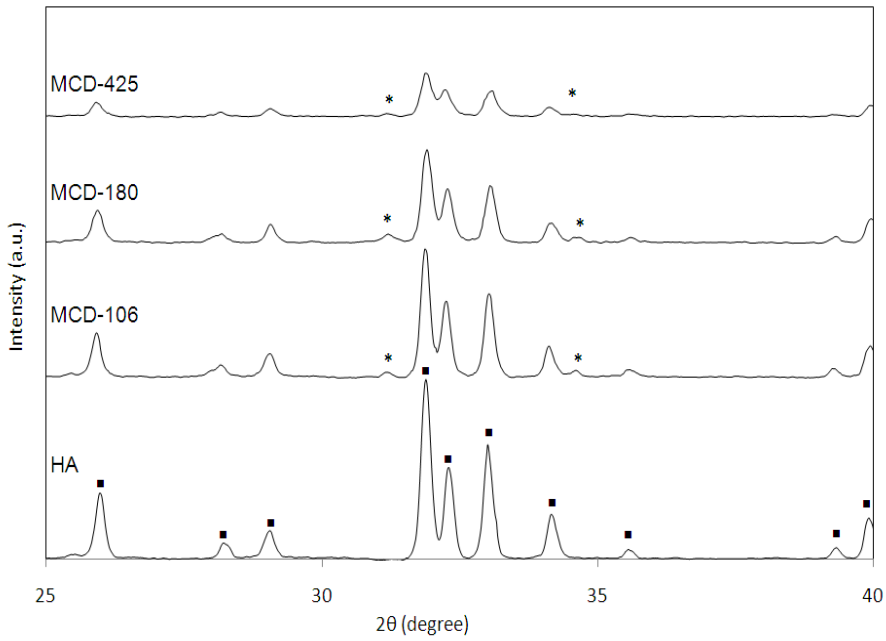

The Fourier transform infrared spectrometer (FTIR) spectra of the powders in the range 1600–450 cm^{-1} are presented in Figure 2. The most intense peaks observed for the crystalline HA powder are those attributable to vibrations of the PO_4^{3-} groups; the ν_1 and ν_3 phosphate bands in the region of 900–1200 cm^{-1} and ν_4 absorption bands in the region of 500–700 cm^{-1}, which are used to characterize apatite structure. The peak at 962 cm^{-1} is assigned to the ν_1 symmetric P-O stretching vibration of the PO_4^{3-} and the ν_3 asymmetric P-O stretching mode are indexed at 1090 and 1045 cm^{-1} [27]. The bands at 601 and 571 cm^{-1} are assigned to ν_4 vibration mode of the phosphate group, which occupies two crystal lattice sites (O-P-O bending mode) according to previous studies [27]. The HA adsorption bands of the ν_1 and ν_4 of the PO_4^{3-} groups determined here are those of stoichiometric HA [16]. The bands at 631 and 474 cm^{-1} correspond to the vibrations of OH^- groups in the structure [27]. The MCD series showed similar finger-print bonds for calcium phosphate bonds but with broader definition, which is representative of the increased amorphous content of these CaP materials [28].

Figure 2. Fourier transform infrared spectrometer (FTIR) spectra of the various apatite powders.

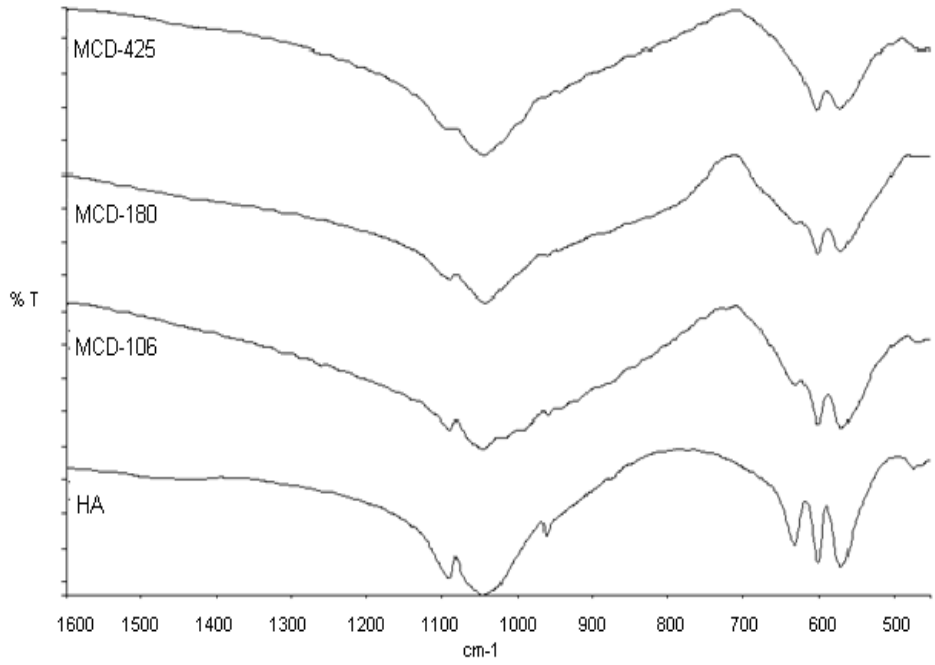

2.2. Characterization of the Modified Titanium Substrates

Titanium (V) was used as the base substrate and the untreated Ti surface was determined to contain 23% O and 77% Ti using EDX analysis. The chemical composition of the microblast surfaces (abrasive blast only, no dopant) are presented in Table 2 and were analyzed for O, Ca, P and Ti only.

Table 2. EDX analysis, coating thickness (PosiTector thickness gauge) and mass of the modified surfaces.

Modification		**O % atm**	**P % atm**	**Ca % atm**	**Ti % atm**	**Ca/P**	**Coating Thickness (µm) (2STD)**	**Coating Mass (mg/cm^2) (2STD)**
Blank	Ti	23	-	-	77	-	0	-
Microblast	MCD-106	59	8	12	21	1.56	3 ± 1	-
	MCD-180	56	6	10	27	1.53	3 ± 1	-
	MCD-425	55	7	11	27	1.57	3 ± 2	-
CoBlast	HA/MCD-106	63	13	21	2	1.59	6 ± 3	0.48 ± 0.4
	HA/MCD-180	67	12	18	3	1.53	6 ± 1	0.44 ± 0.4
	HA/MCD-425	65	12	20	5	1.61	7 ± 3	0.44 ± 0.3

The % atm Ti determined reflects the exposure of the underlying substrate and can be used to represent the degree of coverage resulting from apatite materials. A high Ti level represents a thin or

patchy coating and conversely, a low Ti concentration signifies a thick coating. The EDX results reveal that after a wash treatment, the MCD microblasted surfaces show a reduction in Ti concentrations to 21–27% atm, compared to 77% atm for the Ti substrate. Also the presence of Ca and P which are the main constituents of the MCD abrasive is noted on the surface. This illustrates that a thin coating of Ca/P material has been blasted onto the surface and successfully deposited as a stable layer onto the Ti surface. The Ca/P values obtained for the microblasted samples treated with the MCD series of the abrasives ranged between 1.53 and 1.57 which is consistent with similar grit blasted studies [18].

The chemical composition of the CoBlast surfaces (blasting with both abrasive and dopant) on Ti are also presented in Table 2. For CoBlast coatings, the levels of O, P, Ca and Ti obtained were determined to be in the range of 63–67%, 12–13%, 18–21% and 2–5% atm, respectively. The reduced level of Ti detected in these samples, compared to the Ti substrate and microblasted surfaces, is indicative of a high degree of coating coverage across all CoBlast samples. The Ca/P values were found to display a ratio of between 1.53 and 1.61, which are relatively close to the value for stoichiometric HA [25]. The % atm Ti, determined using EDX analysis, was observed to increase as the MCD series particle size order increased, indicating a decrease in the thickness of the deposited layer, as outlined in Table 2. This suggests that the smaller the particle size of the MCD abrasive the more HA was deposited, although the coating thickness determined using the PosiTector thickness gauge, and the coating mass values were found to be similar. The coating thickness of all the CoBlast samples was <10 microns which is in agreement with a previous study which used Al_2O_3 as the abrasive [22].

The scanning electron microscopy (SEM) image of the untreated Ti substrate can be seen in Figure 3a which has similar topography to that observed in a previous study [6]. This image reveals a very smooth surface and the morphology of a machined metal. The SEM images of the microblast MCD-106 surfaces, as well as the corresponding CoBlast HA/MCD-106 surfaces, are presented in Figure 3b and c respectively. (More images can be seen as supporting information)

As expected, the microblast process was observed to roughen the untreated Ti surface. Examination of the CoBlast surfaces suggests that the co-introduction of the HA with the abrasive appears to have in-filled some of the surface features that are evident on the microblast sample (Figure 3b). The CoBlast process results in a roughened, highly regular and uniform surface which is consistent with other calcium phosphate coatings produced using simple grit blasting technologies [6,19,20]. It was noted that as the particle size (d90) of the MCD abrasive increased from 106 to 425 microns, the texture (presence of surface features) and the apparent roughness of the resultant surfaces was also observed to increase for both the microblast and CoBlast treatments and this was confirmed by surface roughness measurements.

Figure 3. Scanning electron microscopy (SEM) images (×1000 magnification) of (**a**) titanium; (**b**) microblast MCD 106; (**c**) CoBlast HA/MCD-106.

(a)

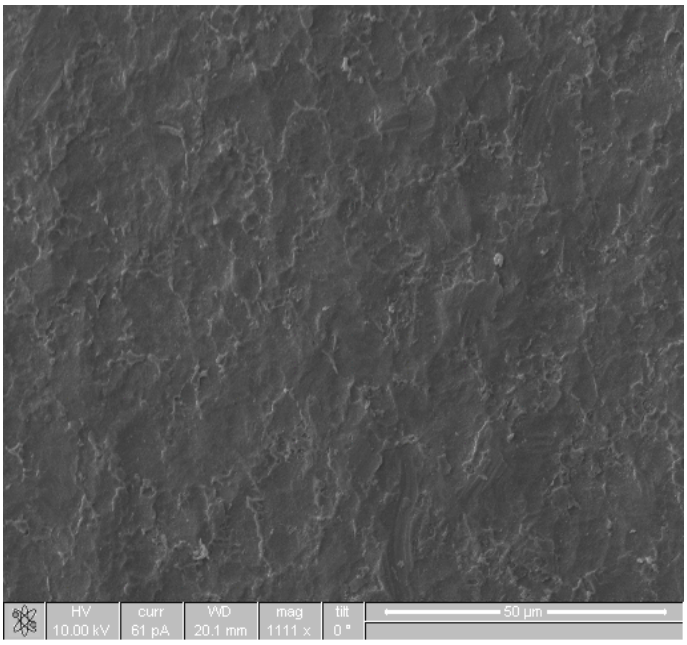

(b)

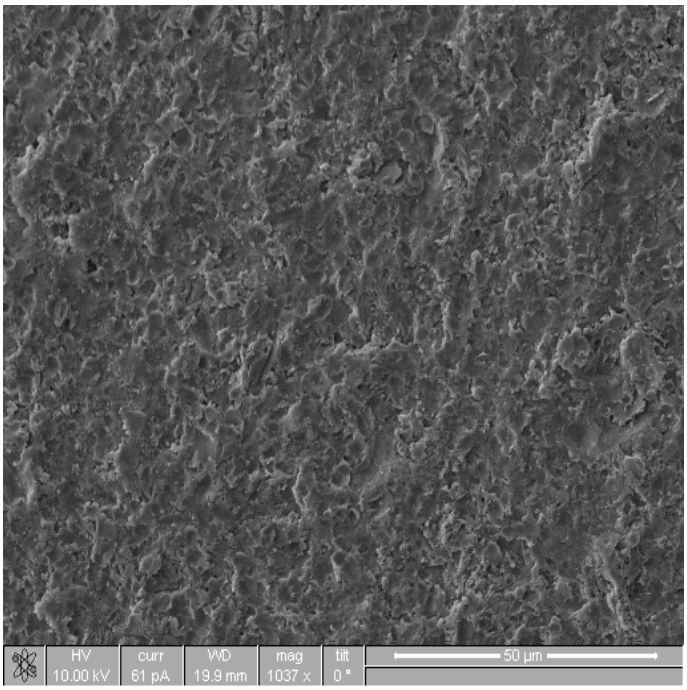

Figure 3. *Cont*.

(c)

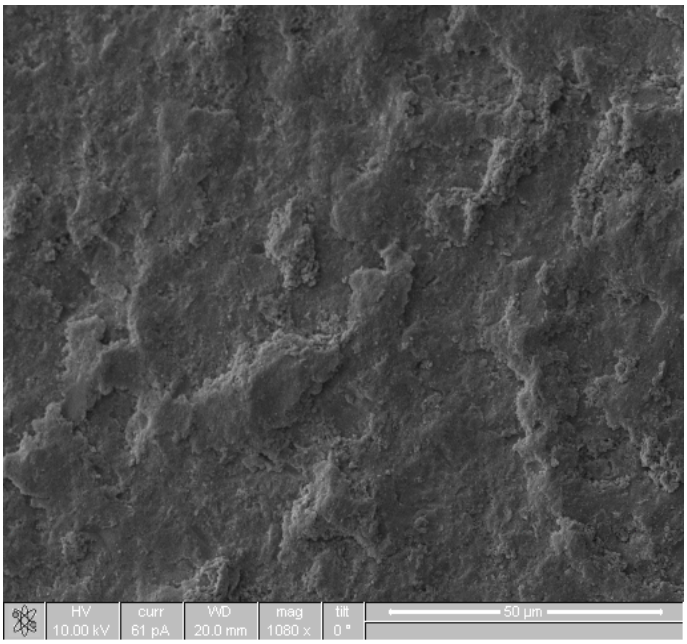

The surface roughness was measured using a stylus method and the results obtained are given in Figure 4. The arithmetical mean roughness (R_a) was used as a measure of the surface roughness, which tended to increase as the particle size of the abrasive increased. Significant differences were observed between the surface treated and the untreated Ti. The average surface roughness of the blank titanium (0.4 µm) increased to 0.5, 0.8, 1.4 µm when MCD-106, MCD-180 and MCD-425, respectively were employed for microblast treatments. It has been previously reported that an increase in surface roughness was observed with the introduction of HA with the Al_2O_3 abrasive using the CoBlast technique and the same trend was observed here on the introduction of HA with the MCD abrasives [21]. Statistically significant differences were noted between the roughness of the microblast and CoBlast samples prepared using MCD-106 and MCD-180 abrasives, though not when MCD-425 was used. A large standard error was observed for the MCD-425 microblasted surface, which may possibly be a feature of the crude microblast process. As per the microblast samples, the level of roughness and irregularity of the CoBlast surface was visibly altered by changes in the abrasive particle size, with a significant increase in surface roughness produced by larger abrasive particle sizes ($p < 0.05$).

Implants with rougher surfaces result in a higher removal torque force and demonstrate excellent osteointegration when compared to those with smoother surfaces [5]. As seen in this study, microblasting offers increased roughening of machined Ti substrates as expected and the use of MCD abrasives results in the deposition of a thin coating layer of calcium phosphate. Furthermore, the roughness of the microblast process can be tuned between 0.5–1.4 µm depending on the particle size of the apatite abrasive employed. This is consistent with previously studies [5,6]. Unfortunately, the coatings deposited using this microblast process have demonstrated poor adhesion to the metal and have not been widely employed as final surface treatments for this reason [21].

Figure 4. Surface roughness (R_a) of the various modifications (* denotes $p < 0.05$ and ** ascribes $p < 0.01$ determined using student's t-test).

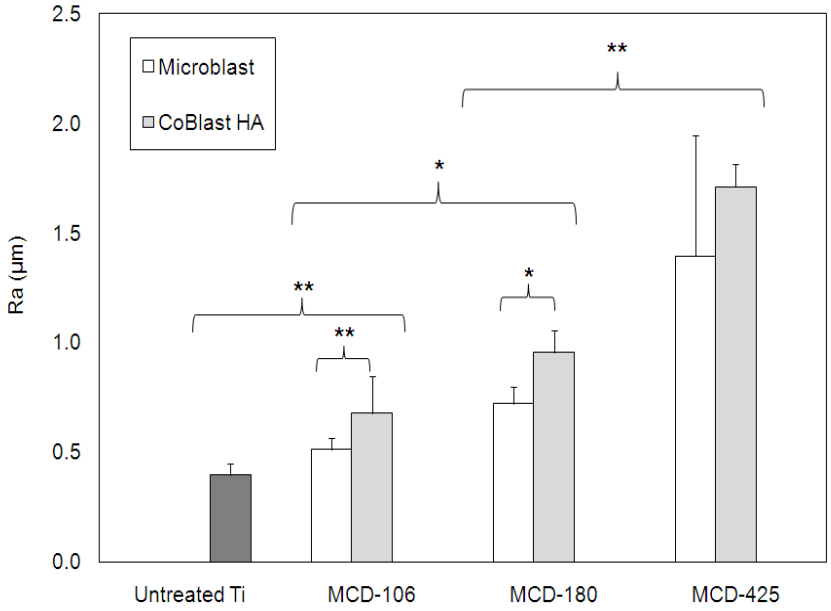

For the CoBlast samples, the tribo-chemical bonding which results from surface roughening, activation and subsequent bonding of the powder to the substrate has been shown to improve the HA bonding to the titanium [21,22]. The deposition of HA *via* the CoBlast process combines the benefits of increased roughness and enhanced bioceramic deposition with the added bioactive property of improved osteointegration compared to the microblasted surfaces. The surface treatment effect was also dependant on the particle size of the abrasive, with the larger particle size producing greater surface erosion and a rougher topography resulting in reduced coating thickness.

In literature, HA coatings, deposited using the standard high temperature plasma spray deposition technique, have been reported to contain a variety of crystalline phases and the presence of altered chemical functionality [9]. This can lead to the formation of intermediates such as calcium oxide (CaO), octa-hydroxyapatite (OHA), α-tricalcium phosphate (α-TCP), β-tricalcium phosphate (β-TCP) and tetra-calcium phosphate (TTCP) [10,11]. The presence of these impurities in a HA modified surface can decrease the crystallinity and subsequently make it more prone to dissolution. The increased solubility of these phases can eventually lead to the poor apposition of bone and compromize the mechanical stability of the implant [12, 29]. This can occur when the coating itself de-laminates over time due to poor bonding strength of the HA onto the underlying surface or as the coating itself resorbs into the surrounding environment [30].

Figure 5 shows the XRD pattern of the CoBlast HA coated substrates. Due to the thin nature of the deposited material and the interference of the background Ti metal, detailed analysis of the XRD profiles was not possible. However, for the CoBlast substrates, the peaks detected clearly correspond to that of HA powder employed. The additional 2θ peaks observed at 35.3° and 38.5° were assigned to the Ti substrate. No evidence of the TCP phase was detected (31° and 34.4°), which suggests that no compositional or crystallographic changes occurred to the HA powder during the blasting process, with negligible uptake of the abrasive, which is in keeping with previous studies [21,22].

Figure 5. XRD of the CoBlast HA modifications (■ denotes HA peaks;*denotes Ti peaks).

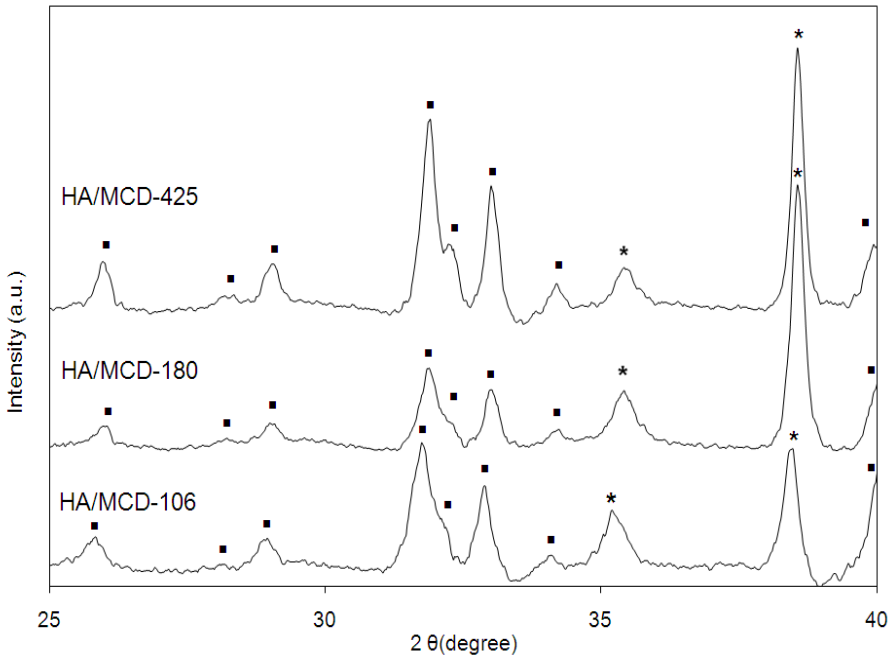

Figure 6 shows the FTIR spectrum in the range 1600–450 cm^{-1} for the HA coated substrates. The FTIR spectra for all CoBlast HA coatings irrespective of the abrasive used are very similar and display the characteristic features of the HA powder used, as discussed earlier. There was no evidence of hydration (broad banding at 3450 cm^{-1}), further demonstrating a pure HA coating has been deposited. Also, the position of the characteristic peak at 962 cm^{-1} represents a highly ordered, non-carbonated apatite and indicates a highly crystalline nature [16]. The banding assignments are in agreement with those of the HA powder as seen in Figure 2 suggesting that the chemistry is retained during the deposition process. This also supports the XRD analysis discussed above, which suggests that there has been minimal uptake of the abrasive powders during sample preparation.

Figure 6. FTIR analysis of the CoBlast HA surface modifications.

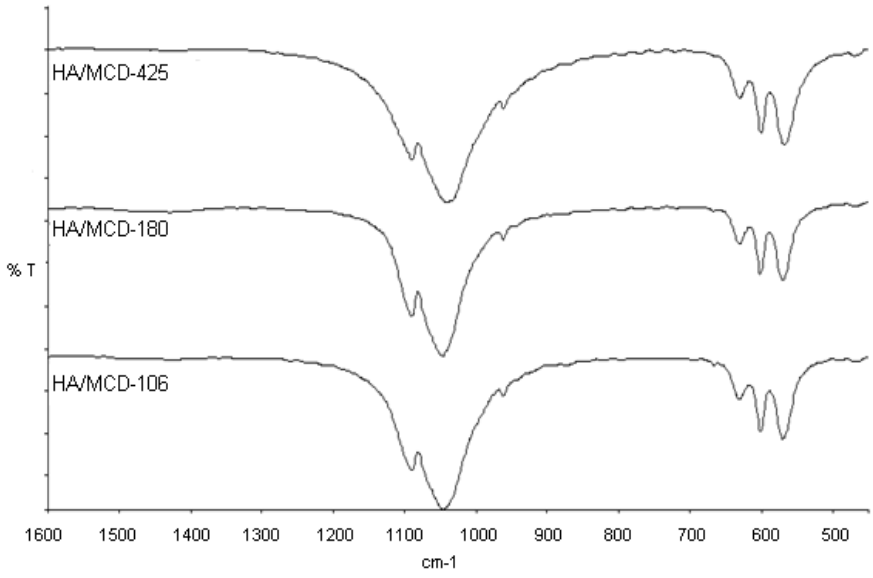

CoBlast demonstrated the ability to deposit a well adhered HA coating with no major evidence of contamination with additional calcium phosphate phases. This is in contrast to the variety of crystalline phases and the presence of altered chemical functionality produced during the standard high temperature plasma spray deposition. The XRD and FTIR analysis does not suggest formation of any such impurities within the CoBlast samples indicating that the HA coating on the CoBlast samples has retained the same properties as the starting crystalline HA powder employed. Therefore it is anticipated that HA modified surfaces prepared using CoBlast should not exhibit the problems associated with the presence of impurities observed for HA modified surfaces prepared using standard high temperature plasma spray which are outlined above.

2.3. Cell Culture Analysis

2.3.1. Cell Proliferation

Osteoblasts are the key cells that are involved in the osteoconduction process. The success of the implantation is strongly influenced by how well the first phase of the attachment and adhesion of these cells will occur, which will then lead to the subsequent proliferation and differentiation upon contact with the implant surface. CoBlast surfaces have exhibited excellent osteoblast attachment and proliferation *in vitro* compared to their respective controls [21-23]. Biocompatability of the modified surfaces was determined via a (3-(4,5-dimethylthiazol-2-yl)-2,5-diphenyltetrazolium bromide) (MTT) assay and the osteoblast proliferation results are presented in Figure 7.

Figure 7. (3-(4,5-dimethylthiazol-2-yl)-2,5-diphenyltetrazolium bromide) (MTT) assay data for MG-63 cells on modified Ti surfaces over five days *in vitro* (* denotes $p < 0.05$ and ** ascribes $p < 0.01$ determined using student's t-test).

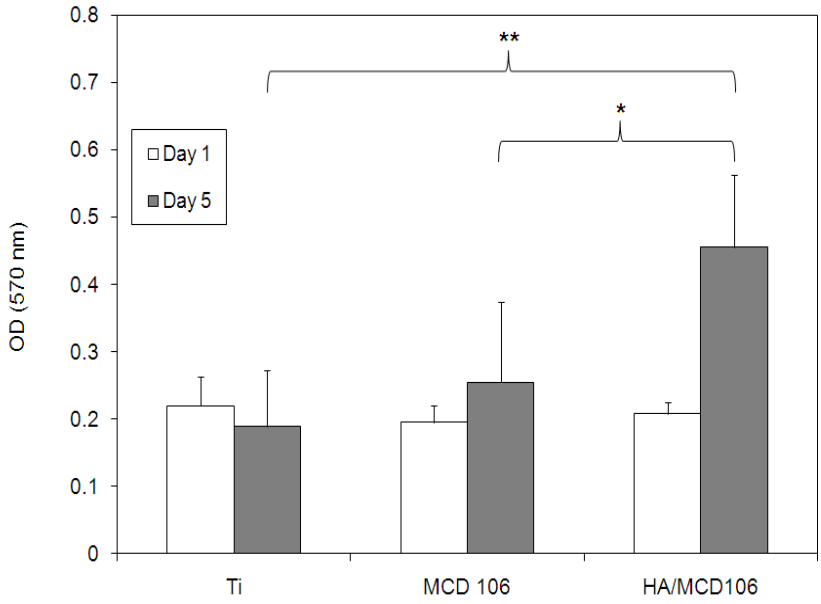

Microblast and CoBlast surfaces prepared using the MCD 106 abrasive were selected for comparison. There was no significant difference in the cell proliferation between samples analyzed at day 1. However, at day 5 there was a significant increase ($p < 0.01$) in cell proliferation on the CoBlast coated substrate compared to the untreated titanium. A significant difference ($p < 0.05$) was also detected between the CoBlast sample and the microblast sample at day 5. The introduction of the bioactive HA layer through the CoBlast process was shown to further increase surface roughness and this combination of surface topography and bioactive surface chemistry was found to offer notably higher levels of cell proliferation after 5 days on the CoBlast surface. No evidence of cytotoxicity was observed using MG63 cells on any of the samples evaluated. However, the surface coating thickness and surface roughness of the CoBlast coatings was found to be lower compared to plasma HA coating in literature (20–300 μm thickness, 3–6 μm Ra)[34] with increased cell proliferation observed on plasma HA compared to grit blasted surfaces [1].

2.3.2. Cell Morphology

Surface modification techniques are extremely important for evoking desired cellular responses through tailoring the implants surface properties. The osteointegration process is greatly enhanced by these modifications, which in turn increases the long term success of the implant. As previously mentioned, HA is well known for its osteoconductive properties and its ability to influence cell adhesion and interaction at the implant-host interface. It is generally accepted that alongside chemical compatibility, the three dimensional surface topography (shape, size and surface texture) of the implant also influences early tissue response.

Figure 8 shows various images of MG63 cells that were cultured on the untreated titanium substrates, Figure 8a; microblasted MCD 106 surface, Figure 8b and CoBlast HA/MCD-106, Figure 8c after 24 hours.

Cells attached well to the untreated titanium surfaces and displayed a fibroblastic morphology synonymous with that of this osteoblastic cell line. The cells are typically polarized in one direction with the average cell length measuring roughly 60–80 μm (Figure 8a). Furthermore, lamellopodia and filopodia extensions (cytoskeletal organisation) from the main body of cells onto the surface are observed. The presence of these processes suggest good cell-substrate interactions where the cell is actively probing for specific topographical features and connects the cell to the substrate (*via* filopodia) from the lamellopida, which is the protrusion of their leading edge indicative of cell spreading and migration. However, the presence of numerous spherical cells indicates that not all cells are actively involved in spreading and migration. The cells cultured on MCD blasted surface (Figure 8b) display morphologies similar to that observed on the untreated titanium surfaces. The cells appeared to follow the contours of the MCD blasted surface where they would sit in the defects on the surface and align themselves along grooves or dents in a process referred to as ‘contact guidance’ [31]. The contact guidance effect has commonly been associated with increased cell proliferation and differentiation [31]. The surface roughness was determined to be 0.4, 0.5 and 0.7 μm for the blank Ti, microblast MCD-106 and the CoBlast HA/MCD-106 respectively and this obviously influenced the proliferation results observed here as mentioned earlier.

Figure 8. MG-63 osteoblasts cultured on (**a**) untreated Ti and (**b**) microblasted MCD 106 treatment × 500 magnification and (**c**) HA/MCD-106 surfaces (CoBlast treatment) (×500 magnification).

(a)

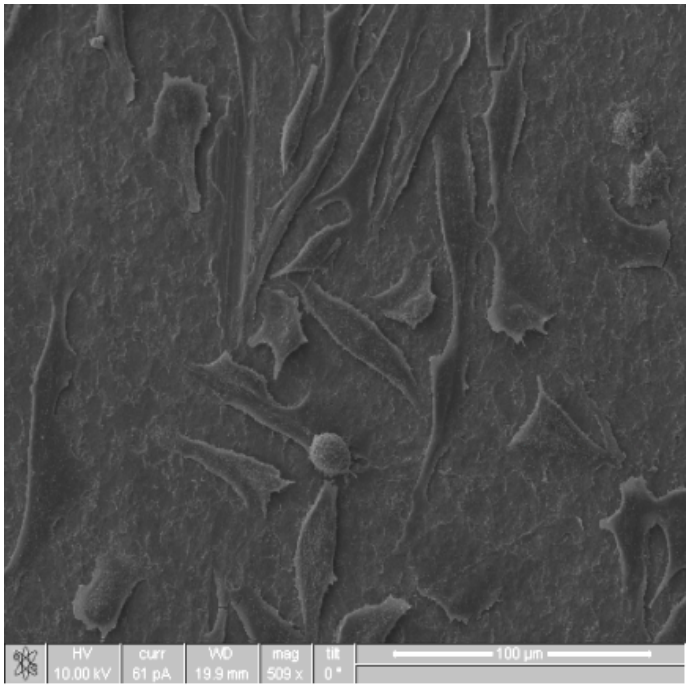

(b)

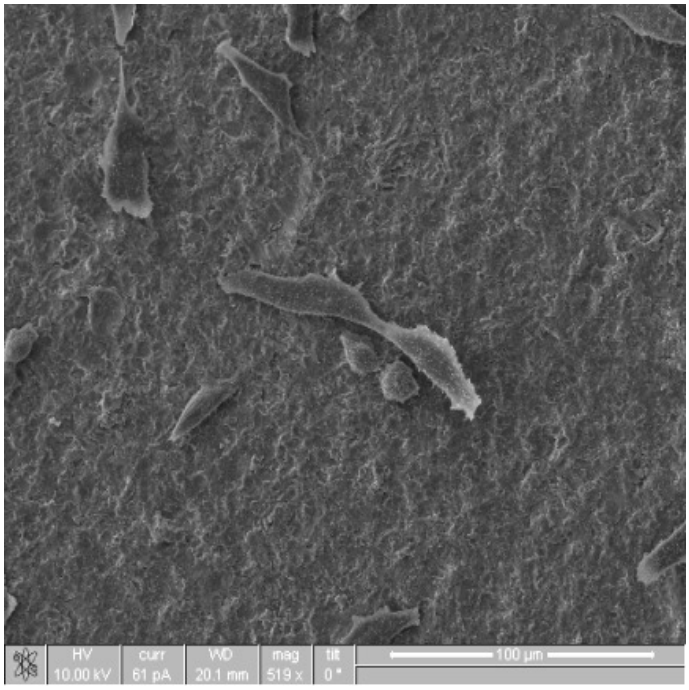

Figure 8. *Cont.*

(c)

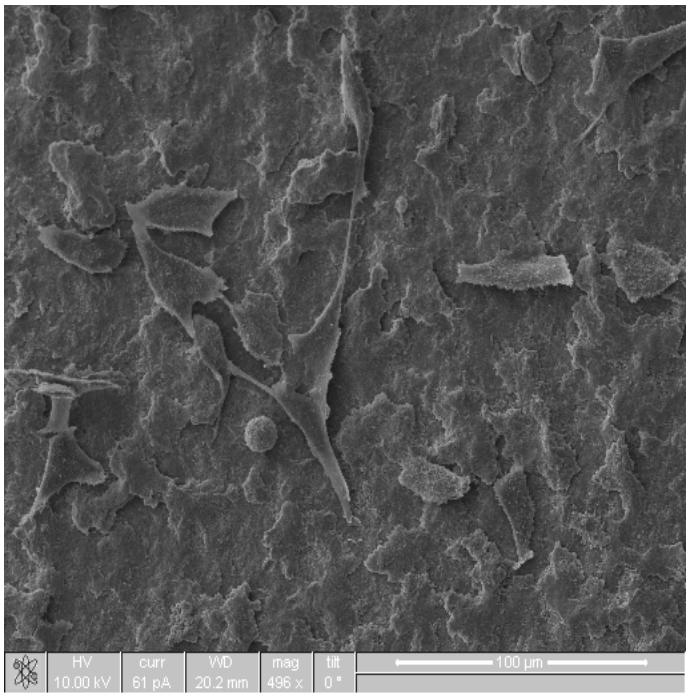

Figure 8c shows an image of MG-63 cells cultured on the CoBlast after 24 hours, it can be seen that these differed from those of the untreated and microblasted titanium in terms of morphology where they had a polygonal shape rather than a polarized fibroblastic morphology indicating increased cell spreading. The cells also tended to align to the surface features created by the addition of the bioactive layer, which was earlier observed to increase the surface roughness (Figure 4). An abundance of lamellopodia and filopodia were present on the CoBlast surface. The addition of a HA coat to the Ti surface, resulted in a higher order of cell spreading and cell focal adhesion attachment compared to the microblasted surface (Figure 8b).

Research has proven that the manufacturing process and patterned topography have a significant influence on long term adherence and cell proliferation *in vitro*, irrespective of composition and surface roughness [32] and early controlled osteoblast alignment was demonstrated on patterned substrates [33]. Therefore, due to the patterned nature of the HA surface after CoBlast treatment, a more favorable surface resulted for cell spreading which subsequently lead to increased cell viability compared to the microblast and blank Ti surfaces. *In vivo* evaluation of CoBlast substrates prepared using an alumina abrasive have already demonstrated early stage lamellar bone growth [21]. This study demonstrates that by employing differing grades of MCD abrasive in the CoBlast process, greater control over surface topography can be achieved, which offers the capability to improve bone-implant contact *in vivo*. Further *in vitro* evaluations such as dissolution studies and bioactive studies in stimulated body fluid (SBF) must be investigated to support these capabilities.

3. Experimental Section

3.1. Materials

Titanium (Grade 5, Ti-6Al-4V) coupons (15 mm × 15 mm × 1 mm), were obtained from Lisnabrin Engineering Ireland. Hydroxyapatite [$Ca_{10}(PO_4)_6(OH)_2$] powder was sourced from S.A.I., France. The MCD apatite abrasives were all purchased from Himed Inc. (NY, USA). HPLC grade 1M hydrochloric acid (HCl), de-ionised water, isopropanol (IPA), ethanol, phosphate buffer solution (PBS), potassium bromide (KBr) FT-ir grade, Trypsin EDTA, MTT assay kit, ACS reagent grade dimethyl sulphoxide, paraformaldehyde, glutaraldehyde, osmium tetroxide and hexamethyldisilizane were all purchased from Sigma-Aldrich UK. MG-63 osteoblast cells were obtained from American Type Culture Collection, Rockville, MD, USA. Minimum Essential Medium (MEM), foetal calf serum, penicillin G sodium, streptomycin, amphotericin B were purchased from PAA Laboratories GmbH, Austria.

3.2. Sample Preparation

Prior to surface modification, the coupons were cleaned ultrasonically in 1M HCl and then in isopropanol to remove any contaminants. The CoBlast technique was used to modify the titanium, through deposition with a HA layer. The processing utilized twin microblast nozzles for the dopant/abrasive system. The HA (dopant) was deposited onto the Ti coupons using compressed air at a pressure of 90 psi, speed of 13 mm/sec and a working distance of approximately 20 mm. The MCD abrasives (either MCD-106, MCD-180 or MCD-425) were blasted out of the second nozzle at a pressure of 75 psi and at a working distance of 8 mm from the surface. The microblast surfaces where prepared under the same corresponding conditions as above, however no HA was delivered through the dopant nozzle. After the surface treatment step, each sample was ultrasonically washed in de-ionized water for 5 mins to remove any loose powder from the surface.

3.3. Surface Characterisation

The elemental composition of the powders and the coatings was carried out using a Jeol JSM 5510 SEM in conjunction with an INCA X-sight EDX spectroscopy detector (Oxford Instruments, Buckinghamshire, UK). Images were also taken using the same SEM system. Gravimetric analysis of the surface treatments on Ti was used to determine the coating mass using an Ohaus DV314C analytical balance by measuring the sample before and after an acid wash (ultrasonic treatment in 20 mL 1 M HCl for 10 mins). PXRD data was collected on a Siemens GAXRD diffractometer using CuKα1 radiation, with an anode current of 30 mA and an accelerating voltage of 40 keV. Data was collected in the range of 20 to 60 2θ degrees with a step size of 0.02 and a scan rate of 1 s per step. Coating thickness was measured using a PosiTector 6000 N thickness gauge (DeFelsko, NY, USA). An average of six readings was used to determine each value. The surface roughness (Ra) was determined using a Talsurf 10 surface profilometer (Talyor Hobson, UK). A Perkin Elmer Spectrum One FTIR was used to determine the structural fingerprint of the powders and the coatings. The coating was scrapped off, gently ground and pressed into a KBR disc (2% wt sample in KBR). Powders for FTIR analysis were prepared in a similar manner. FTIR spectra were recorded in the

1600–400-cm^{-1} range, with 4 cm^{-1} resolution using 20 scans and background subtraction. The spectra gave approximately 70–90% transmittance however the results are presented in an overlay fashion.

3.4. In Vitro Cell Culture

Sample modifications including CoBlast HA/MCD-106 and microblast MCD-106 and the blank Ti were evaluated for osteoconductivity and cytotoxicity using cell culture tests. Prior to cell culture analysis, each sample set was steam autoclaved at 121 °C for 20 minutes. MG-63 cells were used to assess cell proliferation. Cells were cultured in the MEM media supplemented with 10% foetal calf serum and antibiotic/antimycotic (penicillin G sodium 100 U/mL, streptomycin 100 µg/mL, amphotericin B 0.25 µg/mL) in 75 cm^3 tissue culture flasks. Cells were maintained in a humidified atmosphere with 5% CO_2 at 37 °C and were sub-cultured when they reached confluence using 0.25% Trypsin EDTA solution to provide adequate numbers of cells for the various *in vitro* culture studies undertaken.

3.4.1. Cell Proliferation

MG-63 cell attachment to the various treated and untreated Ti substrates was determined after 4 hours in culture using a commercial MTT assay and employing a modified Mosmann method [24]. Cells were seeded onto the samples at a concentration of $1x10^5$ cells/$cm^2$and allowed to adhere during incubation at 37 °C in 5% CO_2 for 4 hrs. The MTT assay reagent was prepared as a 5 mg/mL stock solution in PBS, sterilized by filtration, and stored in the dark. An aliquot of the MTT stock solution (10% of total volume) was added to each well of a six well plate containing the samples (n = 4 for each sample type). After 3 hrs incubation at 37 °C in 5% CO_2, 200 µl of dimethyl sulfoxide was added to dissolve the formazan crystals. The solution was agitated for 15 min on a shaker to ensure adequate dissolution. The optical density of the formazan solutions was read by spectrophotometry using an ELISA plate reader (Tecan Sunrise, Tecan Austria) at 570 nm with the background absorbance value measured at 650 nm. The absorbance values recorded were determined to be proportional to the number of cells attached to the surface in each case. All data reported are expressed as mean ± standard deviation.

3.4.2. Cell Morphology

MG-63 cells were seeded onto each of the above substrates at a cell density of 5×10^5 cells/cm^2 in 6-well plates and were incubated for 24 hours. After cell culture, the samples were gently rinsed with PBS to remove any unattached cells and fixed in a modified Karnovsky's Fixative (2% paraformaldehyde/ 2% glutaraldehyde in PBS) for 1 hour. The samples were then rinsed in PBS and post-fixed in 1% osmium tetroxide and rinsed three times with PBS. The specimens were dehydrated by rinsing in an alcohol series (20, 30, 50, 70, 80, 90 and 95% ethanol), and finally rinsing 3 times in 100% ethanol. The samples were then were chemically dried in hexamethyldisilizane (HMDS) overnight. A 50 nm layer of gold-palladium was deposited onto the substrates using a Polaron E5000 SEM Sputter Coating Unit. The sputtering conditions used a set voltage of 1.4 kV, with a plasma current of 18 mA (argon gas), a deposition time of 2 minutes at a vacuum pressure of 0.05 Torr. The

samples were then analyzed using the Jeol JSM 5510 SEM and subsequently using a FEI Quanta 200 Focused Ion Beam and SEM in backscatter electron mode.

4. Conclusions

Detailed surface studies have shown that the combination of an apatite abrasive and a HA dopant in the CoBlast process produces surfaces with a combination of optimized apatite chemistry and controlled surface structure. The CoBlast process has the ability to retain the chemistry of the starting HA material. This offers advantages over conventional high temperature plasma processing which alters the HA material from its desired chemical, structural and dissolution requirements for its use as an *in vivo* implant material. The study also shows that employing MCD abrasives offer an alternative to alumina for deposition using CoBlast process. *In vitro* studies clearly show that increased roughness of treated surfaces favors enhanced cell proliferation and the CoBlast process offers the ability to tailor the surface texture to produce an optimized surface for osteointegration of a HA modified implant. Enhanced cell proliferation was observed for CoBlast modified surfaces compared to the microblasted surface. The ability of the CoBlast technology to offer diversity in modifying surface topography is clearly shown in this and previous studies and represents foundation work, which supported by bioactivity studies and *in vivo* trials, offers exciting new prospects in tailoring the properties of medical devices for applications ranging from dental to orthopedic settings.

Acknowledgments

The authors would like to acknowledge EnBio for supplying the CoBlast samples for this study.

References and Notes

1. Borsari, V.; Giavaresi, G.; Fini, M.; Torricelli, P.; Salito, A.; Chiesa, R.; Chiusoli, L.; Volpert, A.; Rimondini, L.; Giardino, R. Physical characterization of different-roughness titanium surfaces, with and without hydroxyapatite coating and their effect on human osteoblast-like cells. *J. Biomed. Mater. Res. Part B* **2005**, *75B*, 359-368.
2. Stoch, A.; Jastrze, B.W.; Dlugon, E.; Lejda, W.; Trybalska, B.; Stoch, G.J.; Adamczyk, A. Sol-gel derived hydroxyapatite coatings on titanium and its alloy Ti6Al4V. *J. Mol. Struct.* **2005**, *744*, 633-640.
3. Oh, I.H.; Nomura, N.; Chiba, A. Microstructures and bond strengths of plasma-sprayed hydroxyapatite coatings on porous titanium substrates. *J. Mater. Sci. Mater. Med.* **2005**, *16*, 635-640.
4. Lu, Y.P.; Li, M.S.; Li, S.T.; Wang, Z.G.; Zhu, R.F. Plasma-sprayed hydroxyapatite + titania composite bond coat for hydroxyapatite coating on titanium substrate. *Biomaterials* **2004**, *25*, 4393-4403.
5. Wennerberg, A.; Ektessabi, A.; Albrektsson, T.; Johansson, C.; Andersson, B.A. 1-year follow-up of implants of differing surface roughness placed in rabbit bone. *Inter. J. Oral Maxillofac. Implants* **1997**, *12*, 486-494.

6. Abron, A.; Hopfensperger, M.; Thompson, J.; Cooper, L.F. Evaluation of a predictive model for implant surface topography effects on early osseointegration in the rat tibia model. *J. Prosthet. Dent*. **2001**, *85*, 40-46.
7. Nakada, H.; Sakae, T.; Legeros, R.Z.; Legeros, J.P.; Suwa, T.; Numata, Y.; Kobayashi, K. Early tissue response to modified implant surfaces using back scattered imaging. *Implant Dent.* **2007**, *16*, 281-289
8. Gil, F.J.; Planell, J.A.; Padros, A.; Aparicio, C. The effect of shot blasting and heat treatment on the fatigue behavior of titanium for dental implant applications. *Dent. Mater.* **2007**, *23*, 486-491.
9. Chen, J.; Wolke, J.G.C.; De Groot, K. Microstructure and crystallinity in hydroxyapatite coatings. *Biomaterials* **1994**, *15*, 396-399.
10. Gross, K.A.; Berndt, C.C.; Herman, H. Amorphous phase formation in plasma-sprayed hydroxyapatite coatings. *J. Biomed. Mater. Res.* **1998**, *39*, 407-414.
11. Gross, K.A.; Berndt, C.C. Thermal processing of hydroxyapatite for coating production. *J. Biomed. Mater. Res.* **1998**, *39*,580-587.
12. Heimann, R.B.; Wirth, R. Formation and transformation of amorphous calcium phosphates on titanium alloy surfaces during atmospheric plasma spraying and their subsequent *in vitro* performance. *Biomaterials* **2006**, *27*, 823-831.
13. Weng, J.; Liu, Q.; Wolke, J.G.; Zhang, X.; De Groot, K. Formation and characteristics of the apatite layer on plasma-sprayed hydroxyapatite coatings in simulated body fluid. *Biomaterials* **1997**, *18*, 1027-1035.
14. Li, H.; Li, Z.X.; Li, H.; Wu, Y.Z.; Wei, Q. Characterization of plasma sprayed hydroxyapatite/ZrO_2 graded coating. *Mater. Design* **2009**, *30*, 3920-3924.
15. Katto, M.; Kurosawa, K.; Yokotani, A.; Kubodera, S.; Kameyama, A.; Higashiguchi, T.; Nakayama, T.; Tsukamoto, M. Poly-crystallized hydroxyapatite coating deposited by pulsed laser deposition method at room temperature. *Appl. Surf. Sci.* **2005**, *248*,365-368.
16. Hong, Z.; Luan, L. Paik, S.E.; Deng, B.; Ellis, D.E.; Ketterson, J.B. Mello, A.; Eon, J.G., Terra, J., Rossi, A. Crystalline hydroxyapatite thin films produced at room temperature—An opposing radio frequency magnetron sputtering approach. *Thin Solid Films* **2007**, *515*, 6773-6780.
17. Stoch, A.; Brozek, A.; Kmita, G.; Stoch, J.; Jastrzebski, W.; Rakowska, A. Electrophoretic coating of hydroxyapatite on titanium implants. *J. Mole. Struct.* **2001**, *596*, 191-200.
18. Mano, T.; Ueyama, Y.; Ishikawa, K.; Matsumura, T.; Suzuki, K. Initial tissue response to a titanium implant coated with apatite at room temperature using a blast coating method. *Biomaterials* **2002**, *23*, 1931-1926.
19. Gbureck, U.; Masten, A.; Probst, J.; Thull, R. Tribochemical structuring and coating of implant metal surfaces with titanium oxide and hydroxyapatite layers. *Mater. Sci. Eng. C* **2003**, *23*, 461-465.
20. Ishikawa, K.; Miyamoto, Y.; Nagayama, M.; Asaoka, K. Blast coating method: New method of coating titanium surface with hydroxyapatite at room temperature. *J. Biomed. Mater. Res.* **1997**, *38*,129-134.
21. O'Hare, P.; Meenan, B.J.B.; George, A.; Byrne, G.; Dowling, D.; Hunt, J.A. *In vitro* and *in vivo* response of hydroxyapatite surfaces deposited *via* a novel co-incident microblasting technique for improved orthopaedic implant performance. *Biomaterials* **2010**, *31*, 515-522.

22. O'Neill, L.; O'Sullivan, C.; O'Hare, P.; Sexton, L.; Keady, F.; O'Donoghue, J. Deposition of substituted apatites onto titanium surfaces using a novel blasting process. *Surf. Coat. Technol.* **2009**, *204*, 484-488.
23. O'Sullivan, C.; O'Hare, P.; O'Leary, N.D.; Crean, A.M.; Ryan, K.; Dobson, A.D.; O'Neill, L.D. Deposition of substituted apatites with anticolonizing properties onto titanium surfaces using a novel blasting process. *J. Biomed. Mater. Res. Part B* **2010**, *95*,141-149.
24. Mosmann, T. Rapid colorimetric assay for cellular growth and survival: Application to proliferation and cytotoxicity assays. *J. Immunol. Methods* **1983**, *65*, 55-63.
25. Kim, T.N.; Feng, Q.L.; Kim, J.O.; Wu, J.; Wang, H.; Chen, G.C.; Cui, F.Z. Antimicrobial effects of metal ions (Ag^{+}, Cu^{2+}, Zn^{2+}) in hydroxyapatite. *J. Mater. Sci.: Mater. Med.* **1998**, *9*, 129-134.
26. Fathi, M.H.; Hanifi, A.; Mortazavi, V. Preparation and bioactivity evaluation of bone-like hydroxyapatite nanopowder. *J. Mater. Proc. Technol.* **2008**, *202*,536-542.
27. Varma, H.K.; Babu, S.S. Synthesis of calcium phosphate bioceramics by citrate gel pyrolysis method. *Ceram. Int.***2005**, *31*, 109-114.
28. Pleshko, N.; Boskey, A.; Mendelsohn, R. Novel infrared spectroscopic method for the determination of crystallinity of hydroxyapatite minerals. *Biophy. J.***1991**, *60*,786-793.
29. Legeros, R.Z.; Daculsi, G.; Orly, I.; Gregoire, M. Substrate surface dissolution and interfacial biological minerals. In *The Bone-Biomaterial Interface*; Davies, J.E., Ed.; University of Toronto: Toronto, Canada, 1991; pp. 76-88.
30. Masmoudi, M.; Assoul, M.; Wery, M.; Abdelhedi, R.; El Halouani, F.; Monteil, G. Friction and wear behaviour of cp Ti and Ti6Al4V following nitric acid passivation. *Appl. Surf. Sci.* **2006**, *253*, 237-2243.
31. Anselme, K. Osteoblast adhesion on biomaterials. *Biomaterials* **2000**, *21*, 667-681.
32. Bigerelle, M.; Anselme K. Statistical correlation between call adhesion and proliferation on biocompatible metallic materials. *J. Biomed. Mater. Res. A* **2005**, *75*, 530-540.
33. Puckett, A.; Pareta, R.; Webster, T.J. Nano rough micron patterned titanium for directing osteoblast morphology and adhesion. *Inter. J. Nanomed.* **2008**, *2*, 229-241.
34. Sun, L.; Berndt, C.C.; Gross, K.A.; Kucuk, A. Material fundamentals and clinical performance of plasma-sprayed hydroxyapatite coatings: A review. *J Biomed. Mate. Res.* **2001**, *58*, 570-592.